Grau, teurer Freund, ist alle Theorie

Und grun des Lebens goldner Baum.

JOHANN WOLFGANG VON GOETHE 1749 - 1832

Studierzimmer

THE MINERALOGY AND MODE OF OCCURRENCE OF THE PLATINOID AND ASSOCIATED MINERALS IN THE MERENSKY HORIZON OF THE WESTERN BUSHVELD

by

GORDON ANDREW KINGSTON

A Thesis Submitted for the Degree
of Doctor of Philosophy
University of London

Department of Geology,
Imperial College of Science & Technology,
London.

April 1977

ABSTRACT

Ore samples and platinum mineral concentrates, collected by the author during a field study of the structure of the Merensky Reef at Rustenburg and Union mines in the western Bushveld of South Africa, have been investigated. New details of the geology of the Merensky Reef including the potholes and koppies are discussed in the light of recent theories of origin. New compositional, optical, and physical data for the platinum group minerals in this ore are presented, and critically compared to existing data. Attention is particularly focused on the nature and genetic interpretation of the platinoid mineral intergrowths. The principal methods of investigation were reflected-light microscopy, combining measurements of reflectance and microhardness, electron-probe microanalysis, and X-ray powder diffraction.

The present confusion over the published properties of cooperite and braggite is discussed, and resolved by the presentation of new data. The unique occurrence of an iridium-osmium-platinum zoned laurite is described, as well as two new rhodium sulphides which are believed to be present in the Merensky Reef. Compositional and hardness data on the natural Pt-Fe alloys in this ore supports the unreliability of microhardness as a tool for determining their iron content. The author's original published data for six new bismuthotellurides of platinum and palladium, including type merenskyite, are presented, and are discussed in the light of new observations and published data on other occurrences and synthetic equivalents.

The textural features of the ore are explained in the context of fractional crystallisation of an interstitial platiniferous sulphide melt. Residual pegmatitic and hydrothermal fractions are recognised as responsible for the location of some of the minerals. Intergrowths explained in particular detail include the replacement of pyrite by pyrrhotite, cooperite by braggite, merenskyite by kotulskite, and the exsolution of graphic Pt-Fe alloy from pyrrhotite and pentlandite. The significance of this investigation to the geochemical behaviour of the platinum group metals is finally discussed.

CONTENTS

LIST OF FIGURES

TABLES

MAPS

CHAPTER 1

INTRODUCTION

1.1 The Bushveld Igneous Complex

Although references to rocks of the Bushveld Igneous Complex are to be found in the literature as early as 1872, the first systematic mapping of the Complex began in 1902 with the formation of the Geological Survey of the Transvaal. By about 1916, with the additional incentive provided in 1908 by the discovery of platinum in the chromitite horizons, most of the exposed part of the Complex had been mapped and its general areal distribution shown. Notable amongst those responsible during this period were Hall, Kynaston, Mellor, Wagner, and Molengraaff. This discovery of primary platinum resulted in widespread and intensive prospecting in the area which, with the discovery of the platiniferous(1) dunite pipes and the Merensky Reef, led to extensive mining developments and to the uncovering of valuable fresh petrological and structural data. A summary of previous work and a large bibliography of workers on the Complex up to 1928 is given by Daly (1928) and Daly and Molengraaff (1924), and up to 1932 by Hall in a memoir which still forms the most comprehensive geological account of this great igneous body. However, with regard to the platiniferous deposits and particularly to our knowledge of the Merensky Reef, Percy Wagner's outstanding book (1929) forms a monumental contribution, and still

---

(1) 'platiniferous' is used to refer to rocks, minerals, ores, deposits etc. which contain the six platinum group elements in trace but potentially economic quantities.

stands as a relevant and valuable reference on the subject. Since that time a multitude of publications have followed and, although the knowledge amassed is considerable, there are still important fundamental problems and controversies to be settled. Even without producing further data much could be accomplished from a conscientious assessment of that already available. This evaluation of the data is most valuable when accomplished by a person with extensive first hand knowledge and experience of the region. Review papers by Willemse (1959, 1964, 1969) are particular examples.

1.1.1 The Areal Distribution and Structure of the rocks composing the composite igneous body, appropriately called the Bushveld Igneous Complex by Daly and Molengraaff (1924), is shown on the map by Willemse (1969) in figure 1.1. The Complex is composed of extrusive, hypabyssal, and plutonic rocks which together produce a lobulate form having an areal extent of about 67340 km^2, including that area covered by younger formations. The longest east-west axis of the body is 463 km with the north-south axis from Pretoria of 246 km. The Mafic Zone (Cousins, 1959) or Layered Sequence (Willemse, 1969) forms a nearly continuous belt enveloping the more acid members, attaining maximum thicknesses on the axes of the lobes which have a flat synclinal structure and which plunge towards the centre of the Complex at angles of 9 - 50^{o}. The Mafic Zone consists in the lower part of a high proportion of pyroxenites and chromitites with norite and anorthosites. The greater upper part is composed of gabbroic and dioritic rocks with magnetite bands near the top. A shallow extension of the Mafic Zone occurs west of the Pilanesberg alkaline intrusive mass.

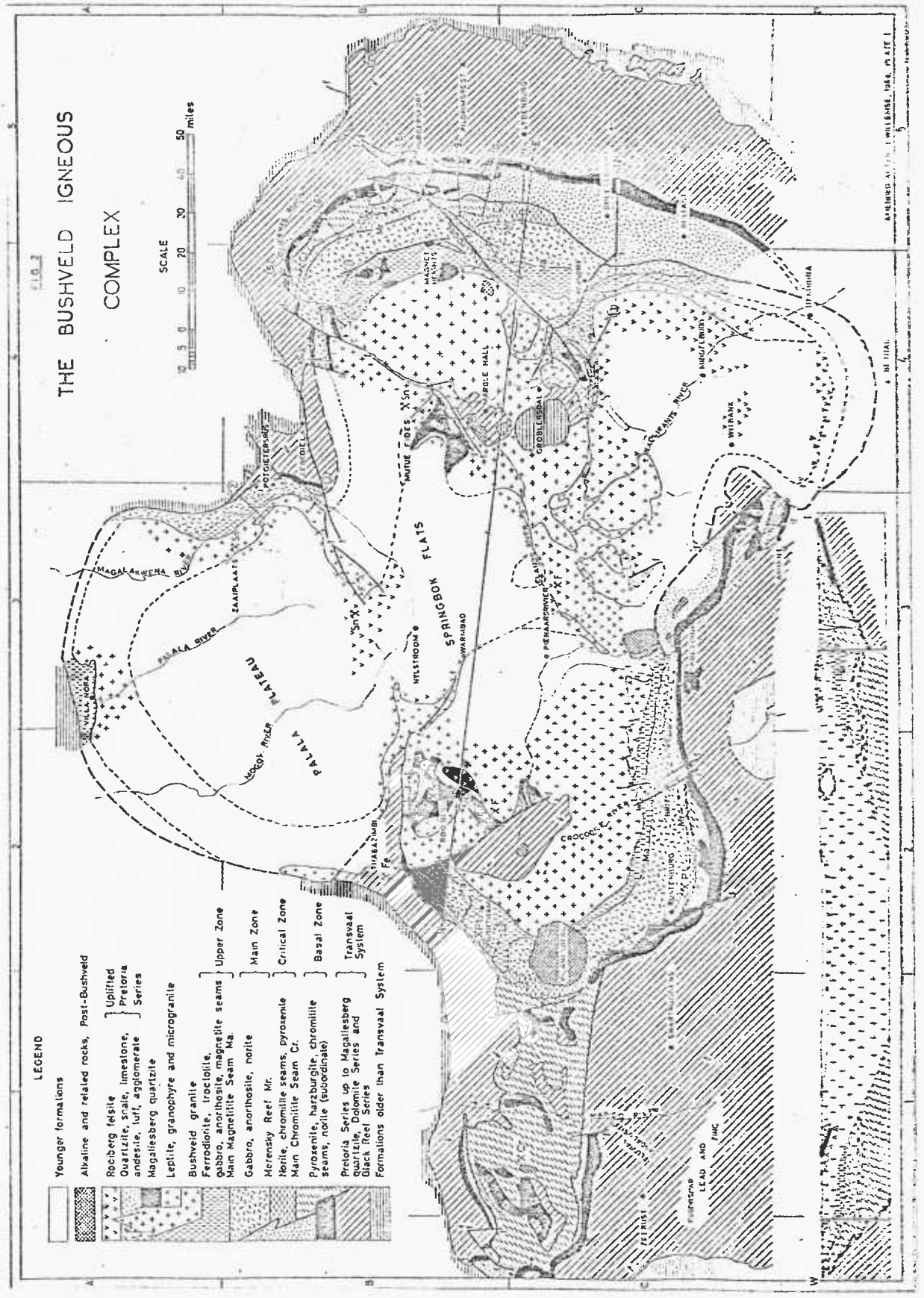

Fig. 1.1 Geological Map of the Bushveld Igneous Complex, Transvaal, South Africa. After Willemse (1969).

The encircling sedimentary rocks of the Transvaal System appear in plan to show a generally concordent dip with the Mafic Zone rocks, although a transgressive relationship has been demonstrated and emphasised by Willemse (1959). These rocks are interbedded with andesitic lava, tuff, and conglomerates, and intruded by diabase sills emplaced along quartzite/shale contacts of the Pretoria Series. Large areas of the Complex are overlain by younger formations, notably rocks of the Waterberg and Karroo Systems. However, sufficient outcrops and borehole data in these regions, combined with the results of a gravity survey published by the Geological Survey in 1958, allow the structure of the Mafic Zone to be seen as five basin-like masses adjoining and perhaps overlapping one another (Willemse, 1964).

The central acid members of the Complex consist dominantly of (a) extrusive felsite (the Rooiberg felsite) with interbedded pyroclastics, (b) granophyre, leptite, and microgranite of controversial and complex genesis, and (c) the extensive Bushveld Granite which intrudes all other rocks except for much later alkaline intrusive masses and Waterberg and Karroo sediments. The Granite/Mafic Zone contact generally conforms to the layering in the Mafic Zone, and the Granite is, therefore, essentially basin-shaped in form, but contacts with the 'roof' felsite and granophyre rocks are mostly transgressive as well as contacts with disrupted fragments of the Transvaal System. A number of later alkaline complexes occur throughout the region, notable amongst them being the Pilanesberg which intrudes and disrupts the Mafic Zone in the western Bushveld. Recent isotopic age measurements (Davies et al, 1970) give an age

for the Complex of 1950 ± 30 million years.

1.1.2 Location of the Bushveld Igneous Complex. The Complex is situated in the Kaapvaal Craton. This is one of eight cratons in Africa established as relatively stable blocks over 2500 m.y.ago (Clifford, 1970). The fusion of subsequent orogenic zones onto these blocks, adding to them and joining them, has resulted in the present African Craton. The broad structural setting of the Complex and related intrusives in this craton is shown in figure 1.2.

Hall (1932) pointed out that a line drawn through the Great Dyke to the Vredefort dome granite bisects the Complex. This line was extended north by McConnel (1955) to include the east African Rift Valley, and southward by Kent (1957). The Trompsburg intrusive is also on this line (Cousins, 1959). Cousins considered that this lineament may mark the position of a fracture in the Earth's crust reaching to extreme depth, through which deep-seated magma was forced at favourable positions to sites at or near the surface. Intersection of this lineament with a possible E-W one through the Pilanesberg intrusive may have been a control factor. However, one should note that the Vredefort dome is some 580 m.y. older than the Mafic Zone, and the Trompsburg intrusive is dated as 600 m.y. younger. Therefore, if this is the case, this lineament has a long history of activity.

Following the Sudbury meteorite impact theory by Dietz (1964), and the later impact theory for the Vredefort Dome, Hamilton (1970) postulated that meteorite impacts were the triggers to magmatism in the case of the Bushveld Complex. He suggested that three separate meteorite impacts were responsible for the convergent arc

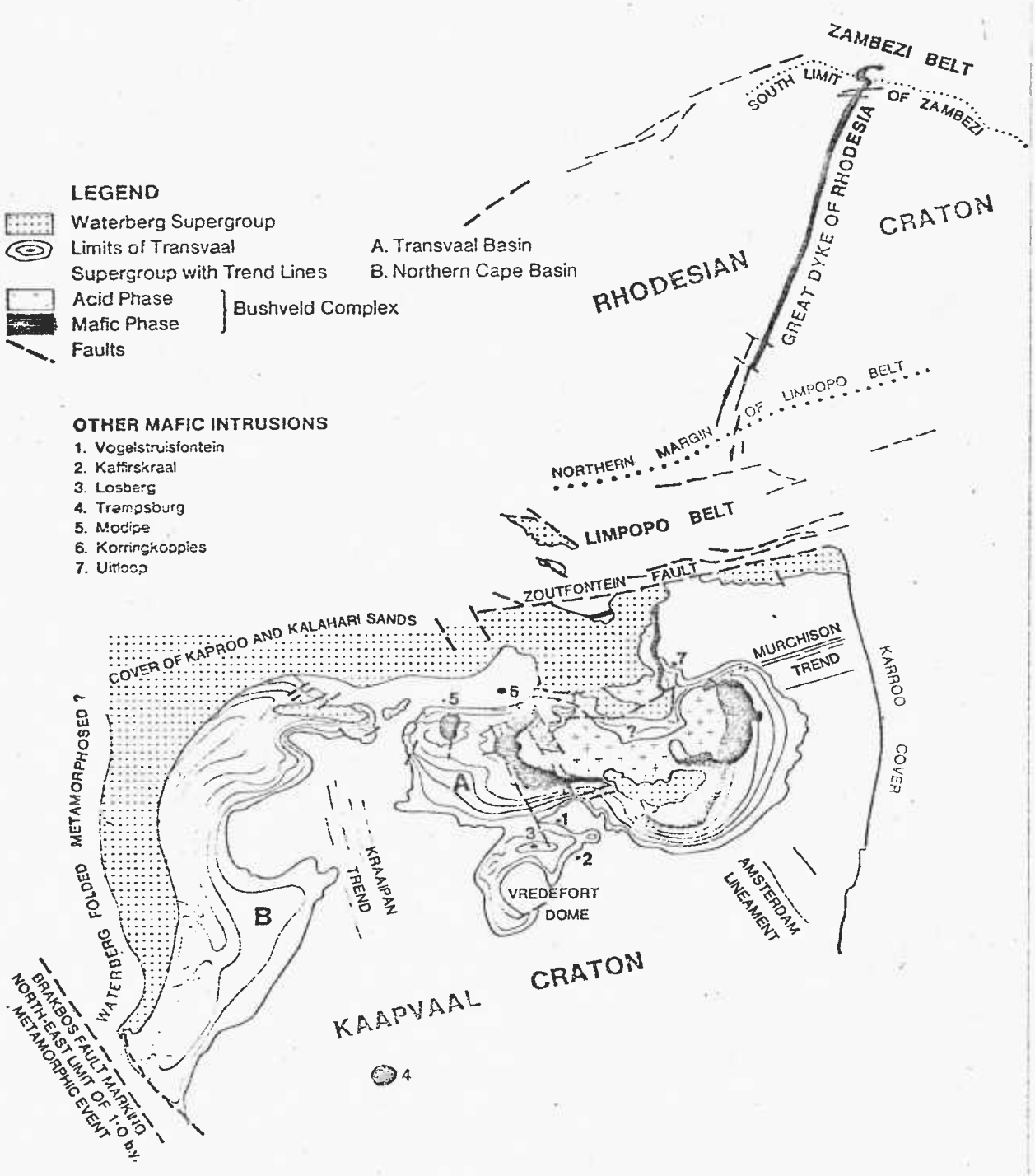

Fig. 1.2 Structural setting of the Bushveld Igneous Complex and genetically related mafic intrusions. After Hunter, 1976.

shape of the Complex and described for each a central area of uplift with a fringing ring structure. Shattering beneath the ring synclines would then form the channelways and receptacles for the rising magma. Each central granitic area formed according to Hamilton by "fusion of crustal and mantle rocks, either instantaneously by shock melting and explosive release of overburden pressure, or shortly after the event as a result of the establishment of a steep thermal gradient by conduction from the mantle through the explosively heated thinned crust". However, no evidence of shock-metamorphic effects have yet been found in the Bushveld rocks.

Recent studies (Crockett, 1969; Hunter, 1976) have shown that a basin was developing on the site of the Bushveld Complex as the lowest stage of the Transvaal System was being deposited, and that a final collapse of this basin took place prior to the intrusion of the Mafic Zone. This basin may have formed by subsidence along a linear fracture perhaps initiated by the formation of the Vredefort Dome. The centipetal dip of the Transvaal rocks, which increases towards the margin of the Bushveld Complex, was thus a result of this subsidence. Around the major portion of the flanks of the basin the strata accommodated themselves to such subsidence in a broad sinusoidal curve. Thus the dip of the Transvaal System gradually increases inwards from the basal Black Reef series. Dips may have been flat in the central part of the basin. In the western area of the Transvaal, Crockett reported decollement and gravity sliding structures in the Pretoria series. Isolated Transvaal System 'rafts' in the middle of the Bushveld Complex were interpreted as tectonic slides translated along low-angle fracture planes.

One might note that this collapse could still be of meteoritic origin, but that the collapse is also a natural progression of crustal instability evident in the Transvaal System rocks.

Crockett (1969) has suggested that the cause of basin formation on the Kaapvaal Craton is linked with intermittent ductile flow of mantle material away from the foci of subsidence. The outbreaks of mafic andesite volcanicity that preceded the Bushveld Complex are considered to be the products of the periodic heating and melting of the base of the steadily sinking crust. He postulates that the significantly different nature of the Bushveld magmas, which display a differentiation into basalt and granite, may be indicative of a more sudden collapse of the Transvaal basin which would leave little time for magmatic mixing so that th?oleiitic magmas were injected, while the granite represents mobilization of sialic crustal material.

Hall (1932) was of the opinion that the pronounced and regular basining of the Transvaal System was due to its gradual bending down by the magma load of both the granitic and mafic portions of the Complex, combined with lack of adequate support through the withdrawal and ascent of originally underlying magma. Visser (1957) held a similar opinion but thought it was just due to the weight of magma. However, these views are contradicted by the subsequent geological and geophysical work (Cousins, 1959; Smit et al.,1962) which shows that the Mafic Zone consists of three or four distinct bodies and not a single lopolith. Gravity surveys also show that the weight of gabbroic rocks is small compared to the Bushveld Basin as a whole.

1.1.3 The Sequence of Events leading to the formation of the Bushveld Complex are considered therefore to be as follows:

1. Deposition of the Transvaal System in a subsiding basin on the Kaapvaal Craton, with some contemporaneous volcanicity. The Smelterskop Stage of the Pretoria Series consists of a high proportion of lavas and pyroclastics and represents an approach to the peak of volcanic activity prior to the emplacement of the Mafic Zone. The most widespread extrusion, extending some 500 km to the SW beyond the Bushveld Complex, is the Ongeluk Lava which occurs about halfway up the Pretoria Series and reaches thicknesses of up to 1500 metres in the Zeerust area.

2. Final collapse of the Bushveld Basin initiating gravity sliding of Transvaal System rocks round the margin.

3. A sill phase of diabase sheets injected into the now inclined Pretoria Series. Although the composition and mineralogical character of these sills is very variable, due in part to varying degrees of assimilation of sedimentary material, two main types of diabase have been defined. Close to the Mafic Zone is the Maruleng Type with orthopyroxene as a typical constituent, and which includes at least some of the noritic rocks of the erratic Chill Zone of the Mafic Zone. Away from the contact with the Mafic Zone the sills become more aluminous and less disrupted and contaminated with products of assimilation. These hornblende-clinopyroxene bearing diabases have been termed the Lydenburg Type. They are believed to represent the original undifferentiated magma of the Complex in chemical composition (Willemse, 1964).

4. An epicrustal phase represented by the Rooiberg

felsite, leptite, and granophyre. Although it is generally accepted that processes such as felspathisation of sediments, anatexis of sedimentary rocks, replacement of alkaline solutions, and metamorphic recrystallisation have taken place in the formation of these rocks, it is generally considered (Willemse, 1969; Fourie, 1969) that the rocks were for the most part initially products of volcanism.

5. The mainplutonic phase which produced granodiorite, dioritic, mafic and ultramafic rocks of the Layered Sequence or Mafic Zone. Now universally accepted as formed by magmatic differentiation, although controversy still arises with regard to its structure at depth and to the mechanisms involved in producing the layering.

6. A plutonic phase represented by the Bushveld Granite.

1.1.4 The Mafic Zone is a layered sequence of mafic and ultramafic rocks some 7600 m thick forming a lobulate belt from 8 to 20 km wide round the periphery of the Complex. The intrusive nature of this zone is in little doubt, with the layering and diversity of rocks due to magmatic differentiation. The layering conforms fairly closely to the strike and dip of the Pretoria Series, varying from 5 to 50°. At Rustenburg mine the average dip is $9\frac{1}{2}^{\circ}$ and at Union mine 20°. As seen in figure 1.1 the layering dips everywhere towards the centre of the Complex. The thickness of the zone varies, and increases towards the axes of the embayed areas as in the Rustenburg and Northam embayments. Also the Northam (Union mine) Mafic Zone sequence, although displaying the same differentiation

pattern as at Rustenburg, is considerably thicker, the increase in thickness taking place across an E-W line approximately through the Pilanesberg mass (Vermaak, 1976). Mapping of marker horizons, particularly chromitite layers, has demonstrated that the lower parts of the sequence are not continuous round the Complex, but are best developed in the embayed areas and 'cut out', with overlap of higher layers, against the edges of the embayments such that, as recorded by Cousins (1959) "the contact between the Mafic Zone and its floor closely resembles that between sea and land along a coast line which, in places, has been drowned".

The differentiation trend is broadly from magnesium-rich undersaturated rocks at the base towards iron-rich and alkaline oversaturated rocks at the top. In general the first 2400 m is highly differentiated with a bewildering diversity of rocks forming extensive sheets and lenses from one or a few centimetres to many metres thick, often persistent over many miles. A prime example is the Merensky Reef pyroxenite which is traceable round most of the Complex. The remaining 5200 m is generally more uniform and less differentiated, although layering is still a prominent feature. It must be remembered, however, that because of the occurrence of economic chromite and platiniferous horizons in the lower part of the Mafic Zone much more is known of this part, from borehole and underground observations, than is the case for the remaining 'monotonous' and poorly exposed upper two thirds.

For a considerable time now the Mafic Zone has been divided into zones based on the recognition of certain easily recognised and laterally continuous marker horizons (fig. 1.3). Thus the

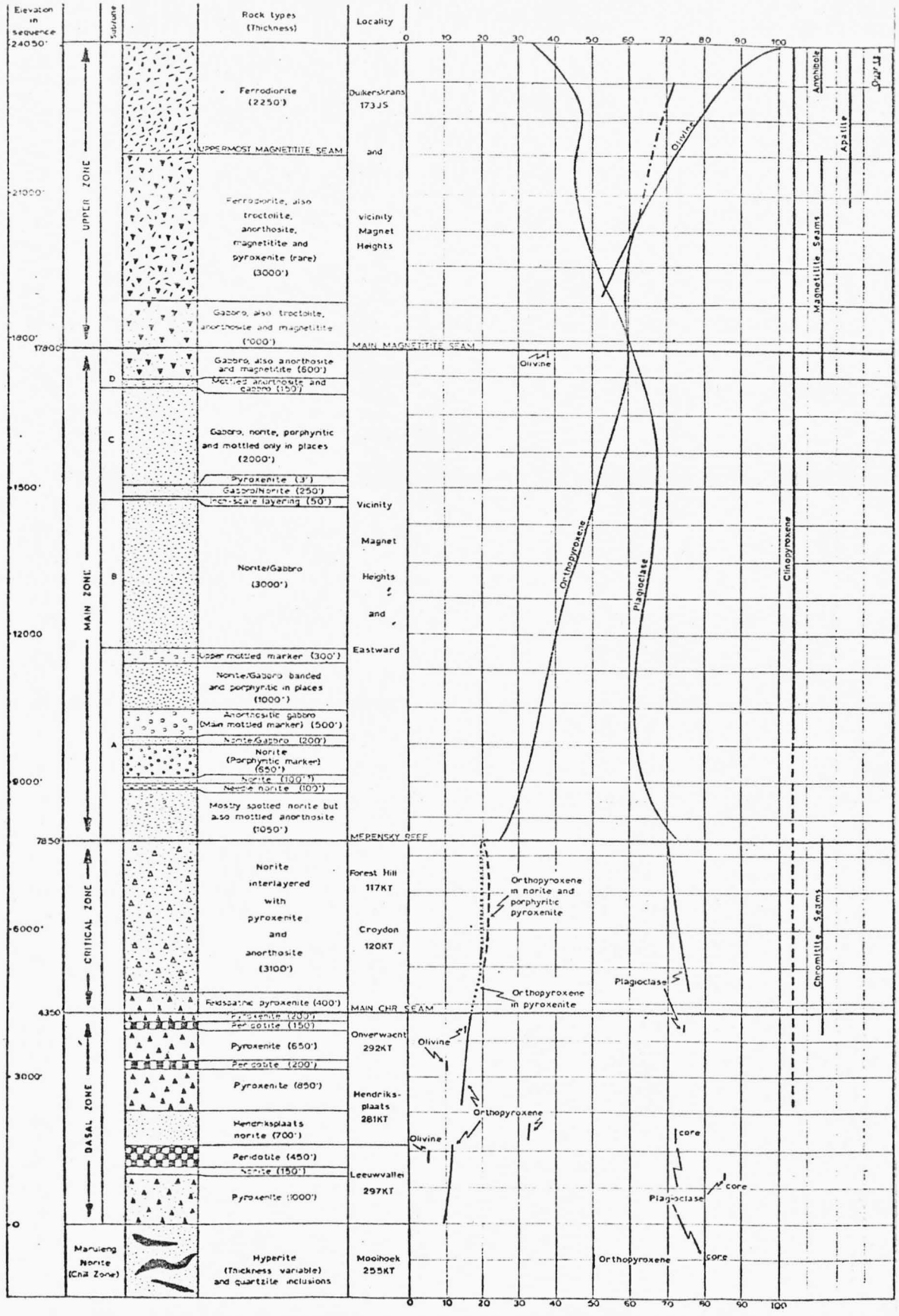

Fig. 1.3 The divisions of the Mafic Zone as illustrated by a composite section through the Eastern Bushveld by Willemse (1969). The silicate compositions are expressed in mol.% of $FeSiO_3$ in orthopyroxene, Fe_2SiO_4 in olivine, and An in plagioclase.

top of the lowermost and dominantly pyroxenitic portion, named the Basal Zone, is taken as the first prominent and thick chromite layer. In the eastern Bushveld the exploited Main Chromitite Seam or Steelport Band is used. In the western Bushveld this chromite horizon is also present but the Magazine Reef, traceable from west Brits to beyond Swartkop Chrome mine, could be used instead (Willemse, 1964). The dominantly pyroxenitic Basal Zone gives way to intensely layered and rhythmic sequences of chromitite, pyroxenite, norite, and anorthositic rocks of the Critical Zone, the top of which is considered to be the Merensky Reef. The top of the succeeding Main Zone, poorly differentiated noritic to gabbroic portion, is taken as a prominent magnetite horizon called the Main Magnetite Seam. The Upper Zone rocks above range from gabbro to ferrodiorite and diorite, and contain numerous magnetite horizons.

Although petrologically these divisions are perhaps not justified, there is some broad coincidence of these marker horizons with mineralogical and chemical breaks (fig. 1.3) as well as with some major unconformities. The mining companies, however, use other equally persistent marker horizons in correlating borehold data, as for example the UG1,UG2,UG3, etc. chromite seams in the Rustenburg area (Cousins and Feringa, 1964). However, in using these marker horizons in correlations throughout the whole Bushveld it should be born in mind that the Mafic Zone was probably intruded as two or more separate arcuate sheets fed from separate feeders, involving periodic influxes or surges of new magma which, quite reasonably, have produced a similar overall differentiation sequence.

1.1.5 The Critical Zone. Since the Merensky Reef is a product

of the formation of this highly layered zone by magmatic differentiation, it is relevant to this thesis that some of the main characteristics of this zone are mentioned.

This portion of the Mafic Zone consists of a generally repetative sequence of chromitite, pyroxenite, norite, anorthositic norite and anorthosite, with the chromitites and pyroxenites subordinate. In the eastern Bushveld the thickness is about 1100 m, in the Rustenburg embayment it varies between 350 - 670 m, and in the Northam embayment about 840 m (Willemse, 1969). Most of the chromitites occur in this zone and have been described in detail by Cousins and Feringa (1964) for the western Bushveld, and by Cameron and Desborough (1969) for the eastern Bushveld.

The Critical Zone is particularly noted for its easily visible parallel layered structure, the layers behaving like stratigraphic units traceable over many miles, even layers of a few centimetres thick. This remarkable continuity of the layers and the reliance that can be put on it has made the exploration of the economic horizons a relatively easy task, especially as the layers have not undergone any deformation, except for some major regional faulting. The layers range from less than a centimetre to many metres in thickness, with gradational and sharp boundaries between them. In some parts of the sequence a distinct separation plane is present, as between the Bastard Reef pyroxenite and the underlying mottled anorthositic norite at Rustenburg mine. Other sharp breaks appear to be disconformities marked by an irregular contact, as at the base of the Merensky Reef pyroxenite at Rustenburg where the Reef pegmatitic pyroxenite rests on an undulating anorthosite surface.

Cameron and Desborough (1969) record numerous disconformities in the eastern Bushveld which "are extensive over distances of miles and marked by scour and other features indicative of erosion, by abrupt changes in rock type, or by changes in composition of one or more phases" during magmatic sedimentation. The intensity of the layering was illustrated by them in the north-eastern Bushveld where 160 distinct layers occurred over a thickness of 12 m.

The visible layering is produced by differences in cumulate phases, intercumulus phases, phase proportions and in texture, giving rise to various field descriptive terms like anorthosite, spotted anorthosite, mottled anorthosite, spotted anorthositic norite, pegmatitic pyroxenite, chromitite, spotted mottled anorthositic norite etc. Although parallel layering is by far predominant 'crossbedding' features do occur. Also large scale unconformable relationships occur as in the case of the 'pots' at Rustenburg mine where, in extreme cases, the Bastard Reef, lying some 12 m above the Merensky Reef, dips downward through the layering and rests directly against it, forming a marked inclined separation plane. Koppies are another example of an unconformable relationship between the Merensky Reef pyroxenite and its footwall anorthosite. Features like this may be indicative of magmatic convection currents but an alternative explanation is given later by the author.

A further feature of the Critical Zone is the existence of a rhythmic sequence of magmatic sedimentation creating a series of units, each commencing with a chromite seam displaying a sharp lower contact and passing upwards into pyroxenite and then into more anorthositic rocks. The next unit begins again at a chromitite seam.

The ideal rhythmic unit is often terminated by the start of another one. It is possible that this broad rhythmic pattern is a result of intermittent surges of magma into the chamber, each new surge triggering a new differentiation sequence and producing a repetition of the previous one. A further mechanism suggested by Lauder (1964) may also have operated by which layers of magma were isolated from each other in the chamber by the formation of 'rafts' of cumulate crystals at various levels.

The cryptic compositional variations have been studied to some extent (Cameron & Desborough, 1969), but more research needs to be done in this field to provide a more fundamental picture of the magmatic differentiation process for this body. A generalised picture of the compositional trends of plagioclase, orthopyroxene, and olivine through the whole mafic zone was summarised by Willemse (1969) from various sources from 1934-1956. The trends (fig.1.3) do indicate that the Mafic Zone is compatible with a layered sequence produced by progressive differentiation of an intrusive mass. However, the occurrence of periodic surges of new magma is considered an important factor in explaining breaks in the sequence.

1.1.6 The Merensky Reef is a horizon of platiniferous feldspathic pyroxenite containing disseminated Fe-Cu-Ni sulphides and situated at or near the top of the Critical Zone. The term Merensky Horizon or Merensky Suite is often used to describe the whole pyroxenite horizon, and Merensky Reef is used to describe that part which is mined. In most places the pyroxenite is in part pegmatitic. At Rustenburg and Union mines the lower part of the Merensky Horizon is pegmatitic and delimited by a thin chromite band at the base and

top. At these mines the platinum group metals are concentrated in the pegmatitic facies and associated chromite bands, although at Union mine, where the pegmatitic pyroxenite is up to $5\frac{1}{2}$ m thick, only the top part is of economic grade. Some of the finer grained hanging-wall pyroxenite is included during mining. The Merensky Horizon forms a generally traceable layer of varying character which has been located and followed round most of the Mafic Zone. There are, however, numerous other platiniferous pyroxenite horizons below the Merensky Horizon, and most of the chromitite horizons contain values of up to 2 ppm of platinum group elements. Some of the pyroxenite horizons are very close to being of economic grade. Any genetic explanation of the concentration of platinum group metals in the Merensky Reef must, therefore, embrace these other occurrences. Unfortunately the economic importance and extensive exploitation of the Merensky Reef has led to an unjustified emphasis of its geological uniqueness, and has given rise to unique explanations for its origin. It is considered that magmatic differentiation and fractional crystallisation of interstitial platiniferous base-metal sulphide liquid adequately accounts for the minerals and textures that can be seen. Residual hydrothermal fluids would naturally be derived, from which some platinum group mineral precipitation would take place.

The Merensky Reef is being exploited at Rustenburg Mine which is still the World's largest individual platinum producer, and occupies a strike length of about 30 km. Other producing areas (fig. 1.1.) include the Bafokeng Mine near Rustenburg, the Western Platinum Mine (Alpha Mine) in the Brits area, the Union Mine near Northam, and the Atok Platinum Mine in the Lydenburg district. The

Amandelbult Mine, situated 30 km NE of Union Mine, is still in the development stages.

1.2 Discovery and Development of the Merensky Reef

1.2.1 The Discovery of the Merensky Reef in 1924 was a climax to a series of discoveries of platinum group elements (PGE) in the area, which commenced with investigations into the presence of these elements in the chromitite layers by Hall and Humphrey of the Geological Survey, and independently by Merensky and Von Dessauer. Results of these investigations published in 1908 indicated the presence of platinum group elements, particularly platinum, in sub-economic amounts. In 1923 Adolph Erasmus located a platiniferous lode deposit in the Rooiberg felsite of the Waterberg District. This was mined until 1926. In 1924 discoveries of alluvial and eluvial 'platinum' in the eastern Bushveld by Lombaard, a prospector-farmer, and Dr. Hans Merensky led to a primary source in a dunite pipe on Mooihoek 147. In September 1924 Lombaard located 'platinum' in a pyroxenite in the Lydenburg district, which was first called the Lombaard Reef and later changed to Merensky Reef in honour of Merensky who was mainly responsible for the success of the prospecting programme. Under his guidance the Merensky Reef was later located in the Potgietersrust area, and also in the Rustenburg district where it is at its richest, and in the equally important location just north of Northam. The Merensky Reef was soon traced

---

Footnote

The abbreviations PGE for platinum group element(s), and PGM for platinum group mineral(s) will be occasionally used in this thesis. Introduced by Cabri (1972), and now internationally accepted by Commission on New Minerals and Mineral Names.

round most of the Mafic Zone, and other occurrences of platiniferous dunites of the Mooihoek type were also found and exploited at Onverwacht 330 Mine and Driekop Farm Mine, about five km north of Mooihoek, by about 1928. At the same time sub-economic platiniferous pipes of disseminated, poikilitic, and solid sulphide ore were found in the Rustenburg district on the farm Vlackfontein 902 and also in the Marico district WNW of Vlackfontein (Wagner 1924); further indications of similar deposits were found north of Pretoria.

1.2.2 The Early History of Development of the primary platiniferous deposits, especially the Merensky Reef, is well documented (Beath, Cousins and Westwood 1961). Immediately on the discovery of these deposits, a short-lived mining boom took place as numerous mining companies began to work them. This was followed in the late 1920's by a slump as the price of platinum fell rapidly. Out of this situation two mining companies, namely the Potgietersrust Platinums Ltd. and the Waterval (Rustenburg) Platinum Mining Company, survived and merged to form Rustenburg Platinum Mines Limited in 1932 to work the Merensky Reef in the Rustenburg district. The Merensky Reef outcrop on Swartklip farm near Northam was later worked by the Union Platinum Mines Company which was formed in 1947, and which by 1949 had amalgamated with the Rustenburg Company. The Swartklip development now constitutes the Union section of the Rustenburg Platinum Mines Limited. For eighteen years Rustenburg and Union mines were the only producers of PGE in the Bushveld and produced approximately 40% of the World's platinum. In September 1967 the Union Corporation confirmed that an exploration programme on the Bafokeng area NW of Rustenburg had proved the Merensky Reef

there to be satisfactory for exploitation. A lease for the mining rights was obtained, and in November 1968 Impala Platinum Ltd. was formed with Union Corporation holding 46.75% of the equity and UC Investments 11.69%. Following development of the Bafokeng mine on the farm Vaalkop, concentrates were first produced in January 1969. This mine, with its two other Wildebeestfontein sections is now the second largest primary PGE producer in the World. In 1970 the Lonrho group, after drilling an area between Brits and Rustenburg, began shaft sinking operations on the farms Wonderkop and Middalkraal at Marikana near Brits. In August 1970 Lonrho Ltd. joined with Falconbridge Nickel Mines Ltd. and Superior Oil Company of Housten, Texas to develop this area under the subsidiary Western Platinum Ltd. Milling of ore from the now named Alpha Mine (Western Platinum Mine) started in 1971 with the shallower Middelkraal section and has now extended to the deeper Wonderkop section. In late 1970 the Atok Platinum Mine was established in the Lydenburg district on the farm Middelpunt by Atok Mines, a subsidiary of African Triangle Mining, Prospecting and Development Co. (Pty) Ltd., and administered by the Anglovaal group.

1.2.3 Mining of the Merensky Reef is generally on the herringbone system down dip, with a stoping width of about 74cm. Ore is trammed from the face to central winzes via tracks(drives) spaced at about 12m intervals. The ore is then moved by scrapers to ore passes connected to the main footwall haulage drives from where it is trammed to the main ore pass at the shaft or up main inclines to the surface. Rustenburg and Union Mine 'heavy' concentrates from the corduroy tables go to James tables for the recovery of the PGM ('metallics')

which are despatched direct to the refinery at Wadeville near Johannesburg. The remainder goes through conventional flotation processes and the resulting sulphide concentrate is smelted to converter matte. This is sent for the extraction of nickel and copper to Matte Smelters Ltd. at Rustenburg. Johnson and Matthey and Company has a 50% interest in this company. The matte is roasted and leached with sulphuric acid which dissolves the nickel and copper. These by-products are then extracted from the solution by electrolysis and the sludge treated to produce a product containing about 60% PGE plus gold. Further refining is carried out at Wadeville, which has been in operation since late 1969, or at Johnson Matthey's refinery at Brimsdown in Great Britain. For the Western Platinum Mine's concentrates the Kristiansand plant in Norway is used. The concentrates from Bafokeng mine are refined at Springs at a refinery completed in mid-1969 on the site of East Geduld Mines. The PGE from this mine are marketed by Ayrton Metals. Impala Platinum Ltd. also controls Metallurgical Processes Ltd. who process the nickel and copper by-products into alloys.

1.3 Ore Minerals of the Merensky Reef.

The petrology of the Merensky Reef, particularly with regard to the occurrence of the PGE and PGM, has been the subject of extensive investigations over the last ten years by research mineralogists working for the various mining companies exploiting this orebody. The incentive came from the increasing demands of the industrial processors and metallurgists to understand the mineralogy precisely, both from the need to reduce losses in the tailings, and from the problems arising from the production of the refined metals

from the mineral concentrates and smelter mattes. The decision by the mining companies to form PGE research groups was aided by their eventual realisation of the value of the electron-probe microanalyser in this field and that it was an essential analytical tool to possess. However, these companies have been reticent about allowing the publication of their results. Although earlier reports on the silicate-oxide and base-metal sulphide petrology of the Merensky Reef have appeared (van Zyl, 1970; Liebenberg, 1970), it is only within the last two years that some of the PGE data has become available with the publication of the results of mineralogical investigations at the Atok Platinum Mine by Schwellnus et al (1976), the Western Platinum Mine (Alpha Mine) by Brynard et al (1976), and, for the properties in general of the Johannesburg Consolidated Investment Co. Ltd., by Vermaak (1976), and Cousins and Vermaak (1976). Until this 1975-76 outburst, the first and last published electron-probe and quantitative microscopic study of the PGM of the Merensky Reef was by the author in 1966.

Before the discovery of platiniferous deposits in the Bushveld during the period 1923-1928 a number of the PGM which were to be later found in the concentrates from these deposits, had already been described from other parts of the world. Sperrylite $PtAs_2$ had been found in the Vermilion mine at Sudbury and described by Wells and Penfield in 1889. Laurite RuS_2 had been recorded from the platiniferous gravels of Borneo by Wohler in 1866 and also from Colombia. Native platinum, generally alloyed with iron, was well known by 1923 since its occurrence was first described from the river gravels in Colombia in 1748, although the actual recognition of

platinum as an element occurred in 1750 mainly through the work of Professor Wollaston. The first concentrates obtained from the Bushveld were, therefore, assumed to contain mostly native platinum, but mineralogical and chemical studies of the concentrates from the various deposits revealed other mineral phases to be present.

Sperrylite was the first other phase to be found, besides ferroplatinum, as bright metallic specks in a concentrate obtained by panning the oxidised sulphide ore from one of the nickel-sulphide pipes on the Vlackfontein farm 902 in the Rustenburg district in 1923. These grains were confirmed as sperrylite by Wagner and Rogers (Wagner 1924). Crystals of sperrylite in crushed zones of banded ironstone underlying the norite were also described from the Waterberg district by Spencer (1926), and later, large octahedral and pyritohedral crystals up to 1.85cm. across were found in the Potgietersrust district (Wagner 1929). The crystals from both these districts were confirmed as sperrylite and studied by X-ray techniques by Bannister and Hey (1932). By 1929 sperrylite had also been confirmed as occurring in the Merensky Reef in the Lydenburg and Rustenburg districts.

The first new mineral to be found was cooperite PtS which was located in the concentrates from the Rustenburg district by Cooper in 1928. Confirmatory tests and analyses were carried out by Adams (1931) and the crystal structure of cooperite determined by X-ray techniques by Bannister (1932). Another new mineral, stibiopalladinite Pd_3Sb, was found in the contact metasomatic and pegmatitic deposits of the Potgietersrust district and was described by Adam (1927). More recent studies (Clark, *et al.* 1974) suggest the com-

position Pd_5Sb_2. In 1932 Bannister confirmed laurite as being present in concentrates from the Potgietersrust area, and also discovered a new mineral braggite (Pt,Pd,Ni)S in material collected by Cooper from the Rustenburg district. This was the first new mineral to be isolated and determined by X-ray methods.

It was not until 1961 before any further new minerals were found, although a geochemical study of the Pt, Pd, and Au contents of the igneous rocks of the Bushveld had been completed by Hagen in 1954. Then, with the advent of the electron-probe microanalyser, Stumpfl (1961) found and analysed nine new platinoid phases - geversite $PtSb_2$, PtSb, Pt(Sb,Bi), $(Pt,Ir)As_2$, $Pt(Ir,Os)_2As_4$, Pd_2CuSb, Pd(Sb,Bi), Pd_8CuSb_3, and $Pt_4Sn_3Cu_4$ - in concentrates from the Dreikop mine, followed by the mineral hollingworthite $(Rh,Pt,Pd)(As,S)_2$ in 1965 from the same locality. At this time the author (1966) discovered four platinum and palladium bismuthotellurides in the Merensky Reef at Rustenburg and Union mines. Two were new minerals, namely merenskyite $(Pd,Pt)(Te,Bi)_2$ and $(Pd,Hg)_x(Te,Bi)_y$, and two, moncheite $(Pt,Pd)(Te,Bi)_2$ and kotulskite Pd(Te,Bi), constituted a second reported occurrence in the world, having previously been found in the Monchegorsk deposit by Genkin et al (1961, 1963).

No additional minerals were reported in the Bushveld until 1975 when rustenburgite $Pt_{0.398}Pd_{0.386}Sn_{0.217}$ and atokite $Pd_{0.486}Pt_{0.302}Sn_{0.212}$ were described by Mihalik et al. in concentrates from the Merensky Reef, and stumpflite Pt(Sb,Bi) and irarsite IrAsS from the Dreikop pipe by Tarkian and Stumpfl. These were followed by paolovite Pd_2Sn from the Atok Mine in 1976 by Schwellnus et al. Irarsite and paolovite had been described previously by

Genkin et al in 1966 and 1974 respectively. Schwellnus et al also mentioned the occurrence of an As-Sn-Pd and an Sb-As-Pd intergrowth.

1.4 Aims of the Thesis

Prior to the initiation of the author's investigations in 1962, the silicate petrology and to a lesser extent the structure of the Merensky Reef at Rustenburg and Union mines had been described satisfactorily by various workers such as Wagner (1929), Schmidt (1952), and VanZyl (1960). However, studies of the opaque mineralogy, particularly the PGE and PGM and their mode of occurrence, left ample scope for further work. Developments in determinative techniques, such as the electron-probe microanalyser, had provided an incentive to mineralogists to research into the mineralogy of platiniferous ores and, in the author's case, to re-examine the Merensky Reefwhose opaque mineralogy had not been examined since the pioneering ore microscopic study by Schneiderhohn (1929). Up to 1962 the PGE in these ores had only been recognised as occurring in a relatively small number of platinum group minerals. The platinum mineralogy was generally thought to be fairly simple, consisting of five or six major minerals together with a large proportion of the PGE content accounted for by Schneiderhohn as occurring in solid solution in the base metal sulphides, pyrite, pyrrhotite, pentlandite and chalcopyrite. However, workers on other platiniferous deposits, in particular Stumpfl on the Dreikop pipe (1961), Borovski et al (1959) and Genkin et al (1961, 1963) had described a large number of new platinum group minerals. It was thus reasonable to suspect that many of these phases, together with other unreported PGM were present in the Merensky Reef. An important aim then was to locate

and describe fully the mode of occurrence of any new phases as well as phases previously reported in the literature. In the initial stages of this study all the previously reported PGM from this deposit were recognised as well as a number of other phases, the most important of which were the platinum and palladium bismuthotellurides (Kingston 1966). Two of these bismuthotellurides were new minerals. Since 1966 other workers on the Merensky Reef have reported a further three new but very rare PGM phases (Mihalik et al 1975; Schwellnus et al., 1976).

One particular aim of this thesis, therefore, is to report on and critically assess the present state of knowledge of the composition and properties of the platinum group minerals in the Merensky Reef, particularly in the Rustenburg and Union mine sections. Where published data was already in existence then this is supplemented and discussed on the basis of the author's own results and experiences. Although there have been many determinative studies made of platinum group minerals in other deposits, particularly since 1961, there is still much to be done to define known phases more precisely in terms of structure, composition and compositional variations, their respective compositional systems, and their compositional and structural relationships with their physical and optical properties. Also from a consideration of the geochemical character of these elements many more new phases are still to be discovered.

The form and mode of formation of intergrowths of the platinum group minerals with each other and with the commonly associated base-metal sulphides, and also the significance of these inter-

growths as regards the genesis of the orebody, are obvious sources of disagreement amongst PGE researchers. Therefore, a further contribution in this study is to describe and offer an explanation of the mode of intergrowth of these minerals as exhibited in polished sections of the ore and concentrates, and to discuss their significance with regard to PGE geochemistry and ore genesis.

The geochemistry of the platinum group elements is still far from being completely understood, particularly with regard to their 'inclusion' in the lattices of silicate and oxide minerals. Geochemical data on the platinum group elements in the Mafic Zone has not been substantially added to since Hagen's study (1954), although some new data on the partitioning of these elements in the Merensky Reef have recently been reported by Crocket (1976). Chapter 9 introduces and discusses what is known about their geochemical behaviour, in particular the evidence for their separation during the genesis of the Merensky Reef.

Finally it should be noted that the descriptions of the nature and structure of the Merensky Reef at Rustenburg and Union mines are based on personal observations during a period of ten weeks of sampling and underground mapping at these mines in 1962.

CHAPTER 2

STRUCTURE AND PETROLOGY OF THE MERENSKY REEF AT RUSTENBURG AND UNION MINES

2.1 Introduction

The first description of the petrology and structure of the Merensky Reef was by Wagner (1929) who provided valuable data on this platiniferous pyroxenite at its early stage of exploitation, including the present Rustenburg and Union mine areas. His objective descriptions still make up a valuable reference on this subject and include much data and conclusions which have often been overlooked by others in this field in more recent years. Schneiderhohn (in Wagner, 1929) was the first to study and describe the nature and paragenesis of the base-metal sulphides, and to attempt to examine the platinum group minerals in polished sections of the ore. His report is still a useful reference, although the only other mineralogical report on the base metal sulphides of the Bushveld Complex in general by Liebenburg (1970) has largely superseded it. Since 1929 several accounts of the petrology and structure of the Merensky Reef at Rustenburg and Union mines, particularly at Rustenburg mine, have been published. Schmidt (1952) provided, in addition to Wagner, petrological descriptions of the various rock units at Rustenburg mine, which included a detailed comparative study of the orientation of the orthopyroxenes and feldspars composing the normal undisturbed Merensky Reef with those of the potholes. Van Zyl (1970) carried out an even more comprehensive petrological study at Union mine. Legg (1967,1969) completed an electron-probe microanalyser and X-ray dif-

fraction study of the UG1 chromite seam, and the chromite bands of the Merensky Reef at Rustenburg mine. General accounts of the composition and structure of the Merensky Reef have been provided by Cousins (1964,1969) and Beath, Cousins, and Westwood (1961).

Recent papers specifically on the Merensky Reef by Vermaak and Hendriks (1976), Vermaak (1976),Schwellnus et al (1976), and Brynard et al (1976) provide further data on the structure and silicate-oxide mineralogy as introductory parts to their treatment of the economic and genetic aspects. Vermaak and Hendriks provide a particularly useful condensation of petrological data, which includes information from an unpublished company report by Ramsden and Wilmshurst. The general structure and composition of the Mafic Zone in the western Bushveld is adequately covered by Feringa (1959), Cousins and Feringa (1964), Coertze (1970), and Vermaak (1970,1976), together with the various review papers already mentioned in the introduction. These papers include the broad structural and stratigraphical aspects of the Merensky Reef.

There is still a lack of uniformity in the use of the several available terms for describing the economic platiniferous horizon near the top of the Critical Zone. An example of the present confusion is the term 'Merensky Reef' itself which was originally used to describe the first discovery of this horizon at Lydenburg, where no pegmatitic layer was present and the platinum-metal carrier was a medium grained pyroxenite. Wagner (1929) reported the upper part of this pyroxenite horizon as being "platinum-bearing Merensky Reef" and the lower portion as being "platinum-poor or barren Merensky Reef". A coarse pegmatitic pyroxenite was later found to

be the principal PGE carrier in the Rustenburg area, but the term 'Merensky Reef' was still retained for the platinum-poor overlying finer grained pyroxenite. During the period when Rustenburg and Union mines were the only working mines, the term 'Merensky Reef' became established as describing the whole pyroxenite horizon, and during the authors visit in 1962 the pegmatitic pyroxenite was referred to as the 'Reef' pyroxenite, and the overlying finer grained pyroxenite as the 'Merensky' pyroxenite. Underground the term 'Merensky Reef' was naturally also used for that part of the pyroxenite being mined, as for example at Union mine where only the central part of the whole pyroxenite horizon is being mined (fig.2.1). The use of this term for the whole thickness of pyroxenite has also been adopted at Atok mine (Schwellnus et al, 1976) and at Western Platinum mine (Brynard et al, 1976). Unfortunately Vermaak and Hendriks (1976) have caused further confusion by redefining the "economically valuable pegmatoidal layer" in the Western Bushveld as the Merensky Reef. To avoid confusion in this thesis the terms to be used in describing this horizon are as follows.

Merensky Unit or Merensky Suite refers to the layered succession extending from the footwall contact of the Merensky Reef up to the footwall contact of the Bastard Reef. The succession (fig. 2.1, 2.2, 2.3) begins with a platiniferous pyroxenite layer containing two or more thin chromitite bands, which grades upwards into norite, spotted anorthosite (spotted leuconorite) and finally into mottled anorthosite (mottled leuconorite). The Bastard Reef is the basal pyroxenite member of a similar but thicker sequence which extends to the Main Zone contact, and which makes up the

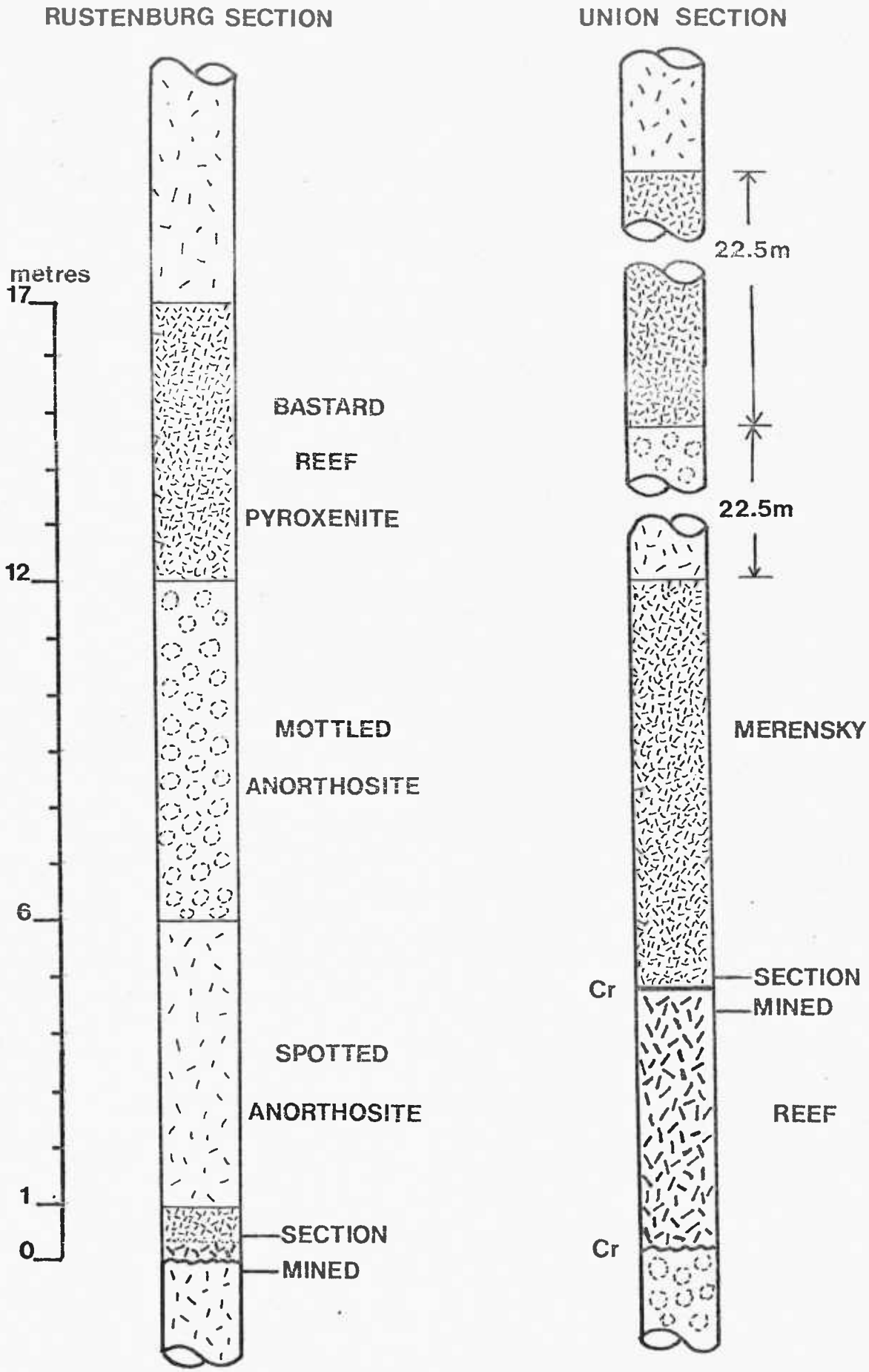

Fig. 2.1 Geological sections through the Merensky Unit at Rustenburg and Union mines, showing the difference in thickness of the Merensky Reef and the ore sections which are being exploited.

Bastard Unit or Suite.

The Merensky Reef or Merensky Horizon are synonymous terms to describe the basal pyroxenite layer of the Merensky Unit, which is usually underlain by 'light' anorthositic rocks, particularly spotted and mottled anorthosites. This layer is platiniferous, although usually only part of it is of economic grade. In the western Bushveld about 40% of this pyroxenite layer is usually very coarse and pegmatitic (fig.2.1). However, at Western Platinum mine there is a rapid decrease in this pegmatitic proportion from 40% to 10% or less in going from west to east across the property (Brynard et al., 1976). At Atok mine in the eastern Bushveld (Schwellnus et al., 1976) a pegmatitic pyroxenite layer forms about 25% of the Merensky Reef and occurs towards the top. Contrary to common belief the pegmatitic pyroxenite component (s) of the Merensky Reef is not always the main platinum-metal carrier. Although it is true for much of the western Bushveld, in the eastern Bushveld the pegmatitic pyroxenite is more noted for being barren. Concentration of PGE is far more related to thin chromitite bands in the Merensky Reef, as shown later in chapter 3. Two or three of these bands may occur, one of which is invariably at or close to the basal contact in the western Bushveld.

2.2 The Merensky Reef at Rustenburg Mine

2.2.1 The Hanging Wall and Foot Wall Rocks of the Merensky Reef as exposed in the mine are illustrated in figures 2.2 and 2.3. A considerable amount of the uppermost part of the Critical Zone is exposed in the various crosscuts in the mine, and a good section from the Merensky Reef to the start of the Main Zone, and from the

Fig.2.2 RUSTENBURG MINE SECTION

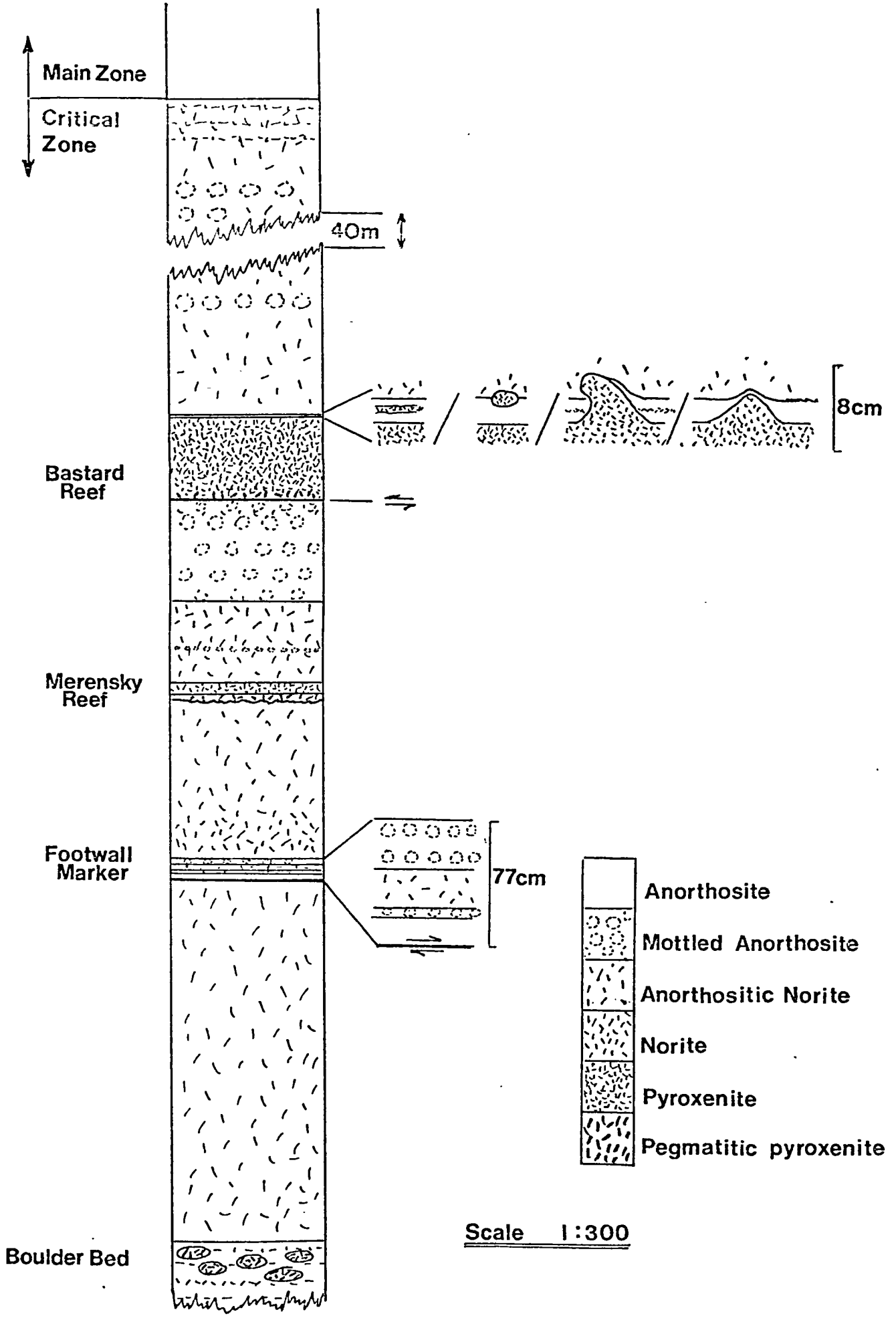

Fig. 2.3a Geological section along 12 Level X-cut, Rustenburg Mine, showing the nature of the Footwall Rocks from the lowest exposed 'Boulder Bed' to the 'Footwall Marker'. Scale 1 : 200.

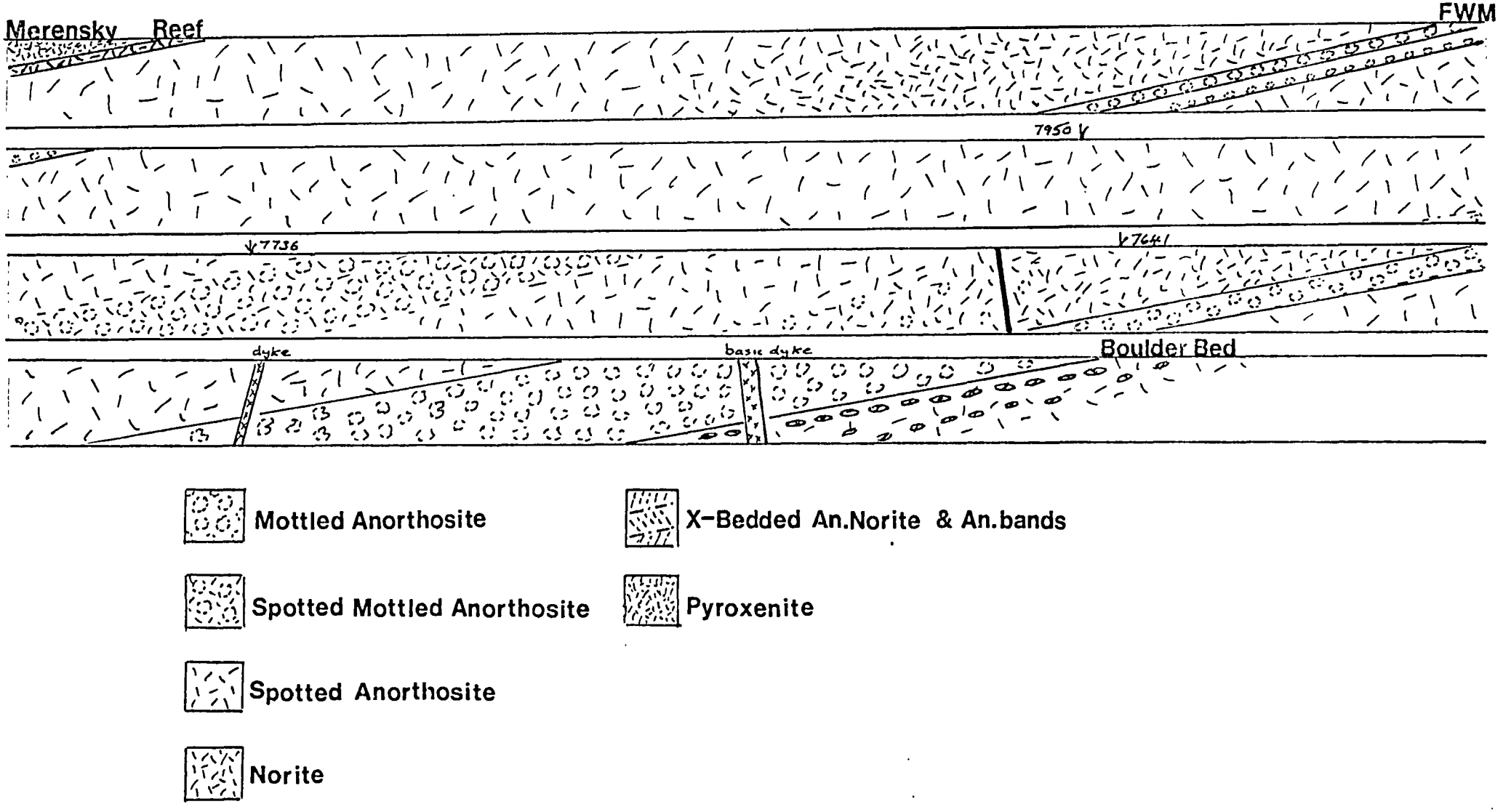

Fig. 2.3b Geological section along 8 Level X-cut, Rustenburg Mine, showing the nature of the Hanging Wall Rocks from the Merensky Reef to the base of the Main Zone. Scale 1 : 200.

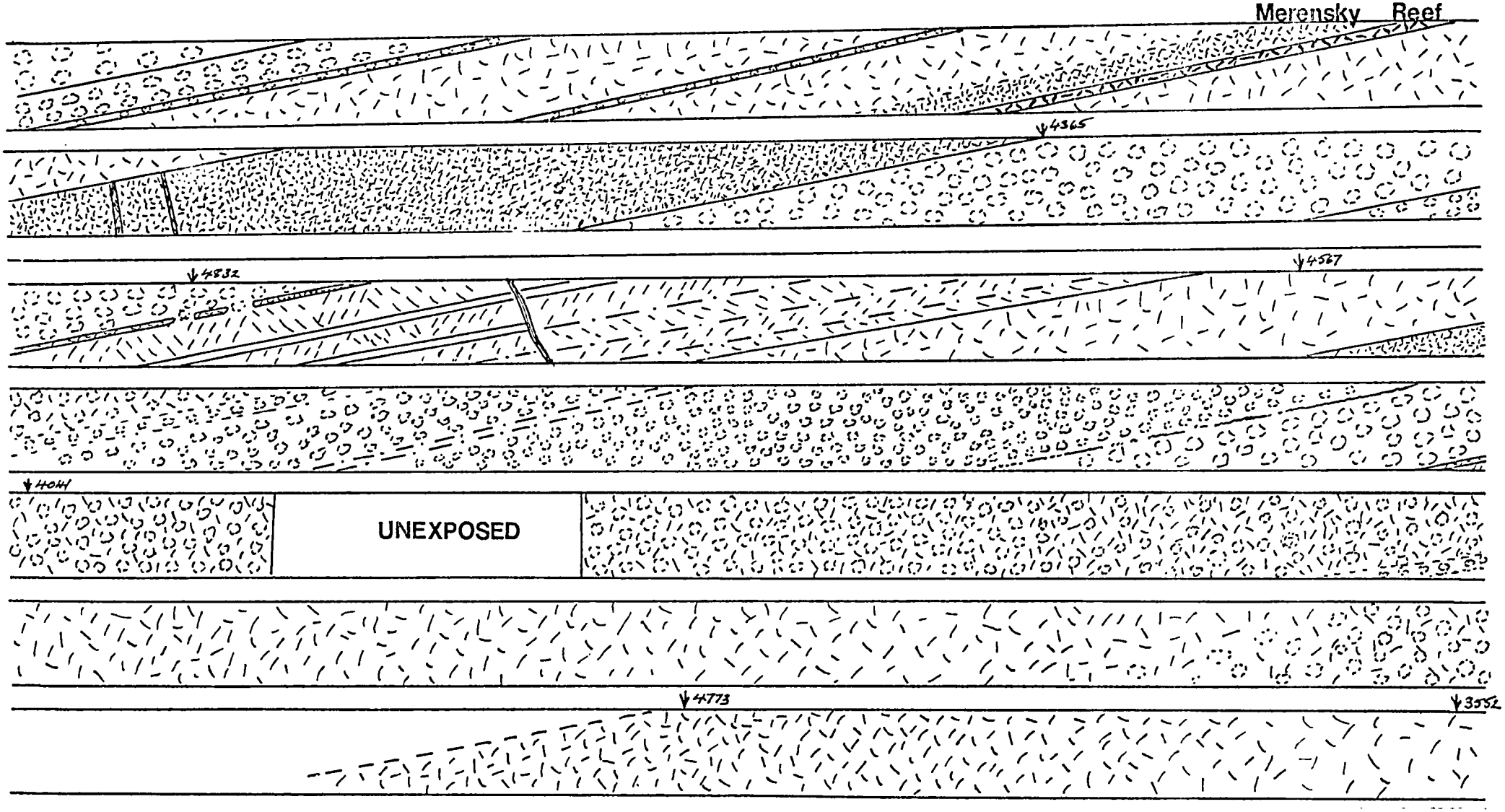

'footwall marker' to the 'boulder bed' was mapped along 8-Level Crosscut South (fig.2.3b), and 12-Level Crosscut North (fig.2.3a) leading off from the Central Deep shaft. This provided an accurate picture of the field appearance and thickness values of the various components of the Merensky Unit and Bastard Unit. A simplified diagrammatic section showing the position of the Merensky Reef relative to other prominent horizons in the mine is given in figure 2.2. The whole succession dips north at an average dip of $9\frac{1}{2}^{o}$. Local changes in this dip are brought about by structural features like pots and koppies which will be dealt with later together with other structural aspects.

The Boulder Bed is probably equivalent to the 'pseudo reef' in the footwall at Union mine, and may represent a partly formed or disrupted pyroxenite horizon at the base of another differentiation unit. The 'boulders' consist of oblate Reef-like pyroxenite masses containing some disseminated peripheral chromite which occasionally forms a weak concentration at their base. They are circular in plan but oval in vertical section, presumably as a result of compaction. They are enclosed by spotted and mottled anorthosite (fig.2.4).

The Footwall Marker is about 9m below the base of the Merensky Reef. This horizon is used to position the haulage ways. A prominent separation plane (fig.2.2) occurs at the base of this marker unit at the contact of a pure anorthosite layer with the underlying spotted anorthositic norite. Cousins (1969) and Barry (pers. comm. 1962) consider that between 6 - 9m of movement has taken place along this plane. A further marker horizon called the 'ten foot mar-

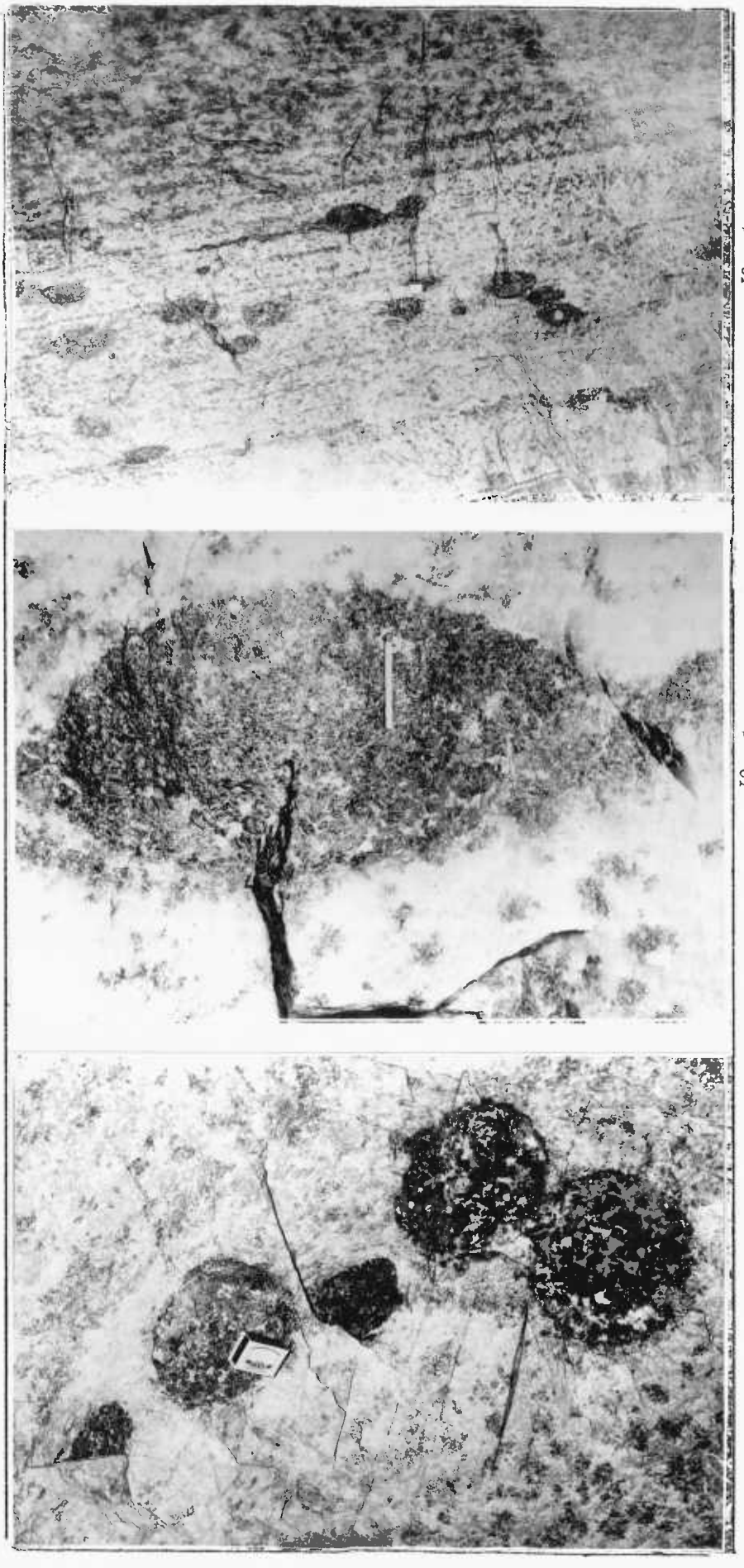

VERTICAL SECTION

VERTICAL SECTION

PLAN VIEW

Fig. 2.4 The Boulder Bed at Rustenburg Mine.

ker' occurs 3.3m above the footwall contact of the Merensky Reef, and is especially useful in mapping pothole structures and in determining the depth to which the downthrown Reef occurs in them.

Fig. 2.5 The Merensky Reef at Rustenburg Mine. This is an example of Normal Reef Facies showing the typical light footwall spotted anorthositic norite, the thin white anorthosite at the undulating contact with the basal chromitite band and Reef pegmatitic pyroxenite, and the overlying finer grained Merensky Pyroxenite. For scale see figure 2.6.

The Bastard Reef is a medium grained pyroxenite of 5m thickness. Its appearance is identical to the Merensky pyroxenite. A few centimetres thickness of the base is often pegmatitic, and some sulphides occur together with low platinum metal values. Sometimes a very thin discontinuous accumulation of chromite occurs at the base. A prominent separation plane filled with a 'mud seam' occurs at the basal contact with mottled anorthosite (fig. 2.2). The extent of the movement along this plane is not known, and even

where the Bastard Reef dips into a pothole this plane is often present. The nature of the top contact of the Bastard Reef is illustrated in figure 2.2, and suggests that it was still in a plastic condition when the overlying spotted anorthositic norites were forming. The top of the Critical Zone occurs about 57m above the Bastard Reef.

2.2.2 The Merensky Reef is variable in appearance throughout the property when examined in detail. These various forms can be classified into three types according to whether the Merensky Reef occurs at the normal reef-elevation in the mine (Normal Reef Facies), is downthrown below the level of the footwall contact by potholes (Pothole Reef Facies), or is elevated on or around footwall domes (Koppie Reef Facies).

(a) Normal Reef Facies accounts for most of the Merensky Reef in the mine and spatially corresponds to a plane which dips to the north at $9\frac{1}{2}^{o}$. Intersection of the Reef by the workings at the position of this plane gives rise to the term 'normal reef elevation'. Marked downward and upward deviations from this plane mainly occur in the area of potholes and koppies respectively. Normal Reef facies largely conforms to the structure and lithological arrangement illustrated in figures 2.5 and 2.6. At the base there is a thin chromitite band of variable thickness (as in fig. 2.6) which forms an irregularly dimpled or undulating and sharply defined contact with a thin pure anorthosite band, which grades rapidly into the footwall spotted anorthositic norite. It was observed, in agreement with Cousins (1969), that the majority (about 70%) of the 'rises' of this contact corresponded to a thickening of the bottom

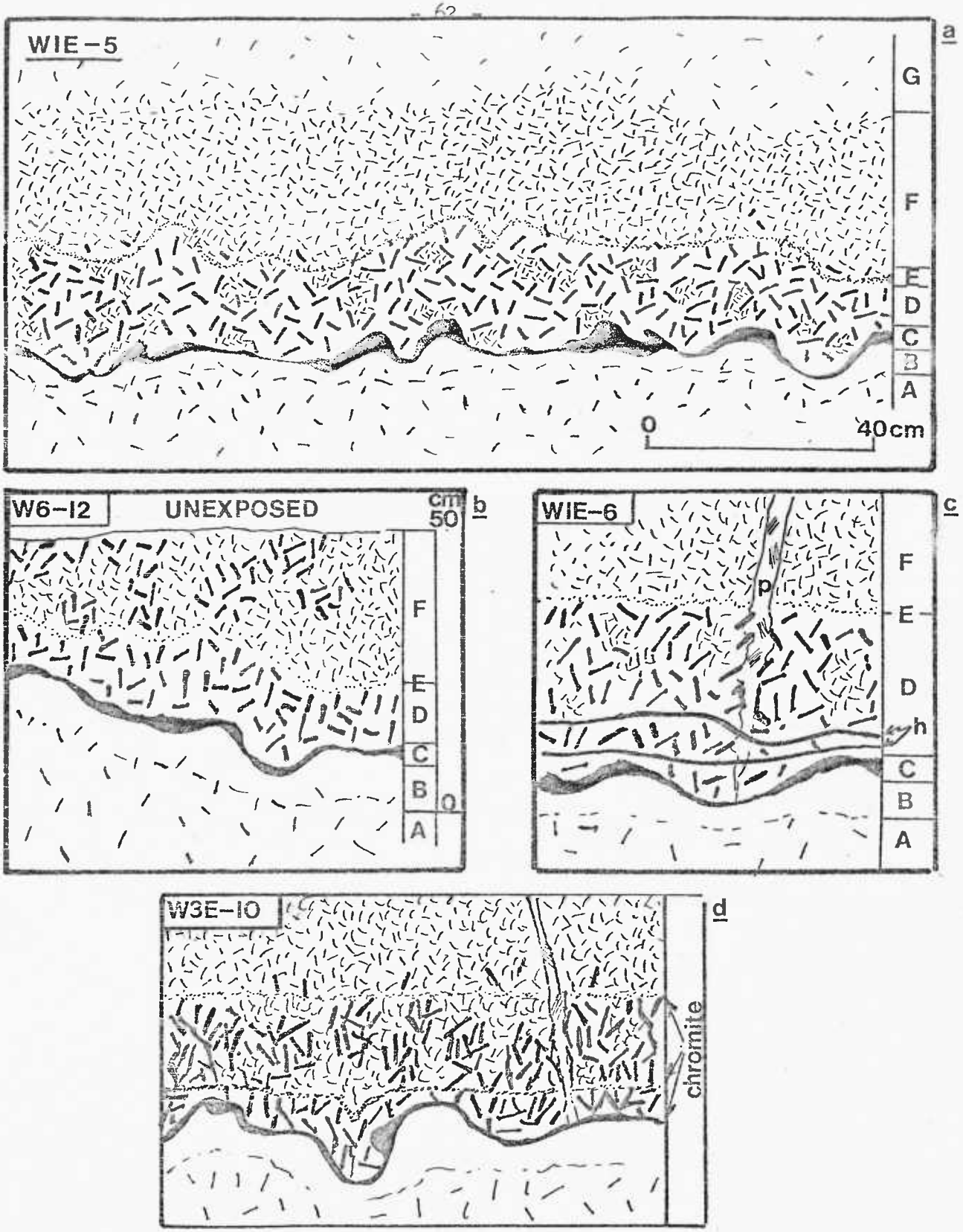

Fig. 2.6 Examples of Normal Reef Facies at Rustenburg mine, showing its structure and the relationships between the footwall spotted anorthosite (A), the thin white anorthosite (B), the basal chromitite band (C), the Reef pegmatitic pyroxenite (D), the top chromitite band (E), and the Merensky pyroxenite (F), grading into the hanging wall spotted anorthositic norite (G). Quartz-feldspar-mica veins (P). Scale 1 cm = 0.1 m.

chromitite band at their crests. The bottom diffuse contact of the thin (2-4cm) white anorthosite layer with the footwall spotted anorthosite usually undulates sympathetically with its sharp top contact with the chromitite, but with far less amplitude. The result is that the anorthosite is generally thicker in the cores of the 'rises'. Although discussed more fully later, it is considered that the Merensky Reef was formed on a still plastic cumulate crystal mush, and that the dimpled structure described above has been produced by a mechanism analogous to that for sedimentary load casts.

The basal chromitite band grades rapidly up into a coarse and partly pegmatitic feldspathic pyroxenite, commonly known as the 'Reef', which has an average thickness of about 18 cm, with a range of from 10 - 30 cm. The Reef is not all coarse and pegmatitic. A large proportion is composed of medium grained 'granular' Merensky-type patches (fig. 2.6) which are fairly evenly distributed throughout the Reef, and are often quite well defined from the pegmatitic material. The overall appearance is one of clots of pegmatitic pyroxenite in a matrix of finer grained pyroxenite. It is tempting to compare these clots with the pegmatitic pyroxenite aggregates in the Boulder Bed. This has been done by Vermaak (1976) who considers that coarse aggregates like these formed under the influence of volatiles within an isolated layer of magma, which had been confined above the present footwall by a floating anorthosite mat. He considers that these pegmatitic pyroxenite 'boulders' sank in the magma unit (from which the Merensky Unit was finally formed), dimpled the early-formed chromite layer and formed the basal Reef pyroxenite.

At the sometimes sharp contact or within the sometimes gradational contact of the Reef with the overlying less coarse Merensky pyroxenite occurs a very thin irregular and discontinuous chromitite band. This band becomes more pronounced and thicker as the margin of a pothole is approached and the contact between the Merensky and Reef pyroxenite is then very clearly defined by it (fig. 2.11). The Merensky pyroxenite is usually from 40 - 60 cm thick, and grades rapidly through norite to the hanging wall spotted anorthosite. Thus at Rustenburg mine the Merensky Reef is generally up to 1 m thick.

Variations from this typical section are to be found in the mine. In the Waterval section, to the extreme west of the property, the Merensky Reef contains a third 0.5 mm thick chromitite band in the centre of the Merensky pyroxenite (fig. 2.8). This band is bordered by Reef-like pyroxenite. The chromitite band at the Reef/Merensky contact is also very thick (1.3 cm) and persistent, whereas the bottom chromitite band is thin, and the undulations at the contact with the footwall are small. Figure 2.6d is a further example to the immediate east of the Waterval section where a third chromitite band occurs, in this case within the Reef.

Thin pegmatitic veins of dominantly quartz, brown mica, and feldspar, together with some sulphides, occasionally occur within the Merensky Reef as illustrated in figures 2.6 & 2.7. They strike roughly E-W and are nearly vertical to the layering. The veins wedge out towards the hanging wall contact and basal chromitite band, although in some cases a thin greyish line marks its continuation into the footwall (fig.2.7a). The walls of these veins are straight

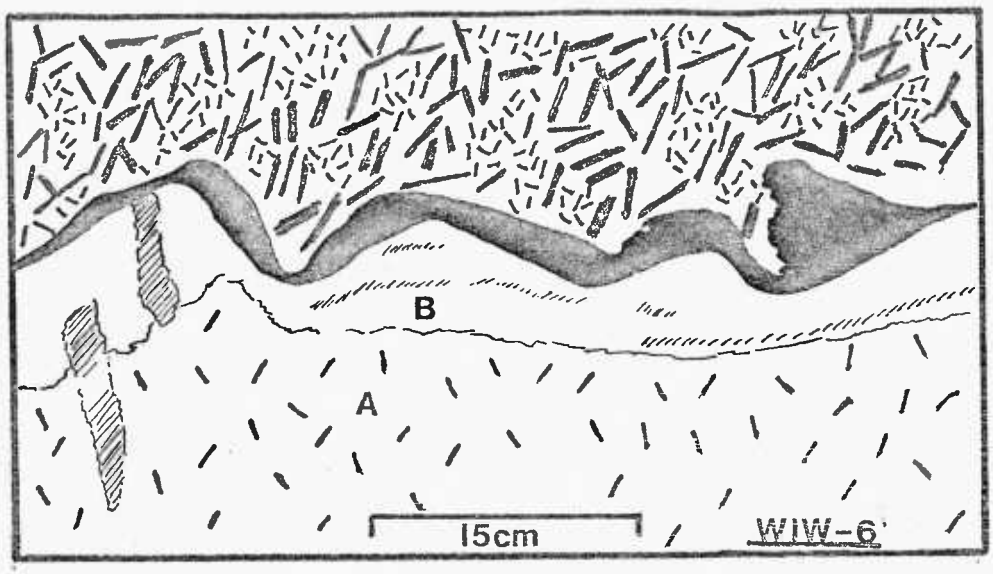

(a)

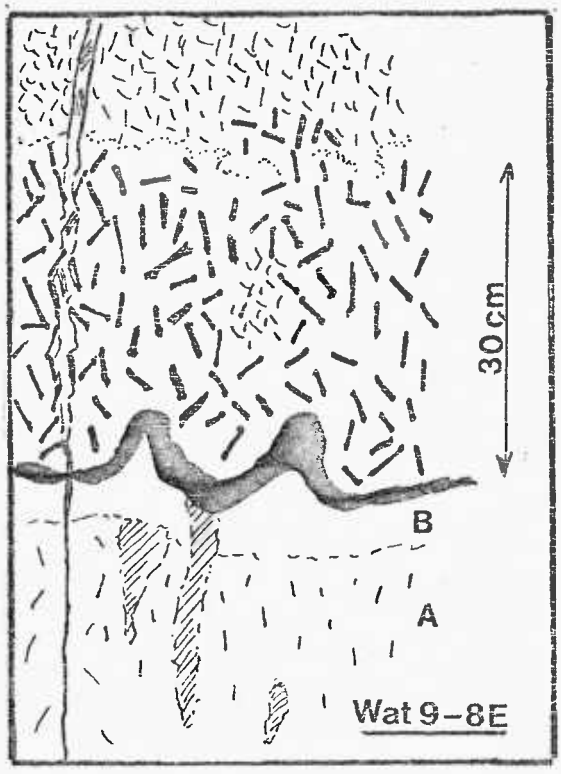

(b)

Fig. 2.7 Details of the footwall contact of the Merensky Reef at Rustenburg mine, showing the appearance of grey diffuse sulphide-bearing 'pipes' and 'layers' in the footwall white anorthosite (B) and spotted anorthosite (A). Figure 2.7b also illustrates the wedging out and continuance of a quartz-mica-feldspar pegmatitic vein into the footwall. Sulphide mineralisation at this locality was visible for approximately 60 cm below the basal chromitite band.

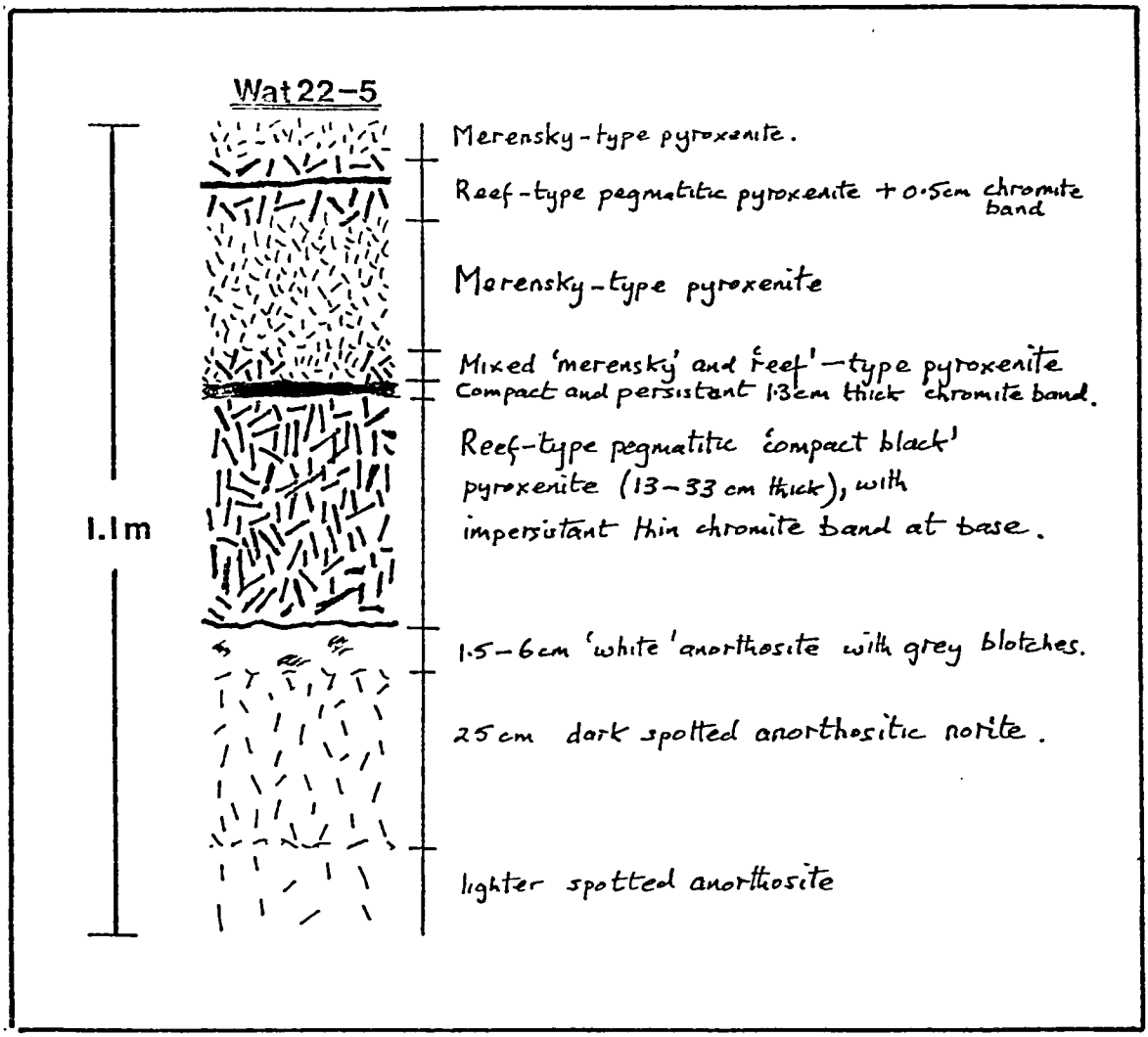

Fig. 2.8 A variety of Normal Reef Facies found in the Waterval Section of Rustenburg mine. The ore section exhibits three chromitite bands. Scale 1 : 10.

and sharply defined in the Merensky pyroxenite but become irregular and diffuse on passing into the pegmatitic Reef. Pegmatite patches of the same mineralogy as the veins are sometimes found within the Reef, isolated from the veins. Wagner (1929) considered these veins to be shrinkage cracks mineralised during the pneumatolytic stage of the crystallisation of the Merensky Reef. He also reported calcite, chlorite, serpentine, and one instance of fluorite in these veins. These type of veins appear to be characteristic of the pyroxenite layers, since similar ones occur and are restricted within the Bastard Reef pyroxenite.

Often the bottom half of the Reef pyroxenite is cut by long gently curving chloritic fractures ('h' in fig. 2.6c). As a result the Reef appears greenish and darker than the normal brown half above. These fractures lie in the plane of the Reef and provide no evidence of any lateral movement, even where they cut through some of the 'rises' of the chromitite/footwall contact, or the pegmatitic veins.

The visible Cu-Ni-Fe sulphide mineralisation extends from 43 cm below the footwall contact to 45 - 50 cm above. The sulphides occur within the Reef as disseminated interstitial aggregates of dominantly pyrite, pyrrhotite, pentlandite and chalcopyrite. The bulk of the platinum group metals occur within the Reef and basal chromitite band. The sulphide mineralisation is noticeably patchy, and concentrations of interstitial sulphides are particularly associated with the finer grained Merensky-like pyroxenite patches within the Reef, where presumably a greater total intergranular 'pore space' was available to localise the interstitial sulphide melt. Sulphide

mineralisation in the footwall corresponds particularly with greyish diffuse bands in the thin white anorthosite layer underlying the basal chromitite band, and with pipe-like areas projecting down from the chromitite band and within the footwall spotted anorthosite (fig. 2.7a & b). The layers usually conform to the undulations at the base of the Reef, although they are sometimes 'cut off' by them. The pipe-like areas are at right angles to the footwall contact and are often seen to start at it. Stope-wall sections of these 'pipes' presumably account for the apparantly isolated patches which decrease in size and number downwards. In the immediate vicinity of these patches the pyroxene spots of the anorthosite become diffuse. They are clearly related to the sulphide mineralisation in the overlying Merensky Reef.

One occurrence of a massive banded chalcopyrite-rich sulphide body of up to 2 m in diameter, and containing about 155 g/tonne of PGM, was exposed during the authors time at the mine. This sulphide pegmatite contained near its margin very large and perfectly formed pyroxene crystals, often with a core of sulphide. The margin was gradational into the Reef and Merensky pyroxenite but sharp against the footwall spotted anorthosite. In the latter case thin veins penetrated the rock but wedged out after about 20 cm. The body extended from the bottom of the Merensky pyroxenite to about 1.5 m into the footwall. Above the top contact the Merensky was rich in disseminated sulphides. A similar sulphide mass rich in pyrrhotite and poor in chalcopyrite and pentlandite was also exposed near the crest of a koppie-type structure, where intensive metasomatism of the Merensky Reef had taken place. This body was very poor

in PGM, assaying around 2-3 g/tonne.

(b) Pothole Reef Facies refers to the Merensky Reef where it occurs in circular to elliptical depressions which range from 15 - 100 m in diameter and 1 - 50 m in depth relative to normal reef elevation. These potholes can be catergorised into two types, namely 'Normal Potholes' which depress the Merensky Reef by 1 - 5 metres, and 'Bastard Potholes' which depress it by amounts of the order of 100 m, bringing the Bastard Reef pyroxenite down to or below normal reef elevation.

'Normal potholes' are by definition the most common by far, and miners follow the ore section into these and extract it without much problem. Typical sections through these pots as exposed in the winzes are illustrated in figures 2.9a & b, and map 1. The larger the diameter of these potholes the more likely is there to be secondary or even a tertiary pothole development within it, with a consequent greater depth to the whole structure. As the edge of a pothole is approached, the thin impersitent top chromitite band of the Normal Reef facies becomes thicker and marks the contact between the Merensky and Reef pyroxenite very clearly. At the edge the Merensky Reef suddenly dips downwards, and the pegmatitic Reef together with the top and bottom chromitite bands 'wedges out' and is cut off by the Merensky pyroxenite (figs. 2.10, 2.11, 2.9). Where the pothole sides are gently dipping the basal chromitite band may continue at the contact (fig. 2.9b, 2.10b), although the undulations are either not so prominent or not present at all. The thin white anorthosite layer is also absent. Sometimes the Reef pinches out, at normal reef elevation, several metres from the edge. In this

case the bottom chromitite band may persist to the edge of the pothole. The side contact of the pothole, where the Merensky pyroxenite rests directly on the footwall spotted anorthosite, may vary from being gently sloping to overturned and undercutting into the footwall. This contact is usually sharp but a gradational boundary may be found (fig. 2.10a). This figure also shows a case where the Merensky pyroxenite has undercut the Reef and footwall and isolated a remnant of the basal chromitite band.

On the floor of the potholes the Merensky Reef is still clearly recognizable, with pegmatitic Reef pyroxenite overlain by Merensky pyroxenite, and of a similar thickness to the Normal Reef facies. It similarly contains economic platinum-metal values together with disseminated sulphides. However, there are four significant differences which any theory for their origin has to explain. Firstly there is no white anorthosite band at the contact of the Reef with the footwall spotted anorthosite. Secondly there is no basal chromitite band, although there may be a top chromitite band. Chromite grains are, however, disseminated throughout the pothole Reef and clots and stringers of chromite may occur. Thirdly there are no small amplitude undulations at the footwall contact as at normal reef elevation. Fourthly the patches of non-pegmatitic pyroxenite in the Normal Reef are usually absent in the Pothole Reef. In one case the author recorded a section (fig. 2.11) of a pothole in which there was no pegmatitic constituent, and the Merensky pyroxenite rested directly on a gently undulating footwall contact. At the top of the 'rises' the thick bottom chromitite band and underlying white anorthosite was still preserved. Some minor faulting towards

Fig. 2.9 Two examples of Normal Potholes at Rustenburg mine. The Pothole Reef pyroxenite has no chromitite band at its base but a well developed chromitite band at its top contact with the Merensky pyroxenite. In the pothole chromite grains are disseminated throughout the Reef pyroxenite. A- Footwall spotted anorthosite. B - Reef pegmatitic pyroxenite. C - Merensky pyroxenite. D - Hanging wall spotted anorthosite.

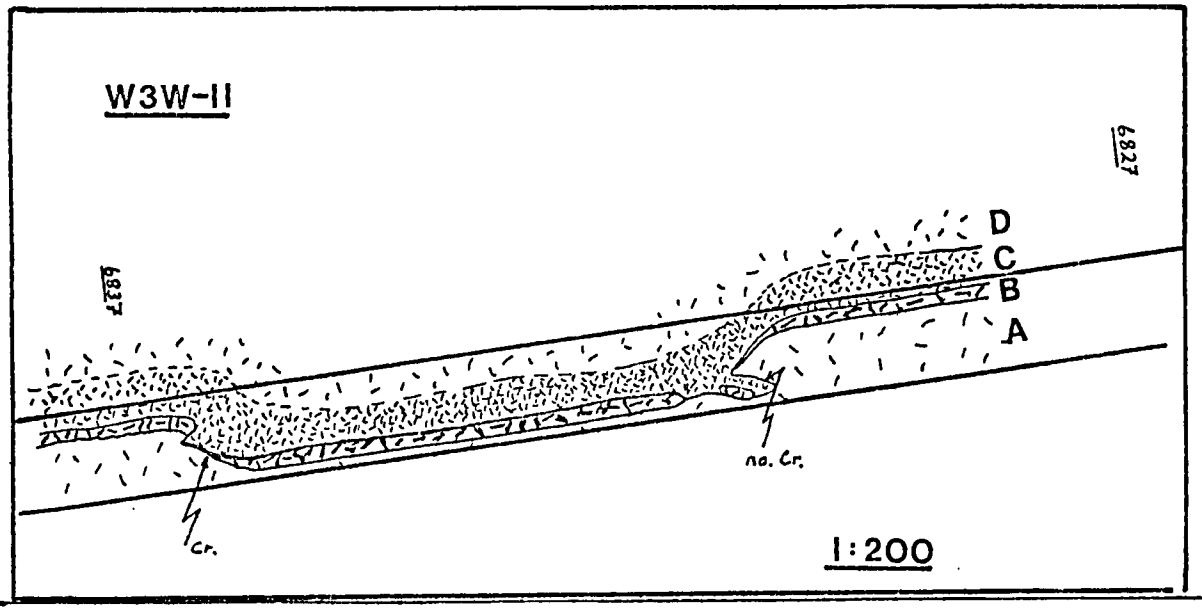

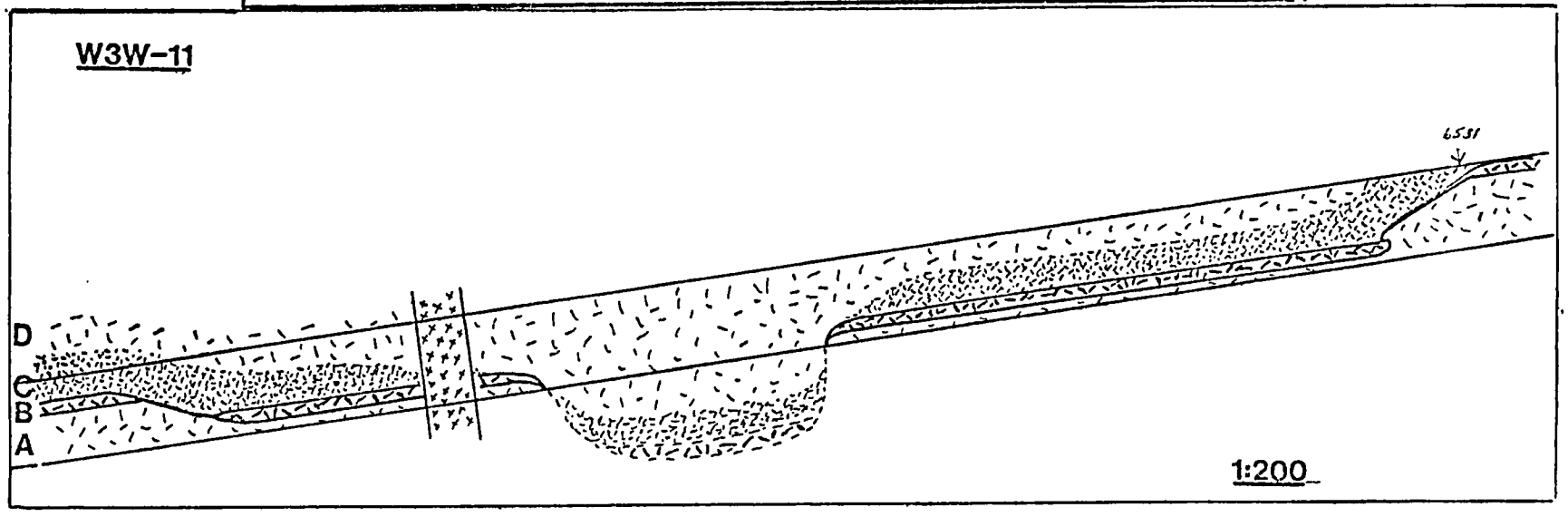

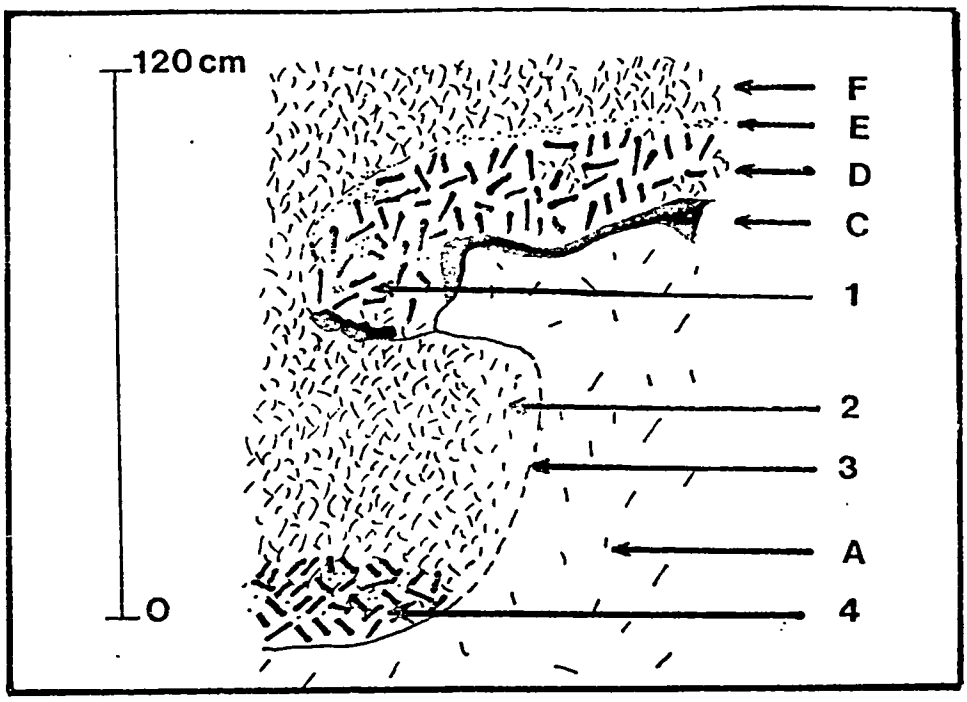

(a)

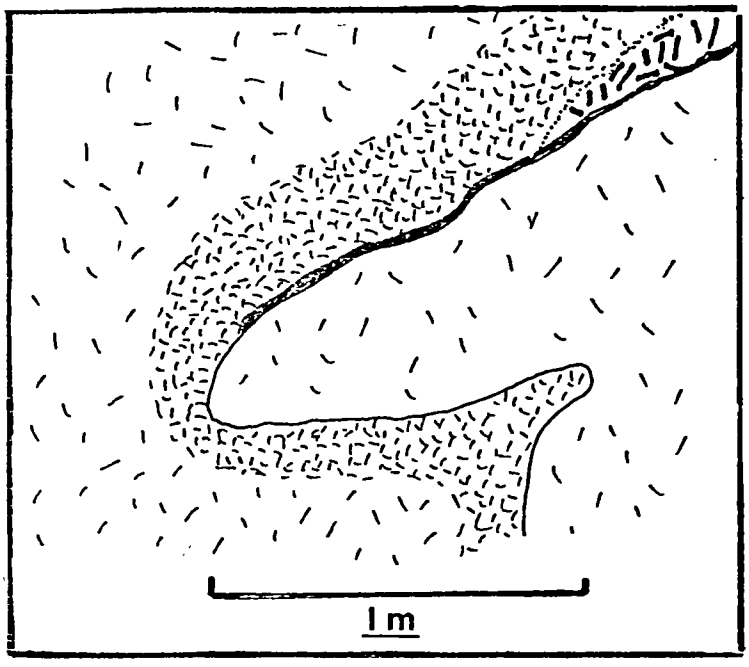

(b)

Fig. 2.10 (a) Edge of shallow Normal Pothole near W1E-5, Rustenburg mine. Spotted anorthosite (A), bottom chromitite band (C), Normal Reef pegmatitic pyroxenite (D), thin irregular top chromitite band (E), and Merensky pyroxenite (F).

At the lip of the pothole the Reef contains disseminated clusters of chromite (1), the Merensky is less pyroxenitic (2) and exhibits gradational boundary (3) with footwall. The Pothole Reef contains disseminated chromite and no bottom chromitite (4). No undulations at the contact with the footwall in the pothole.

(b) Edge of shallow Normal Pothole exposed in Waterval 9 Inc.

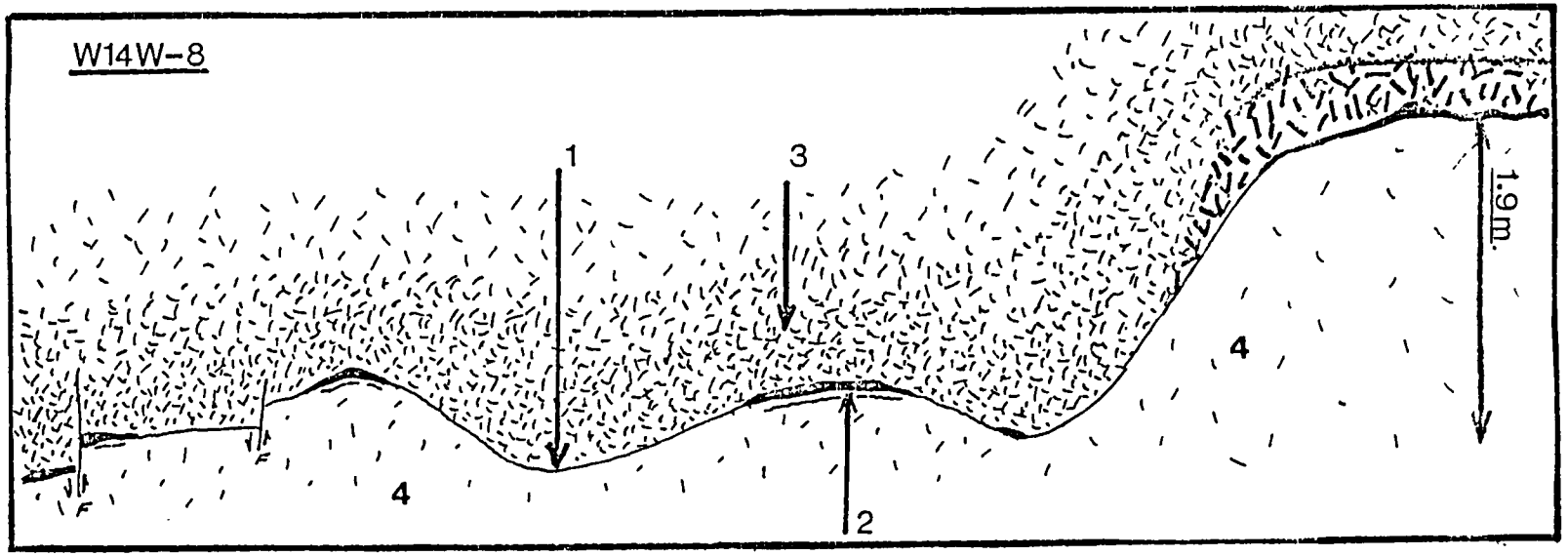

Fig. 2.11 This is a section of one half of a shallow normal pothole on W14W-8 at Rustenburg mine illustrating the occurrence of Pothole Facies in which the Merensky pyroxenite (3) rests directly on the footwall spotted anorthosite (4). Where the bottom chromitite band is absent (1) in the pothole, there is no thin white anorthosite at the contact. Where remnants of the chromitite band are present, the white anorthosite is also present (2). The Merensky pyroxenite grades upwards into norite. At Normal Reef Elevation the top chromitite band becomes well defined towards the edge of the pothole.

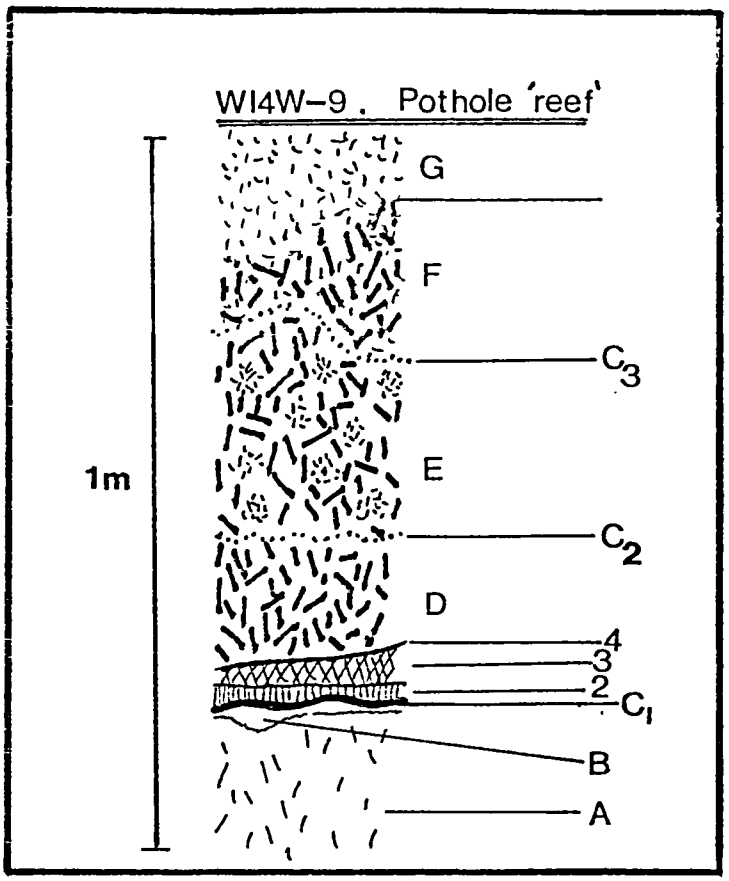

Fig. 2.12 A variety of Normal Pothole Reef Facies. Around the pothole at normal reef elevation the Merensky Reef was as in fig.2.6. The various features of the section above are:

A - Footwall spotted anorthosite

B - White anorthosite

C_1 - Thin bottom chromitite band

2 - Black pitch-like Reef

3 - Fragmented earthy decomposed Reef

4 - Separation plane of 1-2 mm thick

D - Reef pegmatitic felspathic pyroxenite

C_2 - Thin impersistant middle chromitite band

E - Reef pegmatitic feldspathic pyroxenite with patches of Merensky type pyroxenite

C_3 - Thin disseminated impersistant top chromitite band

F - Reef-type pegmatitic pyroxenite

G - Fine grained Merensky pyroxenite

the centre was also seen. A rare variety of pothole reef facies is illustrated in figure 2.12.

Bastard Potholes are fortunately of minor occurrence from the economic point of view. Because of the depth (50 m or more) to which the Merensky Reef is 'displaced' from its normal reef elevation, it is not economic to extract the ore from them. The edge, side, and, as far as can be determined from boreholes, the floor features of these structures are similar to the Normal potholes. The nature of the floor contact is illustrated by figure 2.13. A number of features are of particular significance with regard to the origin of these structures. Firstly the layers of hanging wall rocks above the contact roughly conform to the shape of this contact. Secondly the hanging-wall spotted anorthosite progressively thickens towards the centre and deepest part of the pothole, 'filling' and 'smoothing off' the irregular topography of the contact. The succeeding mottled anorthosits shows a similar but less marked increase in thickness, and the Bastard pyroxenite is of fairly constant thickness. Thirdly the layers of footwall rocks on the side of the pothole are transgressed by the hanging wall rocks and are generally undisturbed. However, there is evidence of disturbance of the layering beneath these pots, as for example at Union mine where a thick chromitite bed (the UG1) is in a vertical position beneath a particularly large Bastard pothole. Finally the pegmatitic Reef pyroxenite is restricted to the low angle contacts of the pothole floor.

All the features so far described for both types of pothole are considered to be most easily explained by a sedimentary

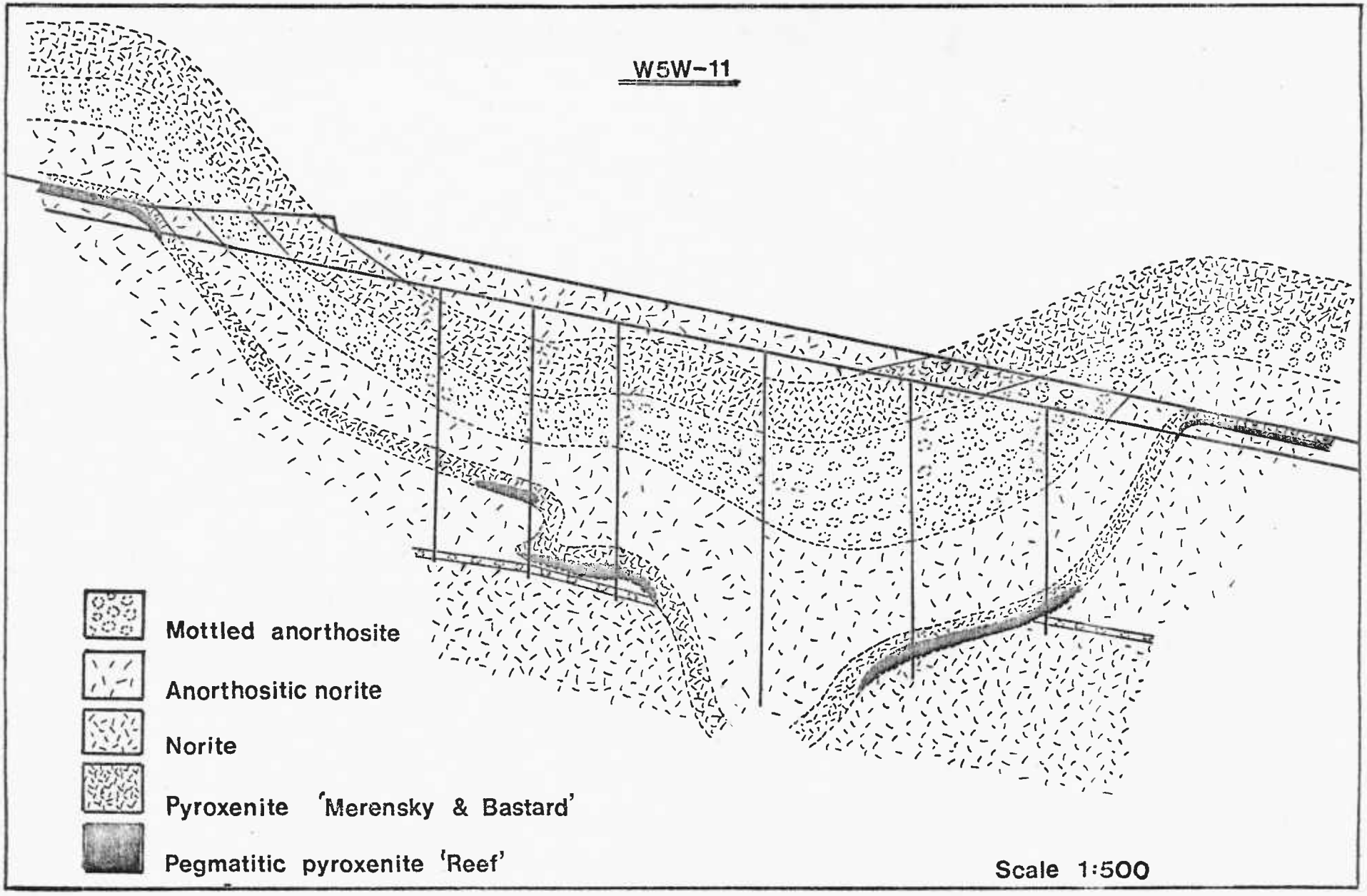

Fig. 2.13 Geological section through the only Bastard Pothole to be tested by drilling at Rustenburg mine. The central borehole was stopped whilst still in the hanging wall spotted anorthosite (anorthositic norite).

process of infilling of hollows formed largely by the magmatic scouring of a compact but still plastic footwall crystal cumulate. All the features clearly indicate a disruption of the Normal Reef pegmatitic pyroxenite and associated chromitite bands during pothole formation. This disruption and pothole formation is considered to have been produced by localised eddies in the magma at the crystal cumulate/magma interface during a time when the Reef pegmatitic pyroxenite was accumulating over an already formed chromitite layer. The currents producing the eddies were turbulent and acted over a short space of time. They were probably produced by influxes of new magma. Apart from giving rise to eddies, which scoured out hollows, the currents also spread and compacted the 'clots' of pegmatitic pyroxenite which were accumulating and which gave rise to the Reef. However, it must be stressed that there were processes operating in the footwall 'cumulate pile' which are considered to have influenced the formation of the potholes by localising and thus intensifying the activities of the eddies. The results of these footwall processes are evident at the level of the Merensky Reef as updomed areas called 'koppies'. Localisation of the magma current eddies by incipient sags in the footwall are considered to have been another product of these processes, particularly in the case of the large Bastard potholes. Therefore, before discussing the formation of potholes any further it is particularly important to first mention the nature and possible origin of Koppies and Koppie Reef facies, since they are the evidence of footwall activity during the formation of the Merensky Reef.

(c) Koppie Reef Facies refers to the Merensky Reef as

it occurs on updomed areas of footwall rocks. Cousins (1964) in describing a typical koppie says that the contact between the Reef and its footwall forms a low dome usually only a few feet high. As the contact rises it gradually eliminates more and more of the Reef, until only a thin chromitite seam follows the contact between the Merensky pyroxenite and the footwall anorthosite. No folding in either the hanging wall or footwall layers was seen.

This description rather oversimplifies the nature of koppies. Unfortunately the complete koppie structure is rarely exposed by mining because the economic Reef wedges out against the limbs. Updomed footwall areas are in fact more common than accounts by Cousins (1964,1969) would lead us to expect, and the idea that koppies and potholes "may be likened to minor protuberances on an otherwise almost perfectly plane surface" gives a wrong impression. The Merensky Reef conforms to a highly irregular footwall surface when treated as a whole. This is illustrated by Map I, showing the relationship between Pothole, Koppie, and Normal Reef facies along C2W-9. Two types of updomed footwall areas occur.

The first type is that described above by Cousins. As illustrated in Map I however, the shape of these koppies can be quite irregular and are not necessarily circular. The second type is illustrated in Map II. This type is associated with discordant intrusive-like bodies of very coarse to pegmatitic feldspathic rock which occupies the central part of the updomed footwall spotted anorthosite. The pegmatitic body of the koppie in Map II exhibits a gradational contact with the footwall rocks and Merensky Reef through which it passes. In the haulage way below, the footwall marker was

bent down and became diffuse near the pegmatitic body which was surprisingly 'fading out' at this point. The pegmatitic body increased in size upwards through the Merensky Reef. Unfortunately, the further upward passage of this body was not exposed. In other parts of the mine similar bodies were seen in the core of some of the first type of koppies. In this case they did not reach the footwall contact of the Merensky Reef. Similar bodies were also mapped where pothole-type conditions were present. In these areas the relationships between the various lithological components were very complex. Barry (pers. comm. 1962; in Cousins 1969) considers that the formation of these pegmatitic bodies or 'alteration pegmatites' provide a mechanism for pothole formation by the readjustment of mobilised footwall rock under differential pressures. The inference is that the hollows formed by this readjustment were filled by the collapse of the hanging wall cumulate crystal mush into them. Although the author does not agree with this 'collapse theory', the formation of hollows by such a mechanism prior to enlargement by 'scouring' and filling by 'sedimentation' is considered likely in the case of the Bastard potholes.

In the case of the koppie of Map II, the Merensky pyroxenite and Reef pyroxenite were seen to be progressively and selectively replaced towards the pegmatite body, becoming more and more feldspathic. However, the top chromitite band became thicker, and the bottom chromitite band still persisted on its undulating footwall surface. Thus finally the Reef and Merensky pyroxenite changed to an anorthosite with shadowy grey patches of pyroxene and sulphides, and 'remnant' patches of pyroxenite. The two chromitite

bands were, however, still present in their normal positions. The sequence graded into the pegmatitic body which is probably metasomatic rather than intrusive. At one point a large (2 m diameter) pyrrhotite rich massive sulphide body occurred. This was low in platinum metals.

Although the exact field relationships and mineralogy of these pegmatitic bodies needs to be investigated, their presence shows that residual magmatic processes were operating in the footwall. These processes are especially important to the formation of potholes since it is considered that they helped to provide an irregular surface in the form of koppies prior to the final deposition of the Merensky Reef, and thus localised and intensified the scouring action of magma eddies on the floor.

Other structures such as jointing, minor faulting, and early basic, and later syenitic dykes radiating from the Pilanesberg Complex, are not dealt with here. Some redistribution of the precious metals at the contact of some of the dykes has been reported (Wagner 1929).

2.2.3 The Formation of the Potholes was first explained by Schmidt (1952). He considered that they were formed by the swirling motion of currents in the magma caused either by convection, or more probably by the influx of new magma. He envisaged that these eddies picked up the large pyroxene crystals of the Reef pegmatitic pyroxenite and, by using them as an abrasive material, cut through the bottom chromitite band into the underlying spotted anorthosite which had not yet become completely consolidated. He provided mineralogical evidence to support his conclusions, notably that in compar-

ing Pothole with Normal Merensky Reef.

(1) the volume percentage of the feldspar in the Merensky Reef was greater inside the pothole because of the addition to it of previously eroded feldspars from the footwall;

(2) there was a more even variation upwards in the composition of the orthopyroxenes compared to outside the pothole;

(3) the orthopyroxene crystals inside the potholes have a greater elongation and the orientation is such that they are aligned parallel to the sides

This explanation was supported by Ferguson and Botha (1963). However, because of the large size of the Bastard potholes in particular, it was difficult to imagine such extensive scouring, and other explanations were sought. Cousins (1964) considered they were slump structures, but was unable to account for the lost rock material necessary to form the cavities into which the Merensky Reef and hanging wall rocks would collapse. Coertze (1963) considered they were faulted fold-structures. Barry (pers. comm; in Cousins, 1969, and in Vermaak, 1976) has suggested a genetic relationship with the feldspathic pegmatitic bodies which trangress the central parts of some of the potholes and koppies, and has proposed that readjustments in the footwall during the formation of these bodies provided the mechanism for the removal of material required for the theory by Cousins. Barry maintains that postmagmatic introduction of volatiles preferentially mobilized the low-temperature leucocratic rocks, thereby causing slumping of the high-density layers into the resulting potholes. Evidence (Cousins, 1969) that pothole formation postdates movement along the Footwall Marker fault is based on sparse bore-

hole data, and could be an error in interpretation, since it is inconceivable that the features of these structures already described could be produced after the rocks were consolidated.

The author is, therefore, in general agreement with the first explanation by Schmidt, although it is considered that the additional existence of updomed and downwarped footwall areas controlled the siting of the potholes by affecting the pattern of magma flow over the floor, and thus localising and intensifying the scouring eddies. In addition the formation of the very large potholes would also promote the development of minor eddies in the vicinity. This could explain an often close spatial relationship between small Normal potholes and the large Bastard potholes. Unfortunately the existence of disturbed layers beneath the Bastard potholes has not been properly studied since mine workings rarely pass beneath such structures. However, they can be used as further evidence for processes operating in the footwall during the formation of the Merensky Reef, and they do not contradict Schmidt's explanation, since any irregularities of the depositional surface produced by such processes have already been proposed here as important to pothole formation by magma scouring.

2.3 The Merensky Reef at Union Mine.

At Union mine the various components of the Merensky Reef at Rustenburg mine are present but considerably thicker (fig. 2.1). The bottom 2-3 cm thick chromitite band rests on an undulating footwall surface of mottled anothosite with an intervening thin white anorthosite band, as at Rustenburg mine. The chromitite is overlain by a very coarse and pegmatitic feldspathic pyroxenite of

3 to 5.5 m thickness that can be equated to the Reef at Rustenburg. It is, however, noticeably coarser. At the top of this layer is a well defined contact with the overlying finer grained pyroxenite, equivalent to the Merensky pyroxenite at Rustenburg. At the contact is a 2-3 cm thick chromitite band which is very persistent. The Merensky pyroxenite grades upwards, after about 7 m, into a spotted anorthosite. Studies of the platinum-metal distribution (see chpt. 3) have shown that only in the vicinity of the top chromitite band are the 'values' economic. The result is that, despite the great difference in thickness between the Merensky Reef at Union and Rustenburg mines, the sloping width is the same. The section mined (approx 0.6 m) consists of about 46 cm of Reef, the chromitite band, and, in order to fully recover this PGM-rich chromitite, about 10 cm of the hanging wall Merensky pyroxenite.

Because of the large thickness of the Merensky Reef and Merensky Unit at Union mine the potholes and koppies are naturally usually not exposed in their entirety. However, Normal and Bastard type potholes occur, and according to Cousins (1964,1969) and Barry (pers. comm.) they are similar in size, number, and character to their counterparts at Rustenburg mine. Since the author's visit to this mine was brief there was no opportunity to study these structures at first hand.

2.4 The Silicate and Oxide Mineralogy

2.4.1 The Merensky Reef mineralogy has been critically reviewed, together with the addition of much new data, by Vermaak and Hendriks (1976). They concluded that the Reef pegmatitic pyroxenite was a coarse grained feldspathic pyroxenite or melanorite (orthopy-

roxene cumulate) in which either quartz or olivine may be present. They determined its weighted average composition (in volume %) as 61.5 % orthopyroxene, 23.7 % feldspar, 9.6 % clinopyroxene, 0.1% quartz, and 5.0% combined accessories which includes the base-metal sulphides, chromite, biotite, phlogopite, hornblende, magnetite and ilmenite. They also reaffirmed that the coarse grained fraction of the Reef occurs in clots or roughly ovoid bodies surrounded by finer grained aggregates. Consequently a grain size range for orthopyroxene of 0.8 - 6.0 cm has been reported, although the grain size is clearly bimodal with averages given by Vermaak and Hendriks of 2.60 mm and 1.29 cm.

The Merensky pyroxenite is described by them as a porphyritic pyroxenite of very variable grain size and texture. According to them it is usually a medium-grained granular aggregate of cumulus bronzite and variable intercumulus plagioclase, with characteristically large (1.5 cm) oikocrysts of clinopyroxene enclosing 1 mm-sized chadacrysts of bronzite and biotite. Throughout the rock there is an invariable patchiness of coarser grained aggregates of either dark (bronzite, hornblende, tourmaline) or light (sodic plagioclase, quartz, calcite, phlogopite) minerals, usually accompanied by biotite. They also reported some unpublished work by Wilmshurst whose electron-probe microanalyses of the plagioclase showed a vertically increasing anorthite content from An_{69} to An_{79}, with decreasing enstatite content of the orthopyroxene from En_{81} to En_{78} in moving from the Reef into the Merensky pyroxenite.

The chromite mineralogy of the Merensky Reef was first generally reported on by Sampson in 1929 (1932), and specifically at

Union mine by van Zyl (1960,1970) and Legg (1967, 1969), and at Rustenburg by the same people together with Ramsden and Wilmshurst (1972). The immense amount of literary speculation that revolves around the problem of the formation of chromite and chromitite deposits in general also applies to the thin bands and disseminations of chromite in the Merensky Reef. It is not within the written scope of this thesis to review and discuss chromite formation. However, a few of the more important features and opinions on the Merensky Reef chromite resulting from the above studies and those of the author need to be mentioned.

The consensus of opinion (Vermaak and Hendriks, 1976) is that these chromitite bands are formed by the gravity settling of early formed cumulus chromite. The resulting cumulate texture was subsequently modified by postcumulus resorbtion and crystal growth (Cameron, 1969). The suggestion by van Zyl (1970), that the chromite bands were not an early crystallization product but crystallised after the orthopyroxene from a chromiferous liquid which had settled as a result of gravity, has received less support from other workers. The existence of an immiscible chromite liquid has, however, been proposed before by Fockema and Mendelssohn (1954), Fourie (1959), Groeneveld (1960), and McDonald (1965).

The textural nature of the basal chromite band at Rustenburg mine and the top chromitite band at Union mine is illustrated in figure 2.14. The basal chromite band at Rustenburg and Union mines consists, according to Legg (1967), of three distinct parts. The bottom contact with the white anorthosite displays irregular, strongly embayed, elongate and crescent-shaped chromite

Top Chrome Band **1985** Union Mine

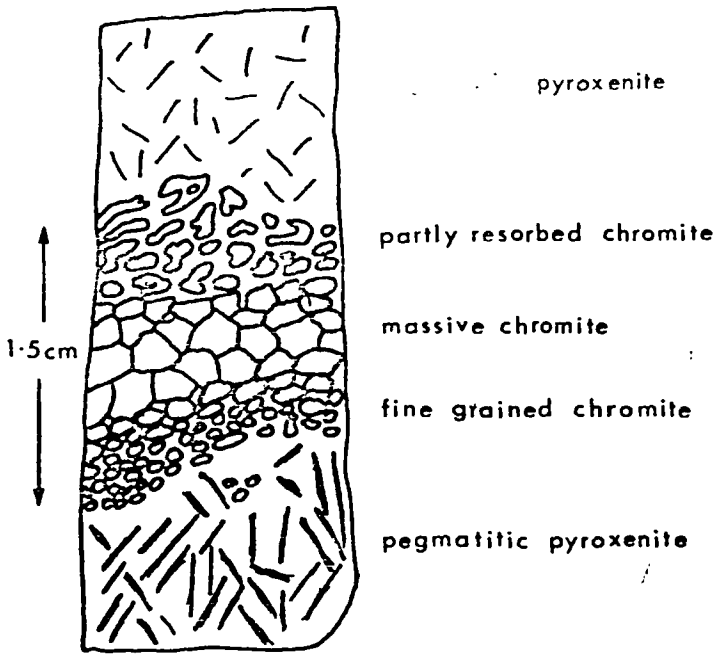

Basal Chrome Band **BL 13** Rustenburg

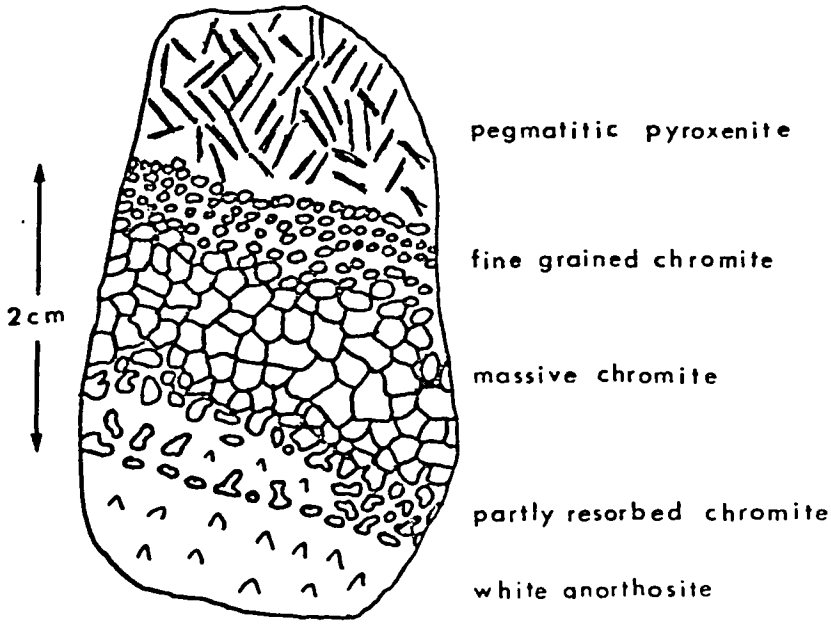

Fig. 2.14 The textural characteristics of the bottom chromitite band at Rustenburg mine and the top chromitite band at Union mine. After Legg (1967).

grains enclosed by the silicates. This contact zone passes up into a compact and coarser grained zone showing a polygonal mutual boundary structure with very little interstitial silicate material. This is generally considered to be a result of adcumulus growth. The top part of the chromitite band consists of fine-grained and disseminated euhedral chromite. Where the chromitite band is very thin the irregular-shaped grains may persist throughout. The irregular embayed grains at the bottom contact strongly suggest resorbtion in their present position. This may have been caused by reaction with the intercumulus liquid from the underlying anorthositic norite. There is clearly some direct relationship between the formation of the white anorthosite band and the partial resorbtion of the bottom part of the band.

The texture of the top chromitite band at Union mine is the reverse of the bottom chromitite band already described. In this case resorbtion appears to have taken place at the contact with the Merensky Pyroxenite. Rare and complex intergrowths of chromite with ilmenite have been described by Legg (1967,1969). He interprets them as being formed by high temperature exsolution at low oxygen fugacity of a chromiferous ulvospinel from a titanium-rich ferrian chromite, which later oxidised to form ilmenite and iron-poor chromite.

The first study of the compositional difference between chromite of the top and bottom chromitite bands at Rustenburg and Union mines was by Legg (1967). From an electon-probe microanalyser study of the composition of chromite at ten levels through the thick UG1 chromitite horizon, he established that for these chromites

the reflectance increased with increasing ferric iron content. He then used reflectance measurements to monitor the change in ferric iron content from the bottom to the top chromitite bands of the Merensky Reef. He found that the reflectance of chromite increased upwards by 1.5 to 2.5 percent units of reflectance, and concluded that this represented a marked increase in ferric iron content. For the bottom chromitite band Ramsden and Wilmshurst are reported by Vermaak and Hendriks (1976) to have indicated a decrease in iron content upwards across it. Their three electron-probe microanalyses (FeO 34.9, 36.8, 35.3 wt.%) do not, however, support this.

Legg considered that the enrichment in iron in the top chromitite band was caused by an increase in oxygen fugacity, probably produced by the formation of immiscible sulphide liquid droplets in the magma, with the oxygen fugacity being increased by the release of oxygen from SO_2. However, according to Page (1971) and Haughton et al (1974) the removal of iron from the magma, as by chromite precipitation, decreases the sulphur-carrying capacity of the magma, may bring it to saturation, and thereby cause immiscible sulphide droplets to form. Depletion of Fe^{2+} is considered by them as the most important requirement for sulphide separation from the magma, although other variables such as oxygen and sulphur fugacities and temperature also correlate with and influence it. In the Merensky Reef there is clearly a correlation between chromitite formation and sulphide segregation from the magma. Thus at Union mine where there is a well developed top chromitite band the greater proportion of the total sulphides of the ore section occur immediately above it in the Merensky pyroxenite (chapter 3.1.3). This is

also the case at Rustenburg where the bulk of the sulphides occur in the Reef pyroxenite immediately above the well developed bottom chromitite band. Sulphides are also concentrated above the bottom chromitite band at Union mine. In contrast there is only a small quantity of sulphides above the thin impersistent top chromitite band at Rustenburg. The spatial separation of the chromite from the sulphides can be explained by differential gravity settling combined with the slightly earlier formation of the former.

2.4.2. Other Main Rock Types making up the Bastard, Merensky, and footwall units at Union and Rustenburg mines are summarised below from descriptions by van Zyl (1970).

The Norites are holocrystalline, hypidiomorphic, and consist mainly of cumulus plagioclase (An 64 - 76; 59 vol.%), and orthopyroxene (Of 17-40; 34 vol.%), with clinopyroxene (6 vol.%) and accessory biotite, quartz, and magnetite (1 vol.%).

The Spotted Anorthosites (spotted anorthositic norites or spotted leuconorites) are holocrystalline, hypidiomorphic rocks with about 14 vol.% of orthopyroxene (Of 18-33), 84 vol.% plagioclase (An 72-80), 2 vol.% of clinopyroxene, and less than 1 vol.% accessory biotite and magnetite. The spots are produced by sparsely scattered irregular crystals of orthopyroxene. The order of crystallisation was first plagioclase for a short period, followed by both plagioclase and orthopyroxene, and finally interstitial ortho- and clinopyroxene.

The Mottled Anorthosites are holocrystalline, hypidiomorphic rocks consisting mainly of plagioclase (An 75-82; 93 vol.%) with subordinate orthopyroxene (Of 22-29; 4 vol.%), clinopyroxene

(about 2 vol.%) and accessory biotite and magnetite (1 vol.%). The dark mottles of 2-4 cm in diameter consist of large, irregular clusters of pyroxene which is interstitial to the plagioclase.

The Boulder Bed (fig. 2.4) mineralogy has been studied by Kinloch (in Vermaak, 1976, p.1288) who reports the average composition of one boulder as being in volume % 12.9 olivine, 22.2 plagioclase, 27.0 alteration products like talc, serpentine, chlorite, and amphibole, 12.6 orthopyroxene, 16.9 clinopyroxene, 2.0 quartz, 1.6 biotite, 2.8 amphibole, 0.6 carbonate, and 0.4 spinel, chromite, magnetite, and sulphides. From the centre of the boulder to the edge there was an increase in clinopyroxene and olivine, a decrease in orthopyroxene and alteration products, an increase in sulphide and oxide minerals, and texturally the plagioclase became finer grained and the mafic minerals became coarser. Vermaak interpreted this as indicating its formation in a "foreign rapidly changing, volatile environment with which there was continuous reaction as indicated by the significant amount of alteration", and that the increase in olivine outwards shows that "the magma from which the aggregate formed became progressively more basic". He uses the occurrence and mineralogical features of these mafic aggregates to support his genetic model for the formation of the Merensky Unit and particularly the Reef pegmatitic pyroxenite.

2.5 The Formation of the Merensky Reef

The Merensky Reef is considered not to be unique with regard to its genesis, which must apply also to the many other pyroxenite layers, all of which contain significant amounts of platinum-group metals in association with base-metal sulphides, and usually

chromitite bands within them or at their base. Pegmatitic facies are also not peculiar to the Merensky Reef. There are four aspects to the genetic picture of the Merensky Reef, namely:

1. The mode of formation of the Merensky Unit as well as other cyclic units above and below. This includes the formation of the Merensky Reef and associated chromitite bands.

2. The mode of formation of the potholes and koppies.

3. The mode of formation of the interstitial base-metal sulphides.

4. The source and concentration of the platinum group metals, and the explanation of their mineralogical and textural form of occurrence in the ore i.e. as discrete minerals and as trace constituents in the sulphides, silicates, and oxides.

Past discussions and theories on the genesis of the Merensky Reef have largely failed to embrace and integrate these four aspects and explain all the known data. Even the most recent genetic model by Vermaak, to explain the cyclic differentiation units and the Merensky Reef, has ignored the potholes, and results in additional problems in explaining the ore mineralisation. Similarly hydrothermal theories have dealt in isolation with the platinum-metal mineralisation (Lauder, 1970; Stumpfl, 1974), have treated the Merensky Reef as merely a favourable site for ore localisation, and have ignored its previous ore forming differentiation history and its many field and laboratory-observed characteristics, which clearly point to the syngenetic nature of this mineralisation.

Some genetic aspects have already been dealt with during this and the previous chapter, particularly in connection with

potholes and koppies. Implicit in their explanation was the author's agreement with the consensus of opinion that (1) the Merensky Unit represents one of several cyclic differentiation units in the top part of the Critical Zone; (2) fractional crystallisation and gravity settling was responsible for the visible mineral layering and cryptic compositional variations, and (3) the footwall anorthositic rocks were relatively consolidated but still plastic whilst the Merensky Unit was forming. In addition the author considers that the field evidence provided in this chapter shows that the bottom chromitite band and Reef pegmatitic pyroxenite, together with the bulk of the still liquid interstitial sulphides, had already formed on the footwall spotted anorthosite floor after koppie but prior to pothole formation. It is also considered that turbulent magmatic currents from the influx of new magma were responsible for the scouring and enlargement of existing sags in the footwall, producing the Bastard Potholes, and for scouring new and shallower hollows, producing the Normal Potholes. Updomed 'koppie' areas in the footwall controlled the flow of the magma current over the surface and localised the scouring action of the eddies. Sags and updomed areas in the footwall were probably caused by the metasomatic processes envisaged by Barry, but the draining away of magma at depth could be a possible mechanism to produce incipient collapse of the partially consolidated layers higher up in the intrusive mass. The potholes were eventually filled during the continuing cyclic differentiation of the overlying magma, such that the layers of the Bastard Unit were also affected. This mechanism for their formation does not accord with the recent theory for the formation of cyclic units by

Vermaak (1976), who envisages that the Merensky and other cyclic units were formed from the separate differentiation of isolated layers of magma delimited at the top and bottom by rafts or mats of floating cumulus plagioclase. In the case of the Merensky Unit, the footwall unit was presumably already largely differentiated. If this theory is correct then the effect of the potholes on the layers of the Bastard Unit would be difficult to explain in terms of sedimentation into footwall hollows, although Vermaak conveniently considers potholes and koppies as "not pertinent to the origin of the Merensky Reef".

Vermaak cites work by van Zyl (1960,1970) and Meyer (1969) as evidence that an upward increase in anorthite content of the plagioclase is the general rule for each cyclic unit. He then considers that "the only logical explanation for this reversal lies in the floating of plagioclase in a magma of similar density, and that if the floating was arrested by a compositional, density, or temperature inversion, a mat of crystals would form and later crystals would underplate the mat to form the anorthosite layer". However, there appears to be conflicting opinion, and confusion about this reversal, since Van Zyl (1970), despite some of his data, clearly states several times that "there is a regular <u>decrease</u> in the anorthite content of the plagioclase from the bottom upwards in each sub-unit" (cyclic unit). He also confirms a corresponding <u>increase</u> in the orthoferrosilite content of the orthopyroxenes.

With regard to the Merensky Unit, Vermaak envisaged that the entrapped magma differentiated as follows:

1. Progressive 'underplating' of the floating plagio-

clase mat by early formed plagioclase crystals. This explained the 'evidence' for a progressive decrease in anorthite content downwards.

2. Removal of the plagioclase by this mechanism caused enrichment in ferromagnesium constituents in the magma.

3. Volatiles collected beneath the floating anorthosite mat and created a low viscosity environment.

4. Aggregation of mafic minerals into dark, rounded, boulderlike masses in the volatile rich zone immediately beneath the anorthosite mat. The existence of these aggregates is based on their occurrence in the 'boulder bed', and in some weathered portions of the Reef.

5. The bottom chromitite band formed by gravity settling onto a 'plastic' footwall. Resorption of chromite represents reaction with the interstitial liquid of the preceding cycle.

6. The pegmatitic pyroxenite boulders sank to the base of the Merensky magma unit and dimpled the bottom chromitite seam, producing the undulations now seen.

7. The boulders formed the Reef and were buried by subsequent sedimentation of cumulates to produce the finer grained Merensky pyroxenite and layered footwall anorthositic rocks.

This genetic model has much to support it. However, it does add to the problem of explaining the potholes, and a satisfactory explanation of the difference in mineralogy between the highly altered boulders of the 'boulder bed' and the relatively unaltered 'clots' of the Reef is lacking, especially as both are reputed to have formed in a volatile rich environment and by the same process. Other problematical points are:

1. The apparant absence of these mafic aggregates in anorthosites at other levels in the top part of the Critical Zone;

2. That such a high concentration of platinum-group metals and sulphides should result at Rustenburg from the differentiation of only a 12 m thick layer of magma;

3. The lack of any folding, sagging, breaks, etc (other than those associated with Bastard Potholes) at the level of the proposed anorthosite mat, especially as, according to Vermaak, there was "extensive magma turbulence and movement causing the mixing and subsequent winnowing of these cumulates";

4. The existence of the potholes as evidence of magma currents which would be expected to disrupt the mat;

5. The existence of only sporadic and thin pegmatitic patches at the base of the thick Bastard Reef pyroxenite, which is the basal member of cyclic unit five times thicker than the Merensky Unit, and thus would be expected to give rise to a correspondingly thicker pegmatitic layer than the Reef.

However, the origin of the Reef as an accumulation of clots of coarse mafic minerals produced in a volatile-rich environment is consistent with the features of this layer as described in this chapter. Whether these and the cyclic differentiation pattern could be produced without the necessity of plagioclase rafts is a subject for a further thoughts and more quantitative evidence. Finally, the author sees no strong objection to the alternative suggestions by Schmidt (1952) and Van Zyl (1960,1970) that the cyclicity in the Critical Zone probably corresponds to intermittent surges of new basaltic magma.

In conclusion, the following platinum metal mineralogy of the Merensky Reef ore is dealt with in the context of magmatic differentiation and the fractional crystallisation of immiscible base-metal sulphide droplets which, during their separation from the magma and subsequent gravity settling to the base of the Merensky Unit, are believed to have scavenged the magma of its platinum metals. The droplets finally underwent fractional crystallisation within the interstitial confines of the Merensky Reef pyroxenite. The resulting platinum-group minerals, their textural relationships with each other and with the base-metal sulphides, are described and explanations offered in this thesis. The paragenesis of the ore minerals, and the physico-chemical conditions under which they were formed, are discussed in chapter 9.

CHAPTER 3

INTRODUCTION TO THE ECONOMIC MINERALOGY OF THE MERENSKY REEF

3.1 The Economic Metals and their Distribution

3.1.1. The Economic Metals in the Merensky Reef are the six platinum group elements Pt,Ir,Os,Pd,Ru,Rh, together with Au. Nickel and copper are also an important source of revenue, their contents in the ore being on average 0.19 %Ni and 0.11 %Cu. Mineralogical studies have shown that small amounts of silver, mercury, tin, lead and zinc also occur, although no information is available as to whether these metals are recovered during the refining process. No assay data is available for them. According to Newman (1973) the revenue from each of the ore metals, expressed as a percentage of the total revenue, is Pt 58.01, Pd 8.6, Rh 5.67, Ru 1.96, Ir 1.08, Au 2.32, Ni 19.01, and Cu 3.35 percent. Their relative abundance in the ore is given in table 3.1.

Table 3.1 The content of precious metals in the Merensky Reef expressed as a percentage of the total, from various sources.

Atomic Number	Element	(1)	(2)	(3)	(4)	(5)
79	Au	5	4	3.2	4.00	1.90
78	Pt	61	60	59	58.5	65.18
77	Ir	1	0.7	1.0	0.70	0.08
76	Os	--	0.6	0.8	0.60	0.04
46	Pd	24	27	25	27.90	27.30
45	Rh	4	2.7	3	2.60	2.60
44	Ru	5	5	8	5.70	2.90

(1) Newman, 1973. (2) Cousins, 1969. (3) Cousins & Vermaak, 1976. (4) Rustenburg mine, 1952 (unpublished report by Lever, Todd & Powell). (5) Union mine, 1952 (unpublished report by Lever, Todd & Powell).

3.1.2. The Overall Grade of the ore from Rustenburg mine, and Union mine, is privileged company information. Some grade figures for the Merensky Reef are, however, available from Wagner (1929) whose data has been summarised by Vermaak and Hendriks (1976). They quote an average overall grade over a width of 76cm of 8.8 g of platinum-group elements (PGE) per tonne, with a range of 7 - 12 g/tonne. Newman (1973) gives a range for PGE plus Au, based presumably on his knowledge of the Western Platinum mine, equivalent to 3.9 - 7.8 g/tonne over a milling width of 76 cm (i.e. quoted as 2.5 - 5.0 dwt/$\frac{s}{\lambda}$ton, corresponding to 75 - 150 inch-dwts over 30 inches).

Any statistical treatment of the mine assay data to determine the presence of zonal patterns, or high grade zones, which might be related to petrological or structural features, has not been reported. However, no obvious indication of 'ore shoots' or element zonation at Rustenburg mine was apparant to the author from a brief examination of the assay results up to 1962. One broad feature was the general increase of grade with depth (i.e. distance down dip). This may in part reflect leaching of the precious metals in the oxidised zone, as well as a progressive improvement in the efficiency of the assay technique.

3.1.3 Element Distribution Data for the Merensky Reef in the western Bushveld has been given by Cousins (1969), Newman (1973), and Brynard et al (1976). Cousins graphical plots of average Ni, Cu, and Cr_2O_3 content against average PGE plus Au content for the Merensky Reef at Rustenburg mine display strong positive correlations in the case of Ni and Cu, but only a weak positive correlation

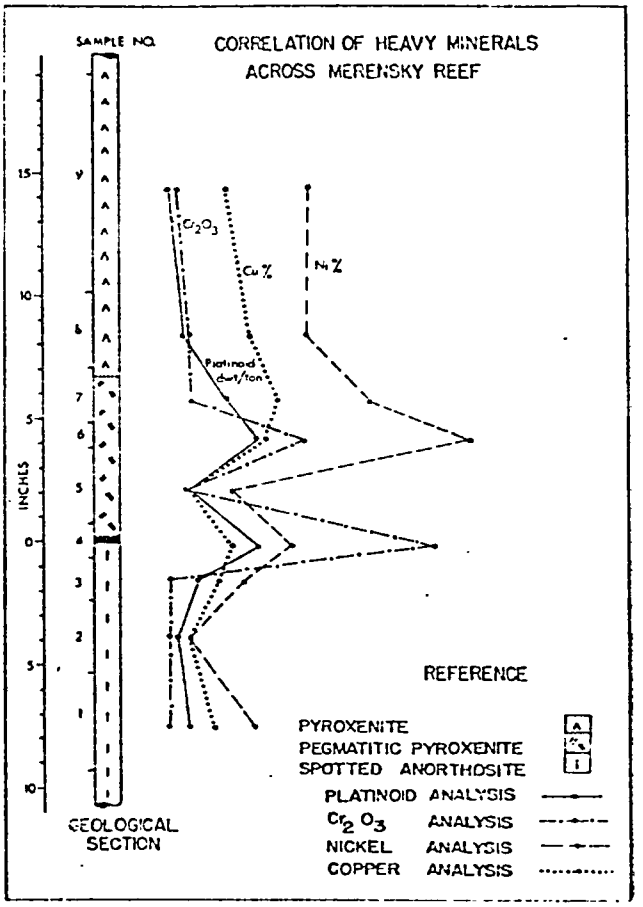

Fig 3.1 Relationships between platinum group metal content in the Merensky Reef at Rustenburg mine and Cu, Ni, and Cr_2O_3 content, according to Cousins (1969).

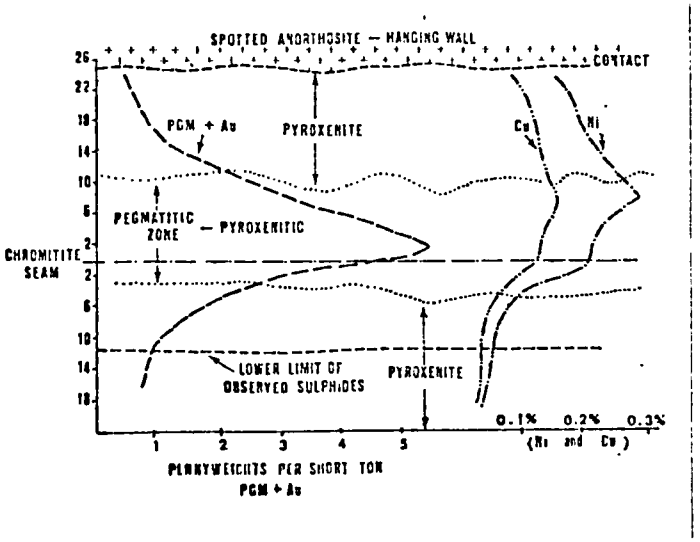

Fig. 3.2 Vertical distribution of metals in the ore section of the Merensky Reef at Western Platinum mine, according to Newman (1973).

in the case of Cr_2O_3. With regard to the detailed vertical distribution plots (fig. 3.1) he concludes that "peak platinoid values normally occur in the Basal Chromite band and that the peak sulfide values occur immediately above it".

Newman (1973) provides some further quantitative vertical distribution data for the Western Platinum mine, where the Merensky Reef is from 2 - 12 m thick, and where major PGE plus Au mineralisation occurs at the top chromite band, as in figure 3.2. He also concludes that where there is sulphide mineralization PGE plus gold will be present, although the highest PGE and gold values are not necessarily associated with the highest nickel and copper values but are invariably concentrated in or about the chromite band. Brynard et al (1976) also confirmed this strong positive correlation at Western Platinum mine of PGE plus Au with Ni and Cu, although they found a weaker or negative statistical correlation with chromium. However, their graphical representation of the vertical element distribution shows a peak value correlating with the chromite band.

No published data on the precious metal distribution is available for Union mine. However, Zermatten et al (unpublished report) have carried out an excellent study of pillar and borehole sections through the top 'ore section' of the Merensky Reef at Union mine. Although the quantitative vertical distribution plots cannot be presented here, their qualitative conclusions are presented because of their genetic importance. They concluded that:-

1. The PGE plus Au values peak at the chromite band which may contain 30 wt.% or more of the total PGE plus Au content.

2. The Merensky pyroxenite immediately above the

chromite band contains 26 wt.% of the total PGE plus Au content, whereas the Reef pegmatitic pyroxenite immediately below the chromite band contains 42 wt.%.

3. The highest concentration of Cu and Ni occurs immediately above the chromite band.

4. The chromite band contains only 10 wt.% of the Cu and 9 wt.% of the Ni content of the ore section.

5. The Merensky pyroxenite contains 69 wt.% of both the Ni and Cu content of the ore section.

6. The Reef pegmatitic pyroxenite contains only 21 wt.% of the Cu and 22 wt.% of the Ni.

It is considered that the weak to negative statistical correlation between Cr_2O_3 content and PGE plus Au content previously reported (Cousins, 1969) is misleading, since it is abundantly clear from the vertical distribution plots that the chromite bands are heavily enriched in platinum group elements. The apparant lack of correlation is because of the small thickness of the chromite band relative to the large remaining chromium poor part of the ore section. Thus the relationship with chromium content is obscured by comparing the bulk chromium content of the ore section with PGE plus gold content. It is considered, therefore, that, in relation to its thickness, the chromite band at these mines has in fact acted as a very effective PGE collector and, in all cases so far reported, corresponds to PGE plus Au distribution peaks. The strong positive correlation of the PGE content with Cu and Ni agrees with past and recent ore microscopic studies in which the platinum group minerals are commonly found enclosed or at the margin of the interstitial base-metal

sulphides, in particular chalcopyrite and pentlandite. It is considered probable that the PGE content of the chromite band is largely accounted for by Pt-Fe alloy and other alloys types, whereas the PGE content of the sulphide bearing Reef and Merensky pyroxenites are accounted for by the platinum group sulphides, arsenides, antimonides and bismuthotellurides. This will, however, be discussed later.

3.2 Economic Metal Occurrence

3.2.1 The Economic Base Metals in the Merensky Reef are nickel and copper, which display a fairly constant ratio at the producing mines in the western Bushveld of 1.7:1, corresponding to grades of around Ni 0.19 and Cu 0.11 wt. percent (Newman, 1973). These two metals mostly occur as the base metal sulphides pentlandite and chalcopyrite. The small remaining Cu and Ni is accounted for by rare to very rare copper and nickel sulphides and arsenides, as major and minor constituents of some platinum group minerals, and as trace amounts in ore and gangue mineral lattices. Subsidiary 'non-revenue' elements like zinc, tin, cobalt, and lead occur either in trace amounts in other minerals or as very rare minerals. The following list of minerals have so far been reported or found in the present investigation to account for the above elements:

Common occurrence in the ore

Copper & Nickel

pentlandite $(FeNi)_9S_8$ with up to 0.9 wt.% Co.

chalcopyrite $CuFeS_2$

pyrite FeS_2 some nickel detected

pyrrhotite FeS with 0.2 wt.% Ni, and 0.1 wt.% Co.

Rare to very rare occurrence in the ore

Copper & Nickel

cubanite $CuFe_2S_3$

mackinawite (Fe,Ni,Cu)S with 5 - 7 wt.% Ni, 0.4 - 6 wt.% Cu.

valleriite $\lceil CuFeS_2 \rfloor . \lceil (Mg,Al,Fe)(OH)_2 \rfloor$

bornite Cu_5FeS_4

chalcocite Cu_2S

niccolite NiAs

skutterudite $(Co,Ni,Fe)As_{3-x}$ (unconfirmed)

braggite (PtPdNi)S

cooperite PtS with less than 1% combined Cu and Ni.

Pt-Fe alloy with less than 3 wt.% Cu and 0.5%Ni.

Lead, Zinc, Tin, Mercury and Bismuth

galena PbS

PdPb phase

sphalerite ZnS

paolovite Pd_2Sn

rustenburgite $(Pt,Pd)_3Sn$

atokite $(Pd,Pt)_3Sn$

unnamed (Pd,Hg)(Bi,Te)

bismuthinite Bi_2S_3

bismuthotellurides (see 'precious metals' below)

Tellurium and Antimony (see 'precious metals' below).

3.2.2 The Precious Metals were first believed by Schneiderhohn (in Wagner, 1929) to be largely in solid solution in the base metal sulphides. Wagner was clearly not of this opinion, but conceded that a significant amount could be. They are now known to occur

Table 3.2 The precious metal minerals of the Merensky Reef at Rustenburg and Union mines, together with qualitative and quantitative (in vol.%) relative abundance estimates by the author, and Vermaak and Hendriks (1976) respectively.

MINERAL	ABUNDANCE RELATIVE TO TOTAL PGM		
	Rustenburg Mine	Union Mine	Vermaak & Hendriks Vol.%
Braggite (PtPdNi)S	v.common	minor	35.90
Cooperite PtS	v.common	minor	13.36
Laurite (RuIrOsPt)S	minor	v.common	9.77
Sperrylite $PtAs_2$	rare	rare	0.29
Pd_4Sb	v.v.rare	v.rare	----
Pd_xAs_y	v.v.rare	N.R.	----
Pt-Fe alloy	minor	v.common	
(a) free grains	minor	minor	0.51
(b) myrmekitic	common	v.common	35.39
(c) int.cooperite	rare	rare	3.46
Au-Ag-Pd alloys	minor	v. minor	0.40
Moncheite $(PtPd)(TeBi)_2$	rare	v.rare	0.44
Merenskyite $(PdPt)(TeBi)_2$	rare	v.rare	0.07
Kotulskite Pd(TeBi)	rare	v.rare	0.02
Michenerite PdTeBi	N.D.	N.R.	0.01
(PdHg)(BiTe)	v.v.rare	N.R.	----
Atokite $(PdPt)_3Sn$	N.D.	N.R.	----
Paolovite Pd_2Sn	N.D.	N.R.	----
Rustenburgite $(PtPd)_3Sn$	N.D.	N.R.	----
Silver telluride	v.v.rare		

N.D. Reported but not detected by author.

N.R. Not reported as being present so far.

mainly as discrete minerals, although an important but unknown proportion of the total PGE plus gold content is still not accounted for. Rhodium is a particular example. Recent studies of the Merensky Reef by Vermaak & Hendriks (1976), Brynard et al (1976), and Crocket et al (1976) have added further weight to the probability that solid solution of PGE or submicroscopic inclusions of PGM in the base metal sulphides, and even in the silicates and oxides, accounts for a significant proportion of the PGE content of the ore. The exact nature of the occurrence of these precious metals in these sulphides, assuming the samples to have been pure, is controversial and difficult to resolve. It is apparant from the present mineralogical study that it would be impossible to be sure of the purity of any sample, unless no platinum group metals were detected. Homogeneity of results for a large number of separately prepared samples would be strong evidence for lattice held PGE, or even dispersed submicroscopic inclusions of colloidal size as suggested by Vermaak and Hendriks. The theoretical aspects of diadochic substitution of PGE in sulphide, silicate and oxide lattices is discussed in chapter 9. The previous minerals known to occur at Rustenburg and Union mines are listed in table 3.2, together with a qualitative estimate of their relative abundance by the author (1966), and a quantitative estimate by Vermaak and Hendriks (1976).

3.3. Material Studied

The results of the present ore mineralogical study are based on an examination of approximately 150 polished sections of ore and concentrates. The ore specimens were collected by the author during a three month field investigation of the general mine

geology, and structural and petrological characteristics of the Merensky Reef at Rustenburg and Union mines in 1962. Dr.J.Zermatten of Johannesburg Consolidated Investment Co.Ltd. generously provided a collection of prepared concentrate material, as well as samples of high grade 'metallic' concentrates from both mines. Platinoid alloys for use as electron-probe microanalyser standards were kindly donated by Messrs. Johnson and Matthey Ltd.

Details of the mineral beneficiation process at Rustenburg mine are given by Beath, Cousins, and Westwood (1961). The concentrates studied by the author were 'metallic' table concentrates. These are obtained from the ore, after crushing, grinding and classification, by gravity concentration when the pulp is passed over tables covered with corduroy blankets. The heavy platinum group minerals are subsequently released by washing the blankets, and the corduroy concentrate is then dressed on an elaborate system of James tables up to a final concentrate. This is sent direct to the refiners. The thickened tailings, containing the Cu-Ni-Fe sulphides and a large proportion of platinum group metals, go to the flotation plant. The flotation concentrate is thickened and dried, after which it goes to the smelters, and a platinum metal-rich Cu-Ni converter matte is produced.

Many of the samples in the polished sections of the table concentrates provided by Dr. Zermatten had been acid treated and split into various magnetic fractions prior to mounting and polishing. This separation on the basis of resistance to various acid attacks and magnetic susceptibility was a help by selectively concentrating some of the phases, and thus providing sections of

dominantly one or two minerals. For example, myrmekitic Pt-Fe alloy intergrowths with pyrrhotite were found in abundance in an untreated magnetic fraction of a Union mine concentrate, whereas grains of this intergrowth type were absent or rare in magnetic fractions which had been previously acid treated. This was because all the magnetic pyrrhotite matrix had been leached out, leaving only the weak to non magnetic Pt-Fe myrmekitic alloy form. Magnetic fractions of acid treated concentrates from Union mine would, however, often contain abundant examples of large Pt-Fe alloy grains of textural type V, to be described later. Treatments with aqua regia resulted in non magnetic fractions from Union mine being rich in laurite. The acid treatment also served to remove concentrate components which were not part of the ore, as for example tungsten carbide, lead, pure copper, and iron. Thus the first treatment was to dissolve the tramp iron with 20% ferric sulphate and 10% sulphuric acid. A further acid treatment to remove base metal sulphides, remaining tramp iron, copper, lead and lead compounds, involved boiling with nitric acid. Some had been further treated with aqua regia, and also with HF to remove silicates. This acid leaching, however, may have produced changes in the concentrate grains which could be mistaken for original depositional textures. One such possible occurrence was the replacement of cooperite by a dendritic growth of Pt-Fe alloy in an acid treated concentrate from Union mine. This intergrowth was common in this particular section but was not found in any others. However, other acid treated concentrates displaying cooperite and braggite did not shown any signs of such a replacement. The interpretation of this is, however, dealt with later.

3.4 Mineralogical Methods Employed

3.4.1 Reflected-light Methods. Qualitative observations of the ore in polished sections formed an important part of the study, as only one in every three sections of the ore revealed any platinum group minerals. It should also be born in mind that Schneiderhohn (1929) did not locate one example of a platinum group mineral during his detailed study of these ores. The concentrates enabled the various phases to be characterised, but the concentrate grains were generally free of attached base metal sulphides, and thus paragenetic considerations required their location in the ore. The microscopy was also an essential preliminary to and control on all electron-probe microanalyser work. This instrument is not a substitute for sound ore microscopic observation. Use of it as such by some workers has resulted in false analyses, particularly in the case of fine intergrowths of minerals of similar composition e.g. kotulskite - merenskyite intergrowths, and braggite-cooperite intergrowths.

Spectral reflectivity measurements at the internationally recommended wavelengths of 470, 546, 589 and 650 nm were obtained with the Reichert reflex spectral microphotometer, which incorporates a photomultiplier tube and wedge dielectric filter. A description of this instrument together with the results of standardization experiments are given by Santokh Singh (1965). This instrument enabled rapid and accurate spectral reflectivity measurements to be made on areas down to 1 μm diameter. In the present context the size of the area used for any particular mineral grain corresponded to the maximum flawless and flat area available and

ranged from 1 to 24 μm in diameter. In the case of the bismuthotellurides the rarity of grains of a suitable size and having a flat area limited the number of reflectivity measurements that could be made.

The standards used varied as the investigation progressed. For cooperite and braggite a secondary standard was used. This had been calibrated against N.P.L. Measured pyrite by Millman (pers. comm.). For laurite and the bismuthotellurides the author is grateful to S.H.U. Bowie for the loan of an N.P.L. Measured pyrite (N.1915.1), and also for the loan of N.P.L. Measured silicon standard (N.2538.36) for prassoite and zappinite.

Indentation Microhardness values were obtained with a Durimet hardness tester fitted with a Vickers diamond, as described by Young and Millman (1964). Some later measurements were done with the pneumatically loaded Vickers hardness tester. The problems of measurement are dealt with under the respective mineral descriptions.

3.4.2 X-ray Diffraction. In this particular investigation a procedure was required which would enable a very small (0·3-0·01 mm) and previously analysed grain to be extracted, with minimum contamination from the enclosing silicates and sulphides, and to be suitably mounted for X-ray powder analysis. A steel needle, a tungsten carbide pick, and a microdrill were found too unmanageable and not practical for extracting such small grains. However, by using a diamond marker in the way described by Williams (1962) it was found that with practice very small areas can be pulverized with some precision. A method suggested by A. P. Millman (pers. comm.), which entails using the Leitz Durimet microscope fitted with a standard

Leitz wedge-type scratch diamond, was found to have a much greater precision of positioning. The problem of picking up the very small quantity of powder which results from this method of extraction was solved by the author (1966) as follows.

The diamond, after being lowered on to the required spot, is moved, using the micrometer stage, in the opposite direction to the normal one used for scratch purposes. A mound of mineral powder is formed at the end of the scratch, the length of which can be very precisely controlled. The mineral powder is mounted as follows: a clean glass slide is taken and a spot of 'Cow' gum or other rubber solution is allowed to adhere to it; the slide is then inverted and held over the polished section whilst still observing the powdered area under the ore microscope with a low-power objective (some refocussing is required because of the intervening glass slide); the rubber-cement spot, which can now be seen through the back of the glass, is lowered on to the powdered area to engulf the fragments of broken mineral. After a short while the solvent begins to evaporate and the cement can be rolled into a ball containing the mineral powder. The slide and adhering rubber ball are then raised from the surface of the polished section. Further grinding of the powder can be accomplished between two slides, as described by Hiemstra (1956), followed by the mounting of the ball on the end of a glass fibre. The ball should generally not be greater than 0·5 mm in diameter. The larger the ball the more scattering of X-rays occurs with consequent fogging of the film. An X-ray photograph of a globule of pure cement should be taken first since some varieties yield lines in the front reflection region.

Before destroying the rare mineral grains in the case of the bismuthotellurides some preliminary experiments, similar to those by Hiemstra (1956), and Genkin and Korolev (1961), were carried out on cleavage fragments of galena to determine approximately the minimum quantity of material required to produce a distinct powder patter. It was found that a cleavage fragment of dimensions 0·06x 0·05x0·025 mm and of approximate weight 0·6 µg produced a weak but measurable pattern.

3.4.3 Electron-probe Microanalysis

For most of the electron-probe microanalyser work a Cambridge Microscan Mark 1 was used. This is a scanning analyser with a vertically incident electron beam and X-ray detection at an angle of 20° to the surface of the specimen. It does not have paraxial optics, but positioning is facilitated by the use of a back-scattered electron image also obtained at an angle of 20° to the surface. The counts for the characteristic radiation are detected with a semi-focusing spectrometer that incorporates a flow-proportional counter with a 'dead time' of 5 µsec. A pulse-height analyser is used for discrimination against unwanted noise while scanning photographs are being taken, but it is rarely used while counting in order to avoid errors due to pulse-height depression.

The count rates were corrected for statistical errors due to the 'dead time' of the electronics, and also for counts due to the background radiation. The apparant mass percentages given by these count rates were in most cases further corrected for absorption, fluorescence, the effect of the difference in atomic number, and overvoltage. These corrections were done graphically

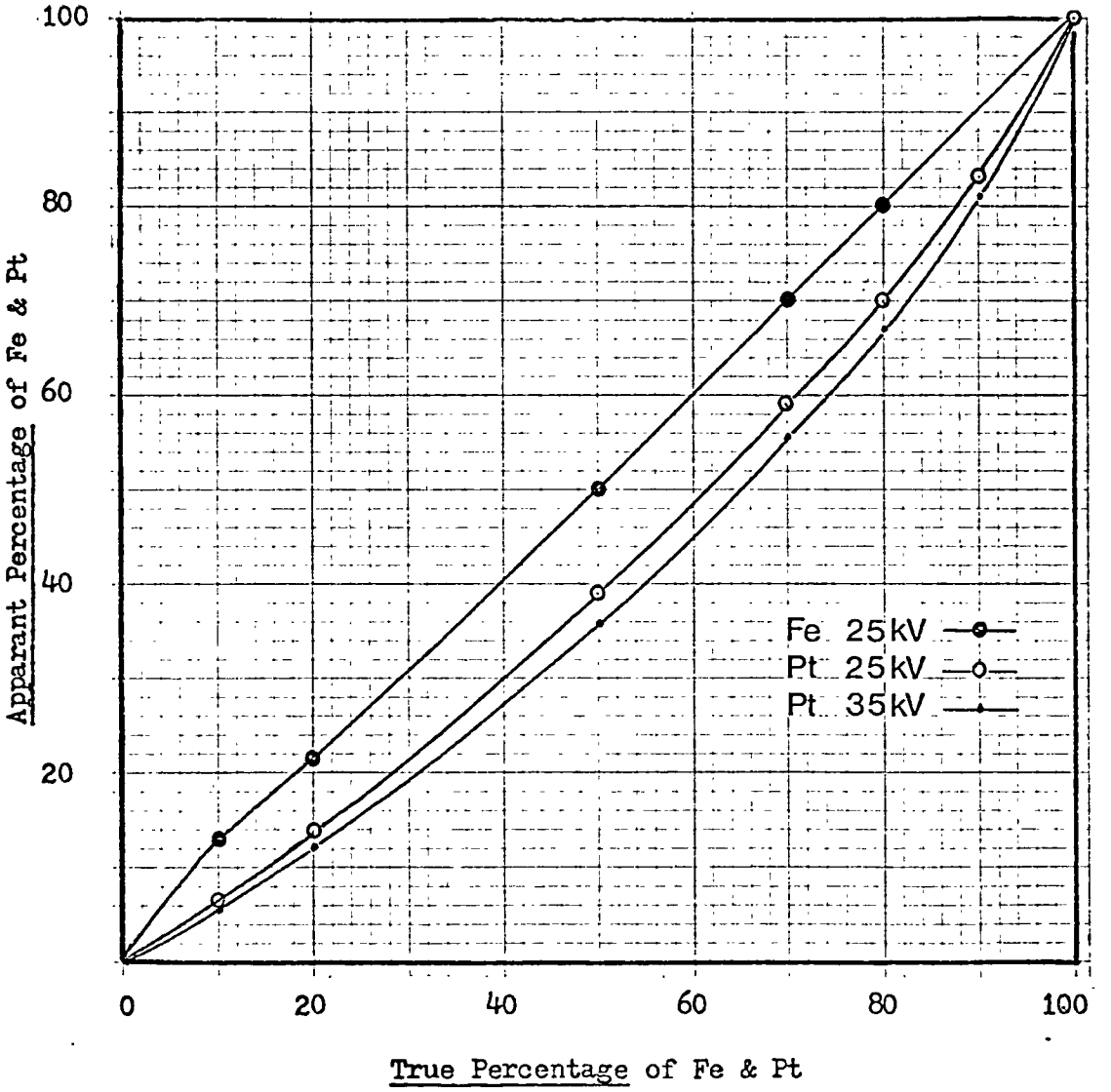

Fig. 3.3 Matrix correction curves for the electron-probe microanalysis of platinum-iron alloys.

in the case of Pt-Fe alloy analyses, and numerically for the others.

Pt-Fe-Alloy analysis. At the start of the whole investigation, the natural and artificial Pt-Fe alloys were the first to be studied. At that time, although there were various methods available for the theoretical correction of absorption and electron penetration, there were no methods available to correct for the effects of fluorescence, atomic number, and overvoltage. Much early and unpublished work was done by Kelly, Millman, and the author on the theoretical aspects of correction, particularly with regard to mass absorption coefficients (Kelly, 1966), and the Pt-Fe system. It is not now relevant to present these results here. However, a study of artificial Pt-Fe alloys at that time indicated that an early solution to the problem of the inadequacy of the available theoretical corrections was not imminent. Therefore, in order to proceed with the mineralogical study of these alloys the only solution was to use a graphical correction. The correction curves of apparant percentage against true percentage at 25 and 35 kV are given in figure 3.3.

Platinoid bismuthotelluride analyses were completed at a later date when a reasonably good matrix correction procedure had evolved. Absorption was corrected for by a method by Philibert (1962); fluorescence by using Castaing's formula (1951); the effect of difference in atomic number by using Ziebold's method (1964); and overvoltage by using a modification to Philibert's formula made by Duncumb (1964). Background fluorescence effects were ignored. The values of the absorption coefficients were those given by Kelly (1966). Table 3.3 illustrates the effect of these corrections. It is noteworthy that the absorption correction is by far the most

important.

Table 3.3 The effect of theoretical matrix corrections on the apparant mass percentages for the platinoid bismuthotellurides merenskyite (1) and kotulskite (2).

Element	Apparant Mass %.	Corrections		
		Absorption	Atomic No.	Fluorescence i.e. Final %
Pd (1)	40.7	35.6	34.0	33.2
(2)	56.8	48.8	46.6	45.9
Te (1)	54.0	57.4	56.6	56.3
(2)	32.1	38.8	38.3	38.0
Bi (1)	15.7	16.3	18.2	15.1
(2)	18.3	18.9	21.1	17.2

Rhodium sulphide analyses were corrected using the internationally accepted B.M.-I.C.-N.P.L. computer programme by Frost, Mason, and Reed (1969).

Other analyses have only been corrected for absorption. The results are, however, considered satisfactory for purposes of mineral identification, and to determine the nature of any substitutional trends.

CHAPTER 4

THE BASE METAL SULPHIDES

The main base metal sulphides at Rustenburg and Union mines are pyrite, pyrrhotite, pentlandite, and chalcopyrite, the latter occasionally containing exsolved cubanite, valleriite, and mackinawite. Co-Ni-Fe arsenides like niccolite and skutterudite are known to be present, are very rare, and have not been studied in any detail. Bornite, chalcocite, galena, and sphalerite are similarly of rare occurrence.

Two recent independent abundance estimates by J.C.I. company geologists (in Vermaak and Hendriks, 1976) of the sulphide content of the ore at Rustenburg mine are 2.9 and 1.89 [1] vol.% the latter being estimated from ten chemical analyses of the ore, and corresponding to volume percentages of pyrrhotite 0.77, pentlandite 0.38, chalcopyrite 0.35, and pyrite 0.39, equivalent to 1.09, 0.61, 0.45, and 0.60 weight percent respectively. An idea of the sulphide proportions in the Reef pyroxenite are provided by Liebenberg (1970) for Rustenburg mine with average volume percent values of pyrrhotite 46.9, pentlandite 32.3, chalcopyrite 17.1, pyrite 3.4, cubanite 0.5, and mackinawite 0.2. No specific data are available for Union mine. However, ore microscopic observations suggest the proportions to be similar. Available data (in Vermaak and Hendriks 1976, and by Brynard et al, 1976) indicate relatively constant proportions throughout the western Bushveld as a whole, with an average pyrrhotite: pentlandite: chalcopyrite: pyrite

---

Footnote (1) recalculated from weight percent data.

ratio of approximately 10:8:3:1. Rustenburg mine is approximately 10:7:4:1. Marked variations can be expected. For example at Atok mine in the eastern Bushveld, pyrite is the main sulphide (Schwellnus et al, 1976) forming 45 vol.%, with chalcopyrite 30, pentlandite 13, pyrrhotite 8, and violarite 4.

The textures, mineralogy, and paragenesis of the base metal sulphides in the Merensky Reef of the Rustenburg district was first studied by Schneiderhohn (in Wagner 1929, pp. 207-215,239-246). Because of the relatively consistent mineralogy of the interstitial sulphide aggregates, his account has not been rendered obsolete by later accounts, although new data can be found in the hundred pages of Liebenberg's account of the sulphide mineralogy of the whole Mafic Zone, and additional observations in publications on the Merensky Reef by Kingston (1966), and Schwellnus et al, Brynard et al, and Vermaak and Hendriks (1976). Much additional data is no doubt hidden in the files of the mining companies, as indicated by Vermaak and Hendriks during their frequent references to unpublished and unavailable company reports.

4.1 General Textural Features

The large scale structural features of the orebody have already been dealt with in chapter 2. On a hand-specimen and polished section scale the textural relationships between the silicate-oxide aggregates and the interstitial sulphides are essentially the same as those seen in disseminated ores of basic magmatic sulphide deposits throughout the world. Thus essentially the textures have been produced by the entrapment of base-metal sulphide droplets in the interstices of a cumulus aggregate of silicate and

oxide crystals which were progressively modified by postcumulus enlargement, overgrowth, and alteration by reaction with residual pore liquid. Reaction between the sulphide droplets and the silicates produced reaction products, mostly hornblende in the case of pyroxenes and biotite in the case of plagioclase according to Schneiderhohn. The hornblende and biotite are orientated crystallographically with the minerals from which they have developed. The sulphides are intimately intergrown and interfingered with these reaction minerals. Subsequent crystallisation of the sulphide droplets and any residual silicate liquid gave rise to residual pneumatolytic and then hydrothermal fluids which caused further alteration of the silicates, as well as some very minor redistribution of sulphides and platinum metals. Most of this latter alteration is embraced by the term serpentinisation.

As a result of the process of entrapment and fractional crystallisation, much of the ore consists of scattered isolated irregular interstitial aggregates of BMS of 1 mm to several centimetres across. Where the proportion of the sulphides is high they may join and poikilitically enclose the silicate grains. Where these poikilitic patches (up to 10 cm across) occur they usually correspond to the finer grained pyroxene aggregates between the coarser pegmatitic 'clots'. Richer accumulations have resulted in the rare footwall sulphide pegmatites.

Most of the interstitial base-metal sulphide aggregates consist of an irregularly shaped pyrrhotite core enclosed by pentlandite exhibiting its characteristic polygonal fracture pattern. The pentlandite may be separated completely or in part from contact

with the enclosing silicates by chalcopyrite. Rarely is chalcopyrite in direct contact with pyrrhotite. Exsolution flames of pentlandite occur within the pyrrhotite, and often flame-like projections occur at the contact of pyrrhotite with the enclosing granular pentlandite 'mosaics'. Pyrite is mainly found within the pyrrhotite, and displays varying degrees of replacement by the latter, appearing as small ragged inclusions to partly replaced euhedral crystal aggregates. It also occurs as subhedral to anhedral grains in pentlandite and at the pentlandite-pyrrhotite contact. Exsolution laths of valleriite, cubanite, and especially mackinawite may occur in the chalcopyrite. Platinum group minerals are found mostly near or at the margins of the BMS aggregates, although platinum-iron alloy and cooperite in particular do occur centrally.

The effect of early entrapment of the sulphide droplets by cumulus silicates and chromite, and later entrapment by adcumulus growth, may be seen as fine disseminations of minute rounded specks within the silicates, notably plagioclase, or along the margins of the silicate grains. Veinlets of sulphides can also be seen, even in hand specimens, to penetrate outwards from the interstitial aggregates. Many of these are composed almost entirely of chalcopyrite, the latest main product of fractional crystallisation, whilst others have clearly resulted from the original BMS liquid which has migrated outwards into fractures and cleavage planes. The author finds no necessity to invoke the "tectonic remobilisation" or "partial redistribution" of already crystallised sulphides to account for these veinlets, particularly the chalcopyrite-rich ones, as is currently being proposed by Vermaak and Hendriks (1976) and Stumpfl

(1976) respectively, especially as the Merensky Reef is noted for its lack of tectonic deformation and metamorphism. The deposition of sulphides, together with some solution and redeposition of early formed material, by residual hydrothermal fluids derived from the differentiation of all intercumulus liquid (sulphide and silicate-oxide) can be considered to explain other types of primary depositional textures and mineral assemblages in the ore. For example serpentinization has mostly obliterated the original sharp contact between the silicates and the sulphides (figs. 4.1 and 6.6 etc).

4.2 Mineralogy and Microtextures

4.2.1 Pyrite - Pyrrhotite Intergrowths

Although Schneiderhohn (in Wagner, 1929) reported that pyrite at Rustenburg was nickeliferous, only trace amounts were detected in the present study, and at Western Platinum mine Brynard et al (1976) only detected 0.4 wt.% Ni and 0.3 wt.% Co. The reflectivity and colour of Rustenburg pyrite are certainly consistent with a low Ni and Co content. However, there are four forms of occurrence of pyrite in the ore and the composition above only refers to the most dominant one.

The average composition of the main hexagonal form of pyrrhotite in the ore has been determined by Ramsden and Wilmshurst (in Vermaak and Hendriks, 1976) as Fe 59.9, Ni 0.2, Co 0.1, and S 37.9 wt.%, copper was not detected. Vermaak and Hendriks also refer to "nickel-rich pyrrhotite which occurs either as entrainments within ordinary pyrrhotite or along its gangue contact". Brynard et al have provided two electron-probe microanalyses of what they consider to be hexagonal and monoclinic pyrrhotite. Their

analyses show Ni and Co contents of 0.5-0.6, and 0.3-0.4 weight percent respectively in both.

Pyrite dominantly occurs at Rustenburg and Union mines in a matrix of pyrrhotite, and is invariably replaced by it to varying degrees. All stages of its replacement by pyrrhotite can be found, from large euhedral inclusion-free rectangular pyrite crystals and aggregates, which may exhibit some corrosion features, to its complete replacement by a granular 'mosaic' pyrrhotite (figs. 6.6, 4.3, 4.1, 4.2). The first stage was the formation of embayments and the 'rounding off' of corners, with the overall crystal outline still being retained. This is considered to have been produced by magmatic corrosion by the remaining sulphide liquid after crystallisation of the pyrite. It is noteworthy that the pyrrhotite in the embayments is in optical continuity with the enclosing pyrrhotite. The remaining stages of replacement by pyrrhotite are believed to have resulted from a process of desulphurisation after the crystallisation of the pyrite-inclusion free pyrrhotite, and pentlandite.

In the initial stages of this pyrite breakdown extensive pyrrhotite veining was developed, forming an irregular rectangular network (fig. 6.6). The veins, which have careous margins and display an irregular thickening at their intersections, are clearly formed by replacement, and a crystallographic control of it exists (notably along the 100 & 111 planes). Under crossed nicols the pyrrhotite veins are granular and not optically continuous with the enclosing pyrrhotite. The degree of pyrrhotite veining varies greatly in different sections and in different interstitial aggregates within a section. Figure 4.3 illustrates a more advanced stage

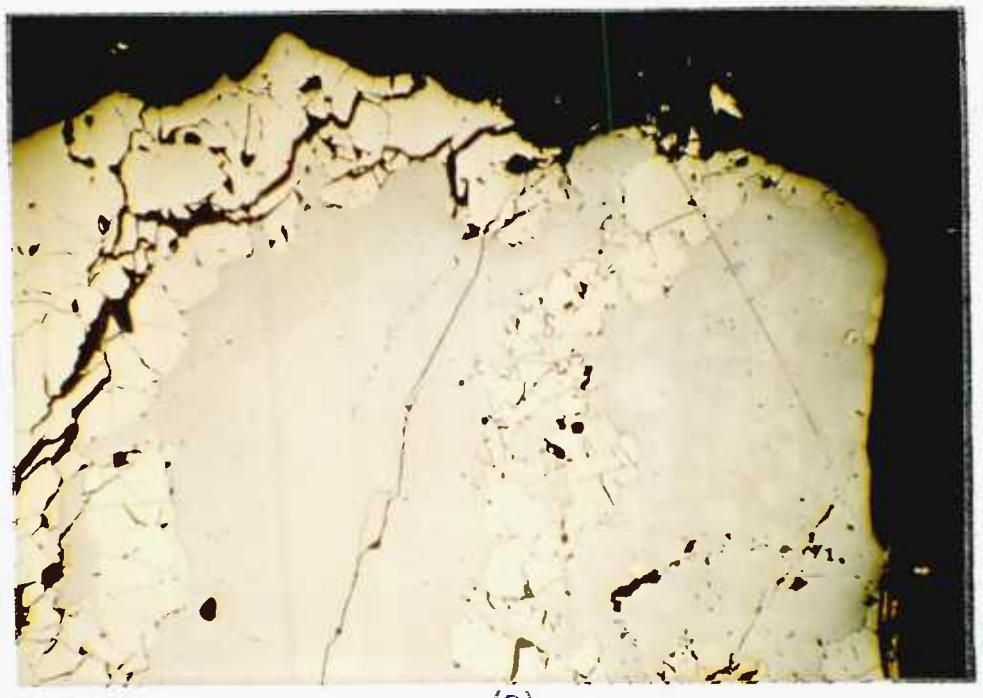

(a)

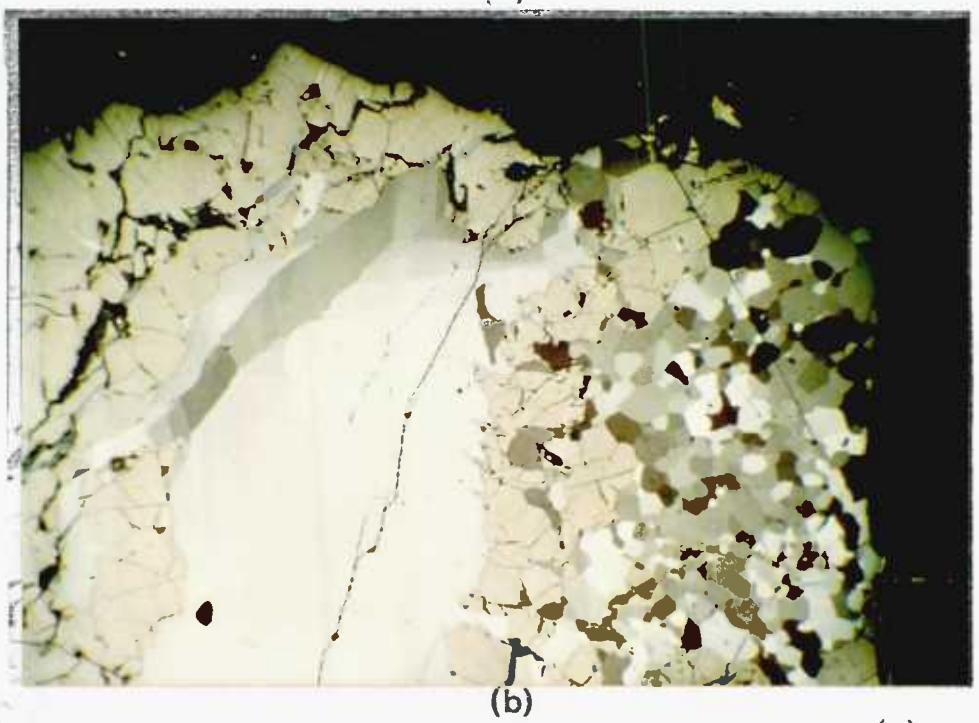

(b)

Fig. 4.1 Two photomicrographs under plane polarised light (a), and under crossed nicols (b), showing the structure and typical distribution of pyrrhotite and pentlandite in an interstitial sulphide aggregate at Rustenburg mine, as well as their irregular and embayed boundary relationship, the characteristic shrinkage partings and fractures of the marginal pentlandite, and the typical separation of fine granular 'mosaic' pyrrhotite from the coarse pyrrhotite by intervening pentlandite. Scale 1 cm =180 µm.

(a)

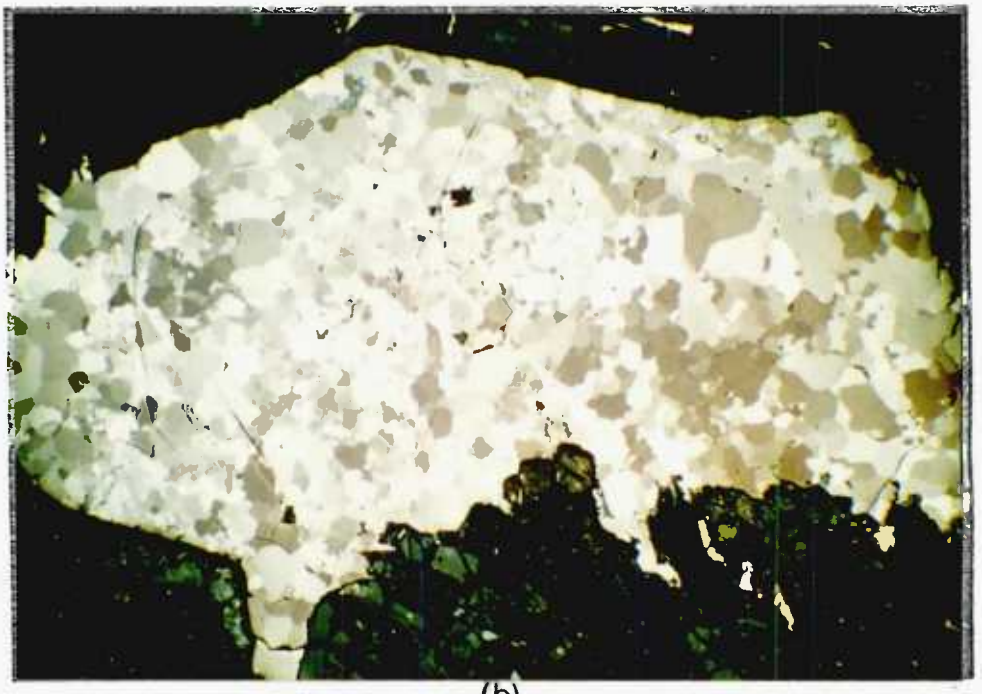

(b)

Fig. 4.2 Photomicrographs of polished section under PPL (a) and XN (b) showing ragged residuals of pyrite enclosed in a granular interlocking aggregate of anhedral pyrrhotite grains which are considered to have been formed by the replacement of pyrite. The pyrite originally filled the whole silicate interspace. The patchy nature of the crystalline pyrrhotite suggests a re-crystallisation process was involved. Rustenburg mine. Scale 1 cm = 180 μm.

a

b

Fig. 4.3 Photomicrographs of polished section under PPL (a) and XN (b) showing an early stage in the formation of 'mosaic' pyrrhotite from the replacement of pyrite, and the typical separation of it from the adjacent coarse pyrite-inclusion-free pyrrhotite by granular pentlandite. Rustenburg mine. Scale 1 cm = 60 µm.

of replacement, the development of the mosaic pyrrhotite and the separation from the pyrite-free pyrrhotite by pentlandite. In the stage before complete replacement the pyrite occurs as illustrated in figure 4.2a. This shows a case where a pyrite crystal or aggregate, whose shape had been controlled by the interstitial space it filled, has been nearly completely replaced, and only 'wispy' ragged pyrite inclusions remain. The granular structure of the resulting 'mosaic pyrrhotite' is well illustrated in figure 4.2b.

The existence and consistent structure of these 'mosaic pyrrhotite' areas resulting only from pyrite replacement, and the fact that they are always separated from the large pyrite-inclusion free pyrrhotite areas by pentlandite, is evidence that this replacement could not have been produced by pyrite resorption by an enclosing sulphide liquid from which pyrrhotite subsequently or simultaneously crystallised. The replacement process is considered to have involved solid diffusion of sulphur atoms out of the system with simultaneous recrystallisation perhaps activated by internal or externally imposed strain. Whatever the exact mechanism of this replacement it is at least certain that this pyrite was the first of the base-metal sulphides to crystallise. At Union mine this pyrite is rarer and shows less replacement by pyrrhotite, and a greater euhedralism than at Rustenburg mine.

Finally, complex myrmekitic intergrowths of pyrite with pyrrhotite and chalcopyrite are very common in the banded sulphide pegmatite previously described. These still remain to be studied. The apparant absence under the microscope of visible platinum group minerals to account for the very high assay values is a further prob-

lem with regard to this body.

4.2.2 Pyrrhotite - Pentlandite Intergrowths

The composition of the marginal granular pentlandite is reported by Vermaak and Hendriks as being Fe 32.95, Ni 33.5, Co 0.9, and S 31.85, with copper not detected. The composition of the feathery exsolution lamellae in pyrrhotite have not been determined. Pentlandite from Western Platinum mine has a composition range from three electron-probe microanalyses (Brynard et al, 1976) of Fe 32.8, 33.3, 35.8, Ni 35.2, 32.3, 34.3, Co 0.8, 0.8, 0.8, and S 31.8, 31.6, 32.1, weight percent.

Most of the pentlandite occurs as granular shells rimming large irregular-shaped pyrrhotite cores of 'mosaic pyrrhotite, and pyrite-inclusion free pyrrhotite. The nature of the boundaries between pentlandite and pyrrhotite is well illustrated in figure 4.1b, and suggests some resorption of pyrrhotite. These features together with a pyrrhotite:pentlandite ratio of at least 10:7 points to the direct crystallisation of pentlandite from the sulphide melt after pyrrhotite. This pentlandite is also a good example of the well established volume reduction which takes place on cooling to produce octahedral partings and cracks, giving it a granular appearance. These shrinkage partings are filled with serpentine, chlorite, calcite and other hydrothermal products precipitated by the activity of residual fugitive constituents. The partings and cracks terminate abruptly against the pyrrhotite cores.

Exsolution 'flames' of pentlandite occur in the pyrrhotite, but are not common. These 'flames' were seen at twin boundaries, where a classic 'herring-bone texture' was produced, adjacent

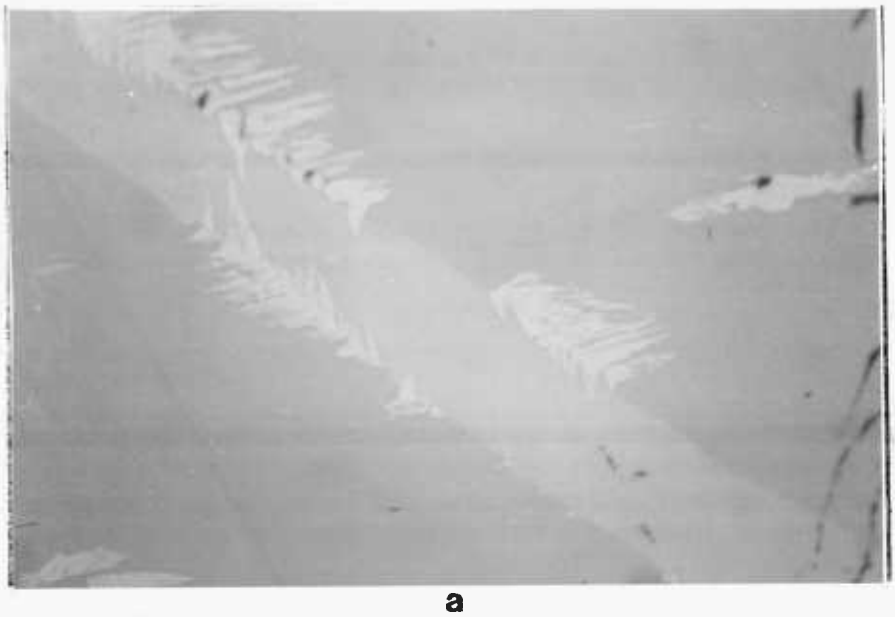

a

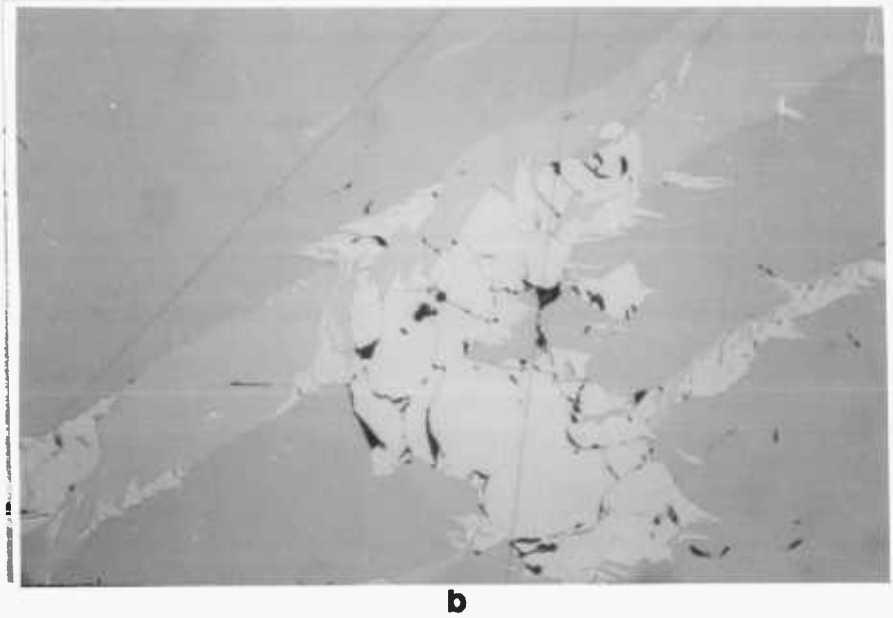

b

Fig. 4.4 Photomicrographs of a polished section under PPL showing exsolution 'flames' of pentlandite in pyrrhotite along (a) pyrrhotite twin planes producing a 'herring-bone texture', and (b) along pyrrhotite twin planes and the boundary of granular pentlandite with pyrrhotite. Rustenburg mine. Scale 1 cm = 15 μm.

to fractures filled with gangue, and also at the pyrrhotite margins (fig. 4.4). In all cases shrinkage cracks were absent. Pentlandite 'flames' were also found in chalcopyrite which was replacing pyrrhotite along grain boundaries (fig. 4.5). Pyrite was also a product of this replacement.

Pentlandite often encloses deeply corroded grains of pyrite. Pyrite enclosed by chalcopyrite is rare. Where the ore has been subjected to supergene influences pyrrhotite is often partially or sometimes completely replaced by a 'bleached' variety which pervades the primary pyrrhotite along the cleavage planes. This 'bleaching' is also to be seen in the 'mosaic' pyrrhotite in which a halo of lighter pyrrhotite is found round each grain. As a result of this change, particularly in the case of the large optically continous areas, shrinkage has occurred along the cleavage planes which have been infilled with transparant gangue material.

4.2.3 Chalcopyrite Intergrowths

The chalcopyrite is the last formed base-metal sulphide of the "liquid magmatic stage" of sulphide fractional crystallisation envisaged by Schneiderhohn (1929). It is consequently found at the margins of the sulphide aggregates in contact with the silicates and separated from the pyrrhotite 'cores' by pentlandite. It rarely completely rims these aggregates but is often concentrated as one or two marginal patches, so that pentlandite is commonly in direct contact with the silicates. The chalcopyrite corrodes and penetrates the granular pentlandite and may completely enclose some grains. As reported by Schneiderhohn it is also found in the interior of the sulphide aggregates following the intergranular bound-

aries (fig. 4.5). Because a high proportion of the platinum group minerals appear to have formed near or at the silicate contact of the sulphide aggregates, they are often found partly or completely enclosed by chalcopyrite. Where fractured hard platinum group minerals like braggite occur at the margin, the fractures are filled with chalcopyrite and later silicates. Platinoid bismuthotellurides are particularly concentrated in chalcopyrite. The chalcopyrite penetrates into the cleavages of the enclosing silicates and is also found as a major filling constituent of microveinlets along silicate fractures and grain boundaries.

With regard to its composition Schneiderhohn reported traces (0.00001 wt.%) of cobalt and nickel from an arc spectrographic analysis of material extracted directly from the polished section. A recent electron-probe micrcanalysis (Vermaak and Hendriks, 1976) detected only the major elements Cu 33.7, Fe 30.5, and S 33.1 wt.%.

The other important intergrowths of chalcopyrite are with mackinawite, a brown valleriite-type phase, and cubanite.

Mackinawite is defined as a tetragonal FeS with up to 15 atomic % substitution of Fe by Ni, Co, and/or Cu (Uytenbogaardt & Burke, 1971). It was first named by Evans et al (1962,1964), although several occurrences of this mineral had been described earlier but confused with valleriite (Liebenburg, 1970). At that time the published properties of valleriite were confusingly largely those of mackinawite. Birks et al (1959) provided the first electron-probe microanalysis of type mackinawite, giving Fe between 51-58 wt.%, Cu less than 5 wt.%, and sulphur assumed as the rest. Kouvo

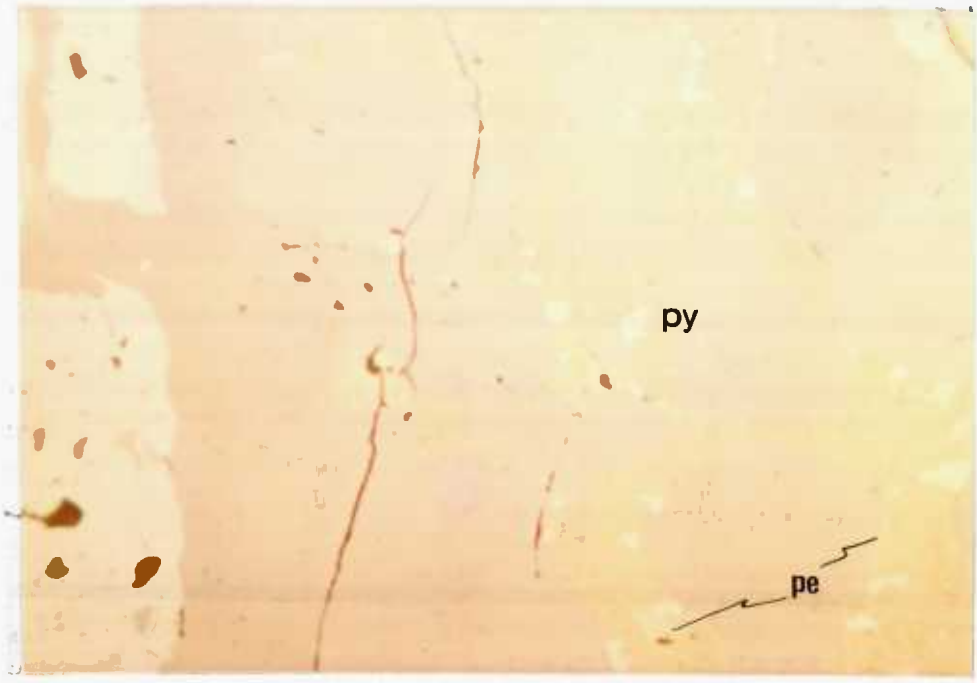

Fig. 4.5 Polished section photomicrograph under PPL showing chalcopyrite, containing small 'flames' of pentlandite (pe) and wisps of anhedral pyrite (py), occuring as intergranular veins in pyrrhotite. Rustenburg mine. Scale 1 cm = 40 µm.

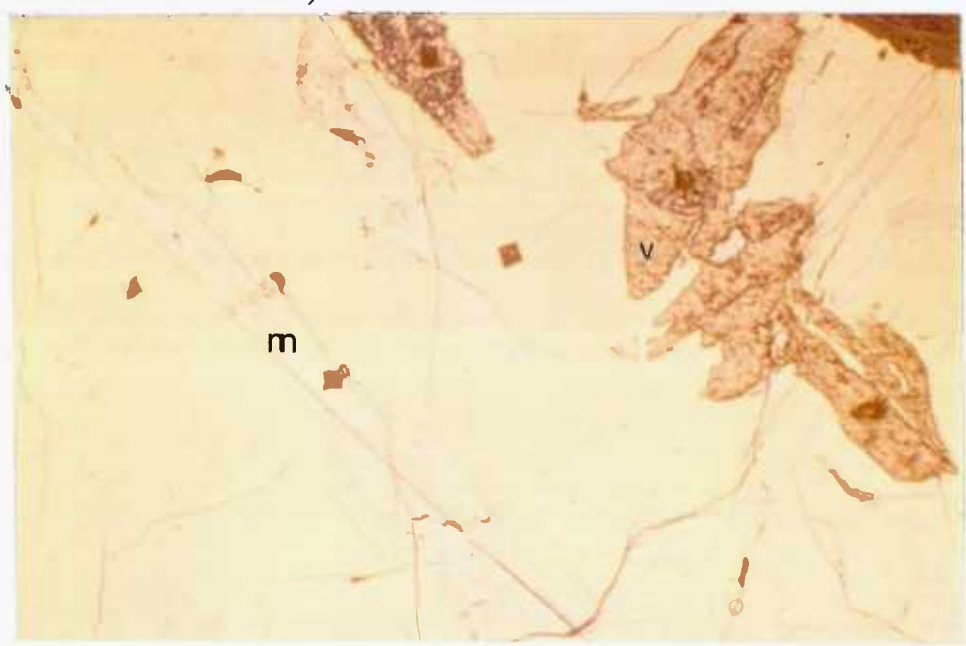

Fig. 4.6 Polished section photomicrograph under PPL showing ragged orientated laths of mackinawite (m) and a 'valleriite-looking' phase (v), of the same composition as mackinawite, enclosed along the margin of chalcopyrite with altered primary silicates. Rustenburg mine. Scale 1 cm = 40 µm.

Fig. 4.7 Polished section photomicrograph under PPL showing mackinawite as small branching replacement bodies after pentlandite. Rustenburg mine. Scale 1 cm = 15 µm.

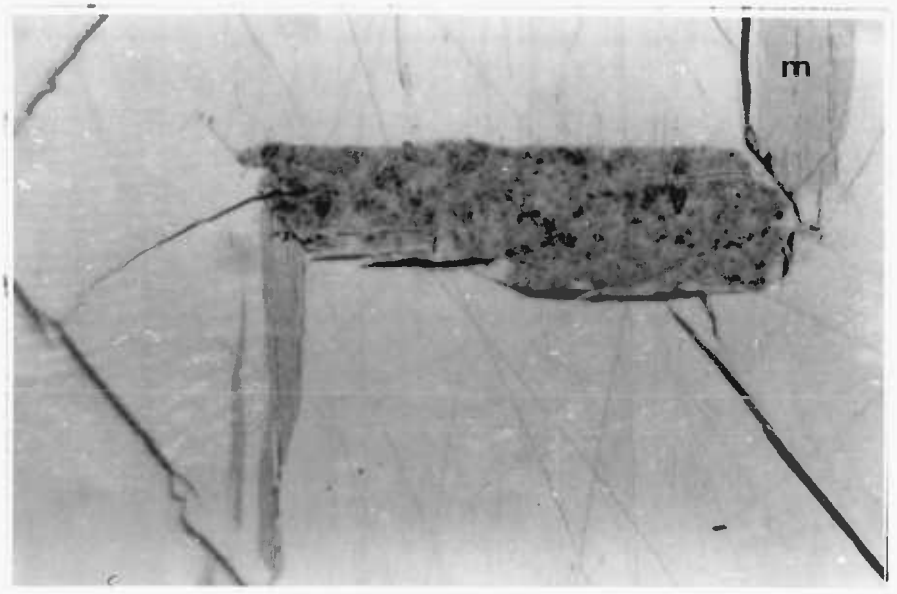

Fig. 4.8 Polished section photomicrograph under PPL showing a lath of 'valleriite-looking' iron sulphide (v) with 5-6 wt.% Ni and up to 6 wt.% Cu, occurring in chalcopyrite, and apparantly resulting from the replacement of mackinawite (m) by inversion, since there is no compositional difference between them. Rustenburg mine. Scale 1 cm = 15 µm.

et al (1963) recorded it in several Finnish orebodies and gave X-ray diffraction, wet chemical analysis and electron-probe microanalysis data which showed it to be tetragonal (Fe, Ni, Co)S with Fe 64-54, Ni 0.2-8, and Co< 0.2 - 11 wt. percent. This data was in agreement with that of Evans et al which first became available as an abstract of a verbal presentation in 1962. Their analysis detected no copper, and they determined the structure as tetragonal with a 3.68, and c 5.03 Å, and a space group $P4/nmm$ containing 2FeS.

Schneiderhohn (1929, pp 213,217,218) gave comprehensive details of an 'unidentified ore mineral' in the Merensky Reef occurring as orientated inclusions in chalcopyrite, which were very strongly pleochroic from "bright yellow with a pink tint to dark grey". A spectrographic analysis by him gave major iron and nickel, minor cobalt and palladium, and trace iridium, antimony, silver and gold. Despite the precious metals in his analysis, his description of its properties and forms of occurrence strongly suggest mackinawite. The author subsequently reported mackinawite in the Merensky Reef in 1966, although the X-ray powder data and electron-probe microanalyses were not given. The analysis of two laths of mackinawite from Rustenburg mine gave, after correction for absorption, Fe 50.0, 56.0, Cu 6.0, 0.4, Ni 5.0, 6.0, and S 32.0, 36.0 weight percent. The X-ray data is given in table 4.1. The poor correlation with data by Kouve et al (1963) requires further investigation. No previous electron-probe or X-ray diffraction analyses have been reported for Rustenburg mackinawite.

Table 4.1 X-ray powder diffraction data for Rustenburg 'mackinawite' (Co radiation), compared to mackinawite from Outokumpu mine by Kouvo et al (1963).

Rustenburg		Outokumpu	
I	d (obs)	I	d (calc)
5	5.07	vs	5.03
1	3.90	s	2.97
1	3.54	vw	2.60
10	3.04	s	2.31
2	2.84	m	1.838
2	2.49	m	1.727
3	2.29	w	1.676
2	2.10	mw	1.563
2	1.92	w	1.526
2	1.88	w	1.409
			etc

Rustenburg mackinawite occurs as ragged orientated laths in chalcopyrite (fig. 4.6), commonly at or near the margin with the silicates. Their mode of formation is not clear. When mackinawite occurs in chalcopyrite, a mineral of identical properties to it occurs in the adjacent pentlandite as small dendritic bodies at the junction of and along cleavage partings (fig.4.7). These are definitely replacement bodies. The mackinawite laths are strongly pleochroic from a light pinkish or brownish cream to grey, with a bireflectance of from Rp 36.6% to Rg 40.7% at 589nm. Extinction under crossed nicols is parallel to the long axes of the laths, and its anisotropy is very strong. One reliable indentation

gave a VHN_{25} of 155, within a range quoted by Vaughan (1969) of VHN_{25} 94-181.

A brown 'valleriite-type' phase with a spotted and spongy looking surface (figs. 4.6 and 4.8) and which was distinctly anisotropic, pleochroic from light to dark brown of very low reflectance, and slightly softer than mackinawite, may be the "valleriite" reported by Liebenburg (1970) and others to occur in the Merensky Reef. It appears (fig. 4.8) to have been formed by the replacement of mackinawite, since 'residual' mackinawite areas can be seen as part of it. Some incipient alteration can also be seen in the mackinawite laths along its cleavage. Two electron-probe microanalyses, however, showed that it was of the same composition as mackinawite with Fe 48.0, 53.0, Cu 1.0, 0.5, Ni 7.0, 5.0, S 35.1, 36.2. It is, therefore, not valleriite.

Cubanite is rare in the Merensky Reef chalcopyrite. It occurs as thin orientated exsolution laths. No compositional data is available for it.

4.2.4 Other base metal sulphides

Bornite is rare but can be found in near surface ore as lamellar replacement intergrowths in chalcopyrite. Vermaak and Hendriks (1976) report that most of the bornite occurs either together with pentlandite and chalcopyrite as small crystals in chromite, as relatively large particles in the silicates, or as composite grains with chalcopyrite. They also reported small free grains of chalcocite in feldspar or attached to grains of chalcopyrite.

Sphalerite exsolution 'stars' have been reported in chalcopyrite by Liebenburg, but are extremely rare.

Galena has been reported by Vermaak and Hendriks as clusters of fine crystals in feldspar. They also reported one small grain of bismuthinite intergrown with pyrrhotite in a fracture in a feldspar, and the arsenides niccolite, and skutterudite. The author has located one intergrowth of the latter. Finally, a Bi-Sn-S phase was detected by the author, associated with a silicate inclusion in a myrmekitic intergrowth of two Fe-Ti-(o) phases.

4.3. The paragenesis of the base metal sulphides is intimately related to the paragenesis of the platinum group minerals and will, therefore, be discussed in [redacted] chapter 9. The evidence clearly points to pyrite as the first formed, followed by pyrrhotite, pentlandite and then chalcopyrite. This simple sequence is, of course, complicated by overlapping deposition, exsolution, and replacement. Thus a second generation of pentlandite segregated as exsolution 'flames' from pyrite-inclusion-free pyrrhotite after the main mass of marginal granular pentlandite had crystallised. Mosaic pyrrhotite is also considered to be a second generation pyrrhotite formed from the breakdown of pyrite after pentlandite formation but prior to chalcopyrite. Some redistribution of the sulphides is evident where serpentine veins cut the sulphide aggregates. The suggestion (Vermaak and Hendriks, 1976) that tectonism has been important in mobilising chalcopyrite, pentlandite, and pyrrhotite (in that order) to form veinlets and stringers in the silicates does not agree with the observed lack of post-depositional deformation of the orebody in the field.

CHAPTER 5

PLATINUM GROUP ALLOYS AND INTERMETALLIC COMPOUNDS

5.1 Platinum-Iron Alloys

These are by definition natural mineral alloys composed dominantly of Pt and Fe, with Fe not exceeding 50 atomic percent, equivalent to 22·3 weight percent. The minor amounts of other platinum group elements, which are often present substituting for Pt, rarely exceed 6 wt. per cent total. Similarly the content of metals like Cu and Ni, which substitute for Fe, rarely exceed 8 wt.%. The contents in both cases are usually far less. No examples of an iron-platinum alloy in which Fe significantly exceeds 50 at.% has yet been reported.

5.1.1 The Nomenclature for these alloys has been highly confusing and inconsistent. This was because it was based on composition alone and defined according to weight percent of the various constituents. The result was that minor substitution of other elements gave rise to numerous unnecessary names for essentially the same material. Fortunately the terminology has been rationalised by a study of the composition and crystal structure of synthetic Pt-Fe alloys and their natural equivalents by Cabri and Feather (1975). This new nomenclature has been approved by the Commission on New Minerals and Mineral Names, I.M.A., and dispenses here with the need to review the now obsolete past terminology. The platinum-iron alloys are classified by them as follows:

1. native platinum for disordered face-centered cubic platinum alloys which contain greater than 80 atomic % Pt (i.e.

greater than 93·32 wt.% Pt).

2. ferroan platinum for disordered face-centered cubic platinum-iron alloys which contain from 20 - 50 atomic % Fe (i.e. from 6·68 - 22·3 wt.% Fe). The atomic percent content of any substituting element is included in the value of atomic % of Pt (in the case of Ir,Pd,Rh,Os,Ru,Au,) or Fe (in the case of Cu,Ni,Sb etc). The high-iron varieties will have increasing magnetic susceptibility.

3. isoferroplatinum for ordered primitive cubic platinum-iron alloys with compositions usually near Pt_3Fe (Pt 91·3, Fe 8·7 wt.%). Minor amounts of other platinum group elements are considered as Pt, and minor Cu and Ni etc. considered as Fe. Cold-working may produce ferromagnetism in the mineral and disordering of the structure to face-centered cubic.

4. tetraferroplatinum for ordered tetragonal platinum-iron alloys with compositions usually near PtFe (Pt 77·75, Fe 22·25 wt.%). Minor substitutions of other elements are considered as before. This mineral is weakly anisotropic under oil immersion, and thought to be ferromagnetic.

Finally they propose the term platinum-iron alloy or Pt-Fe alloy for use when only compositional data are known and the structure has not been determined by X-ray diffraction. An equivalent term used by metallurgists and geologists in the platinum mining industry is ferroplatinum.

In the present investigation the structures of the analysed grains were not determined. It is, however, considered most probable that of the large homogeneous grains of Pt-Fe alloy

found in the concentrates, those that are weakly anisotropic, strongly magnetic, and have a high iron content are tetraferroplatinum, and those that are not hand magnetic, isotropic, and of low iron content are isoferroplatinum. The myrmekitic Pt-Fe alloy in pyrrhotite is the most likely candidate for being the disordered variety, ferroan platinum.

However, although it is recognised that a study of the structure of the Pt-Fe alloys in the Merensky Reef would be of value, there are several difficulties to consider. In order to study the genetic relationship between structure and mode of occurrence and paragenetic position, it is particularly necessary to analyse grains in situ, where their paragenetic position can be determined, as well as the influence of any deformation or recrystallisation processes. The difficulty in locating grains in the ore is an obvious drawback. The alternative procedure of studying Pt-Fe alloy concentrates from the mine should take into account the strong possibility of deformation (cold working) of the grains during mineral beneficiation. This could produce a disordering of the primitive cubic structure. Similarly, cold-working effects are very likely to be produced during the extraction of material for X-ray powder diffraction. Finally the high temperature face-centered disordered structure can develop into an ordered primitive cubic or tetragonal structure on cooling (Elcock, 1956), and the present doubt as to whether the disordered phase is quenchable anyway (Cabri and Feather, 1975, p.119) is a further reason why its presence in an ore, and particularly in a concentrate, need not necessarily be related to a primary depositional process.

5.1.2. The Occurrence. Platinum-iron alloy (syn, with ferroplatinum) is the most common alloy form and one of the most abundant platinum group minerals in the Merensky Reef. It is the most common constituent of magnetic fractions of samples of table concentrates from both Rustenburg and Union mines, although, despite the small difference in Pt content between the two mines, it accounts for a greater proportion of the total Pt content of the Union mine than of the Rustenburg mine. Thus at Union mine approximately 70 wt. % of the total platinum mineral content is Pt-Fe alloy, whereas there is only approximately 25 wt.% at Rustenburg mine, with most of the remaining Pt content being accounted for in both cases by cooperite and braggite (Zermatten, pers. comm.) In polished sections of ore specimens, Pt-Fe alloy, as with the other platinum group minerals, is of rare occurrence, and only a few areas showing it intergrown with the base-metal sulphides have so far been located. Fortunately, further information on its mode of occurrence in the ore can be deduced by studying composite grains in polished sections of the concentrates.

Platinum-iron alloy has so far been found to occur at both mines in five main intergrowth forms.

Texture Type I - intragranular myrmekitic intergrowths with pyrrhotite, pentlandite, and chalcopyrite, as in figures 5.1, 5.2 & 5.3.

Texture Type II - intragranular fine and often diffuse spongy intergrowths with pentlandite and chalcopyrite, as in figures 5.4 & 5.9.

Texture Type III - intragranular aggregates of skeletal

'idioblastic' crystals of cubic form in pyrrhotite, pentlandite, and chalcopyrite, as in figures 5.6, 5.7 & 5.8.

Texture Type IV - intragranular fine spongy to graphic intergrowths with cooperite, as in figures 5.11, 5.12 & 6.2.

Texture Type V - homogeneous and relatively large euhedral to subhedral crystals (fig. 5.13 and 5.14) which are usually found as free grains in the concentrates, and rarely with attached base-metal sulphides or other platinum group minerals.

If a quantitative study of the distribution of platinum-iron alloy in the ore is to be of genetic value, then it should distinguish between these various textural types during modal analysis. These types are considered to have resulted from distinctly different formational processes. Vermaak and Hendriks (1976) classified these intergrowths into three types for the purpose of their mineral distribution study. They suggested a general mechanism to account for the occurrence of Pt-Fe alloy with cooperite and pyrrhotite, although they did not relate it directly to the different intergrowth types.

A description of the main features of the textural types is presented below, and an attempt to explain these features and types is presented separately. A discussion of these observations with regard to mineral paragenesis is dealt with in Chapter 9.

Textural Type I includes those intergrowths between Pt-Fe alloy and the base-metal sulphides which can be described by any of the synonymous terms such as graphic (Edwards, 1960), myrmekitic (Ramdohr, 1969, p113-127), or eutectoid (Spry, 1969, p102-103). Although myrmekitic intergrowths can be produced by replacement, the

intergrowths described under Type I are considered to be formed by exsolution. This type is a very common form of occurrence of Pt-Fe alloy in the 'metallic' concentrates, together with Type III with which it often may occur in concentrates as part of the same composite grain or in the same area of an ore section. Pyrrhotite is by far the most common matrix mineral, and occurrences in pentlandite are rare, although homogeneous pentlandite may be attached to some of the concentrate grains. Frequently chalcopyrite and pyrrhotite jointly form the matrix (fig.5.2).

Of all the terms, myrmekitic probably best describes the whole textural form, illustrated by figure 5.1, of a worm-like intergrowth of pyrrhotite and Pt-Fe alloy, with 'graphic' being used to describe only the form of the Pt-Fe alloy. These intergrowths are often so fine as to be hardly resolved, even under the highest magnification in oil. The graphic Pt-Fe alloy pattern varies from being fairly random to being strongly orientated, even within individual concentrate grains. Often a strong orientated wavy or radiating plumose structure occurs across a complete concentrate grain (fig. 5.3), although plumose patches occur within grains (fig. 5.1). Coarser skeletal veins, giving the appearance of a fishbone or backbone, often form an intimate part of the myrmekitic form, and may in part be composed of partly formed euhedral crystals (figs. 5.1 and 5.9). Although these coarser veins laterally interfinger and show an obvious continuity with the finer graphic areas, there is a reduction in the quantity of the finer graphic Pt-Fe alloy in their vicinity (fig. 5.1). This strongly supports a segregation process rather than replacement.

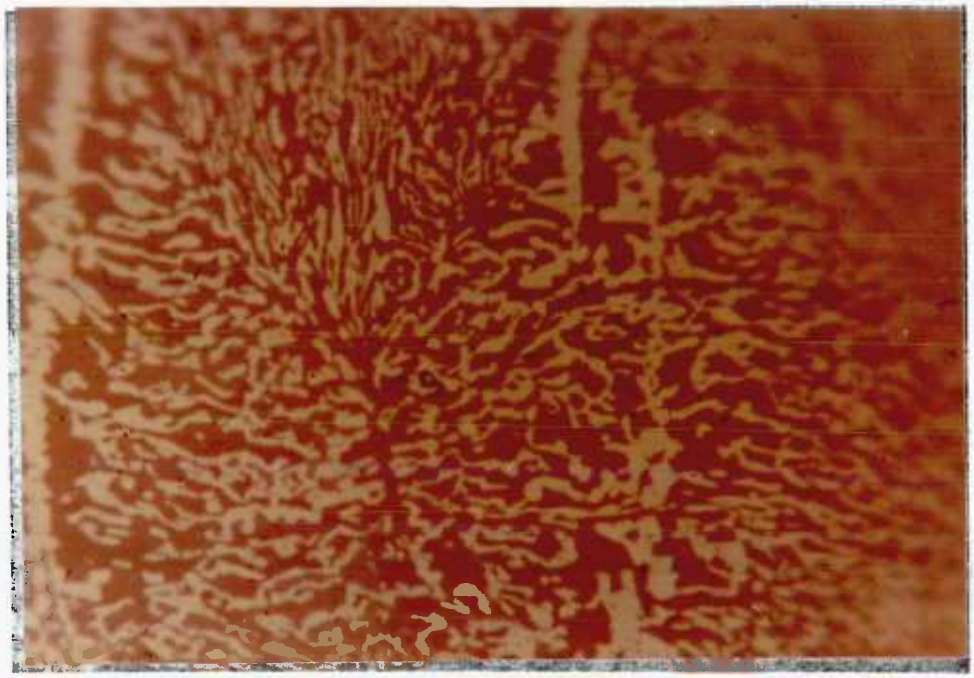

Fig. 5.1 Type I - controlled myrmkitic intergrowth of Pt-Fe alloy with pyrrhotite, showing the common structural components of skeletal veins adjacent to finer radiating plumose areas. High grade concentrate from Union mine. Scale 1 cm = 8 μm.

Fig. 5.2 Type I - random myrmekitic intergrowth of Pt-Fe alloy with pyrrhotite* and chalcopyrite☆, displaying a slight coarsening of the graphic Pt-Fe alloy where enclosed by chalcopyrite. High grade concentrate from Union mine. Scale 1 cm = 18 μm.

The growth structure of the Pt-Fe alloy is particularly well displayed when the myrmekitic grains are leached with acid to remove the matrix base-metal sulphides, as in figure 5.3. Partial leaching of this nature may also occur during mineral beneficiation (fig.5.5.)

A further feature is that the graphic Pt-Fe alloy is contained by either optically continuous pyrrhotite areas or coarse granular pyrrhotite areas. In the latter case the grain boundaries of pyrrhotite can be seen, under crossed nicols, to delimit areas exhibiting different patterns. Thus composite grains may display textural combinations and variations of orientated coarse skeletal veins, plumose or wavy myrmekitic types and random myrmekitic types.

An example of a myrmekitic form in which the matrix sulphide is partly chalcopyrite is illustrated in figure 5.2. In this case the boundary between pyrrhotite and chalcopyrite is highly embayed, and optically matching patches of pyrrhotite are found enclosed by chalcopyrite. The graphic Pt-Fe alloy is slightly coarser where enclosed by chalcopyrite than by pyrrhotite, although the overall 'worm-like' form is the same. This evidence clearly points to selective replacement of pyrrhotite by chalcopyrite resulting in some redistribution and enlargement of the graphic Pt-Fe alloy. It is possible also that trace platinum held in the lattice of pyrrhotite was released during the replacement and contributed to this thickening.

Textural Type II is a rare and spongy-graphic type which has been found in situ. The nature of this type is shown in figures 5.9 a & b. In this example the 'invisible' boundaries delimiting the triangular spongy areas, as well as the Pt-Fe alloy intergrowth

as a whole,are difficult to explain. However, it is significant that within the area of the intergrowth (as outlined in fig.5.9) the pentlandite shows a granoblastic polygonal structure which is emphasised by a dark grey unidentified intergranular film (possibly and oxide). This structure is not present outside the intergrowth area. Each triangular area of spongy Pt-Fe alloy may be confined to a single pentlandite grain, as already described in the case of pyrrhotite. However, since the pentlandite was isotropic it was not possible to test this under crossed nicols. A further feature to note in figure 5.9 is that the skeletal veins of coarse Pt-Fe alloy, which in places resemble texture type III, are separated

Fig. 5.3 Acid leached grain of an original intergrowth of graphic and idioblastic Pt-Fe alloy in a groundmass of a base-metal sulphide (probably pyrrhotite), showing the nature of the radiating plumose structures common to Type I intergrowths. An acid treated and non-magnetic tailings concentrate from Union mine. Scale 1 cm = 30 um.

from the spongy triangular areas by Pt-Fe alloy-free zones, are not related to any microfractures, and are not controlled by the polygonal structure of the surrounding pentlandite. Finally the intergrowth occurs at the pentlandite-silicate contact, and that part which is enclosed

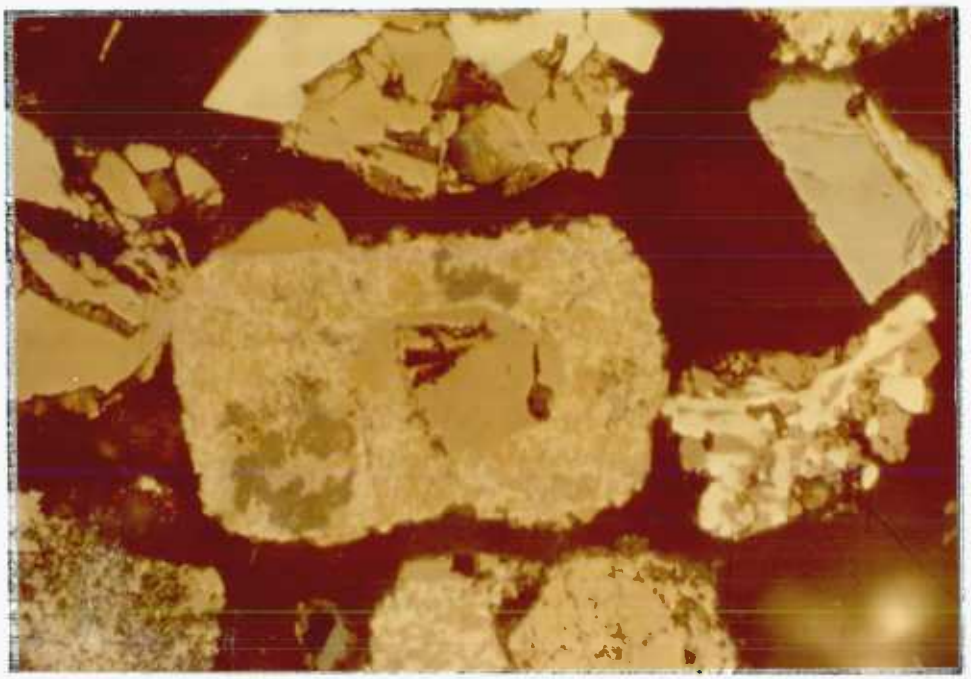

Fig. 5.4 A composite grain (central) showing a euhedral graphic intergrowth of spongy Pt-Fe alloy in chalcopyrite (Type II texture) enclosing a 'barren' subhedral grain of pyrrhotite. A raw high grade concentrate from Union Mine.
Scale 1 cm = 17 μm.

by pentlandite has an angular 'crystalline' outline which is apparantly independent of the pentlandite structure.

A further example of a spongy-myrmekitic type similar to that shown in figure 5.9 is illustrated by the central grain in figure 5.4. In this case the matrix is chalcopyrite, showing a partial replacement by a transparant 'gangue' material, and the spongy graphic intergrowth encloses a central subhedral pyrrhotite grain. The probable euhedral form of the spongy Pt-Fe alloy is indicated by its straight boundary with chalcopyrite to the north, and its rectangular liberated form.

Textural Type III is a common Pt-Fe alloy form in the concentrates (fig. 5.6, 5.7), and like type I is considered to have been produced by exsolution and recrystallisation. The texture consists of aggregates (0.2 – 0.4 mm across) of small euhedral and skeletal crystals which usually exhibit square to rectangular forms of about 20 μm in size, and which are intergrown with a matrix which is most commonly pyrrhotite, and rarely pentlandite and chalcopyrite. The individual Pt-Fe alloy crystals vary in their morphology, and occur as idioblastic homogeneous and matrix-enclosing rectangular to cubic forms (fig. 5.7), partly euhedral forms (fig. 5.6), and skeletal forms showing deeply embayed boundary relationships with the matrix (fig. 5.17). The latter form is similar to the skeletal 'segregation' veins described for type I, except that no myrmekitic form is closely associated. The structure of the Pt-Fe alloy crystals is particularly well displayed in acid-leached concentrate grains (fig. 5.8). An intermediate type, between II and III, is illustrated in figure 5.5. A further feature of type III is that all the idioblastic

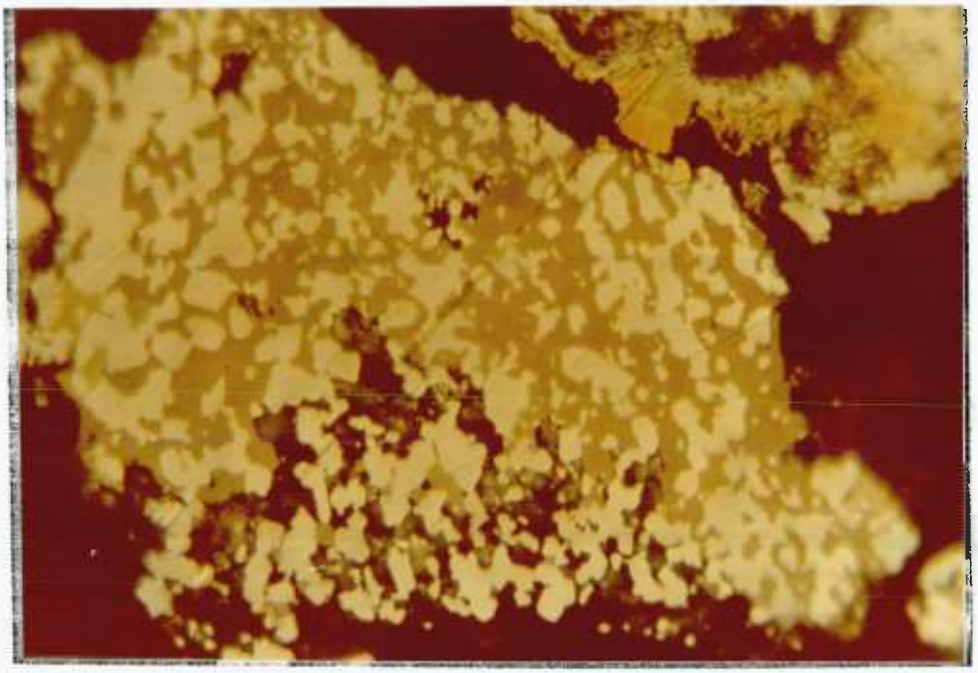

Fig. 5.5 Coarse graphic intergrowth, intermediate between type I and type III, consisting largely of subhedral crystals of Pt-Fe alloy exhibiting cubic forms in a matrix of partly leached pyrrhotite. Raw high grade concentrate from Union mine. Scale 1 cm =17 µm.

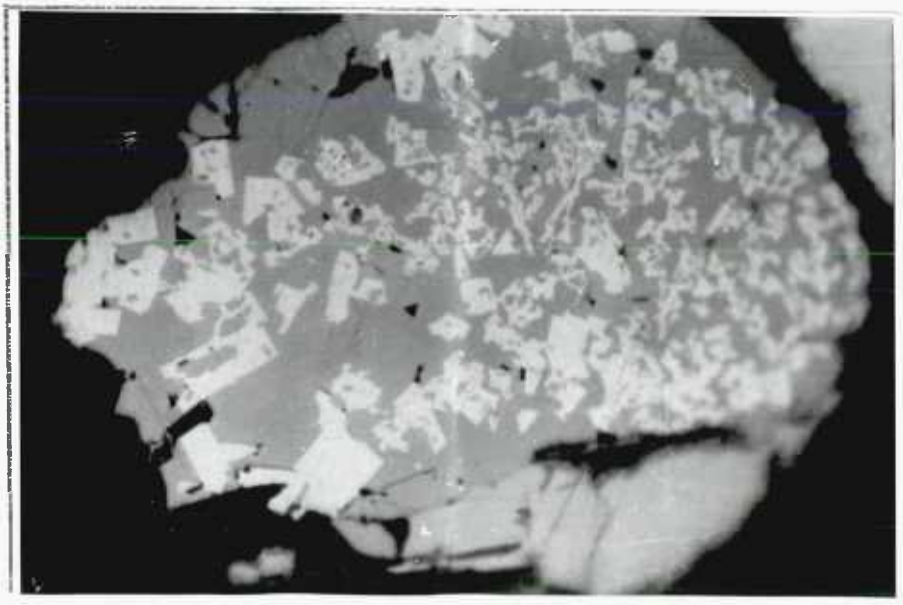

Fig. 5.6 Partly and fully formed skeletal idioblastic crystals of Pt-Fe alloy in pyrrhotite, with attached 'barren' pentlandite. An example of textural type III. Concentrate from Rustenburg mine. Scale 1 cm =33 µm.

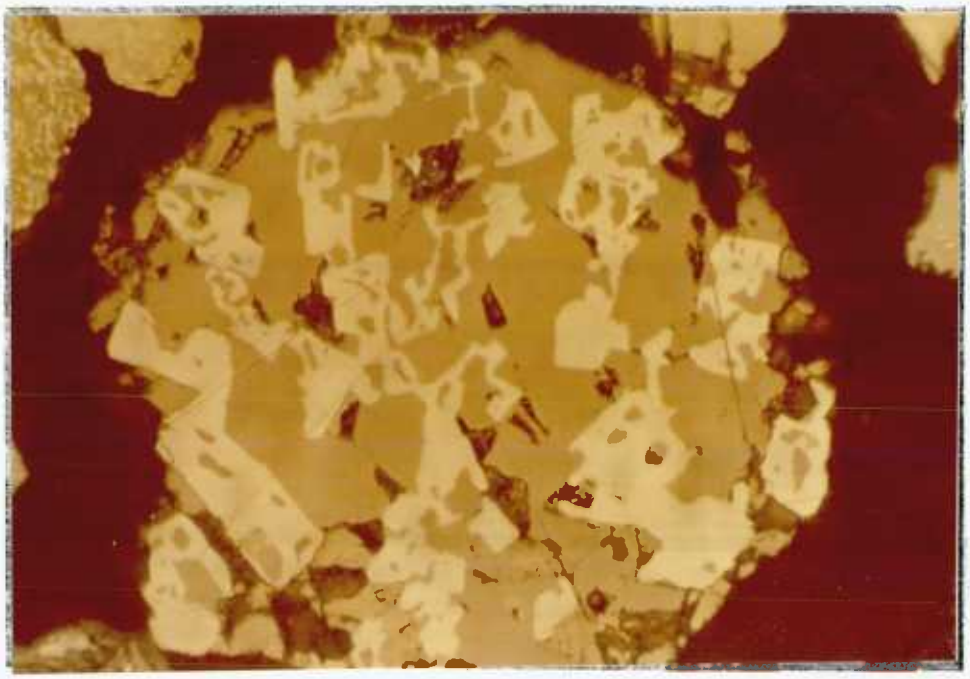

Fig. 5.7 A good example of textural type III, showing skeletal idioblastic crystals of Pt-Fe alloy in pyrrhotite. Raw high grade concentrate from Union mine. Scale 1 cm = 17 μm.

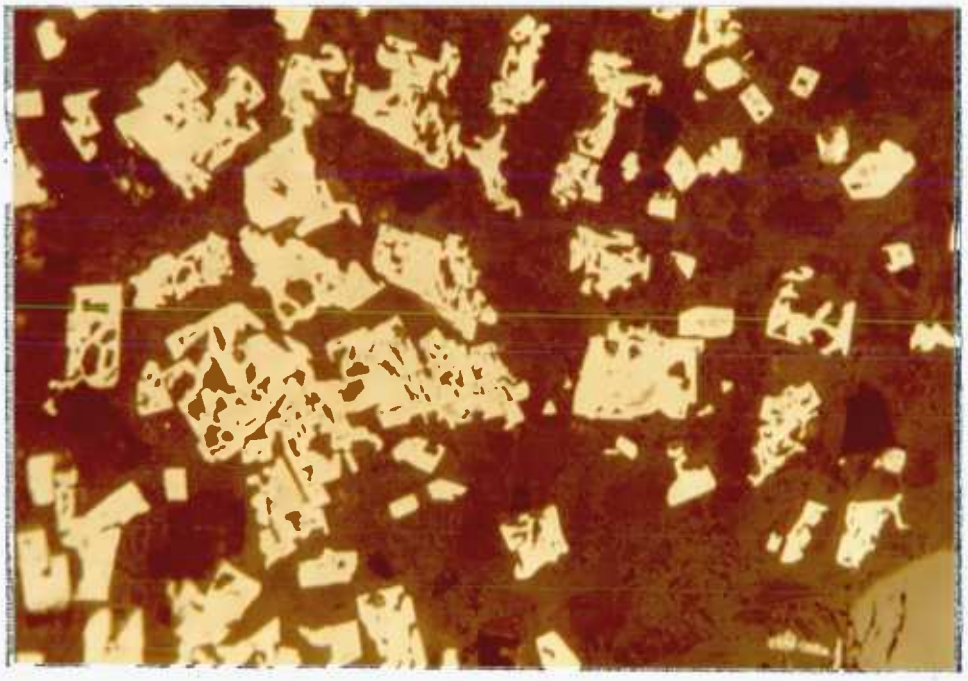

Fig. 5.8 The structure of an aggregate of skeletal idioblastic crystals of Pt-Fe alloy, emphasised by acid leaching and removal of the pyrrhotite matrix. Non-magnetic tailings concentrate from Union mine. Scale 1 cm = 33 μm.

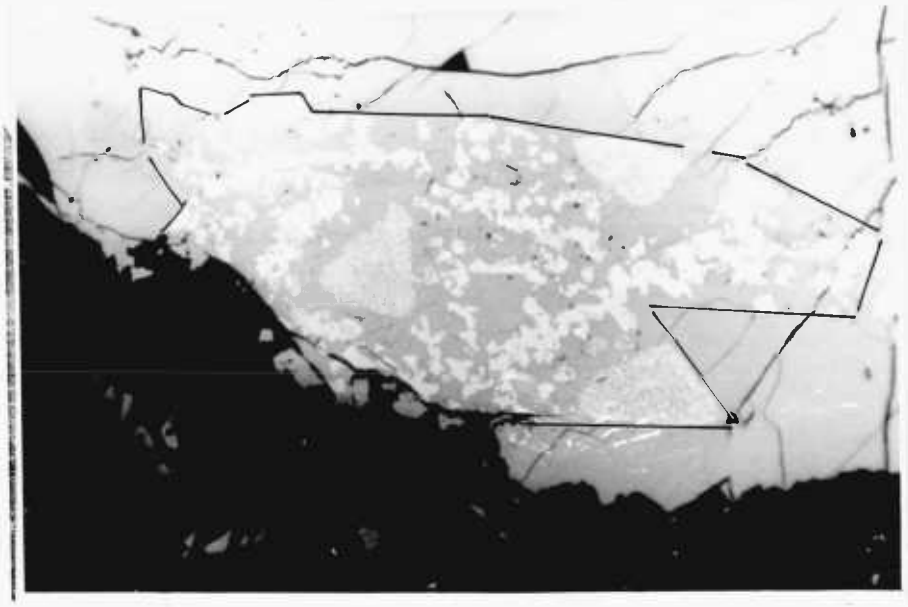

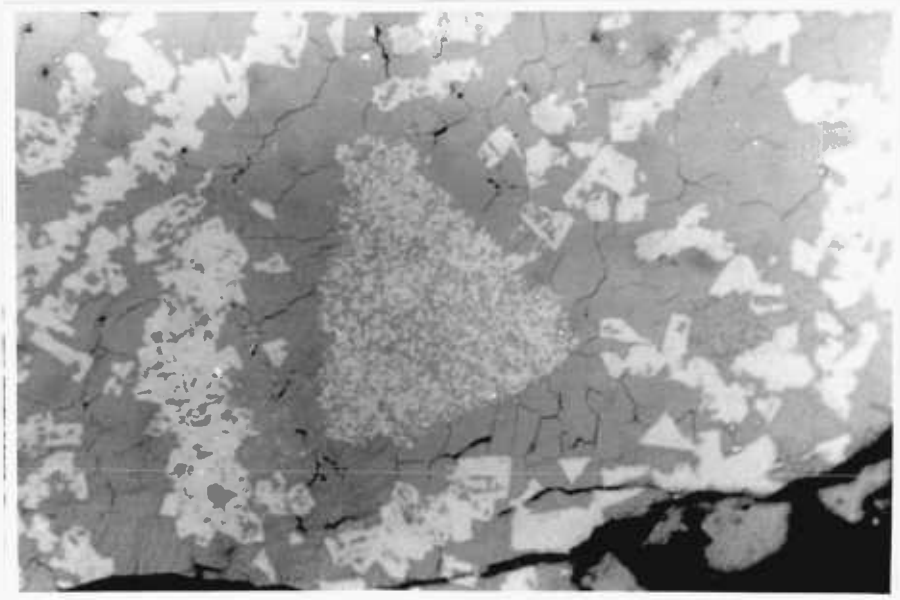

Fig. 5.9 Triangular zones of spongy Pt-Fe alloy of textural type II, and aggregates of euhedral and skeletal crystals of Pt-Fe alloy of textural type III in a matrix of granoblastic pentlandite. Photomicrograph (a) shows the structure of the whole intergrowth which has been outlined to emphasise the angular 'crystalline' nature of its boundary with the barren pentlandite overgrowth. Scale 1 cm =40μm.
Photomicrograph (b) provides detail of the zonal structure and nature of textural types II and III. Scale 1 cm =15 μm.

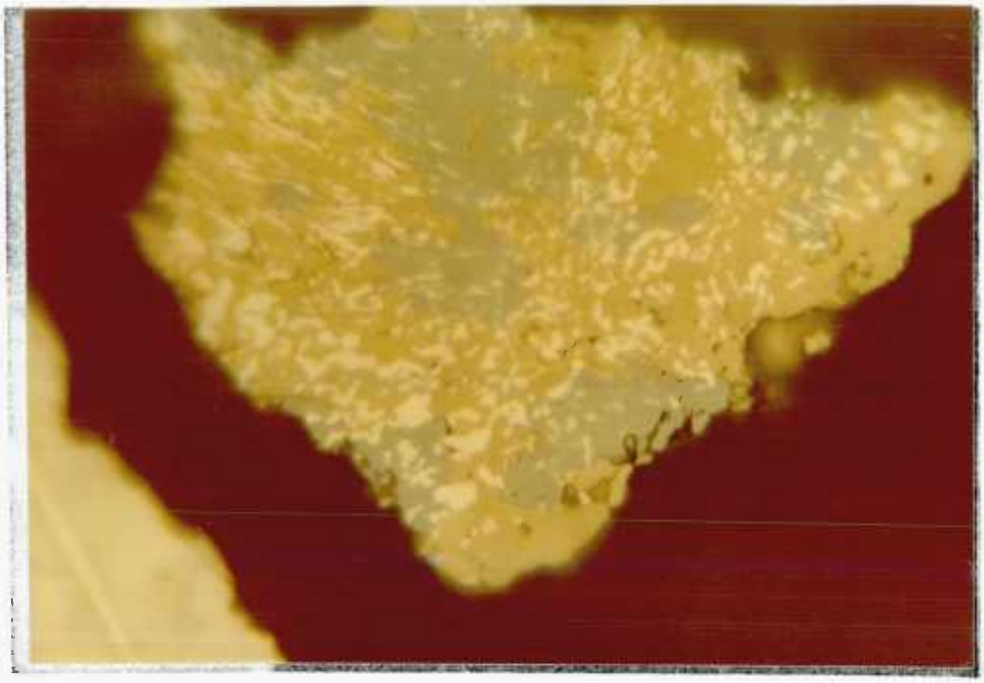

Fig. 5.10 A graphic intergrowth of Pt-Fe alloy (white) with chalcopyrite and a blue-grey unidentified phase similar in properties to laurite. Union mine. Scale 1 cm = 17 μm.

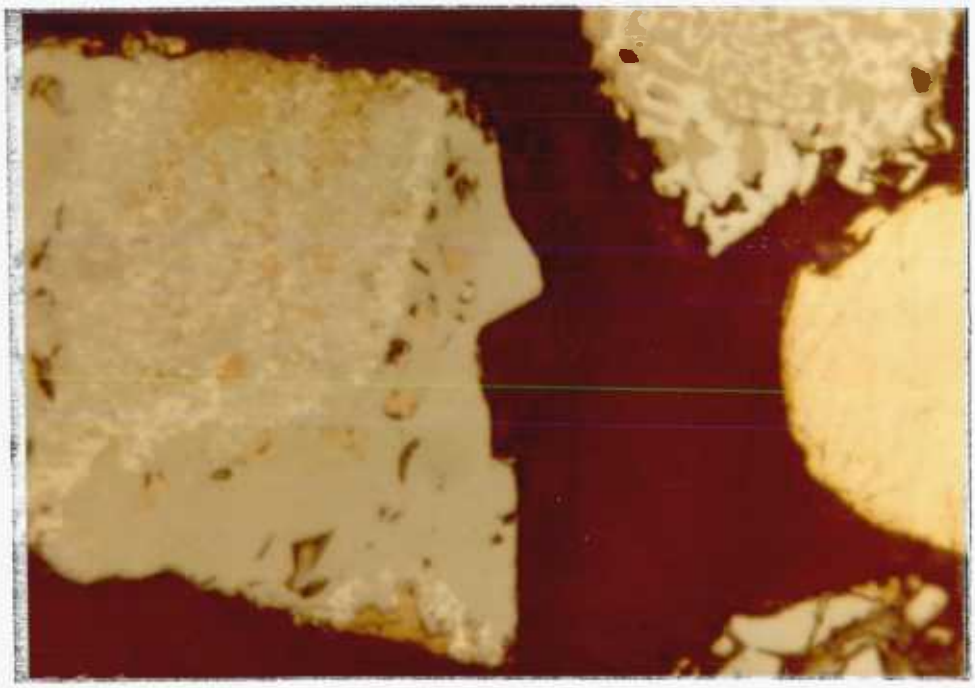

Fig. 5.11 A concentrate grain of cooperite displaying a euhedral intergrowth area of fine spongy Pt-Fe alloy (white). Pyrrhotite appears to be selectively replacing the cooperite matrix to this intergrowth. Grains of myrmekitic Pt-Fe alloy in pyrrhotite, and gold-silver alloy are also displayed. Rustenburg mine. Scale 1 cm = 17 μm.

crystals are small and of a similar size to each other, and their distribution in the pyrrhotite matrix is fairly random. It is only in cases like figure 5.9, where idioblastic crystals occur as part of 'segregation' veins, that any sort of orientation is found.

Textural Type IV includes all fine spongy to graphic intergrowths of Pt-Fe alloy with cooperite. This intergrowth is relatively rare in the concentrates, and has not been found in the ore. Three varieties have been seen:

1. a coarse graphic form (fig. 6.2, chpt.6) which is similar to the coarser myrmekitic forms of type I.

2. a very fine graphic variety (fig.5.12) in which the Pt-Fe alloy occurs as minute ragged crescent-shaped forms, suggesting that they might be intergranular inclusions related to a polygonized cooperite matrix.

3. a spongy or cellular variety similar to type II. The spongy Pt-Fe alloy is restricted to certain euhedral areas within the cooperite grain. This is illustrated in figure 5.11, in which the matrix cooperite is also being selectively replaced by pyrhhotite.

Textural Type V includes the occurrence in the 'metallic' concentrates of Pt-Fe alloy as large and often euhedral to subhedral grains of up to 0.4mm across (fig. 5.14). These grains are easily visible to the naked eye, and under the microscope are generally free of attached or included platinum-group minerals or base-metal sulphides. No iridosmine or osmiridium have been found in these grains, despite the common occurrence of such phases in Pt-Fe alloy grains of this type in many other deposits throughout the World.

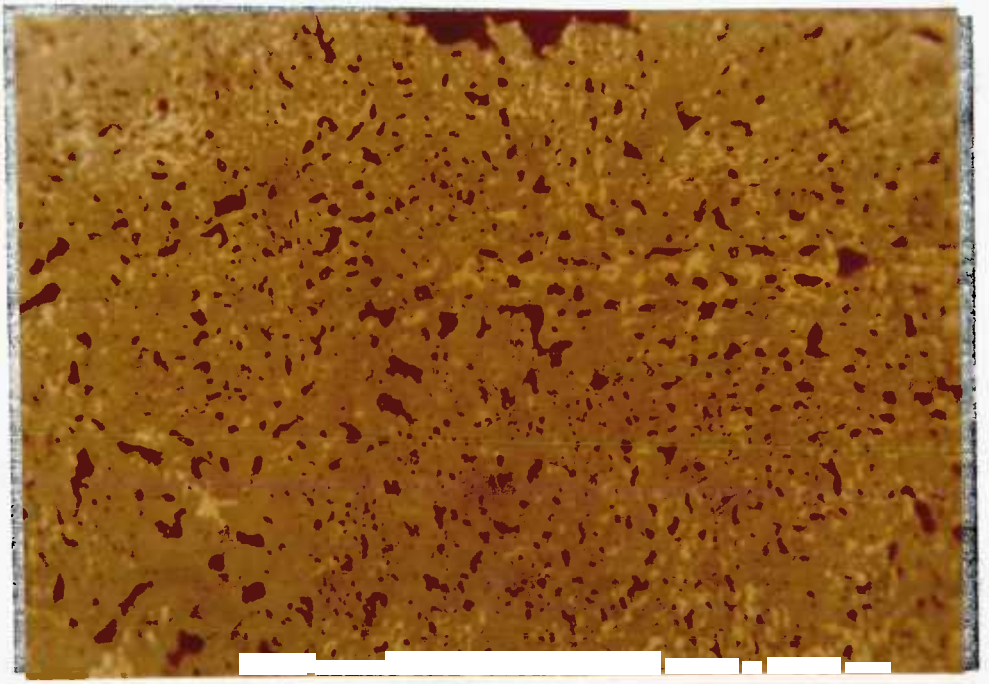

Fig. 5.12 Photomicrograph of a cooperite grain at a high magnification in oil of approx. X 1400, showing the presence of ragged and probably intergranular crescent-shaped inclusions of Pt-Fe alloy (white). Compare with figures 6.2 and 6.3 in chapter 6. Union mine concentrate.

Fig. 5.13 A corroded crystal of Pt-Fe alloy (white) enclosed by chalcopyrite containing laths of grey mackinawite. Silicates are black. Compare with fig. 5.14. Polished ore section. Oil immersion. Rustenburg mine. Scale 1 cm = 40 µm.

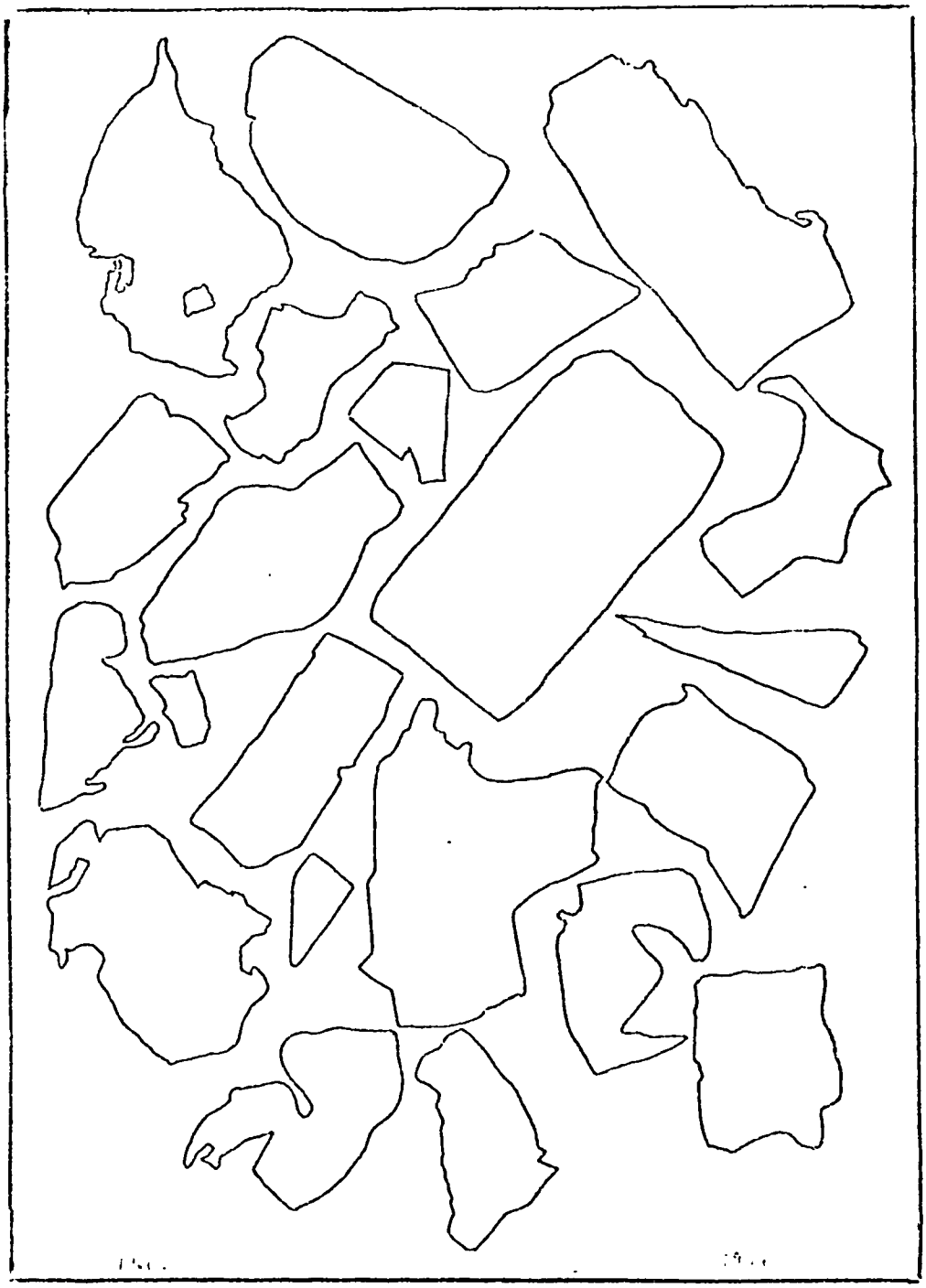

Fig. 5.14 Diagram of a random sample of grain shapes taken from drawings of Pt-Fe alloy grains in sections 1945 and 1946, illustrating the combined deeply embayed and euhedral nature of the grains which has been largely unmodified by the mineral beneficiation process. Compare with figure 5.13. Concentrates from Rustenburg mine.

No other workers on the Merensky Reef have yet reported these two minerals which are relatively easy to distinguish from Pt-Fe alloy, as illustrated in figures 5.15 and 5.16. Only one occurrence of this type has so far been found in the ore (fig. 5.13). Vermaak and Hendriks (1976) have similarly found this form of Pt-Fe alloy to be rare in the ore. They distinguished between Pt-Fe alloy (equivalent to type V), Pt-Fe alloy - BMS intergrowths (equivalent to types I, II, and III), and cooperite-Pt-Fe alloy intergrowths (equivalent to type IV). Their abundance figures, in volume percent of the total amount of precious minerals in the Merensky Reef of the western Bushveld as a whole, were 0.51, 35.39, and 3.46 volume percent respectively.

The shapes of most of the grains are modified by embayments. Often these embayments only effect one or two crystal faces (fig. 5.14). This can also be seen in figure 5.13 in which a crystal has grown across the 'gap' between two silicates and has subsequently been partly replaced by chalcopyrite. With regard to the most common location of such crystals, Vermaak and Hendriks (1976) have determined that in the "silicate ore" (Reef pyroxenite) 99.9 vol% of this form of Pt-Fe alloy occurs associated with pyrrhotite along sulphide-silicate contacts, whereas in the "chromite ore" (bottom chromite band) 90 vol.% occurs in contact and between the chromite grains. It is clear that the common forms found in the concentrates, combined with the limited observations of its occurrence in the ore, can be explained by simple crystal growth from a magmatic sulphide liquid with modification by later corrosion and replacement.

Fig. 5.15 Subhedral crystals and stringers of iridium in an alluvial grain of Pt-Fe alloy from the Urals. Scale 1 cm = 17 μm.

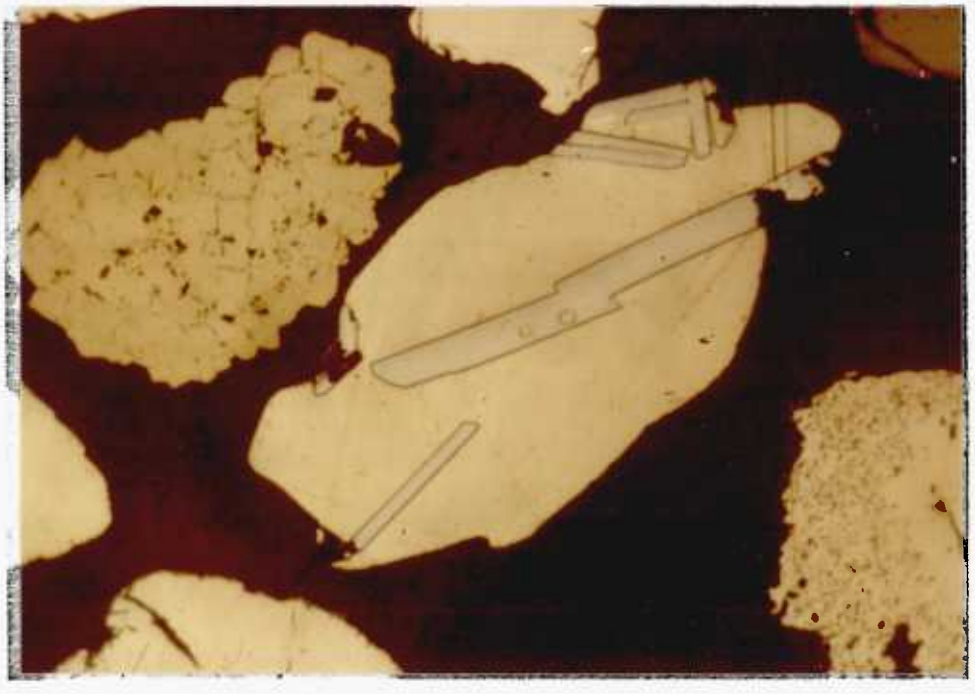

Fig. 5.16 Laths of iridosmine (light grey) in an alluvial grain of Pt-Fe alloy from the Urals. Scale 1 cm = 20 μm.

Other Textural Types and combinations of the types described above can be found in the concentrates. Vermaak and Hendriks (1976) drew attention to this during their brief description of the major types. Future examinations will no doubt reveal more of the rarer types of textures exhibited by composite grains in the concentrates. Examples of particular genetic interest found in this study are:

1. Myrmekitic Pt-Fe alloy in pyrrhotite enclosing a deeply embayed central area of cooperite. This can be interpreted as a reaction between early formed cooperite and iron rich sulphide melt to give an intermediate Pt-Fe-sulphide mixed-crystal which segregates into a myrmekitic intergrowth of Pt-Fe alloy in pyrrhotite.

2. Grains of Pt-Fe alloy rimed by cooperite. These may be interpreted as a result of the interaction of Pt-Fe alloy with interstitial sulphide liquid containing excess sulphur. Alternatively, as suggested by Vermaak and Hendriks, the rim could have been formed by precipitation of cooperite from an interstitial sulphide liquid containing excess sulphur, with the excess sulphur combining with platinum in the liquid.

3. Idioblastic crystals of type III enclosing gold as in figure 5.23.

4. Ragged or sub-graphic inclusions of Pt-Fe alloy (fig.5.10) permeating an intergrowth between chalcopyrite and a blue-grey, isotropic,hard phase having an estimated reflectance of 40% in sodium light. This phase may be laurite. It is possible that replacement

of an original pyrrhotite or pentlandite myrmekitic intergrowth by chalcopyrite has resulted in some remobilisation of Pt-Fe alloy into the 'laurite'. Alternatively the platinum could have been introduced during the copper metasomatism, or chalcopyrite precipitation round the 'laurite' crystal aggregate.

5.1.3. Interpretation of the Textural Types

Textural Types I, II and III are considered to have been produced by unmixing and recrystallisation. This assumes that, during the initial stages of the crystallisation of the base-metal sulphides, crystals of a Fe-Pt-S or Fe-Ni-Pt-S phase were formed. It is suggested that these crystals nucleated on the marginal silicates and grew into the interstitial sulphide droplets (fig. 5.9). This marginal preference of the graphic intergrowths of Pt-Fe alloy was confirmed by Vermaak and Hendriks (1976) who showed that 79.68 vol.% of the myrmekitic type occurs at sulphide-silicate contacts, of which 62.33 vol.% has a matrix of pyrrhotite, 12.78.% a matrix of pentlandite, and 4.57 vol.% a matrix of chalcopyrite. It is considered that the presence of chalcopyrite as a constituent of these intergrowths is due to selective replacement of pyrrhotite.

Breakdown of these mixed crystals by duplex crystallization (Spry, 1969) then occurred. This involved exsolution by conucleation and the mutual growth, during the breakdown of the original mixed crystal, of Pt-Fe alloy and pyrrhotite or pentlandite, to produce a normal eutectoid texture. According to Spry "conditions of growth are such that crystallization takes place rapidly under strong chemical or energy gradients and dendritic growth results. The geometry of the forms produced depends on the branching of the

original duplex nucleus. The spacing between branches or fingers depends on the kinetics of diffusion, the rate of release of free energy of transformation, and on interface energy requirements". Varying Pt concentration throughout the mixed crystal, as well as the possibility of undercooling before precipitation should also be considered.

The type II spongy triangular areas of Pt-Fe alloy illustrated in figure 5.9 may represent mixed-crystal regions of greater Pt concentration, or areas where greater undercooling has taken place. Greater undercooling or greater concentration of the solute is well known to result in a smaller critical radius of the nucleus, and hence easier nucleation, more nucleii, and smaller exsolved bodies (Spry, 1969, P.98). The zonal arrangement in figure 5.9 may reflect an original compositional zoning in the mixed-crystal. However, the barren zones may also be due to depletion by the migration of Pt into the supersaturated zones, or outwards to contribute to the formation of the coarser skeletal idioblastic crystal aggregates.

Type III textures are considered to have resulted from either one or a combination of two mechanisms. Firstly slow cooling, combined with lower concentrations of Pt in the mixed-crystals than for myrmekitic formation, will result in larger critical radii of the nucleii, together with the time for diffusion and crystal development according to surface free energy requirements. The second mechanism involves the initial formation of a myrmekitic texture, and its modification to varying degrees by recrystallisation. The drive to recrystallise comes from a need to reduce lattice strain in the

myrmekitic form, especially as cooling takes place. Deformation may also be a later contributing factor. Nucleation and growth of new strain-free crystals or grains is at the expense of the strained myrmekitic intergrowth, and graphic Pt-Fe alloy recrystallises to euhedral and skeletal forms, whereas a granoblastic texture may develop in the pyrrhotite or pentlandite. This mechanism would help to explain why the matrix pentlandite in figure 5.9 only exhibits a polygonal structure in the area of its intergrowth with Pt-Fe alloy. The angular shape of this intergrowth, its position at a silicate-sulphide contact, its enclosure by 'barren' pentlandite, the termination of enclosing pentlandite fractures at the intergrowth boundary, as well as the granoblastic texture of the matrix pentlandite, and graphic and skeletal form of the Pt-Fe alloy, strongly suggests the original presence of an earlier formed crystal aggregate of a phase which has broken down or unmixed by simultaneous exsolution crystallisation.

Both mechanisms may have operated to produce the euhedral Pt-Fe alloy occurrences of type III. Where the density of Pt-Fe alloy crystals in pyrrhotite is low (fig. 8.3), a low initial Pt concentration is indicated and the former direct mechanism is more likely to have operated without the intervening formation of a myrmekitic form. However, in the case illustrated by figure 5.9, where a high initial concentration is indicated, together with a similarity of the coarse aggregates to the vein-like skeletal forms of myrmekitic type I (fig. 5.1.), recrystallisation is more likely to be responsible.

Although the author favours an exsolution origin for

these textures, it is important to note that a remarkably similar myrmekitic texture can be produced by the replacement of cooperite as illustrated in figure 6.3 in chapter 6. This intergrowth is possibly the result of supergene or serpentinisation processes. It is tempting to compare the residual cooperite areas and the dendritic veins with the triangular spongy areas and skeletal veins respectively of figure 5.9. It could be that resorption of early formed and marginally dispersed cooperite crystals by the base-metal sulphide melt produced the local concentration of platinum necessary for the mixed crystal to form. The mechanism may have even been a simultaneous replacement and breakdown to a myrmekitic intergrowth. Such a process is supported by the rare occurrence of anhedral cooperite enclosed either by myrmekitic Pt-Fe alloy in pyrrhotite or by homogeneous Pt-Fe alloy, as well as graphic cooperite-Pt-Fe alloy associations as in figure 5.11.

Textural Type IV. A mechanism to account for the association of cooperite with Pt-Fe alloy, and which may account for some examples of this type in which Pt-Fe alloy occurs as small inclusions, has been put briefly forward by Vermaak and Hendriks (1976). They suggest that when the interstitial sulphide droplet is oversaturated in iron, and the sulphur fugacity inhibits oxide formation, the platinum combines with iron to produce Pt-Fe alloy. If excess sulphur is available then cooperite will form. Although this could account for grains of cooperite enclosed by Pt-Fe alloy, and vice versa, it does not explain the graphic form of type IV. However, a process of incipient replacement produced by desulphurisation of cooperite is a related mechanism, and may account for the variety

illustrated in figure 5.12. In this case the ragged crescent-shaped forms of the Pt-Fe alloy inclusions suggests that they might be intergranular to a polygonized cooperite matrix, and that their formation may be due to desulphurization during primary recrystallisation.

In the case of the spongy variety in figure 5.11 the cooperite appears to be selectively replaced by pyrrhotite. Complete replacement would account for some occurrences of textural type II. The general confinement of the replacing pyrrhotite to the two regions of spongy Pt-Fe alloy suggests a close genetic relationship, and that the latter could be an incipient replacement produced in advance of the pyrrhotite replacement front.

The coarse graphic form in figure 6.2 has all the appearance of type I intergrowths and may have formed in the same way by simultaneous exsolution crystallisation of a mixed crystal. At presence, however, the author finds this particular texture difficult to explain, especially as 'normal' cooperite is generally associated with braggite and never displays these graphic Pt-Fe alloy textures. Also the author has not yet found type IV intergrowths in the ore itself, and the paragenetic position is therefore a little obscure.

Finally the author has nothing more at present to add to the brief explanations already offered with regard to type V and the other textural types. The paragenetic position of all the various forms of Pt-Fe alloy will be discussed further in chapter 9.

5.1.4 The Composition

At the start of this investigation in 1961, native

platinum alloyed with iron, called then ferroplatinum, was generally accepted as being a major constituent of the concentrates from the Merensky Reef, although the nature of its form in the concentrates and ore was either not known or had not been reported. It appeared to be merely known to those exploiting this deposit as grey metallic grains in the concentrates. The author (1966) was therefore the first to identify and briefly report Pt-Fe alloy as occurring "commonly associated with pyrrhotine as a fine graphic intergrowth, suggesting a eutectic relationship, or as euhedral partially corroded grains". A photomicrograph and X-ray scanning micrographs provided the evidence for textural type III.

In the initial stages therefore the electron-probe microanalyser was used qualitatively to identify the 'white isotropic phase of high reflectance' which occurred in the various forms already described. From this qualitative study and a similar qualitative examination of concentrates from Ethiopia, Columbia, Alaska, Urals and the Witwatersrand (Arias 1968; Toma, 1975) it was clear that past chemical analyses of 'platinum grains' were unavoidably bulk analyses because they had not taken into account the common occurrence of inclusions of iridium, osmiridium, and iridosmine (figs. 5.15 and 5.16), as well as other platinum group minerals like prassoite and zappinite (chpt. 6.4). The advent of the electron-probe microanalyser solved this problem, and since that time many analyses of Pt-Fe alloys from other deposits have been done (Stumpfl and Tarkian, 1973; Tarkian and Stumpfl, 1975; Cabri and Gilles Laflamme, 1974; Stumpfl and Clark, 1965; Cabri and Feather, 1975; Feather, 1976, and others). These have shown that,

apart from iron which is present in amounts up to about 22 wt.%, minor amounts of Pd,Rh,Ru,Os,Ir,Au,Cu,Ni, and Sb may occur in the Pt-Fe alloy lattice. However, as far as the author knows no analyses for Pt-Fe alloys in the Merensky Reef have yet been published.

At the time of this Pt-Fe alloy investigation the development of the present day sophisticated matrix correction procedure was only in its infancy. A preliminary study of artificial Pt-Fe alloys was therefore made in order to check the accuracy of the analyses. It soon became clear that the matrix correction procedure available at that time was inadequate for the Fe-Pt system. Therefore an alternative graphical correction method was adopted. The background to this work, and the graphical plots of true Fe and Pt percentage values against apparant percentage values at different voltages, have been presented in chapter 3.4.3.

Analysis of Pt-Fe Alloy Types I, II, and III Because of the unavoidable subsurface and lateral irradiation of the matrix pyrrhotite in textural types I and II, only a qualitative study was carried out on the graphic Pt-Fe alloy, and it was not possible to determine with certainty whether or not the iron which was present was actually part of the alloy. An examination of acid leached grains may however be a solution to this problem. Unfortunately this has not yet been done. Apart from iron (and sulphur from the underlying pyrrhotite), platinum was the only other element detected.

Electron-probe microanalyses of Pt-Fe alloy of type III are presented in table 5.1, together with a photomicrograph in figure 5.17 showing the nature of the analysed crystals. Because of

the small size of the Pt-Fe alloy crystals, and the possible resultant iron contribution by subsurface irradiation of the enclosing pyrrhotite, all the grains for analysis were selected by line scans to test their homogeneity, and care was taken to avoid pyrrhotite inclusions. The lack of variation in iron content across grains selected for analysis gave some confidence that subsurface pyrrhotite irradiation was negligible. No zonal variation was detected. Trace quantities of other platinum group elements plus copper and nickel were not determined. The analyses were done at 25 kV and the initial percentages were corrected using curves previously constructed from the artificial Pt-Fe alloy study.

Analysis of Pt-Fe Alloy Type V. Prior to the analysis of these large subhedral to euhedral grains of Pt-Fe alloy, forty of them were indented, and their microhardness measured. This served three purposes. Firstly it was a means of selecting suitable grains for analysis so that correlations could be made between hardness and composition, in particular the iron content. Secondly any grains showing an abnormally low or high value of hardness might be compositionally abnormal, or be a different alloy altogether. One example of such a discovery is a Pt-Fe-Au phase. Finally, indenting and drawing grains was a useful means of locating and identifying them under the electron-probe microanalyser.

Grains from a non hand-magnetic fraction and a hand-magnetic fraction were analysed in order to determine the range of iron content and its correlation with hardness, as well as explain the difference in magnetic susceptibility between the two fractions. The results are presented in table 5.2, and suggest that magnetic

Fig. 5.17 Skeletal platinum-iron alloy crystals of cubic outline (white) in a matrix of pyrrhotite (grey). Analyses of grains A, B, and C, are presented in table 5.1 below together with three other grains to the west of the area shown.

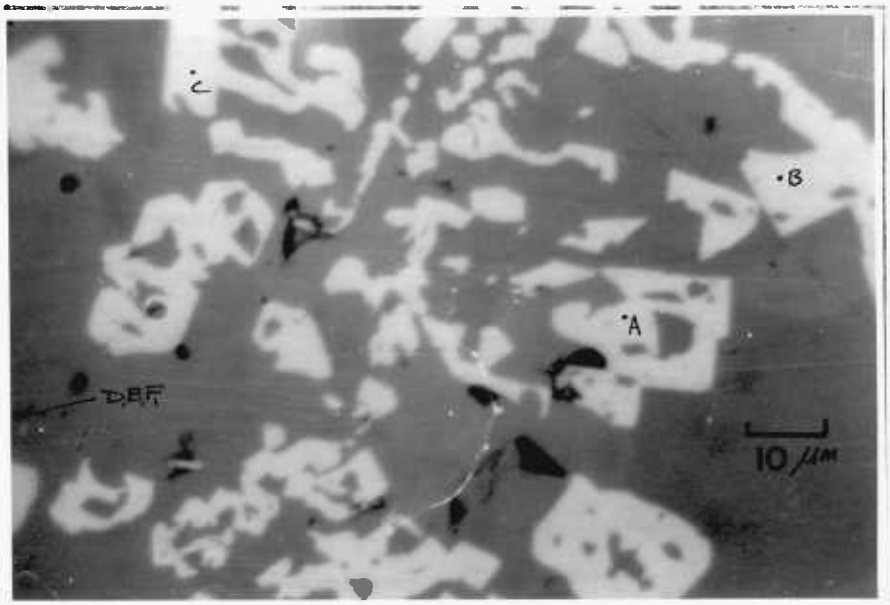

Table 5.1 Showing the range of platinum and iron content of crystals of platinum-iron alloy as illustrated in the figures 5.17 and 8.3

Grain	Composition in wt. %		At. Proportions	
	Pt	Fe	Pt	Fe
A	84.0	15.5	0.43	0.28
E	85.0	12.0	0.44	0.21
B	89.0	11.0	0.46	0.20
D	88.0	10.5	0.45	0.19
C	91.0	10.0	0.47	0.18
F	87.0	9.5	0.45	0.17

Note: a graphical correction method was used. See chpt.3.4.3.

Table 5.2 Electron-probe microanalyses in wt.% of large homogeneous grains of platinum-iron alloy from a hand magnetic fraction of a concentrate (section 1946) and a non hand magnetic fraction (section 1945), from Rustenburg mine.

Section Grain	Pt	Fe	Cu,Ni	Ru Rh Pd	Os	Ir	Total	VHN_{100}
1946 (2)	83.0[b]	21.2[a]	approx.3	nd	nd	nd	102.2	326
(3)	81.0[b]	22.4[a]	2.5, 0.5	nd	tr	nd	106.4	237
(4)	93.0[b]	13.1[a]	nd	nd	nd	nd	106.0	431
(5)	86.0[b]	14.0[a]	?	?	?	?	100.0	---
(6)	92.0[b]	13.4[a]	nd	nd	nd	nd	105.4	297
(7)	93.0[b]	12.6[a]	nd	nd	tr	nd	105.6	249
(8)	86.0[b]	12.6[a]	approx.7	nd	nd	nd	105.6	363
(9)*	95.0[b]	13.6[a]	nd	nd	tr	tr	108.6	340
1945 (4)	95.0[c]	8.0[c]	nd	nd	nd	nd	103.0	380
(8)	97.0[c]	9.0[c]	1.0, nd	tr	nd	nd	108.0	383
(9)	(96)	9.0[c]	tr, tr	nd	nd	nd	(105)	519

Footnotes

a - no matrix corrections, constant specimen current, 16.5 kV.

b - graphical correction, constant specimen current, 35.0 kV.

c - graphical correction, constant specimen current, 25.0 kV.

* - weakly anisotropic under crossed nicols.

nd - not detected or not detected with certainty.

tr - trace

susceptibility is related to Fe content, with the hand magnetic grains having a mean Fe content of 15.4 wt.% compared to 9 wt.% for the non hand-magnetic grains. However, a few noticeably anisotropic grains (e.g. no 9) were seen in section 1946, and therefore crystal structure may be a factor to consider. This combination of anisotropy, high magnetic susceptibility, and high iron content strongly suggests that many of the grains in section 1946 are tetraferroplatinum. Similarly the low iron and non magnetic grains of section 1945 are probably isoferroplatinum.

5.1.5 The Optical and Physical Properties. Pt-Fe alloy at Rustenburg and Union mines appears white in air, and creamy white in oil. The higher the iron content the more creamy or yellowish it becomes. Compared to moncheite and merenskyite it is more creamy. The former are however distinct to strongly anisotropic. Confusion with sperrylite is easily resolved by the measurement of microhardness. Some grains of type V are weakly anisotropic and may be tetraferroplatinum. Most however are sensibly isotropic. The crystal forms in the ore and concentrates have already been described.

The Hardness could only be determined for type V Pt-Fe alloy, for obvious reasons. Values for each grain were obtained from two or three indentations using a 100 g load. The mean microhardness from the measurement of 41 grains in sections 1945 and 1946 (table 5.2) was VHN_{100} 396. The range of values was VHN_{100} 237 - 600, although 90% of the grains fell within the range of VHN_{100} 237 - 446. Comparison of sixteen hand-magnetic grains in section 1946 with twenty-five non hand-magnetic grains in section 1945 gave values of VHN_{100} 237 - 600, mean 363, and VHN_{100} 357 - 519, mean 396, respec-

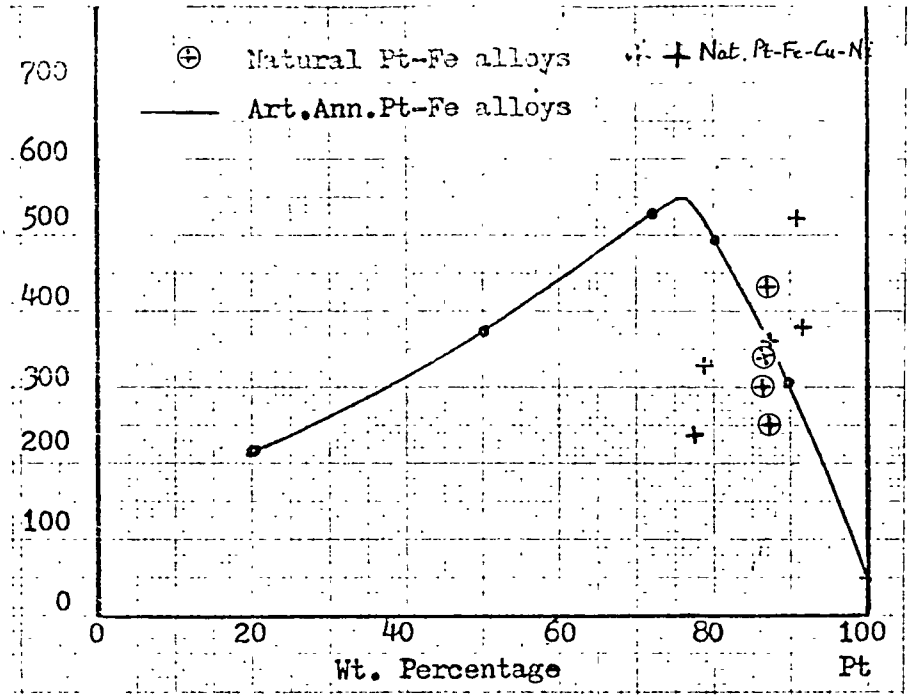

Fig. 5.18 Graph of Vickers indentation microhardness against iron content in wt.% for synthetic Pt-Fe alloys, together with a plot of values for Pt-Fe alloy from Rustenburg mine.

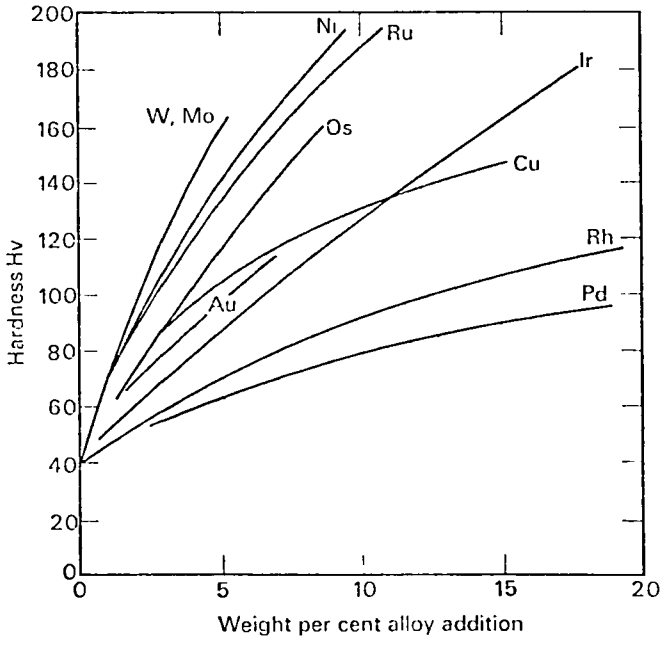

Fig. 5.19 Hardness of annealed platinum alloys. After E.M.Wise in 'Platinum' by International Nickel Ltd., (1976).

tively. All indentations were sigmoidal with no shell, radial or side fractures. Since the grains in section 1946 have a significantly higher iron content than those in section 1945, it might be concluded that an increase in iron content leads to a general decrease in hardness. This would contradict the well known increase in hardness with iron content for artificial Pt-Fe alloys. Figure 5.18 shows this relationship between Fe-content in artificial alloys and indentation microhardness as determined by the author. However, a decrease in hardness with iron content has been reported before, as by Utenbogaardt & Burke (1971) who quote Lebedeeva (1963).

This difference in mean hardness could reflect a structural difference i.e. possibly between isoferroplatinum in section 1945 and tetraferroplatinum in section 1946. If this is the case, then a relationship between hardness and composition can only be expected with Pt-Fe alloy grains of the same structure. However, a plot (fig. 5.18) of indentation microhardness against Fe content for the grains in section 1946 exhibits a random relationship. This is to be expected, since (Cu + Ni) contents vary from not detectable to 7 wt. percent, and there are also trace amounts of Ir,Os,Ru,Rh, and Pd, all of which are known to increase the hardness when alloyed with platinum (Wise, 1935, 1938, 1940, 1953). This is illustrated in figure 5.19.

In conclusion therefore, although microhardness values for the artificial Pt-Fe alloys demonstrate an increase in hardness, reaching a maximum around a composition of PtFe (i.e. 22.5 wt.%), care must be taken in extending this relationship to natural equivalents. In artificial alloys the presence of any of the other five

platinum group metals, and the effect of heat treatment, cold working, and annealing (fig. 5.19), are well known to substantially effect the hardness. In considering the natural Pt-Fe alloys these latter factors could be equated to thermal metamorphism, deformation, and recrystallisation, all of which will produce changes according to the structural possibilities discussed by Cabri and Feather (1975). Cold working can be expected to operate during transport of alluvial grains by rivers (Stumpfl & Tarkian, 1973; Tarkian & Stumpfl, 1975). It is therefore to be expected that the hardness of Pt-Fe alloy grains of the same Fe content but from different sources will vary widely. Even within the same deposit more than one period of Pt-Fe alloy formation may have occurred, as in the case of the Merensky Reef. Hardness may also vary with orientation in the polished sections, although this appears to be a small effect.

A detailed investigation of the relationship between hardness, composition, and structure of natural Pt-Fe alloys combined with their correlation with the factors of environment of deposition and subsequent geological history, would be of great interest. However, it is considered that the usual presence of minor copper, nickel, and other platinum group elements, together with the effect of post-depositional processes and the different structural possibilities, invalidates the use of indentation microhardness as a tool for determining the iron content. It was, however, of value in this investigation in distinguishing these alloys from other platinum group minerals of similar appearance, in particular white isotropic and hard sperrylite.

The Reflectance values of Pt-Fe alloy have not been de-

termined in this investigation. Stumpfl and Tarkian are so far the only ones to have made available reflectance data for these alloys i.e. from Borneo (1973) and Driekop mine (1975). They determined that Pt-Fe grains falling within the three ranges of Fe content in wt.% of 4·4 - 4·9, and 6·6 - 7·8 for Driekop mine, and 10·1 - 10·7 for Borneo gave mean values of reflectance at 589 nm of 69·5, 67·8 and 66·4 percent respectively. However, although this suggests that iron content can be determined by reflectance measurements, it should be noted that all these grains contained similar and small quantities of Cu,Os,Rh,Ru, and Ir, which would allow the effect of the iron to predominate and correlate with reflectance above an even 'background' of trace elements. Often, however, there are several percent of these combined elements which may appreciably add to or subtract from the reflectance influence of the iron. Also it is significant that the Pd content in the Borneo samples exhibits a broad antipathetic correlation with the reflectance. Until more data becomes available it is considered that reflectance, like microhardness, should be used with caution in forecasting the iron content of Pt-Fe alloys, especially as the range of reflectance variation appears to be small at all wavelengths.

5.2 Other Platinum Alloys

5.2.1 Alloy of Pt-Fe-Au. This phase was found in a hand-magnetic table concentrate from Rustenburg mine. The section contained mainly Pt-Fe alloy grains together with rare stibiopalladinite and arsenopalladinite. The Pt-Fe-Au alloy was light grey and isotropic, and formed part of a composite grain with a white isotropic phase of VHN_{100} which was found to consist dominantly of

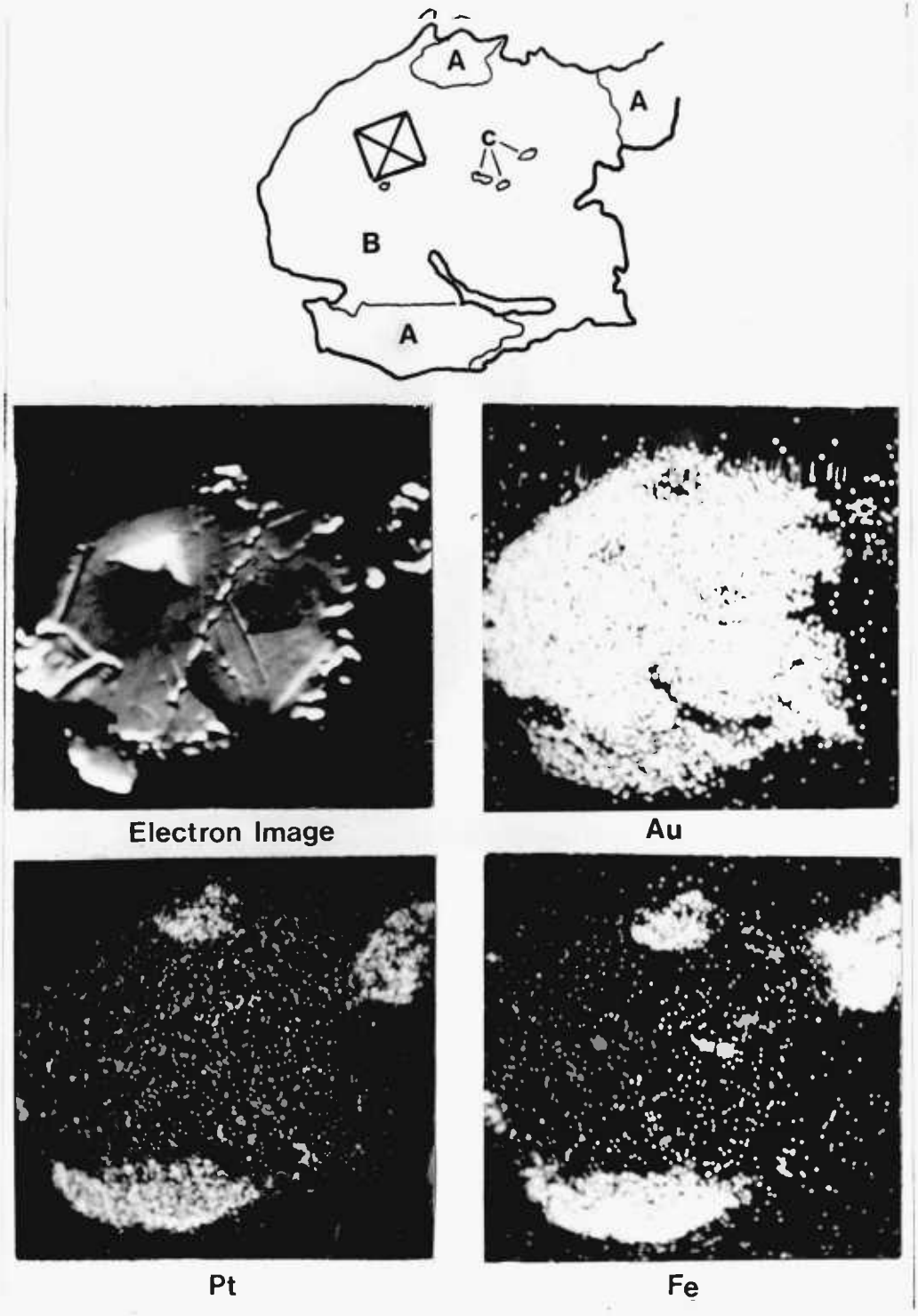

Fig. 5.20 X-ray scanning micrographs showing the distribution of Au Lα, Pt Lα, and Fe Kα, emissions over a composite grain in a hand-magnetic table concentrate from Rustenburg mine. The presence of a Pt-Fe-Au alloy (A), and a Au-Pt alloy (B) is indicated, as well as small inclusions of possibly chromite. Section no. 1946.

gold. Analysis of the Pt-Fe-Au alloy gave initial uncorrected percentages of Pt 41·7, Au 12.0, Fe 13·4 wt. percent, corresponding to an estimated corrected percentage of Pt 45, Au 14, and Fe 13 wt.%. Unfortunately, the possible presence of one or more other elements to account for the apparant deficiency in the total weight percent could not be confirmed because the grain progressively disintegrated under the electron beam, and finally 'disappeared' before a detailed compositional scan could be completed. This also applied to the gold phase. Figure 5.20 shows the nature of the intergrowth, together with X-ray scanning micrographs for Pt, Au, and Fe. Some platinum was present in the gold phase, but in an amount estimated as less than 2 wt.%. This amount is probably not enough to account for the loss in colour of the gold. It is probable that silver was the other element in both cases since a brief semi-quantitative study of another white isotropic grain of VHN_{100}^{50} displayed a small silver content, giving an approximate initial percentage of Pt 60, Fe 15, Ag 5 wt.%.

Schwellnus et al. (1976) are the only others to report gold with platinum in the Merensky Reef. Electron-probe microanalyses by them of three grains gave ranges of Au 79.84-95.55, Ag 3.91-19.56, Pt 0.40-0.52, Cu 0.23-0.68, Ni 0.0-0.02 weight percent.

5.2.2 Pt-Pd-Sn Intermetallic compounds have recently been found as small grains of very rare occurrence in the Merensky Reef at Atok and Rustenburg mines (Mihalik et al., 1975; Schwellnus et al., 1976). Three minerals have been defined. Niggliite, PtSn, has not yet been reported in the Bushveld.

Rustenburgite (Pt_3Sn) and Atokite (Pd_3Sn) are defined

by Mihalik, Hiemstra, and de Villiers (1975) as face-centered cubic end-members of a solid-solution series as shown in figure 5.21 They reported that these two minerals were scarce in the concentrates and ore, and that in each case only one grain of sufficient size (approx. 100 um) for analysis was found. However, the existence of a solid solution series was established by experimental work on the Pt-Pd-Sn ternary system. On the basis of their study the two natural grains which were analysed were defined as palladian rustenburgite $Pt_{0.398}\ Pd_{0.386}\ Sn_{0.217}$, and platinian atokite $Pd_{0.486}\ Pt_{0.302}\ Sn_{0.212}$.

These are both reported as being light cream in colour, weakly anisotropic due to strain, and of high reflectance, with minimum and maximum reflectance values at 589nm for palladian rustenburgite of 59·9 - 60·9, and for platinian atokite of 60·4 - 63·5 percent, and VHN_{25} values of 365 and 357 respectively. Finally they propose that zvyagintsevite (Genkin et al., 1966), a lead-rich equivalent of atokite, be reserved for the composition $(Pd,Pt)_3(Pb,Sn)$, where $Pd > Pt$ and $Pb > Sn$. Where the Pb content is less than Sn, then the names rustenburgite or atokite apply, depending on whether $Pt > \text{or} < Pd$.

The author has not yet found these two phases in the material investigated. However, their identical properties to the bismuthotellurides, combined with their rarity of occurrence and small size, means that to find them a systematic analysis of all 'bismuthotelluride-looking' grains would be required.

Paolovite (Pd_2Sn) was first found by Genkin et al (1974) in the copper-nickel sulphide ores of the Oktyabr deposit, Talnakh orefield, in cubanite-chalcopyrite, cubanite-talnakhite, and

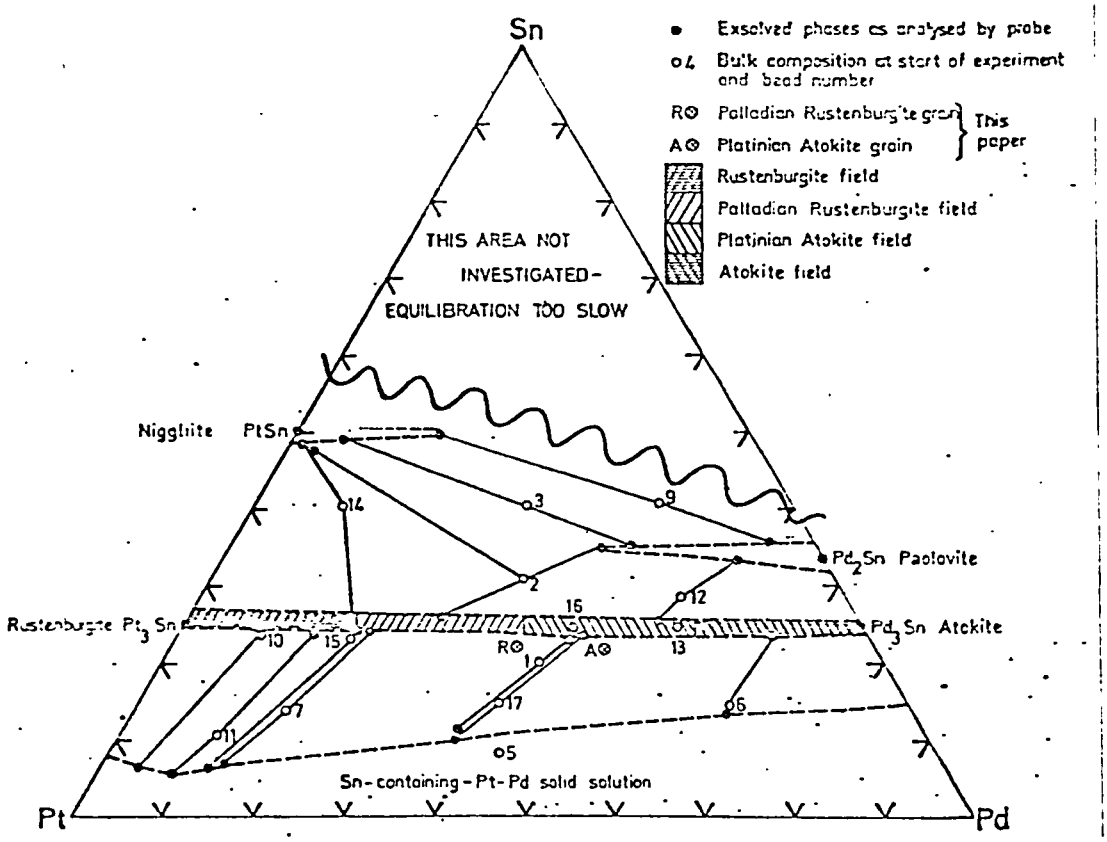

Fig. 5.21 Pt-Pd-Sn ternary diagram showing the relationships between already known minerals in the Pt, Pd-rich portion at room temperature. Diagram from Mihalik, Hiemstra, and de Villiers (1975).

cubanite-mooihoekite ores. It is orthorhombic, with noticeable bi-reflectance and pleochroism from dark lilac-rose to pale rose. Its reflectance at 600nm ranges from Rg 51.0 - 57.6 to Rp 48.4 - 53.8 percent, and it has a VHN_{50} range of 360 - 400 kig/mm^2. Its composition from their three analyses averages to $(Pd_{0.98}\ Pt_{0.02})_{1.98}\ Sn$.

Paolovite was first discovered in the Merensky Reef at Atok mine, eastern Bushveld, by Gasparrini et al. (1975), and subsequently reported in the western Bushveld by Vermaak and Hendriks (1976), although in the latter case no details were given to support it. It was presumably of very rare occurrence. The author has not yet found this phase at Rustenburg or Union mine.

5.2.3 Others. Vermaak and Hendriks (1976) report, but give no details, that the following alloys have been detected:

1. Pt-Sn-Fe-Pd alloy with major Pt and Sn, moderate Fe, and minor Pd.
2. Pt-Cu-Fe alloy.
3. Pd-Pb alloy with Pd:Pb roughly 1:1.

5.3 Gold-Silver-Palladium Alloys

5.3.1 Introduction. The author (1966) was the first to report the occurrence in the Merensky Reef of native gold and electrum containing substantial amounts of palladium. The presence of gold was already known, although, like Pt-Fe alloy, its mode of occurrence in the ore was unknown. There is some confusion in the literature as to the definition of electrum and native gold. Electrum has been variously defined in textbooks as gold containing silver in excess of 20 wt.% (Berry and Mason, 1959), 30-45 wt.% (Ramdohr, 1969), and 25 wt.% (Uytenbogaardt & Burke, 1971). As far as is known binary

and ternary alloys involving Au, Ag, and Pd are probably free of transformations, and natural occurrences of these phases are solid solutions having a face-centered cubic structure. Following the example set by Cabri and Feather (1975) for Pt-Fe alloys, it is considered best to define terms according to atomic percent. Thus the following nomenclature is used here.

Gold or Native gold for an alloy with equal to or greater than 80 atomic percent gold. In the usual case of argentian gold alloyed with silver this would correspond to $\geq$88 wt.% Au and $\leq$ 12 wt.% Ag. Palladian could similarly be used as a prefix where more than trace amounts of palladium were present.

Electrum for a variety of native gold with silver, where the Ag content is between 20 and 50 atomic percent, i.e. greater than 12 wt.% silver. The prefix palladian, platinian, rhodian etc can be added.

Gold-Silver Alloy is used where the composition has not been determined, since silver-free gold has not yet been proved in the ore.

On this basis all the grains analysed both qualitatively and quantitatively can so far be described as electrum and palladian electrum. This now dispenses with 'palladic gold' reported by the author in 1966. Since only a preliminary study of these alloys has been made by the author, they will be treated together, especially as it is not possible to distinguish between the two in reflected light.

5.3.2 The Occurrence of these alloys in the ore and concentrates are in two main forms.

Firstly small anhedral Au-Ag alloy grains or blebs of less than 10 μm in diameter occur at various contacts of chalcopyrite with braggite and cooperite. The majority of the blebs are found in braggite, and occur with some of the small euhedral chalcopyrite inclusions which are generally unrelated to any fractures. These inclusions are invariably bounded by negative crystal faces of the enclosing braggite and cooperite. Other grains occur along the contact of either thin fracture-controlled chalcopyrite veins, or more rarely at external crystal-face contacts with chalcopyrite. A possible explanation for this common association of Au-Ag alloy with braggite is given in chapter 6, in which figures 6.4, 6.5, and 6.12 illustrate the mode of occurrence described above.

The second form of occurrence is as large embayed anhedral grains which may exhibit a maximum dimension of about 0.5mm. These large grains have so far not been located in any of the polished sections of the ore and, since they are relatively free in the concentrates of attached sulphides and inclusions, it is difficult to speculate as to their probable mode of intergrowth and paragenetic position. Some of these grains are euhedral and some may exhibit one or two straight edges (fig. 5.22). It is considered that they are possibly of a late stage of formation, similar to type V Pt-Fe alloy.

A rare example of Au-Ag alloy in association with textural type III Pt-Fe alloy is shown in figure 5.23. The Pt-Fe alloy has overgrown a darker isotropic phase for which the gold inclusions appear to have a preference. The gold also appears to replace the core of the euhedral Pt-Fe alloy aggregates in other parts of the

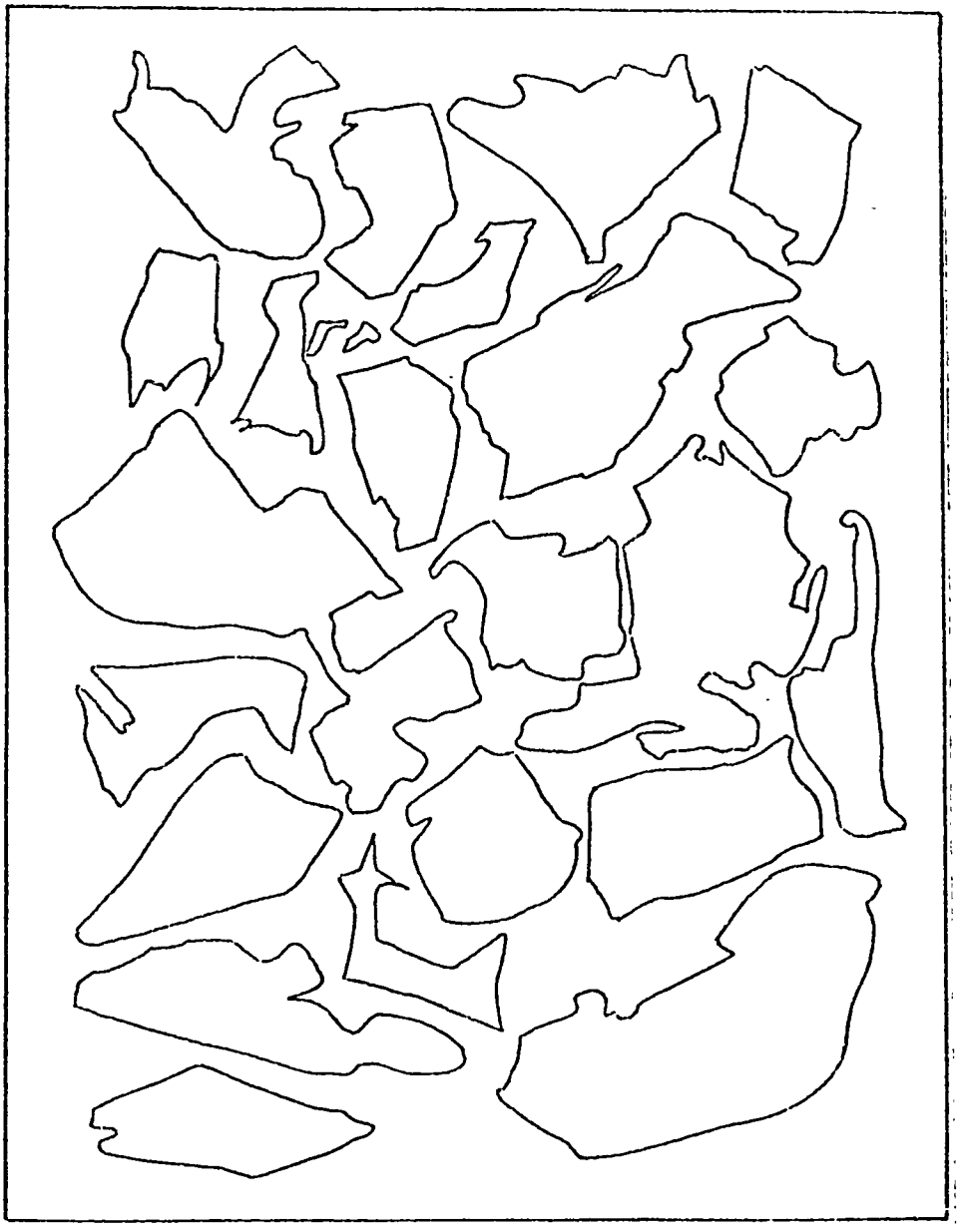

Fig. 5.22 Diagram illustrating the nature of the grain shapes exhibited by Au-Ag and Au-Ag-Pd alloy grains in the 'metallic' concentrates. Rustenburg mine.

intergrowth. However, this texture could still be formed by a process of segregation and crystallisation in the solid state.

5.3.3 The Composition of seven 'gold' grains in a table concentrate from Rustenburg mine were determined by electron-probe microanalysis. The elements detected with certainty were Au,Ag,Pd, Cu, and Fe, although traces of Ru,Rh,Ir, and Os were indicated on the pen-recorder scans.

The seven grains were selected from twenty microhardness-indented grains so as to represent a range of hardness which, it was hoped, would reflect a range of silver content. Prior to this a brief qualitative electron-probe study of some of the indented grains had shown the presence of silver with small amounts of palladium. The electron-probe microanalyses are presented in table 5.3, together with microhardness values. Because only an absorption correction has been applied, the values are still only approximate, and a little lower than they should be. However, this does not alter the fact that these grains clearly fall within the definition of electrum and palladian electrum.

A recent re-examination of these electrum and palladian electrum grains revealed the presence in all cases of nearly submicroscopic disseminated granules of a slightly lower reflectance phase (fig. 5.24). This phase was grey in comparison to the gold matrix and its reflectance was a little lower. It was also too small for resolution and analysis of individual grains by the electron-probe microanalyser.

A phenomenum probably related to the occurrence of these inclusions is that most of the electrum grains tarnish in the

Table 5.3 Electron-probe microanalyses in wt.%* and microhardness values of Au-Ag and Au-Ag-Pd alloys in a table concentrate (no. 1959) from Rustenburg mine.

Grain	Au	Ag	Pd	Cu	Fe	VHN_{50}
1	75·0	17·0	nd	nd	nd	126
5	72·0	14·0	nd	nd	nd	99
16	76·0	18·0	nd	0·1	nd	86
8	62·0	27·0	1·0	0·1	nd	97
9	63·0	20·0	7·0	0·1	nd	109
12	61·0	27·0	4.0	0·1	0·1	86
6	63·0	31·0	nd	nd	nd	72

* corrected for absorption only

nd not detected.

Fig. 5.23 Gold-silver alloy (light yellow) and an unidentified grey phase containing gold inclusions, enclosed by euhedral Pt-Fe alloy. The matrix pyrrhotite of this intergrowth has been removed by acid leaching. Union mine. Scale 1 cm = 7 μm.

Fig. 5.24 Palladic electrum exhibiting minute disseminated inclusions of a grey phase which may be a Ag-Pd alloy. Oil immersion at a magnification of approx. X 1400. Union mine concentrate. Scale 1 cm = 7 μm.

atmosphere after only a few weeks. However, synthetic Au-Ag alloys containing these quantities of silver are naturally not noted for their ability to tarnish in air. It is, therefore, likely that it is the inclusions which are tarnishing and they are a silver-rich phase, possibly alloyed to palladium. This also would explain the lack of correlation in table 5.3 between silver content and indentation microhardness. However, a close study of the X-ray spectrum produced from an area scan compared with an analysis of an inclusion free area may solve its identity.

Under low power magnification these inclusions cannot be seen and the gold appears homogeneous, with the grains exhibiting varying intensities of light yellow. All that can be concluded about the colour is that the lighter yellow 'anaemic' electrum grains generally contain more combined Ag and Pd. Schwellnus et al. (1976) found that gold-silver alloys at Atok mine in the eastern Bushveld varied from orange-gold grains with a silver content of about 4 wt.% to yellow ones of about 20 wt.%. They detected a constant 0·5 wt.% Pt in these grains. They did not, however, report any palladium content. No platinum has so far been detected in the electrum from Rustenburg and Union mines.

CHAPTER 6

PLATINUM GROUP SULPHIDES

6.1 Cooperite PtS

6.1.1 The Discovery of Cooperite is generally attributed to Cooper (1928) who reported the existence of a new mineral $Pt(AsS)_2$ in concentrates from Rustenburg. This formula is reported as having been calculated from a chemical analysis of a concentrate, believed by Cooper to be monomineralic, which gave a composition of Pt 64·2, Pd 9·4, S 17·7 and As 7·7 weight percent. For some unknown reason the palladium content was ignored in the formula. The composition is now known to be PtS, ideally containing Pt 85·89 and S 14·11 wt.% with some minor substitution of generally less than 1% Pd and Ni for platinum. However, contents as high as Pd 5·78, Ni 1·18 wt.% have been recorded by Schwellnus et al. from the Merensky Reef at Atok mine (1976), and Pd 1·5, Ni 1·6 wt.% from Western Platinum mine (Brynard et al., 1976). So far no substitution of arsenic for sulphur has been found.

Cooper determined the composition of cooperite by chemical analysis of a metallic residue resulting from the treatment of a sulphide flotation concentrate from Rustenburg with dilute nitric acid, to dissolve the base-metal sulphides, followed by careful washing "until a

perfectly clean residue of 'metal' was obtained". He appears to have assumed that this residue was dominantly one mineral, even though he was aware that native platinum and sperrylite had been found elsewhere in the Bushveld (chap.1.3). He also ignored the possibility of platinum group elements in the lattices of the sulphides. From his analysis and our present knowledge of the mineralogy of these concentrates it is probable that this insoluble residue consisted of a mixture of dominantly cooperite intergrown with some braggite (fig.6.1), together with sperrylite to account for the high arsenic content, and possibly some ferroplatinum in graphic intergrowth with cooperite (fig.6.2). This mixture was given the name 'cooperite' by Wagner in 1929.

The absence of nickel in the analysis by Cooper might suggest the absence of braggite were it not for the high content of palladium. The palladium could be accounted for by the presence of stibiopalladinite, arsenopalladinite, or the rare tellurides kotulskite and merenskyite. However Schneiderhohn (1928,1931) and Frick (1930) described the reflected-light properties of some 'cooperite samples' sent to them by Wagner (1929, p. 226), and it is clear from their data that they were actually examining grains of braggite. This descriptive error has been transcribed many times since then and still occurs in standard works of reference such as those by Uytenbogaardt

(1968), Ramdohr (1969), and Uytenbogaardt and Burke (1971). It is hoped that in future revised editions this confusion will be rectified.

Adam (1929,1931), in a study of the 'metallics' concentrates from Potgietersrust, isolated a number of grains of similar appearance by treatment of the concentrates with aqua regia followed by magnetic separation and hand picking under a binocular microscope. He obtained what externally appeared to be grains of one phase, and followed this by chemical analysis. The result of the analysis was Pt 71·5, Pd 6·4, S 14·1, Ni 2·0, and insolubles 1·5 weight percent. His analysis of a similar mineral fraction from Rustenburg gave Pt 72·9, Pd 6·2, S 15·0, As 0·2, Ni 2·2, and insolubles 2·6 weight percent. He suggested that the arsenic content was due to insoluble sperrylite. As a result of this Cooper later modified his original view and concluded that the mineral was really platinum sulphide and that the arsenic content of his original material was similarly due to sperrylite. Adam (1931) concluded that the "new mineral is approximately PtS_2, but there is a small excess of platinum over the proportion demanded by this formula and the mineral always contains about 6 wt.% Pd and a little nickel". Braggite, of common occurrence and of equal importance to cooperite in the Rustenburg concentrates (Kingston, 1966), was not known to exist at this time. Adam, however, did recognise

that there were composite grains present and reported the occurrence of ferroplatinum enclosing grains of 'the new mineral'.

The crystal structure and precise composition of cooperite was finally determined by Bannister (1932), and Bannister and Hey (1932). After treatment of some concentrates from Potgietersrust and Rustenburg with aqua regia, Bannister hand picked well developed crystals of sperrylite and laurite from the insoluble metallic residue and determined these by single crystal X-ray diffraction and chemical tests. The remaining fragments, "all steel grey in colour with a metallic lustre and rarely showing crystal form", were divided by X-ray diffraction studies of each grain into two X-ray pattern groups. The first group, after chemical analysis by Hey, proved to consist of a completely new mineral which was named braggite. Unorientated single crystal X-ray diffraction photographs of all grains belonging to the second group were found to fit exactly over a powder photograph of artificial PtS produced by fusing ½ g of Pt, 3 g of K_2CO_3, and 3 g of S in a procelain crucible for 15 minutes (Wartenweiler, 1928). Chemical analyses by Hey of these grains gave a composition close to the theoretical PtS with a slight excess of sulphur. The analyses for the grains from Potgietersrust were Pt 85·6, Pd trace, Ni 0·1, S 14·3 wt.% and from Rustenburg Pt 82·5, S 17·5 weight

percent. Further rotation, oscillation and Laue photographs of an orientated grain by Bannister (1932) showed that it possessed a tetragonal symmetry with unit-cell contents 8PtS, dimensions a_o 4·91, c_o 6·10 Å, space group D_{4h}^9-- P_4/mmc, and structure-type B17. He concluded that the crystal structure of cooperite was made up of planar groups of four sulphur atoms about each platinum atom and tetrahedral groupings of platinum around sulphur, and that it was the first binary compound shown to possess a structure in accordance with Paulings' prediction (1931) that Pt, Pd, and Ni with fourfold co-ordination should form planar MX_4 groups.

It is of historical interest to conclude as to who discovered cooperite. Cooper first showed the existence of a platinum sulphide. He was able to do this because no sulphide of platinum had been reported before, and therefore the presence of major sulphur in his dominantly PGE-containing residue was enough to postulate the existence of a platinum sulphide phase. Adam repeated the studies of Cooper on apparently coarser grained concentrates and was able to provide a slightly better idea of the composition of 'cooperite', although the material analysed was still a mixture. Schneiderhohn described what he thought was cooperite but was from his data most probably braggite. It was Bannister and Hey who finally isolated and defined cooperite. By present day standards

the data provided by Cooper would not be accepted as proof of a new mineral. However Bannister and Hey's data would be internationally acceptable. Therefore on these grounds and on the historical facts presented above they should be credited with the discovery.

6.1.2 The Mode of Occurrence of cooperite in the concentrates is dominantly in the form of free angular grains, and composite grains exhibiting a simple interlocking relationship with braggite (fig.6.1). Both these types are generally free of marginally attached base-metal sulphides, although inclusions may occur. This, together with its angular grain shapes, preserved crystal faces, and irregular fractures, reflects its hard and brittle nature and ease of liberation. In the composite grains, optically matching anhedral areas of cooperite can sometimes be found enclosed by braggite, which may also assume a penetrating vein-like relationship to the cooperite. Generally the boundary between cooperite and braggite is embayed, indicating that if the relationship is one of replacement there is no obvious crystallographic control, although a fracture control could have operated.

Other types of composite grains of rare occurrence are to be seen in the concentrates, and an examination of these is important for a complete understanding of the position of cooperite in the paragenetic sequence.

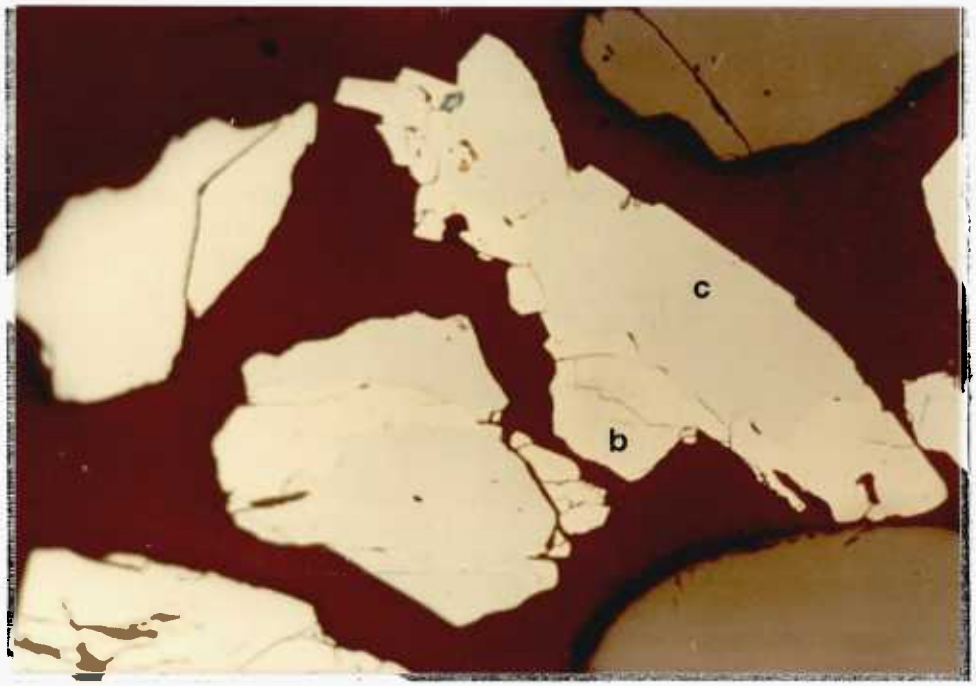

Fig. 6.1 Composite grains of cooperite (c) and braggite (b) showing the nature of the interphase boundary. Concentrate from Rustenburg mine. Scale 1cm =26μm

Fig. 6.2 Ragged inclusions of platinum (white) and chalcopyrite (yellow) in a grain of cooperite (bluish-grey). Concentrate from Union mine. Scale 1cm =10μm

For example at Union mine grains consisting of optically matching fragments of cooperite enclosed by a spongy or finely dendritic form of platinum occurred frequently in a non-magnetic tailings concentrate which had been acid treated (fig.6.3), and rare grains of cooperite with ragged disseminations of platinum were found in most concentrates containing the normal inclusion free and braggite associated cooperite (fig.6.2). The nature and textural interpretation of these has already been dealt with in chapter 5 under platinum and ferroplatinum, and will be discussed further in chapter 9.

In the polished sections of the ore, cooperite has been found as separate euhedral crystals (fig.6.4) and as simple interlocking aggregates with braggite. None of the rare textural forms seen in the concentrates have as yet been found in situ. A particular feature of cooperite crystals and crystal aggregates, when in direct contact with the silicates, is that the silicate-cooperite boundary is irregular or conforms to the shape of the underlying silicate. In contrast, those parts of the same crystal or crystal aggregate enveloped by chalcopyrite and pentlandite are idiomorphic, although some 'corrosion' of the euhedral outline is often seen. This can be interpreted as simple crystal growth from the enclosing silicate walls of a still molten or partly molten base-metal sulphide interstitial liquid. Vermaak and Hendriks (1976) interpret it as "irrefutable evidence" of such a mode of formation. However, whilst the author is largely in agreement with

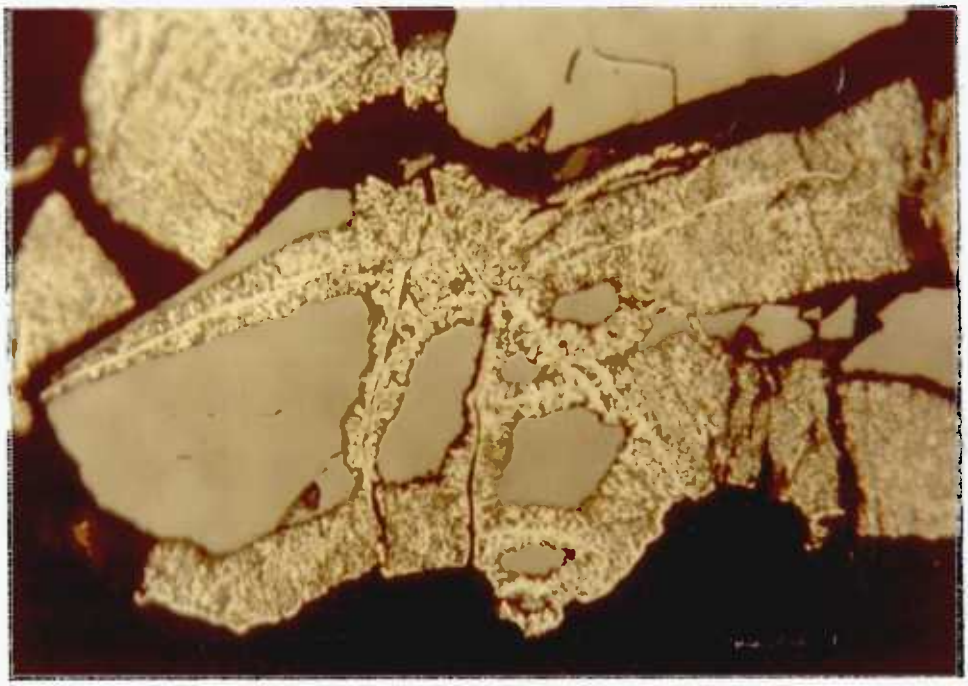

Fig. 6.3 Optically continuous cooperite veined and enclosed by spongy and dendritic platinum. Acid leached concentrate from Union mine. Scale 1 cm = 10 µm.

Fig. 6.4 A euhedral crystal of cooperite (light grey) formed at a sulphide/chromite-silicate junction, and overgrown by pentlandite, gold, and finally chalcopyrite. Fractures in the cooperite are filled with chalcopyrite and later silicates. Basal chromitite band of Merensky Reef at Rustenburg mine. Scale 1cm = 26 µm.

this interpretation, it must be borne in mind that this texture alone is not conclusive evidence that it grew in a liquid environment. Solid diffusion and recrystallisation processes could for example modify a replacement intergrowth near the margin, to produce an idiomorphic crystal, which would naturally assume the irregular boundary in contact with the silicates. However, the clear replacement relationship between cooperite and braggite, discussed below, would support the former interpretation.

In figure 6.5 braggite is everywhere marginally disposed about cooperite areas. Also, as is the case with figure 6.1, small blebs of gold occur near cooperite-braggite boundaries, either totally enclosed by braggite or at the contact with a chalcopyrite inclusion. It should be noted also that braggite in figure 6.5 displays good positive and negative crystal faces in contact with chalcopyrite. These intergrowths strongly suggest a replacement relationship between cooperite and braggite, and at least it is clear in figure 6.5 that braggite formed after cooperite and before the main period of chalcopyrite overgrowth. If replacement is envisaged then it may be that the gold is a by-product, formed either by the release of lattice held gold in cooperite or introduced at the time of replacement, with later segregation from the braggite metasome.

Fig. 6.5 An intergrowth of cooperite (light blue-grey) and braggite (creamy white) exhibiting well developed crystal faces, enclosed by pentlandite to the east, and silicates to the west, and overgrown by chalcopyrite. Rustenburg mine. Scale, 1cm = 17μm

Fig. 6.6 An aggregate of rectangular crystals of a cooperite-braggite intergrowth enclosed by pyrrhotite and pyrite, the latter exhibiting a controlled replacement by pyrrhotite. Rustenburg mine. Scale, 1cm = 80μm

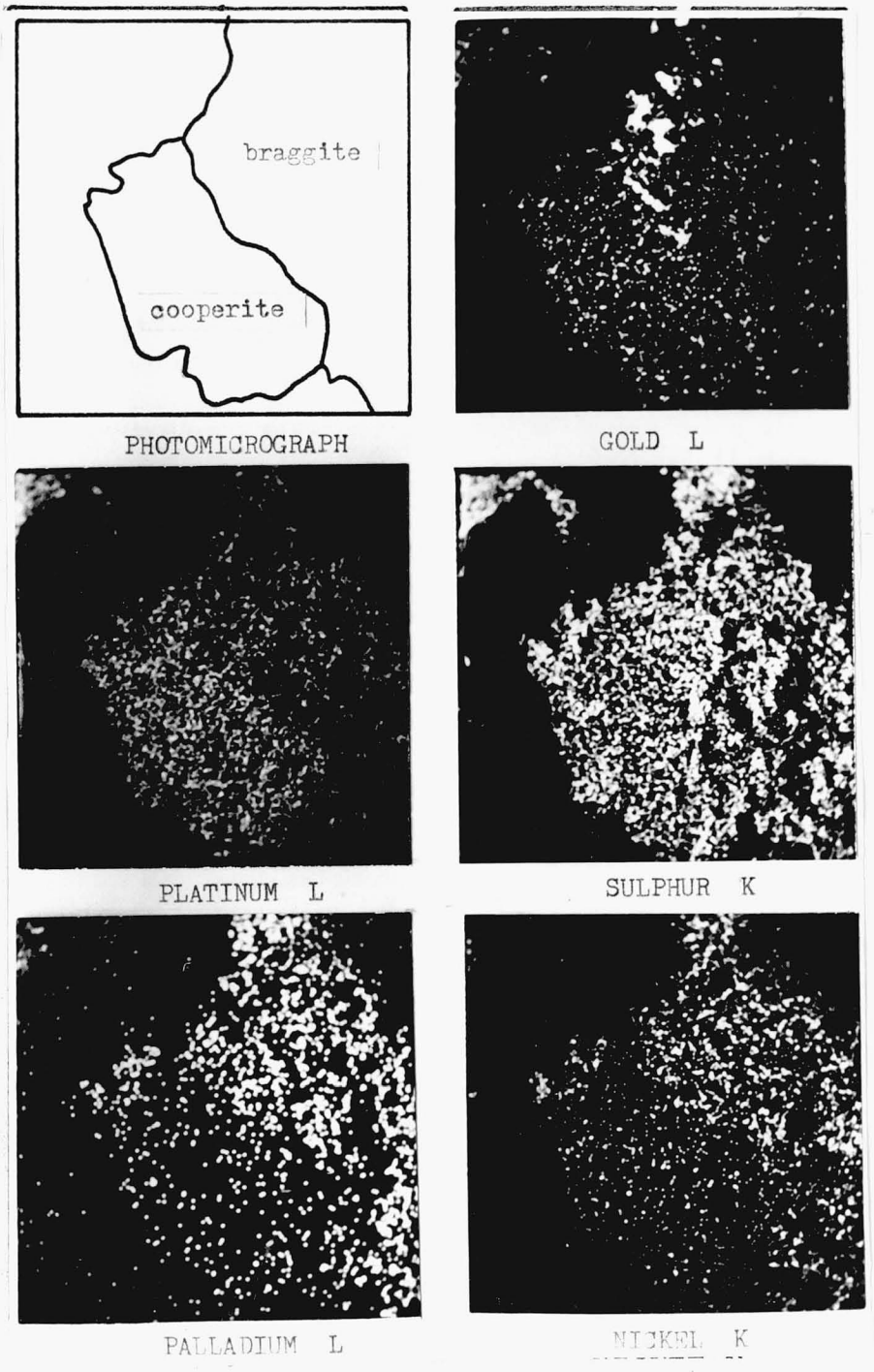

Fig. 6.7 X-ray scanning micrographs showing the distribution of gold, platinum, sulphur, palladium, and nickel in a composite grain of a cooperite-braggite intergrowth containing some free gold blebs. Rustenburg mine.

The author has found no reference to the detection of gold in either braggite or cooperite although trace amounts would be expected to occur. The presence of such small free gold inclusions in braggite would make the proof of lattice held gold difficult in amounts below the detection limit of the electron-probe microanalyser. However the invariable association of braggite with small blebs of gold cannot be mere coincidence. In the present study the X-ray scanning micrograph of Au Lα intensity distribution in a composite grain of cooperite, braggite, and free gold (fig.6.7) shows a higher intensity for cooperite than braggite. This could be used to support the proposal that gold occurs in the lattice of cooperite, and has been depleted in the replacing braggite by solid diffusion to form free gold blebs. The location of a silver-bearing braggite associated with electrum by Brynard et al. (1976) helps to support this idea.

Finally cooperite does not always occur near to or at the sulphide silicate boundaries but may very rarely occur as in figure 6.6. In this case an aggregate of euhedral braggite and cooperite crystals are largely enclosed by pyrite which has undergone partial replacement by pyrrhotite. More commonly, however, cooperite is to be found enclosed by pentlandite and chalcopyrite, with the latter infilling fractures and occurring as inclusions. These qualitative experience-based conclusions have recently

been confirmed by the quantitative study by Vermaak and Hendriks (1976), which determined that 75·28 vol.% of all cooperite occurred at the sulphide-silicate contact, of which 54·2 vol.% occurred in pentlandite, 17·74 vol.% in chalcopyrite, and only 3·34 vol.% in pyrrhotite. Of the remaining cooperite content, 24·26 vol.% was considered to be enclosed by silicates, with only 0·37 vol.% occurring away from the sulphide-silicate contact and enclosed completely by base-metal sulphides. This preference of cooperite, and most of the other platinum group minerals in the Merensky Reef, for occurring at the margins of the interstitial sulphide aggregates, and especially in direct contact with the enclosing silicates, is a feature which is discussed further in 6.22 and 6.3. They also report that 13·36 vol. percent of the total precious mineral content is cooperite, although, as for the previous data, this appears to be an average for the Merensky Reef from several localities.

6.1.3 The Optical and Physical Properties in reflected light of cooperite given in the reference books are still those originally determined by Schneiderhohn (1928,1931) and Frick (1930) for 'cooperite' grains of which some were doubtless braggite. The properties in no way resemble those of cooperite. However they are similar to those for braggite. Some new but incorrect reflectance data is given in Uytenbogaardt and Burke's book (1971).

The data in periodicals are equally confusing, conflicting and overlapping, and Leonard et al (1969) and Cabri (1972) have drawn attention to this. A summary of this data compared to the author's data is presented in table 6.1. The confusion in the literature presumably relates to observations on material which was not confirmed as cooperite by X-ray diffraction or electron-probe microanalysis, unlike the recent measurements of reflectance and microhardness by Schwellnus et al (1976).

The Colour, as can be seen from figures 6.4 and 6.3, is not 'brownish' in air (Uytenbogaardt and Burke, 1971) or 'coffee-brown to olive leather brown' in oil (Ramdohr, 1969). It is light grey in air and exhibits a distinct bireflectance from light grey to a slightly darker bluish grey. In oil this bireflectance is more distinct. Compared to braggite (fig. 6.1), with which it appears to be commonly confused, it is more of a neutral grey whereas braggite appears creamy grey with a slight pink or violet tint in air and is also only very weakly bireflectant. It is only when grains of cooperite and braggite are in close proximity that they can be distinguished from each other by brightness and colour alone with any degree of certainty. Figures 6.5 and 6.6 give some idea of the colour and brightness of cooperite in relation to braggite, pentlandite, chalcopyrite, pyrite and pyrrhotite. Unless the

Table 6.1 Comparison of published reflected-light data for cooperite since 1929.

References

(1) Kingston, 1976.

(2) Schwellnus et al, 1976. (R% data encompasses grains 2, 3, 4, which contain 0·15 - 0·79 % Pd and 0·79 - 1·18 % Ni).

(3) Uytenbogaardt and Burke, 1971. (Data from Ramdohr (1969) plus R% by Vyalsov (1970, pers.comm.) and VHN by Rozhkov et al (1962) in Leonard et al (1969)).

(4) Ramdohr, 1969. (Data in part modified from Schneiderhohn (1929)).

(5) Uytenbogaardt, 1968. (Data from Ramdohr (1950) which is from Schneiderhohn (1929, 1931).

(6) Timofeeva, 1968. (in Leonard et al (1969)).

(7) Zhuravlev et al, 1968. (in Leonard et al (1969)).

(8) Genkin, 1968. (in Leonard et al (1969) and Cabri (1972)).

(9) Pudovkina et al, 1966. (in Leonard et al)1969)).

(10) Rozkov et al, 1962. (in Leonard et al (1969)).

(11) Schneiderhohn and Ramdohr, 1931. (in German).

(12) Schneiderhohn, 1929. (in Wagner (1929), includes measurements of R% made by Frick with a photometer designed by Schneiderhohn). The first reflected-light description of what was believed to be cooperite.

* Young and Millman, 1964.

Table

Please see over

Table 6.1 Comparison of published reflected-light data for cooperite since 1929.

REF.	COLOUR air	COLOUR oil	BIREFLECTANCE PPL	ANISOTROPY XN	REFLECTANCE R in %.	HARDNESS VHN
(1) 1976	light grey to blue-grey Braggite appears creamy grey with a pink or violet tint compared to cooperite.	darker	distinct 470nm 5.2% 546nm 6.7% 589nm 6.4% 650nm 7.6%	strong, 45° position gives yellow brown or brownish yellow. D.Rr blue > orange, noticeable. Rr 2.8-3.8° D.Ar blue concave orange convex noticeable. Ar 1.6-2.2° No polysynthetic twinning.	R_o $R_{e'}$ 470nm 43.5 - 48.5 546nm 40.6 - 47.5 589nm 38.7 - 46.0 650nm 37.5 - 45.5	$\frac{VHN_{100}}{870 - 1033}$ mean 939 $\frac{VHN_{50}}{721 - 935}$ mean 835 ≫ platinum < sperrylite
(2) 1976	no data	no data	470nm 4.1% 546nm 6.4% 589nm 7.0% 656nm 7.5%	no data	R_o $R_{e'}$ 470nm 42.6 - 46.7 546nm 40.5 - 46.9 589nm 39.0 - 46.0 656nm 37.5 - 45.0	$\frac{VHN_{25}}{754 - 894}$ mean 833
(3) 1971	brownish, similar to pyrrhotite	more coffee-brown to olive leather brown than pyrrhotite	very weak, visible in oil on grain boundaries	very weak in air relatively strong in oil. Simple and polysynthetic twinning	460nm 40.5 550nm 39.0 600nm 37.0 650nm 36.5	$\frac{VHN_x}{505 - 588}$ < platinum ≪ sperrylite
(4) 1969	brownish, reminds one of magnetite and similar to pyrrhotite	coffee-brown to olive leather brown	low, noticeable in oil at grain boundaries	moderately strong	green 41 orange 34 red 34	approx. 4 on Mohs scale, (VHN equiv. of 185)*
(5) 1968	brownish, very similar to pyrrhotite	more coffee brown than pyrrhotite	weak or not perceptible	weak or not perceptible	air oil green 41 28.5 orange 34 25 red 34 21	platinum sperrylite
(6) 1968	coffee brown	no data	weak in air but distinctly increased in oil.		< pyrrhotite	$\frac{VHN_x}{203 - 276}$ mean 239
(7) 1968	grey-white	no data	(reflectance data indicates not perceptible).	distinct	600nm 37	no data
(8) 1968	grey-white	no data	negligible in air.	distinct, light grey to greyish-blue.	460nm 40.5 550nm 39.0 600nm 37.0 650nm 36.5	no data
(9) 1966			589nm 2.4% (presumably distinct)		589nm 40.0 - 42.4	$\frac{VHN_x}{505 - 588}$ mean 544
(10) 1962	grey with a creamy brown tint	richer brown	yellow 2.4% (presumably distinct)	distinct	yellow 40 - 42.4	$\frac{VHN_x}{505-588}$
(11) 1931	gelbweiB, ohne rosa Ton	weniger herabgesetz, viel weniger braun	ganz schwach, an Kotngrenzen in Ol eben bemerkbar.	bei + N mit der Schnittlage sind sehr schwach, wechselnd deutlich. Gerade Ausloschung. In der Diagonalsteeung (inOl) graurosa bzw. graugrunlich. Lamellenbau wird oft leicht erkennbar.	air oil green 41 28.5 orange 34 25 red 34 21	Mohn 4-5
(12) 1929	white with distinct greyish-yellow tint			weak to distinctly anisotropic. Grey-pink and grey-green in 45° position. Polysynthetic twinning.	green 37 orange 37 red 36	Mohs 4-5 (VHN equiv. of 185-541)*

material examined by Schneiderhohn was neither cooperite nor braggite it is difficult to understand how he could have considered that 'cooperite' bore any similarity to pyrrhotite. Ramdohr however did refer to its similarity to magnetite.

The Anisotropy under crossed nicols is strong compared to any of the other anisotropic platinum group minerals. Even with the nicols completely crossed the anisotropy is still very noticeable, in contrast to braggite which displays a much weaker anisotropy and is barely visible. This marked difference in anisotropy is very useful in the rapid identification of cooperite from braggite in concentrates, since the difference in their colour and reflectance is far from obvious. Grains showing the strongest anisotropy give brownish yellow colours in the 45^{o} position. The rotation properties as determined by I.M. Gray (1962, pers.comm.) on the author's material are given in table 6.1. These rotation properties are the same as for braggite except that cooperite has a medium isogyre separation (Ar 1·6-2·2°, with Rr 2·8-3·8°) and braggite as a negligible one.

The Reflectance was determined with a Reichert reflex spectral microphotometer at wavelengths of 470, 546, 589, and 650 nm. A secondary standard of pyrite from Kassandra mine was used. This had been calibrated against

N.P.L. Measured pyrite by A. P. Millman (pers.comm.).

Since cooperite is tetragonal it was expected that either the maximum or minimum values of reflectance obtained on a number of sections would be near constant (Cameron, 1963). From reflectance measurements on seven grains at 589nm and at the other wavelengths (table 6.2) it was found that the minimum values are constant and that cooperite is optically positive with a mean Ro and maximum Ré, at 589nm of 38·7% and 46·0% respectively.

The reflectance values compare very well and enforce those by Schwellnus et al (1976) which represent cooperite of similar composition to that of Rustenburg mine (table 6.1). To facilitate direct comparison their values for cooperite containing 3·95 and 5·78% Pd have been omitted in the calculation of mean Ro and maximum Ré. The values at 589nm given by (10) Pudovkina et al (1966) and Rozkov et al (1962) fall in the cooperite range, but in the case of (10) the colour and low hardness discredits the mineral as cooperite, and even as braggite. This probably applies also to reference (9). No other reflectance data needs to be considered in table 6.1 since no other workers have observed and measured the strong bireflection of cooperite. Finally the Ro and Ré spectral profiles confirm the qualitative colour observations in air.

Table 6.2 Spectral reflectance values in percent for cooperite in original material investigated by Cooper from Rustenburg.

Section 1941	Ro				Ré			
	470nm	546nm	589nm	650nm	470nm	546nm	589nm	650nm
gr.1	43·7	40·9	39·4	37·6	48·8	47·1	45·8	44·7
gr.2	43·2	40·2	38·4	37·4	48·5	47·5	46·0	45·5
gr.3			38·3				45·3	
gr.4			38·7				44·2	
gr.5			39·0				43·9	
gr.6			38·3				44·8	
gr.7			38·7					

The indentation Microhardness was determined on eleven grains using a 100g load. Because of the brittle nature of cooperite it was only possible to make two or three reliable indentations on any one grain at this load. The VHN_{100} range was 870 - 1033 with a mean value of 939 and a median value of 951. However with a 50g load up to six correctly spaced and reliable indentations could be made on the largest grains in the concentrates. Therefore an indication of the microhardness anisotropy of individual grain orientations could be obtained by making two indentations at each of three equal rotations of the indentation direction i.e. at N,N30°E, and N60°E. This was done for two grains and gave ranges of 721-935, and 851-895, with a mean of 835. This does not conform to the general rule of an increase

in microhardness with a decrease in load, and on the basis of Young and Millman's work (1964) a mean value lying between 995-1192 was expected (i.e. an increase of between 6 - 27%). However the even lower range of VHN_{25} 754-894 given by Schwellnus et al (1976) adds some weight to the validity of the author's values.

The Van der Veen line test virtually always shows cooperite to be harder than braggite. This is confirmed by the indentation microhardness values for braggite of VHN_{100} 847-882 which suggests a small overlap with cooperite. In only one case was a braggite-cooperite intergrowth found to show no difference in polishing relief using polarisation contrast; values from three indentations in each gave VHN_{50} 822 for braggite and VHN_{50} 803 for cooperite.

The deformation characteristics of cooperite (fig. 6.8) provide a useful means of distinguishing it from braggite. With a 100 g load cooperite usually exhibits three strong angular concave sides, one straight side associated with a strong side shell fracture, and four star radial fractures. With a 50 g load the fractures are less developed and the sides sigmoidal to concave with at least one straight side. Braggite fractures in a similar way but at most only exhibits very weakly concave sides. Finally, prior to 1976 all examples of published

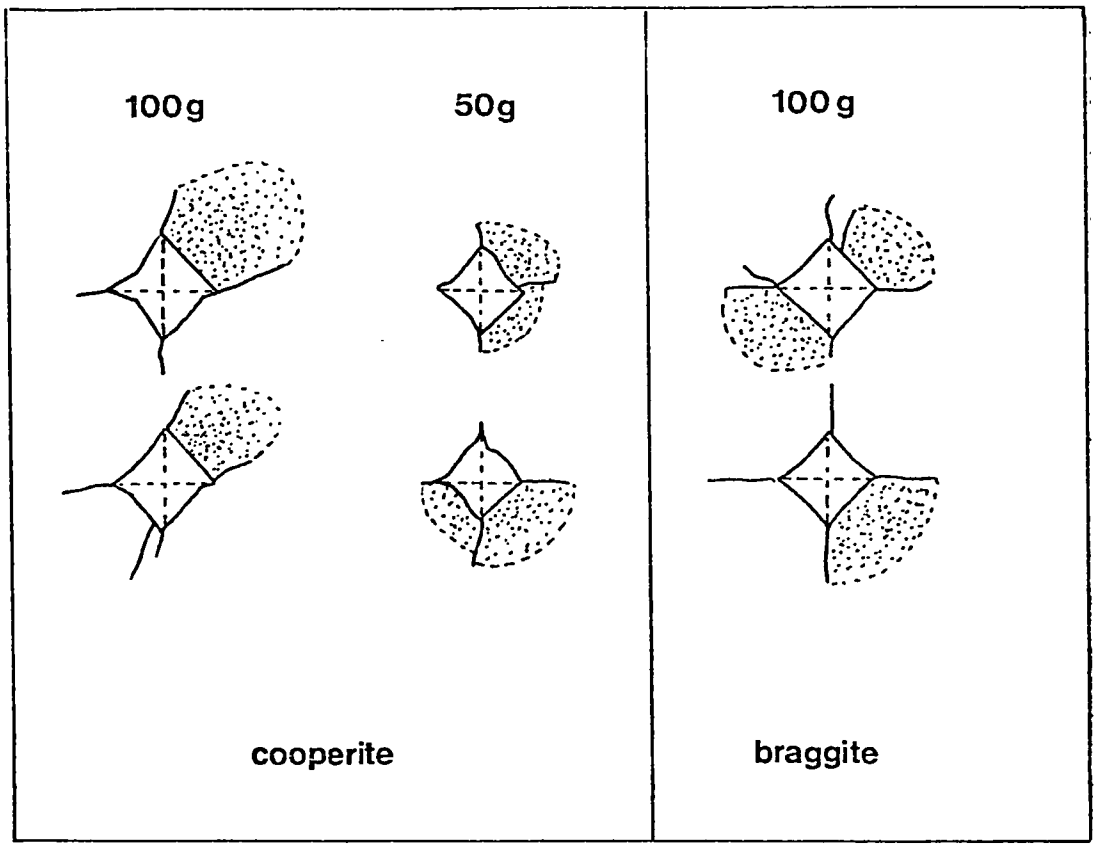

Fig. 6.8 Diagram illustrating the deformation characteristics of cooperite compared to braggite with a 100g and 50g load.

microhardness data given in table 6.1 are far too low. This further supports the author's contention that those descriptions do not refer to cooperite.

6.1.4 The Composition of cooperite, assuming it to be stoichiometric, is ideally Pt 85·89 and S 14·11 weight percent. In this study three grains of cooperite from Rustenburg were examined under the electron-probe micro-analyser which detected major platinum (75·0, 76·9, and 77·2 wt.% Pt before correction, at 35 kV and constant specimen current, and using a pure platinum standard), major sulphur, and in each case less than 1% combined nickel and copper (Ni> Cu). Traces of palladium, ruthenium, and rhodium were indicated but not with certainty. The presence of gold has already been discussed with regard to figure 6.7 which shows the distribution of detected elements in a composite cooperite-braggite grain. No other elements were detected.

Schwellnus et al (1976) record a range of Pd 0·15 - 5·78, Ni 0·68 - 1·18, Pb 1·27 - 1·35, and Bi 0·41 - 0·71 weight percent in cooperite from Atok mine. The negligible range of variation exhibited by the Pb and Bi content (table 6.3) compared to the sympathetic and fairly wide variation of Pt, Ni and Pd suggests four interpretations:

(1) the lead and bismuth atoms do not diadochically substitute for Pt, Pd, and Ni but occupy different and independent lattice positions,

(2) the lead and bismuth occupy interstitial spaces in a non-stoichiometric structure,

(3) the lead and bismuth represent submicroscopic inclusions of a lead-bismuth sulphide,

(4) the lead and bismuth are not present but represent a misinterpretation of second and third order platinum X-ray energy emissions, for example Pt L_{β_6} corresponds exactly with Bi L_{α_1} (fig 8.5).

Since these workers give no details of the emission wavelengths used, it is not possible to be sure which one or combination of these reasons is responsible. However electron-probe microanalyses of cooperite from Western Platinum mine by Brynard et al. (1976)show no detectable Pb or Bi. Therefore it is considered that at least the Bi and Pb content of Schwellnus et al. should be viewed with suspicion until further verified. Also the effect of subsurface intergrowths of braggite (fig. 6.5) with cooperite could be responsible for the unusually high palladium content in the case of two of their analyses (table 6.3). Brynard et al also report <0·02 wt.% Rh.

Table 6.3 Cooperite compositions from various sources expressed as atomic proportions.

Ref.	Locality	Pt	Pd	Ni	Pb	Bi	S	cation:anion
(1)	Rustenburg	0.78	----	----	----	----	1	0.78:1
(2)	Potgietersrust	0.982	----	0.004	----	----	1	0.99:1
(3)	Atok mine	0.94	0.08	0.03	0.01	0.004	1	1.06:1
		0.94	0.007	0.04	0.013	0.007	1	1.01:1
		0.94	0.01	0.03	0.011	0.006	1	1.00:1
		1.002	0.002	0.05	0.01	0.007	1	1.07:1
		0.89	0.12	0.04	0.01	0.007	1	1.07:1
(4)	Western Platinum mine	1.03	0.02	0.02	----	----	1	1.07:1
		0.96	0.03	0.04	----	----	1	1.03:1
		0.98	0.01	0.02	----	----	1	1.01:1
		0.97	0.02	0.06	----	----	1	1.05:1
		1.00	0.03	0.04	----	----	1	1.07:1
		0.97	0.03	0.04	----	----	1	1.04:1
(5)	Noril'sk	0.78	0.07	0.15	----	----	1	1.00:1
(6)	Potgietersrust	1.03	0.02	0.03	----	----	1	1.08:1

(1) & (2) Bannister and Hey, 1932.
(3) Schwellnus, Hiemstra, Gasparrini, 1976.
(4) Brynard, De Villiers, and Viljoen, 1976.
(5) Genkin, 1968.
(6) Cabri, 1972.

Table 6.4. X-ray powder data for cooperite PtS from Rustenburg mine (Cu radiation, Ni filter, and using 11·483 cm.(1) and 6 cm.(2) diameter cameras), and cooperite from Potgietersrust (Berry & Thompson, 1962.

	RUSTENBURG					POTGIETERSRUST			
(1) I	(1) (Cu)	(1) d(meas)	(2) I	(2) (Cu)	(2) d(meas)	I	(Cu)	d(meas)	hkl
1	12·92	3·44	1	12·78	3·48	2	12·85	3·47	010
10	14·83	3·01	10	14·68	3·04	10	14·75	3·03	002 011
-	-----	-----		-----	-----	2	15·9	2·81	---
4	18·34	2·45	3	18·22	2·46	5	18·3	2·46	110
1	19·69	2·29	½	19·57	2·30	2	19·7	2·29	012
5	23·83	1·906	4	23·61	1·923	7	23·7	1·918	112
4	26·01	1·756	3	25·87	1·765	6	25·9	1·765	---
4	26·46	1·729	2	26·22	1·743	6	26·35	1·737	020
-	-----	-----		-----	-----	½	29·65	1·558	120
2	30·38	1·523	1	30·16	1·533	1	30·15	1·535	004
5	30·88	1·501	4	30·63	1·512	8	30·7	1·510	022 121
-	-----	-----		-----	-----	½	33·5	1·397	---
2	36·55	1·293	1	36·25	1·303	3	36·4	1·299	114
3	38·71	1·232	2	38·44	1·239	6	38·6	1·236	123
-	-----	-----				½	38·8	1·230	220
2	41·97	1·152	2	41·94	1·152	½	42·0	1·152	015
2	42·27	1·145				4	42·2	1·148	024
2	42·74	1·135	2	42·52	1·140	5	42·7	1·137	022 031
1	44·70	1·095	½	44·35	1·102	3	44·6	1·098	130
2	48·34	1·031	2	48·03	1·036	6	48·2	1·034	132
1	50.07	1·004	½	49·81	1·008	3	49·7	1·011	
2	53·43	0·959	1	53·24	0·961	4	53·4	0·960	
2	53·71	0·956	-	-----	-----	-	-----	-----	---
1	54·13	0·950	1	54·01	0·951	4	54·1	0·952	
2	55·06	0·940	1	54·74	0·943	3	54·9	0·942	
1	59·90	0·890	½	59·66	0·892	3	59·7	0·892	
1	61·43	0·877	-	-----	-----	2	61·2	0·879	
2	62·39	0·869	1	62·11	0·871	4	62·3	0·870	
2	62·74	0·866	-	-----	-----	4	62·5	0·868	
1	65·67	0·845	½	65·25	0·848	2	65·4	0·847	
1	66·52	0·840		v.faint		3	66·4	0·841	
2	67·63	0·833	1	67·22	0·835	6	67·4	0·834	
-	-----	-----				1	70·3	0·818	
2	77·44	·789				4	77·2	0·790	
1	79·67	0·783				3	79·5	0·783	
3	82·35	0·777				5	82·2	0·777	
3	83·61	0·775							

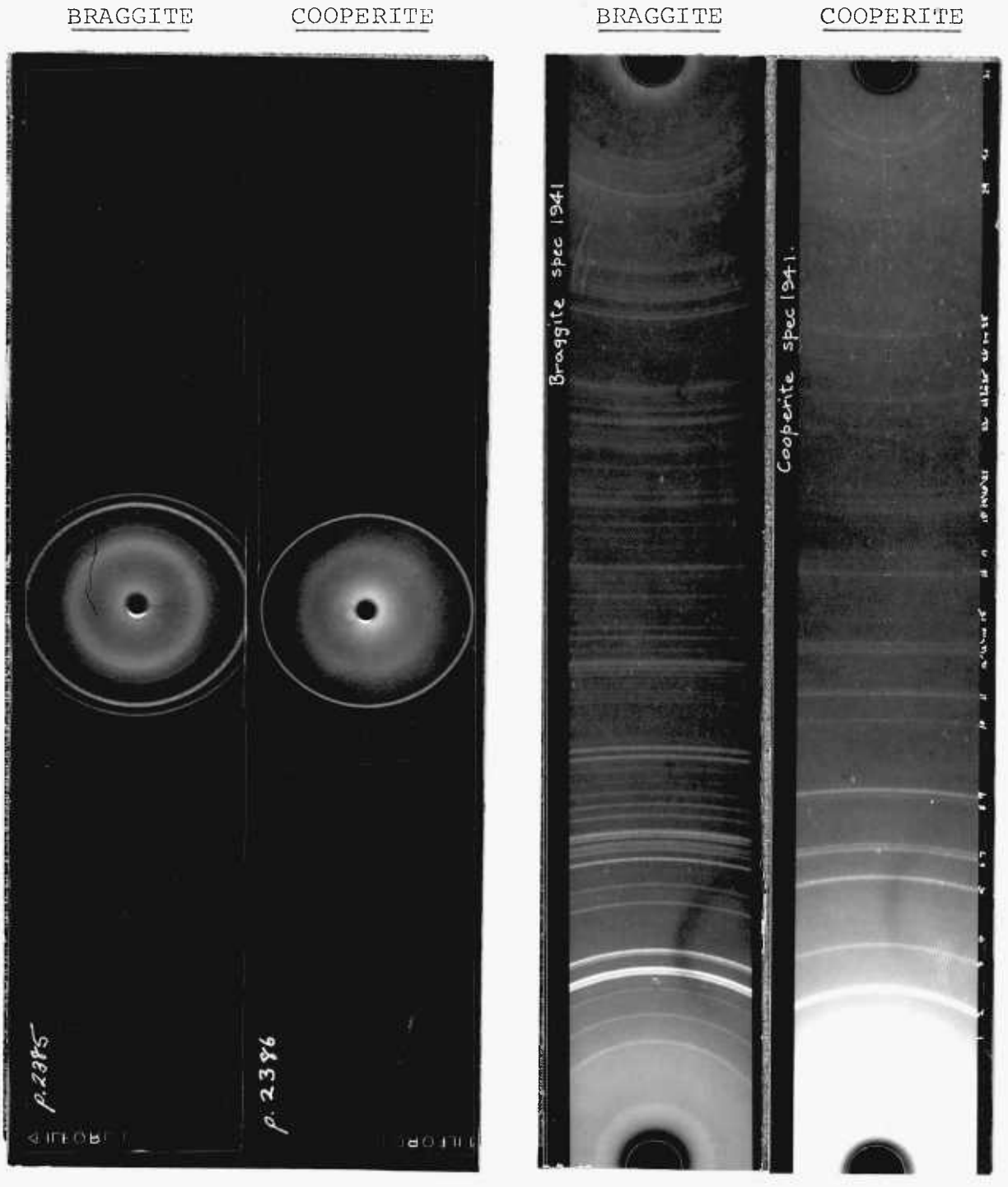

6 cm diameter camera

11·483 cm diameter camera

Fig. 6.9 Contact prints of X-ray powder photographs of cooperite and braggite from Rustenburg mine.

The electron-probe microanalyses together with the X-ray powder diffraction data (table 6.4, and fig. 6.9) provided positive confirmation that the three Rustenburg grains analysed were cooperite, although whether they conform to the 1:1 cation:anion ratio indicated by previous workers (table 6.3) requires further work. It is interesting to note that the analyses of cooperite from Potgietersrust by Bannister and Hey (1932) approximated closely to a 1:1 ratio, whereas their analysis of Rustenburg cooperite was 1:0·8. A correction of the author's analyses for absorption alone gives a 1:0·6 ratio. It may be that Rustenburg cooperite is non-stoichiometric compared to elsewhere. If this is the case then it could account for the gold blebs in braggite as being formed, during the replacement of cooperite, by release of interstitial gold. Finally the reflectance values in table 6.2 agree with the lack of compositional variation shown by Rustenburg cooperite. Compositional studies of Union mine cooperite have still to be done, although optical and physical properties are identical to Rustenburg cooperite.

6.1.5 X-ray Powder Diffraction data for Rustenburg cooperite compared to data for Potgietersrust cooperite by Berry and Thompson (1962) are given in table 6.4. The powder patterns of cooperite and braggite, using 11·483 and 6 cm diameter cameras, are presented for comparison in figure 6.9. In this investigation X-ray

diffraction analysis has only been used, in conjunction with electron-probe microanalysis, to identify cooperite. Having determined the correct properties these were found sufficiently different from any of the other PGM in the concentrates and ore to permit rapid identification during subsequent cooperite-intergrowth studies.

The cell structure and parameters for cooperite from Rustenburg were determined by Bannister (1932, 1937, see 6.1.1). As with other data there is some confusion over the cell dimensions for cooperite. Bannister's values (1937) are a_o 4·91, c_o 6·10, whereas Berry and Thompson (1962) and the ASTM index give values of a_o 3·48, c_o 6·11 Å. The latter values are reported to be by Bannister (1932), although the d-spacings data are for Potgietersrust cooperite and are by Berry and Thompson. Strunz (1970) reports cell data by Wartenweiler (1928) as a_o 3·48, c_o 6·11 which refers to synthetic and presumably stoichiometric PtS. Thus the cell sizes of synthetic PtS and Potgietersrust cooperite appear to be identical but smaller than Rustenburg cooperite. However comparison of the d-spacings in table 6.4 confirms that Rustenburg cooperite has nearly the same cell size as Potgietersrust cooperite.

The atomic structure proposed by Bannister is supported by Evans (1966, pp 140-141) who states that the

sulphides of palladium and platinum have structures closely resembling those of the corresponding oxides, with the metal atoms showing a characteristic planar distribution of four dsp^2 bonds in the divalent state. Thus sulphur atoms are dispersed in a plane almost at the corners of a square, and platinum atoms are tetrahedrally grouped around sulphur (fig. 6.10). The very small difference in electronegativity between platinum and sulphur suggests a small ionic character (less than 18%). However as with other transition-element minerals the bonding characteristics are probably complex and best understood within the crystal

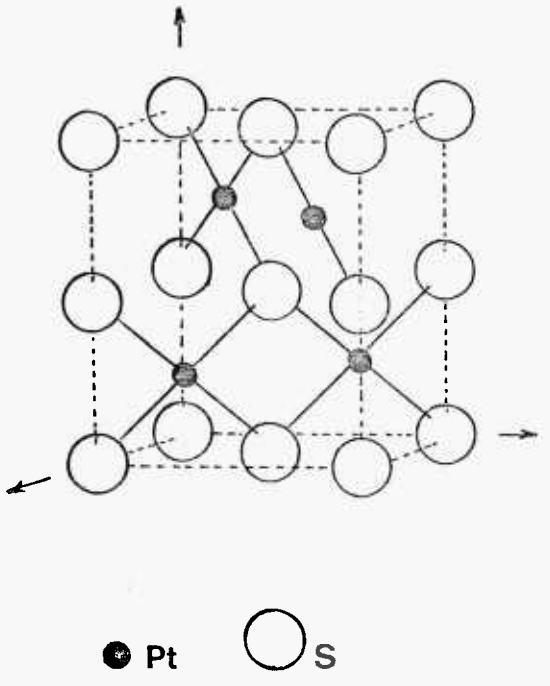

Fig. 6.10 Clinographic projection of the unit cell of cooperite (after Evans, 1966).

field theory. Aspects of bonding and element substitution in the platinum group minerals in general will be dealt with in chapter 9. It is however evident that a thorough re-examination of the crystal and atomic structure of cooperite is required.

X-ray diffraction analysis is considered the most reliable single method of identifying cooperite, especially since good powder patterns can be obtained from material extracted from a polished-section area of 30μm diameter; thus leaving sufficient of the grain for further study. However, with experience of the platinum group minerals, the combined reflected-light properties of cooperite are sufficiently characteristic to facilitate reliable identification during the routine monitoring of processing concentrates and ore. Electron-probe micro-analysis can be used for identification but, if used in a cursory manner or without prior microscopic observations, the results can be misinterpreted, for example where consid-erable substitution by palladium and nickel or intergrowths with braggite occur.

6.2 Braggite (Pt, Pd, Ni) S, with Pt> Pd≥ Ni

6.2.1 The Discovery of Braggite was by Bannister (1932, 1937) who isolated it from Rustenburg and Potgietersrust concentrates by using powder and single crystal X-ray diffraction techniques. It was the first new mineral (together with cooperite, 6.1.1) to be isolated and characterised by X-ray methods and was therefore named in honour of Sir William Henry Bragg and Professor William Lawrence Bragg. The X-ray powder pattern was found to be the same as for artificial PdS (determined by Bannister in 1932 as tetragonal with a_o 6·43, c_o 6·59 Å), and a chemical analysis by Hey (1932) gave a Pt:Pd:Ni ratio of 4·5: 2·5: 1·0 corresponding to Pt 60·15, Pd 18·27, Ni 4·02, and S 17·56 weight percent. Single crystal photos confirmed a tetragonal symmetry, unit cell of 8 (Pt, Pd, Ni) S, a_o 6·37, c_o 6·58 Å, and space group $C^2_{4h} = P^4_2/m$ or $C^3_4 = P^4_2$. Gaskell (1937) redetermined the structure of artificial PdS as tetragonal, with a_o 6·43, c_o 6·63 Å, and space group P^4_2/m. A comprehensive refinement of the crystal structure of braggite has been done by Childs and Hall (1973) who give cell dimensions of a_o 6·380, c_o 6·570 A, and Z=8 with space group P^4_2/m. The basic structure is the same as for cooperite, and results from the combined co-ordination of square-planar co-ordinated metals and tetrahedrally co-ordinated sulphur as in figure 6.14. They tested several different configura-

Table 6.5. Comparison of published reflected-light data for braggite since 1942.

REF.	COLOUR	BIREFLECTANCE & REFLECTANCE R%	ANISOTROPY XN	HARDNESS VHN	COMMENTS
(1) 1976	light creamy grey in air with a faint violet tint against cooperite. Grey compared to pyrite.	very weak but detectable across twin boundaries in oil. 470nm 42.8 - 44.0 546nm 42.9 - 44.8 589nm 43.0 - 44.3 650nm 43.0 - 44.6	distinct to weak, 45° position gives greyish-yellow or brown colours. D.Rr blue orange, noticeable. Rr 3.2° D.Ar blue concave, orange convex. Ar v.small.	VHN_{100} 847 - 882 mean 864	Confirmed by X-ray diffraction and electron-probe micro-analysis.
(2) 1976	no data	Range 470nm 40.9 - 44.3 546nm 41.9 - 46.3 589nm 42.4 - 45.6 650nm 42.3 - 45.9	no data	VHN_{25} 679 -1070 mean 864	Confirmed by electron-probe microanalysis.
(3) 1971	creamy white with a faint violet tinge Bluish or brownish grey compared to platinum.	distinct in oil, bluish tints. 589nm 34.5 - 35.5	rather strong, especially in oil, blue to brown polarisation colours.	VHN_x 742 -1030	Description of a cooperite-braggite intergrowth.
(4) 1969 1960	hard to define because of pleochroism, in oil blue-grey although in part brownish grey.	weak in air, appreciable in oil. R > cooperite > niccolite < a metal ≥ stibiopalladinite	distinct especially in oil.	> platinum > cooperite sperrylite	A confusion of a braggite-cooperite intergrowth as one mineral.
(5) 1968 1951	as for (3)	distinct in oil. R high.	as for (3)	> platinum > cooperite > stibio-palladi-nite ≪ sperrylite	same comment as for £3).
(6) 1962	white in air with weak bluish grey tint.	distinct in air, bluish tints. In oil, bluish grey to brownish grey. R yellow 34.5 - 35.5.	distinct	VHN_x 742-1030	description of cooperite. Large hardness range from cooperite plus braggite.

References

(1) Kingston, 1976. (2) Schwellnus et al, 1976. (3) Uytenbogaardt & Burke, 1971 (refers to reflectance and hardness data by Rozhkov et al, 1962). (4) Randohr, 1960 - 1969 (refers to a note on the optical properties of braggite by Edwards et al, 1942). (5) Uytenbogaardt, 1968 and 1951 (data from Ramdohr, 1950, and Edwards et al, 1942). (6) Rozhkov et al, 1962, in Leonard et al, 1969.

tions of metal ordering for the stoichiometric composition $Pt_5\ Pd_2\ Ni\ S_8$ and proposed that the two Pd atoms preferentially occupy the site 2(d), $(0,\frac{1}{2},\frac{1}{2})$ in the structure, and that this is the minimum requirement in the formation of the braggite rather than the cooperite structure.

As with cooperite there is again some confusion in the standard reference books over the optical and physical properties of braggite under reflected space light. This is illustrated by table 6.5 where it is shown that prior to 1976 descriptions of braggite have been in part confused with cooperite, and cooperite-braggite intergrowths.

6.2.2 The Mode of Occurrence of braggite follows closely that of cooperite. This is one of the main reasons for the confusion in the literature over their respective reflected-light properties. It is one of the most abundant platinum group minerals in the Merensky Reef in general, being common at Rustenburg mine although of minor importance at Union mine. A relative abundance value of 35·9 vol. percent of the precious mineral content is given by Vermaak and Hendriks (1976) for braggite in Merensky Reef ores from the western Transvaal. It usually occurs in the concentrates as part of angular composite grains (fig. 6.1) produced as a result of the brittle fracture of cooperite-braggite aggregates (fig. 6.6) and replacement intergrowths (fig.6.5). Free grains may occur, in which case it is generally diffi-

cult to distinguish it from cooperite with certainty. The general characteristics which can help in this case being its much weaker anisotropy, frequent occurrence of gold inclusions, and common exhibition of lamellar or polysynthetic twinning. When close to cooperite its creamier colour is clearly seen.

Its form of occurrence with cooperite in polished sections of the ore has been dealt with in section 6.1.2 (figs. 6.5 and 6.6). Vermaak and Hendriks (1976) have shown that, with regard to its average distribution in the ores of the western Transvaal, 64·2 vol. % of all braggite occurred at the sulphide-silicate contact associated with pentlandite and chalcopyrite, with the remainder not in direct contact with the silicates but enclosed by pentlandite. Rarely was it enclosed by silicates alone or by pyrrhotite. It is considered that the cooperite-braggite interphase boundary represents a replacement front, and that the replacement took place in the late stages of sulphide formation, just prior to the crystallisation of chalcopyrite. This late stage formation of braggite is in agreement with the mineral distribution results of Vermaak and Hendriks, and explains the rare occurrence of braggite in pyrrhotite, which must have shielded enclosed cooperite grains from replacement. The platinum released by the Pd and Ni substitution contributed towards the later formation of the various

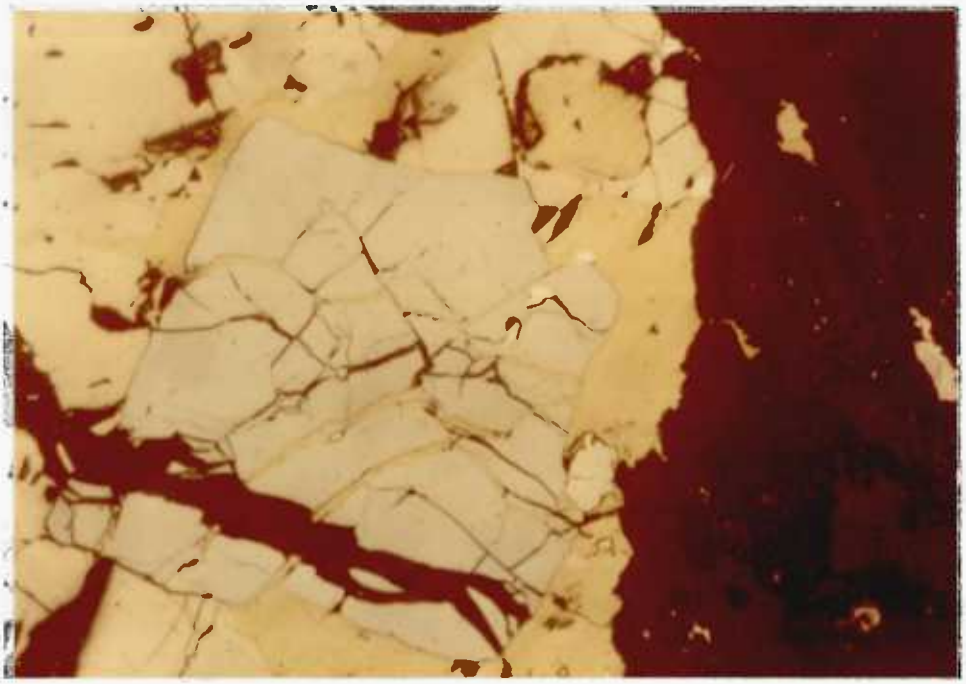

Fig. 6.11 A fractured rectangular euhedral crystal of braggite enclosed by chalcopyrite and pentlandite, and veined by chalcopyrite and 'silicates'. Some small grains of moncheite and kotulskite (white) are also present. Scale 1 cm = 40 μm.

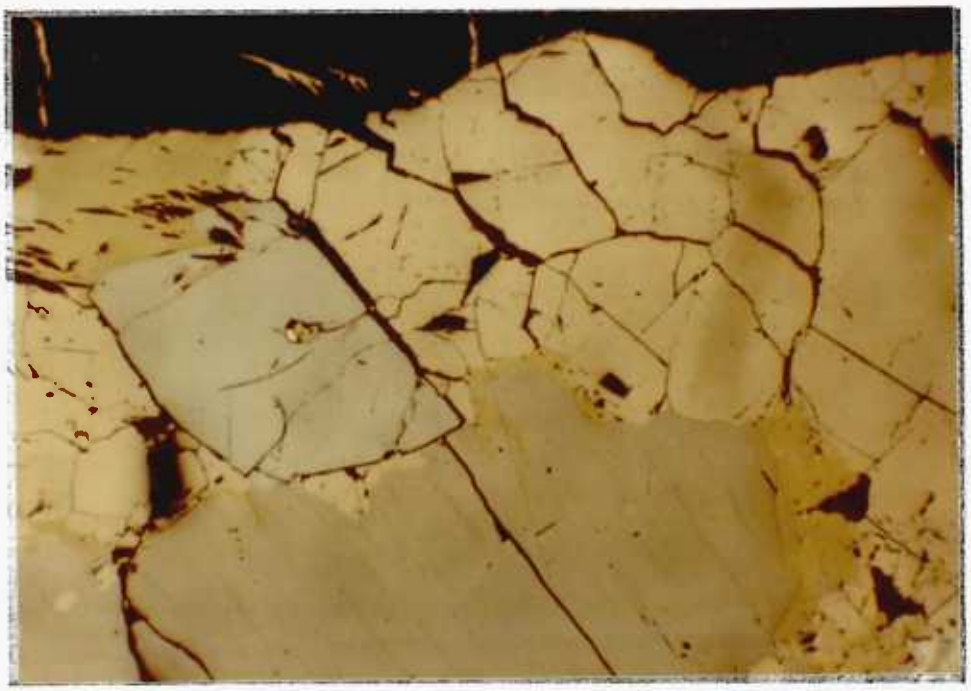

Fig. 6.12 A euhedral rhombic crystal of braggite enclosed by pentlandite and chalcopyrite, and veined by chalcopyrite and 'late-stage silicates'. Small gold bleb is associated with chalcopyrite inclusion in the braggite. Pyrrhotite occupies the area to the south. Scale 1 cm = 40 μm.

platinum bismuthotellurides, which are commonly present in chalcopyrite in the vicinity of cooperite-braggite intergrowths and solitary braggite crystals (fig. 6.11). This late stage palladium metasomatism is also in agreement with the general geochemical behaviour of this element as discussed in chapter 9.

Work on the structure of braggite by Childs and Hall (1973) indicates the ease with which this replacement can proceed. It involves essentially no change in basic structure but a slight change in metal configuration where, although palladium and nickel occupy the vacated platinum sites in the cooperite structure, the metal-to-sulphur distances are different with Pd-S - 2·26 Å and (Pt, Ni)-S - 2·33 ± 0·01 Å. The effect is essentially the formation of a cooperite-like subcell (a - 3·3, c - 6·6 Å) within the cell of braggite (fig. 6. 14A&B).

It may be that not all braggite occurrences at Rustenburg and Union mines are a result of the replacement of cooperite, since euhedral crystals can be found without any internal 'residual' cooperite or any cooperite in the vicinity. Figure 6.11 is a spectacular example of one of these solitary braggite crystals which has fractured prior to chalcopyrite crystallisation. The solution-widened fractures have been infilled with a late stage silicate and chalcopyrite, and a number of

small white grains of moncheite and kotulskite occur in the chalcopyrite around the braggite and in the fractures. In this example it is considered that the braggite crystal was originally cooperite which formed or perhaps gravity settled near to the margin of an interstitial liquid sulphide droplet, and, after some minor sulphide-magmatic corrosion was subsequently partly engulfed by pentlandite. Fracturing of pentlandite and the 'cooperite' crystal coincided with the deposition of a late stage silicate in the fractures and probably palladium and nickel metasomatism. The latter process may have resulted in some further fine fracturing due to a change in volume. Finally chalcopyrite, enriched in platinum from the replacement of cooperite, and in palladium from its geochemical preference for a copper-rich sulphide environment, was deposited in the solution widened fractures and around the braggite. Simultaneous crystallisation and exsolution of platinum and palladium bismuthotellurides occurred with the chalcopyrite formation.

Figure 6.12 is a further example showing that the braggite crystal is clearly overgrown by pentlandite and veined by 'late stage' silicates and chalcopyrite. The characteristic gold inclusions also occur. No occurrence of pentlandite in the fractures in braggite have been found. The relationship with pyrrhotite is not clear here, but in figure 6.6 rectangular braggite-cooperite

crystals are for the most part enclosed by pyrrhotite resulting from the desulphurisation of pyrite. It would appear, therefore, that cooperite is a very early formed 'magmatic' platinum group mineral and that braggite is mostly, if not always, formed from cooperite by a late stage palladium-nickel metasomatism during the residual and more fugitive-element-laden stages of interstitial sulphide melt differentiation. The occurrence of these 'heavy' braggite-cooperite intergrowths near to or at the boundaries of the interstitial sulphide aggregates with the enclosing silicates has been often interpreted as evidence for late stage formation. However, as already indicated, gravity settling could be one of the mechanisms to account for their peripheral location, although early growth on existing silicates, as illustrated in figure 6.5, is also considered to have operated. Figure 6.11 may be an example of a crystal which has 'broken away' during or after crystal growth. Vermaak and Hendriks (1976) have not recognised a replacement relationship between cooperite and braggite. They suggest that 'crystals of these hard platinoid minerals (including laurite and sperrylite) were expelled bodily to the base-metal sulphide-gangue contact by the growing sulphide crystals in the blebs of interstitial base-metal sulphide liquid'. They also try to explain the strong affinity of braggite for pentlandite as being possibly due to a Pt-Pd solid solution in it,

with the resultant exsolution of braggite. However, the evidence presented here for a largely replacement origin for braggite dispenses with the need to envisage such an unlikely physico-chemical relationship, and explains and is compatible with the quantitative mineral distribution data by these two authors.

6.2.3 The Optical and Physical Properties in reflected light are summarised in table 6.5 together with data from various sources. It appears that prior to 1976 confusion has arisen because of the mistaken identification of cooperite for braggite. For example the description by Ramdohr (1969) that braggite in oil appears 'blue-grey although in part brownish grey' is a clear reference to a cooperite-braggite intergrowth. Similarly the range of Vickers microhardness values is considered too great, even in the case of the data by Schwellnus et al (1976).

The Colour in air of braggite is a very light creamy grey, having a pinkish or violet tint when compared against cooperite, and solitary crystals appear grey compared to surrounding yellow base-metal sulphides. In the latter case its weaker anisotropy, polysynthetic twinning and associated gold blebs distinguish it from cooperite. Reflection pleochroism is weak to undetectable according to whether observed under oil or in air. Where twinning is present pleochroism may be detected.

The Reflectance values (table 6.6), using the same photometer and standards as for cooperite, indicate that braggite is optically + ve. The slightly yellow-biased dispersive character exhibited by the R_o and R_e, spectral profiles agrees with the observed colour. Similarly the R_o and R_e, profiles of cooperite (table 6.2) also agree with the observed distinct pleochroism in shades of bluish-grey. The summarised R_o and R_e, values are given in table 6.5 and are closely similar to those given by Schwellnus et al.

Table 6.6 Spectral reflectance values for braggite from Rustenburg

Sp.no.	R_o 470nm	546nm	589nm	650nm	R_e, 470nm	546nm	589nm	650nm
2049	42·8	42·9	43·5	43·3	42·8	43·5	43·9	43·9
1941	42·7	42·9	42·5	42·6	43·8	44·8	44·3	44·6
1942	42·8	-	-	-	44·0	-	-	-

The Anisotropy under crossed nicols is distinct to weak with polarisation colours of greyish-yellow to brown. Rotation properties are the same as for cooperite except that cooperite has a measurable isogyre separation and braggite a negligible one.

The Indentation Microhardness has already been discussed in connection with its use in distinguishing cooperite from braggite (fig. 6.8). It should be noted

that there was difficulty in obtaining measurable indentations because of star radial and shell fracturing combined with a general lack of suitably sized and inclusion free braggite surfaces. Finally it has a high polishing relief against pyrrhotite, pentlandite and chalcopyrite, and commonly exhibits irregular fractures which are often locations for gold, and platinum-palladium bismuthotelluride inclusions.

6.2.4 The Composition of braggite from various sources (Cabri, 1972; Schwellnus et al. 1976; Brynard et al. 1976) demonstrates that it can exhibit a fairly wide range of variation with Pt 49·4-68·1, Pd 9·4-24·5, Ni 2·4-8·0 wt. percent, corresponding to atomic proportions of $Pt_{0·43-0·69}$, $Pd_{0·17-0·39}$, $Ni_{0·08-0·25}$. However if a stoichiometric metals:sulphur ratio of 1:1 is assumed then the proportions will range as in table 6.7. Schwellnus et al also record up to 1·11% Pb and 0·9% Bi, both of which have not been detected before. It is considered that the explanation for the Pb and Bi content is as discussed previously under cooperite, and has therefore been omitted in table 8.7.

In 1962 Genkin and Zvyagintsev described vysotskite which, on the basis of one microspectrographic and two wet chemical analyses, they concluded could be represented by the formula $Pd_{0·68}\ Ni_{0·29}\ Pt_{0·03}\ S_{1·00}$, although other formulae have been quoted from their

Table 6.7 Composition of braggite and cooperite from Rustenburg mine and other localities expressed as atomic proportions of the metals assuming a metal:sulphur ratio of 1:1.

Ref./Grain		Pt	Pd	Ni	Mineral
(i)	a	0.44	0.34	0.22	braggite
	b	0.39	0.40	0.21	braggite
	c	0.43	0.32	0.25	braggite
	d	0.48	0.24	0.28	braggite
	e	0.54	0.27	0.19	braggite
	f	0.46	0.27	0.27	braggite
	g	0.43	0.35	0.22	braggite
(ii)	1	0.55	0.24	0.21	braggite
	2	0.56	0.19	0.25	braggite
	3	0.44	0.40	0.16	braggite
	4	0.56	0.25	0.20	braggite
	5	0.71	0.20	0.08	braggite
	6	0.69	0.17	0.14	braggite
(vii)	1	0.47	0.37	0.16	braggite
	2	0.50	0.32	0.18	braggite
(ii)	1	0.89	0.08	0.03	cooperite
	2	0.95	0.01	0.04	cooperite
	3	0.96	0.01	0.03	cooperite
	4	0.95	0.002	0.05	cooperite
	5	0.85	0.11	0.04	cooperite
(iii)		0.56	0.31	0.13	braggite
(iv)		0.78	0.07	0.15	cooperite ?
(v)		0.95	0.02	0.03	cooperite
(vi)		0.94	0.06		cooperite
		0.91	0.09		cooperite

Refs. (i) Kingston, 1976. (ii) Schwellnus et al, 1976. (iii) Hey, 1932. (iv) Genkin, 1968 (in Cabri, 1972). (vi) Bannister and Hey, 1932 (in Cabri, 1972). (vii) Brynard, De Villiers, and Viljoen, 1976. (v) Cabri, 1972.

results by other workers e.g. Cabri (1972). Vysotskite is isostructural with braggite and, although it has not been found in the Bushveld, at least a partial solid solution relationship exists (fig. 6.13). However further work needs to be done on vysotskite, especially with the electron-probe microanalyser.

The compositions of seven grains of braggite from Rustenburg mine were determined by electron-probe microanalysis. The analyses are presented in table 6.7 in the form of atomic proportions for comparison with other published data, and also are plotted on a ternary composition diagram in figure 6.13. For the purpose of comparison the atomic proportions have been recalculated on the assumption that braggite exhibits a stoichiometric ratio. The non-stoichiometry indicated by some published grain analyses may be real, but probably fall within the small but unknown range of experimental error characteristic of electron-probe microanalyses which are based on theoretical corrections rather than direct comparison with a synthetic standard of the same composition.

The analyses of Rustenburg braggite have only been corrected for absorption. However absorption is by far the most important correction in this system and, since nickel was also analysed at a low voltage to reduce the effect of fluorescence, it is considered that the metal

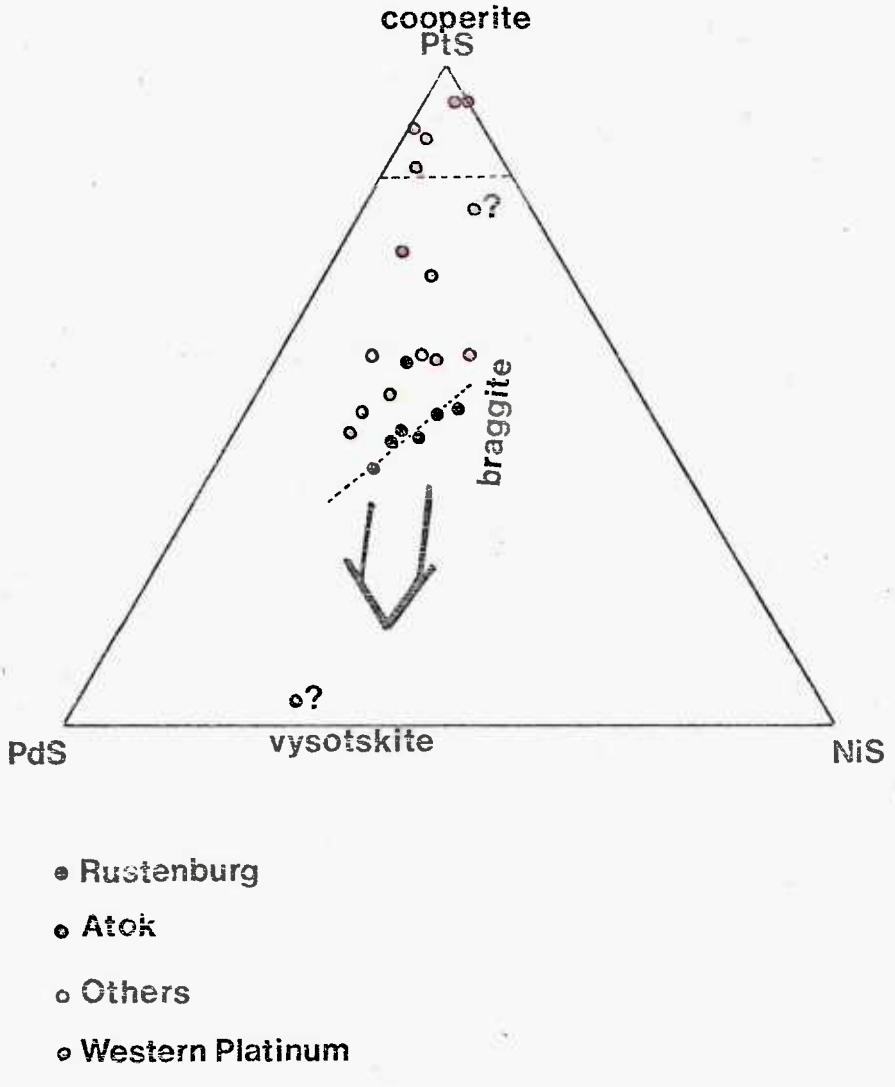

Fig. 6.13 Ternary composition diagram showing the range of composition exhibited by braggite and cooperite, together with the average compositional trend direction towards vysotskite and the local 'Rustenburg trend' towards PdS.

proportions given in table 6.7 are accurate enough to demonstrate the compositional trend. Consideration of these and previously published analyses as a whole indicates an overall trend towards vysotskite by substitution of Pd and Ni for platinum. However consideration of Rustenburg braggite alone clearly shows an antipathetic relationship between Pd and Ni and a trend towards PdS. This is also suggested by the Atok mine braggite. There is much doubt about the true metal proportions for vysotskite, since the analysis was not done by electron-probe microanalysis, but by wet chemical and spectrographic methods which introduce a greater risk of contamination through mineral intergrowth. It is likely that this mineral is merely an intermediate member of a solid solution series between presently known 'braggite' and unknown PdS.

This apparent contradiction between an average compositional trend involving a sympathetic relationship between palladium and nickel and a local trend involving an antipathetic relationship can be explained by the fact that Rustenburg and probably Atok-mine and Western Platinum-mine braggite has been formed largely, if not completely, by the replacement of cooperite. It is considered that there was an initial transformation to braggite by a palladium-nickel metasomatism involving a fairly even balanced substitution for platinum by both these metals. At a

Fig. 6.14A The structural model of braggite with each atom in a single unit cell represented as a thermal ellipsoid.(1)

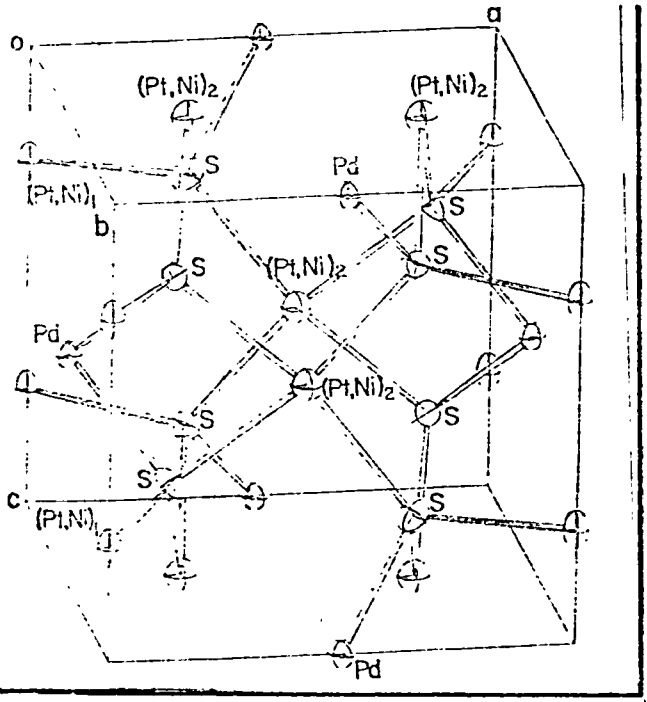

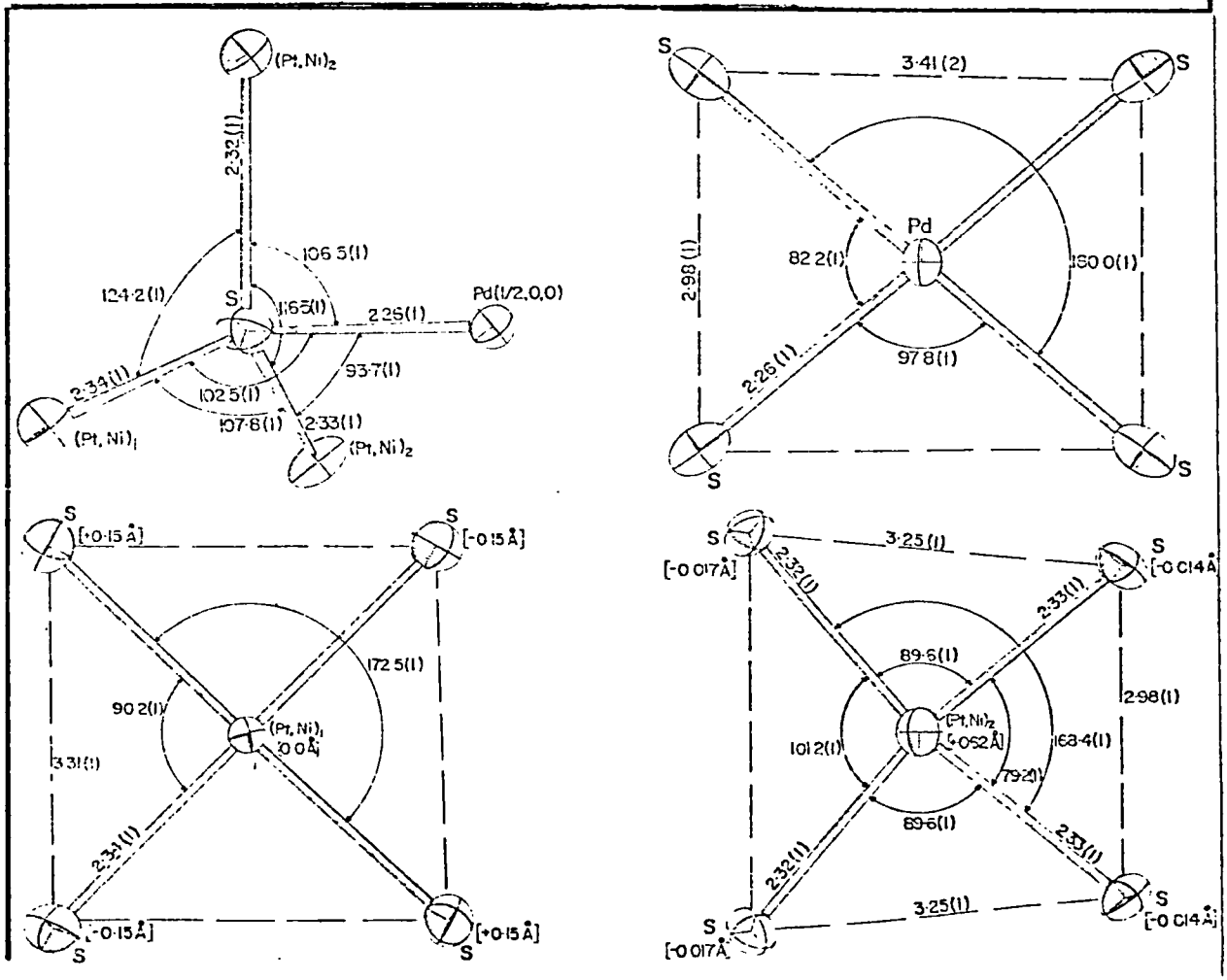

Fig. 6.14B Bond distances and angles about the sulphur site 8(k), the Pd site 2(d), the $(Pt,Ni)_1$ site 2(e), and the $(Pd,Ni)_2$ site 4(j). Displacements of the atoms from a mean plane are enclosed in square brackets.(1)

(1) Childs and Hall,1973.

later time or with a drop in the availability of nickel, palladium continued to substitute for further platinum as well as some of the previously introduced nickel. The compositional variation of braggite exhibited in figure 6.13 reflects, therefore, its replacement origin. This also emphasises the need to correlate or interpret analytical data within a background of microscopic study and control. The reason for the close association of gold blebs with braggite has been discussed earlier (6.1.2).

6.2.5 The Crystal Structure of braggite has already been summarised (6.2.1) and has been fully refined and defined by Childs and Hall (1973). However there is still scope for further work on structural correlations with compositional variation, particularly in the light of progressive palladium and nickel substitution in the cooperite lattice. The present study however confined the use of X-ray powder diffraction to the mere confirmation that the electron-probe microanalyses were of braggite. The data for braggite from Rustenburg mine is given in table 6.8 for comparison with closely similar published data by Berry and Thompson (1962). Its easily identifiable X-ray powder pattern is displayed in figure 6.9 in conjunction with the distinctly different pattern of cooperite.

Table 6.8 X-ray powder data for braggite from Rustenburg mine (Cu radiation, Ni filter, and using 11.483 cm diameter camera).

RUSTENBURG MINE			RUSTENBURG (Berry and Thompson 1962)		
I	θ(Cu)	d(meas)	I	θ(Cu)	d(meas)
½	5.40	8.18	-	-	-
3	9.82	4.52	1	9.7	4.58
3	12.06	3.69	½	11.85	3.75
½	13.67	3.26	-	-	-
1	14.06	3.17	½	13.90	3.21
8	15.39	2.90	3	15.25	2.93
10	15.70	2.85	10	15.65	2.86
3	17.00	2.63	½	16.85	2.66
7	17.21	2.60	3	17.00	2.64
3	21.09	2.14	1	20.90	2.16
2	22.60	2.00	1	22.50	2.01
5	24.61	1.850	3	24.60	1.852
2	25.38	1.797	1	25.25	1.807
1	25.77	1.772			
2	25.99	1.758	1	25.8	1.771
2	26.47	1.728	1	26.45	1.731
4	26.79	1.709	2	26.75	1.713
2	28.13	1.634	1	28.00	1.642
2	29.02	1.588	2	28.95	1.595
1	30.07	1.537	½	29.90	1.547
½	30.88	1.501	½	30.8	1.506
½	31.98	1.454	½	31.8	1.463
4	32.97	1.415	3	32.8	1.423
3	33.61	1.391	2	33.65	1.391
-	-	-	½	34.1	1.375
v.f.	37.42	1.268	-	-	-
½	37.77	1.258	-	-	-
½	38.17	1.246			
1	39.58	1.209	½	39.7	1.207
½	39.98	1.199	½	39.9	1.202
2	40.46	1.187	2	40.5	1.187
½	41.51	1.162	½	41.4	1.166
2	42.52	1.140	2	42.6	1.139
1	43.37	1.122	1	43.2	1.126
1	45.86	1.073	1	45.8	1.075
2	48.20	1.033	2	48.0	1.037
½	51.72	0.981	½	51.7	0.982
-	-	-	1	53.3	0.961
2	59.91	0.890	-	-	-
2	60.10	0.888	-	-	-
1	62.67	0.867	-	-	-
1	68.44	0.828	-	-	-
½	68.77	0.826	-	-	-
1	79.32	0.786	-	-	-

6.3 Laurite RuS_2

6.3.1 Introduction. The occurrence of laurite in the Bushveld was first confirmed by Bannister and Hey (Bannister, 1932) in concentrates from Potgietersrust, although Spencer (1932) had previously drawn attention to the presence of a 'cubic mineral' in these concentrates in his discussion of a paper by Adam (1931). Juza and Meyer (1933) followed this with a study of the Ru-S system and showed that RuS_2 was the only stable sulphide of ruthenium. Laurite was next reported in the Bushveld by Ramdohr (1950) and Stumpfl (1961) from the Overwacht and Dreikop pipes respectively. It is uncertain when it was first confirmed in the Rustenburg and Union mine ores and concentrates. An early report was by Berry and Thompson (1962), who published their own X-ray powder data for laurite using a Royal Ontario Museum specimen from Rustenburg. However its existence in these concentrates appears to have first been known around 1952. This is evident from an unpublished research report at that time for Messrs Johnson and Matthey Ltd by Lever, Todd, and Powell in which they considered that the ruthenium content of the final insoluble residue after progressive acid treatments of concentrates from both mines was due solely to laurite. However in the case of Rustenburg mine, where the ruthenium content of the ore is twice that at Union mine, there was little insoluble residue. This is

connected with the occurrence of most of the ruthenium content in the sulphide flotation concentrate and smelters 'matte' whereas laurite is of rare occurrence in the heavy 'metallic' platinum-group-mineral table concentrates. However at Union mine laurite is one of the most abundant minerals in these 'metallic' concentrates, although the 'matte' contains equally as much ruthenium as at Rustenburg.

The first analysis and in situ record and confirmation of laurite in these concentrates and ores was however by the author (1966). At this time laurite was also shown to be able to contain substantial mounts of iridium, osmium, and platinum. Since then Schwellnus et al have detected the additional presence of iron and nickel in laurite from Atok mine.

6.3.2 The Mode of Occurrence in the concentrates and ore is illustrated in figures 6.15 and 6.16. Laurite is rare in the Rustenburg concentrates and has not been found in any polished sections of the ore. In contrast it is fairly common and easily found in both at Union mine. This is remarkable since, as mentioned earlier, the average ore assay shows a greater content of ruthenium at Rustenburg mine than at Union mine. Since no other ruthenium mineral has been found at Rustenburg to account for this high content it must be concluded that most is locked in the lattice of the base-metal sulphides, although some is

undoubtedly present as trace amounts in the major platinum group minerals already known to occur.

Union mine laurite has so far been found in polished sections of the ore as perfect euhedral crystals enclosed by cobaltian pentlandite (fig. 6.16), either very close to or in contact with the enclosing silicates. It characteristically contains no inclusions. In figure 6.16 the silicate-filled cracks are probably due to a reduction in volume of the pentlandite enclosing the laurite crystal through cooling from magmatic temperatures. This factor, together with the symmetrical compositional zoning of this crystal suggests that laurite, like cooperite, is early formed and pre-pentlandite. The compositional zoning appears to contradict any recrystallisation mechanism involving laurite. Its closeness to the silicate-sulphide boundary could be a gravitative phenomena as suggested for cooperite. Vermaak and Hendriks have quantitatively confirmed laurites' preference for being enclosed by pentlandite and chalcopyrite at the silicate-sulphide contact. They have shown that of the total average laurite content for the Western Transvaal 90·16 vol. % is formed at the sulphide-silicate contact, with 17·24 vol. % in pentlandite, 59·67 vol. % in chalcopyrite, and 13·25 vol. % in pyrrhotite. These figures are, however, not specifically for either Rustenburg or Union mines.

In the concentrates (fig. 6.15A&B) complete euhedral crystals are common, and its highly brittle nature and extreme hardness is reflected in its very high polishing relief against the mounting plastic, the excellent polish, and the often conchoidal curving fracture surfaces which give rise to distinctive angular fragment shapes in the concentrates.

6.3.3 The Optical and Physical Properties of laurite in general are now well documented, a particularly valuable contribution being by Leonard et al (1969) on the microscopy and electron-probe microanalyses of laurites from Borneo, Goodnews Bay in Alaska, and the Stillwater Complex in Montana. However, prior to the authors study, no quantitative data has been available for Union mine laurite.

The Colour in air is light grey with a distinctive bluish tint, especially against the yellow base-metal sulphides. It is not pleochroic.

The Reflectance values in air of six crystals of laurite from Union mine are presented in table 6.9 for comparison with those by Leonard et al. A Reichert reflex spectral microphotometer was used with an Atomic Energy Commission standard pyrite measured by the National Physics Laboratory (S. Bowie, pers comm.). Each value is an average of several measurements, in most cases four.

Table 6.9 Spectral reflectance values for laurite from Union mine (1)-(6) compared to the range exhibited by five laurites determined by Leonard et al. (7), and Gray and Millman (8) (1960).

Wavelength in nm.	R_{air}%							
	(1)	(2)	(3)	(4)	(5)	(6)	(7)	(8)
470	45·7	45·4	45·4	45·5	45·6	45·8	45·8-48·0	39·7 bl.
546	42·2	42·4	42·7	42·6	42·3	42·9	38·5-42·5	43·8 gr.
589	41·1	40·8	41·2	41·2	41·0	41·5	36·4-40·3	45·9 yl. 42·5 or.
650	40·1	40·4	39·8	39·6	40·0	40·4	35·4-38·2	43·4 rd.

The blue biased dispersion profiles are consistent with the qualitative colour observation above, except for those of Gray and Millman (1960). However their values do not warrant the criticism by Ramdohr (1969, p808), based on a visual estimate of laurite as being 'at least as high as that of pyrite', that the values of Gray and Millman are 'questionable and have therefore been omitted'.

The very small variation between the grains agrees with a number of preliminary semi-quantitative comparative electron-probe microanalysis scans which demonstrated that Union mine laurite generally displays a small range of osmium and iridium variation with none to only trace platinum. It was only in the unique

occurrence of zoned laurite (fig. 6.16) that a wide variation in composition was exhibited, and where a higher reflectance than normal corresponded to an (Ir-Os-Pt)-rich marginal zone (Kingston, 1966). It is considered probable that osmium is mostly responsible for the higher reflectance since the Os:Ir ratio is greater in the outer higher reflectance zone than in the (Os-Ir-Pt)-rich inner zone (fig. 8.17) which has the same reflectance as the (Os-Ir-Pt)-poor zones. Similarly the platinum content appears to have little effect since its content is low, its variation small, and it shows no extra enrichment in the marginal zone compared to the central zone. This relationship is supported by data on a 'new ruthenium mineral' by Stumpfl and Clarke (1965) which has an estimated reflectance in white light of 60-65%, and which was of composition 33% Ru, 20·9% Os, 11·4% Ir, and 21·4% S (summation 86·7% from one electron-probe microanalysis). This mineral has a similar X-ray powder pattern to laurite and is weakly anisotropic. It is presumably the substitution by 'hexagonal osmium' which has produced the loss of cubic symmetry, although ruthenium metal has itself a hexagonal structure. However in this case and in the present study it is probably not wise to come to any certain conclusion about the relative role of osmium and iridium in altering the reflectance of laurite, although the evidence suggests to the author that osmium substitution is the more effective. Difficulties in coming to a valid conclusion arise out of the fact (Leonard et al 1969) that there is generally only

a small difference in reflectance between laurites of quite different compositions, and the confidence level for statistical comparison of reflectivity is not high. Also at least a three element substitution is involved, and finally non-stoichiometric variation may have an effect.

The Indentation Microhardness was difficult to determine satisfactorily because of the extreme hardness and brittle nature of laurite, with the consequently small indentation size and strong star-radial and side-shell fracturing (fig. 6.15A&B). Most indentations exhibited distinctly concave sides. Even with a 50g load fractures would often extend to the grain margin. Because of this it was generally only possible to make one indentation per grain, and many grains were indented for every one which could be measured. Where fractures extended to the grain boundary the value was low, even in the case like figure 6.15B. The range of values determined from eleven satisfactory identations are as follows: VHN_{100} 1132-2099, and VHN_{50} 1467-3010 with mean values of VHN_{100} 1531 and VHN_{50} 2291. However, ignoring those values where fine fractures extended to the grain boundary or where large shell fractures were formed, mean values of VHN_{100} 2055 and VHN_{50} 2641 are considered to more closely represent the true hardness. For comparison the following values have been recorded for laurite by other workers:

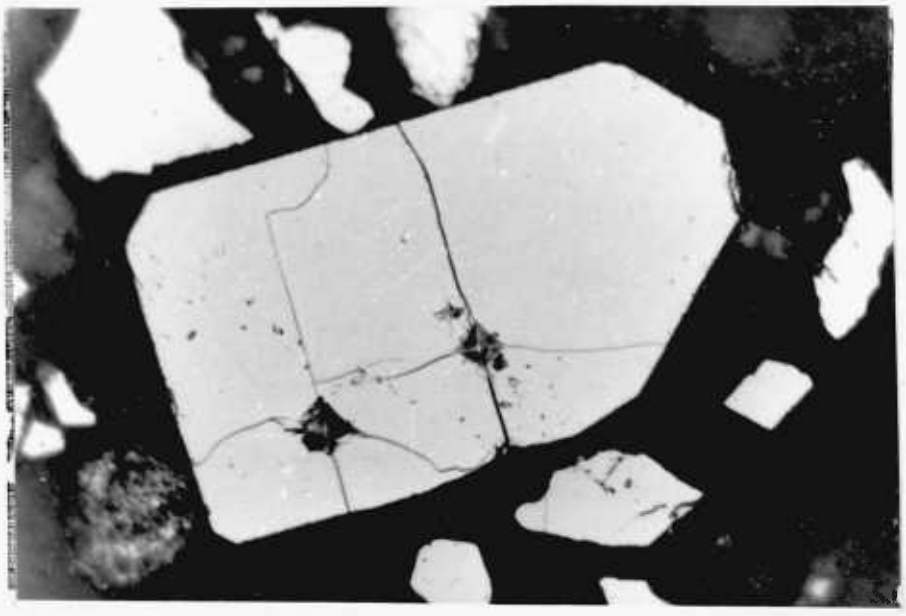

(A)

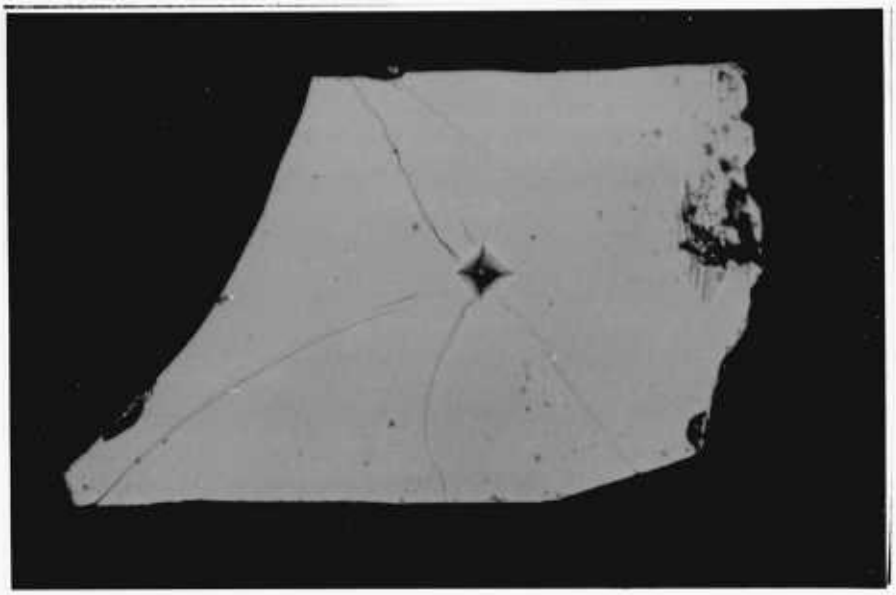

(B)

Fig. 6.15 Photomicrographs of grains of laurite in a polished section of a concentrate from Union mine showing the common euhedral form with indentations and characteristic fracture pattern (A), as well as the fragmental form bounded in part by curving fractures and crystal faces (B).

VHN_{100}	1605 - 2167	(Young and Millman, 1964)
VHN_{x}	1393 - 1670	(Rozhkov et al. 1962)
VHN_{x}	1396 - 1670	(Pudovkina et al. 1966)
VHN_{25}	1250 - 4824	(Leonard et al. 1969, Goodnews Bay laurite)
VHN_{25}	2760 - 2898	(Leonard et al. 1969, Borneo laurite)

The hardness range exhibited by this study and other workers is considered to reflect more the difficulty of obtaining reliable values than a large hardness anisotropy.

That there is a variation of hardness with Os-Ir-Pt substitution was proved when the zoned laurite crystal (fig. 6.16) was examined using a Nomarski interference contrast attachment and two fine depressions parallel to the crystal boundary were seen. These corresponded to the outermost (Ir-Os-Pt)-rich zone displayed by the X-ray scanning pictures on which these two closely parallel zones were not resolved. No softer zone was discernible at the centre of the crystal which was equally rich in iridium and platinum but poorer in osmium, suggesting that osmium substitution is mainly responsible for the decrease in polishing hardness. This is again supported by data on a 'new ruthenium mineral' by Stumpfl and Clarke (1965) which has a VHN_{100} of 1270-1450 with a mean of 1380.

6.3.4 The Composition of laurite from Union and Rustenburg mine was only semiquantitatively determined, and some aspects in relation to reflectance and hardness have already been dealt with. Minor amounts of osmium and iridium were found in most grains with 3 - 5% Os, and Os generally greater than Ir. Some trace arsenic was indicated but could not be identified definitely because Os L_{β_2} coincides with AsK_{α_1}. 1·1% As was reported in laurite from Papua and New Guinea by Harris (1974). The zoned laurite from Union mine is unique so far and the compositional data is presented in figures 6.16 and 6.17, and table 6.10. This is the first time platinum has been detected in any laurite. Schwellnus et al (1976) did not detect any platinum in laurite from Atok mine but did report up to 5·3% Fe and 0·28% Ni with 3·89-7·52% Os and 9·07-17·40% Ir. No hardness or reflectance data was however presented. The range of composition of laurite displayed by published analyses is illustrated in table 6.10.

The zoned-laurite data can be interpreted as simple diadochic substitution for ruthenium. However an alternative explanation by Kostov (pers.comm.1976) is that the zonation is caused by the epitaxial overgrowth of submicroscopic crystals of an Os-Ir-Pt phase, which is probably hexagonal iridosmine with minor platinum. However the relatively low resolution under high magnification of the electron-probe microanalyser will not permit confirmation

Table 6.10 Laurite compositions from various sources compared to those from Union mine (14)-(16).

Ref.	Composition in wt.%						
	Ru	Os	Ir	Pt	Fe	Ni	S
(1)	61·8						38·82
(2)	67·0						33·0
(3)	(65·2)	3·0					31·8
(4)	61·0		1·0				38·0
(5)	59·5	d	2·0				36·0
(6)	40·5	d	13·0				31·1
(7)	53·5	d	7·0				34·4
(8)	30·0	d	20·0				27·0
(9)	43·45	7·52	14·56		1·55	0·27	34·14
(10)	49·00	6·09	9·07		0·22	0·15	36·82
(11)	38·66	3·89	17·40		5·30	0·28	35·52
(12)	46·7	1·8	11·4				38·3*
(13)	33·0	20·9	11·4				21·4
(14)	<42	>10	>8	>5		trace	(34)
(15)	<54	> 3	> 5	> 2		trace	(37)
(16)	33·0	4·0	2·0				43·0

References: (1) Theoretical values for RuS_2. (2) Wohler, 1866; Borneo. (3) Hey, 1932; Potgietersrust, ruthenium by difference. (4)-(7) Leonard et al.,1969; Goodnews Bay, Alaska. Not corrected for matrix effects and osmium 'detected' d. (8) Leonard et al.,1969; Borneo, U.S.National Museum. (9)-(11) Schwellnus et al.,1976; Atok mine, Bushveld. (12) Harris, 1974; Papua and New Guinea, 1.1%. As also recorded*. (13) Stumpfl, 1965; Borneo. (14) Kingston, 1966; (Os-Ir-Pt) - rich zone, semiquantitative. (15) Kingston, 1966; (Os-Ir-Pt) - poor zone, semiquantitative. (16) Kingston, present; an unzoned laurite, uncorrected for matrix effect.

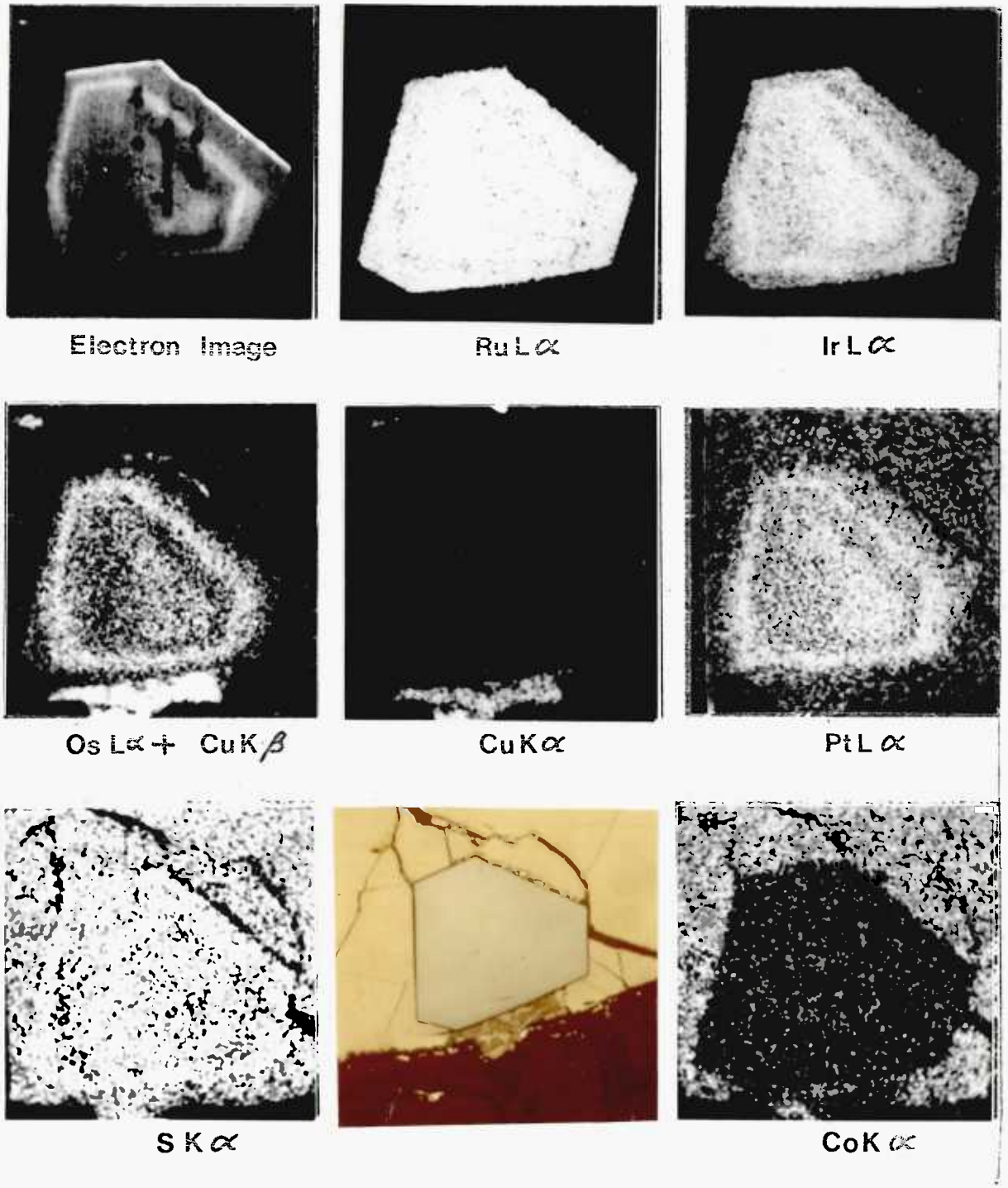

Fig. 6.16 X-ray scanning micrographs showing the distribution of iridium, osmium, platinum, and ruthenium in a zoned laurite crystal enclosed in cobaltian pentlandite from the Merensky Reef at Union mine. The copper rich area to the south of the euhedral laurite crystal corresponds to an area of bornite.

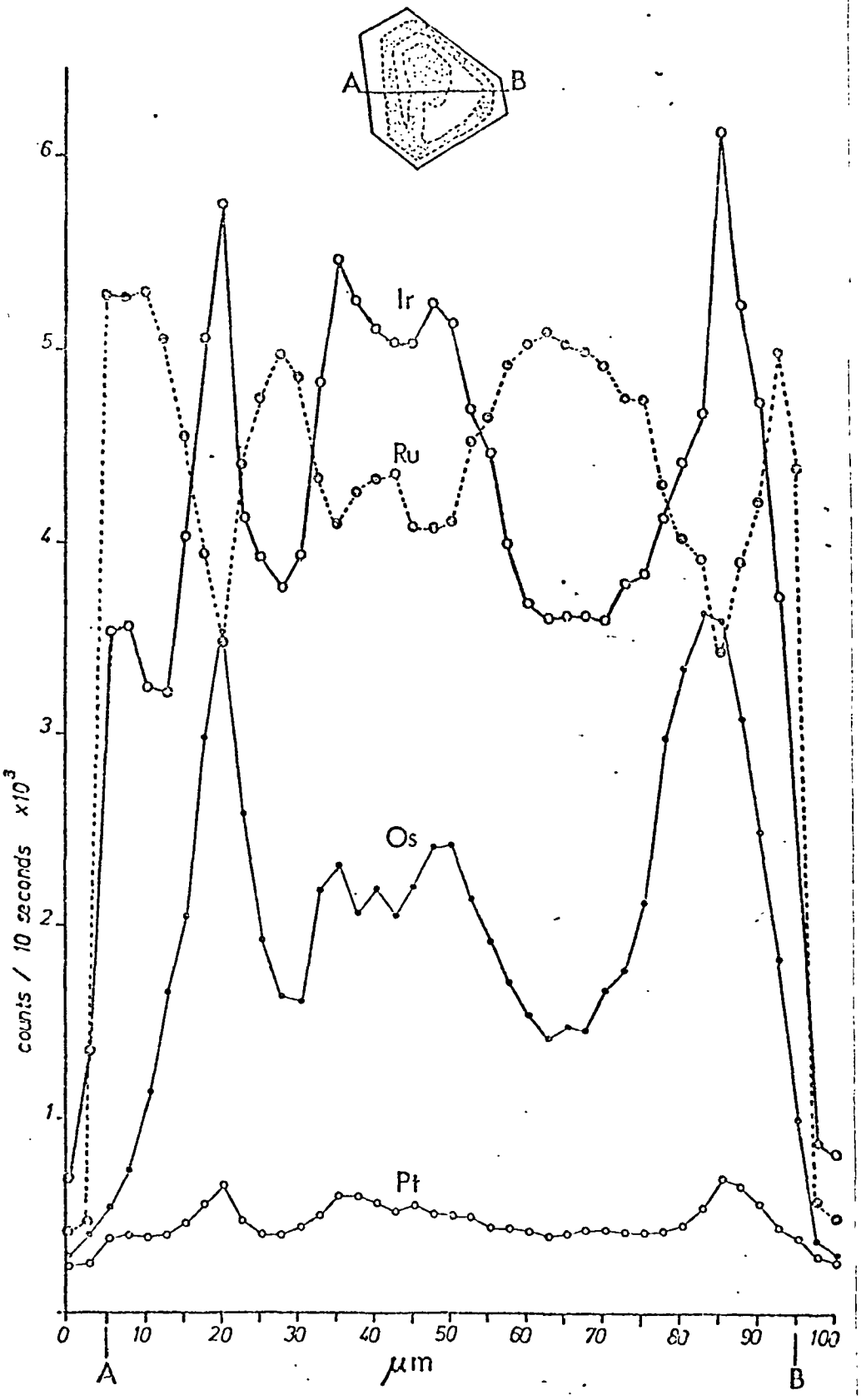

Fig. 6.17 The results of a step scan AB at intervals of 2·5 μm with the electron-probe microanalyser across a zoned laurite from Union mine showing the relative variation in the Ru, Os, Ir, and Pt content.

of this. The existence of similarly high contents of osmium and iridium in homogeneous unzoned laurite crystals would be an argument against his suggestion.

In terms of solid solution of cubic end-member minerals of elements known to substitute in laurite only osmium, iron, and nickel disulphides are known, namely erlichmanite $(Os_{0.85-0.91}\ Ir_{0.036-0.05}\ Rh_{0.094-0.13}\ Ru_{0.01}\ Pd_{0.012-0.02})S_2$ (Snetsinger, 1971), pyrite FeS_2, and vaesite NiS_2. No iridium or rhodium disulphides of the pyrite structure have yet been found.

6.3.5 The Crystal Structure of laurite is a pyrite type with space group T_h6 = Pa3, and Z=4. The cell size is variable depending on Ir, Os, Pt, Fe and Ni substitution. It is often quoted as a_o 5·60 or 5·59Å after Bannister (1932) or 5·57 after Oftedal (1928). Synthetic RuS_2 is 5·6095±·0005 (Sutarno et al 1967). Other values are 5·618 for Rustenburg laurite (Berry and Thompson 1962), 5·6135± ·0025 for Borneo laurite (Leonard et al. 1969), and 5·57 or 5·56 for Inagli laurite (Rozhkov, 1962). As illustrated in figure 6.19 a plot of the compositional data given in table 6.10 shows the range within which the cell size of most laurites can be expected to fall i.e. approximately from a_o 5·61 - 5·63.

Because the difference in cell size between RuS_2 and synthetic OsS_2, a_o 5·6196±0·0003Å (Sutarno et al

Table 6.11 X-ray powder data for laurite from Union Mine (Cu radiation, Ni filter and using 11.483 cm. diameter camera) compared to laurite from Rustenburg.

UNION MINE				RUSTENBURG (Berry and Thompson, 1962)			
I	θ(Cu)	(-) (1)	d (meas)	I	θ(Cu)	d (meas)	hkl
9	13·84	(-)	3·22	8	13·7	3·25	111
9	16·06	(-)	2·78	7	15·95	2·81	002
3	17·97	(-)	2·50	1	17·85	2·51	012
3	19·73	(-)	2·28	1	19·6	2·30	112
9	22·94	(-)	1·976	5	22·8	1·989	022
10	27·21	(-)	1.684	10	27·05	1·695	113
4	28·47	(-)	1·616	3	28·35	1·623	222
2	29·75	(-)	1·552	½	29·55	1·563	023
3	31·00	(-)	1·495	1	30·85	1·503	123
1	33·39	(-)	1·400	2	33·25	1·406	004
5	36·83	(-)	1·285	3	36·70	1·290	133
5	37·96	(-)	1·252	4	37·85	1·256	024
1	39·04	(-)	1·223	½	38·95	1·226	124
½	40·11	(-)	1·196	½	40·00	1·199	233
5	42·35	(1)	1·143	3	42·20	1·148	224
8	45·60	(1)	1·078	5	45·45	1·082	115,333
1	47·71	(1)	1·041	½	47·60	1·044	025,234
1	48·82	(1)	1·023	½	48·65	1·027	125
4	51·01	(1)	·991	3	50·90	·993	044
5	54·34	(1)	·948	4	54·20	·950	135
5	55·47	(1)	·935	3	55·35	·937	006,244
				½	56·40	·926	016
2	57·81	(1)	·910	½	57·65	·913	116,235
4	60·27	(1)	·887	2	60·10	·889	026
5	64·16	(1)	·856	3	64·00	·858	335
5	65·56	(1)	·846	3	65·40	·848	226
				½	66·50	·841	036,245
1	67·06	(1)	·836				
1	68·59	(1)	·827				
1	71·94	(1)	·810	½	71·75	·812	444
½	73·88	(1)	·802				
9	78·54	(1)	·786	7	78·30	·787	117,155
9	81·71	(1)	·778	7	81·30	·779	046

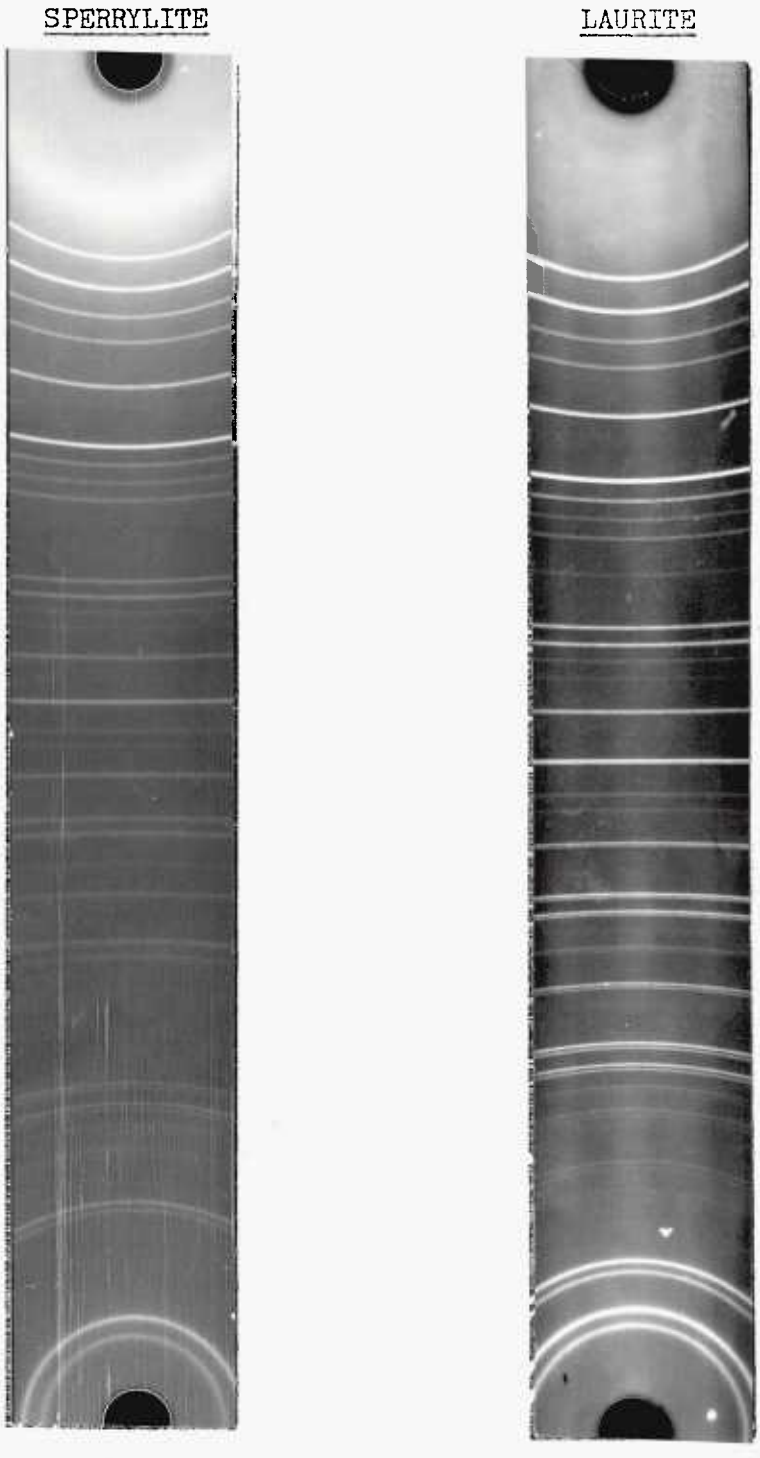

Fig. 6.18 Contact prints of X-ray powder photographs of sperrylite $PtAs_2$ from Rustenburg mine and laurite RuS_2 from Union mine. Copper radiation, Ni filter, and 11.483 cm diameter camera.

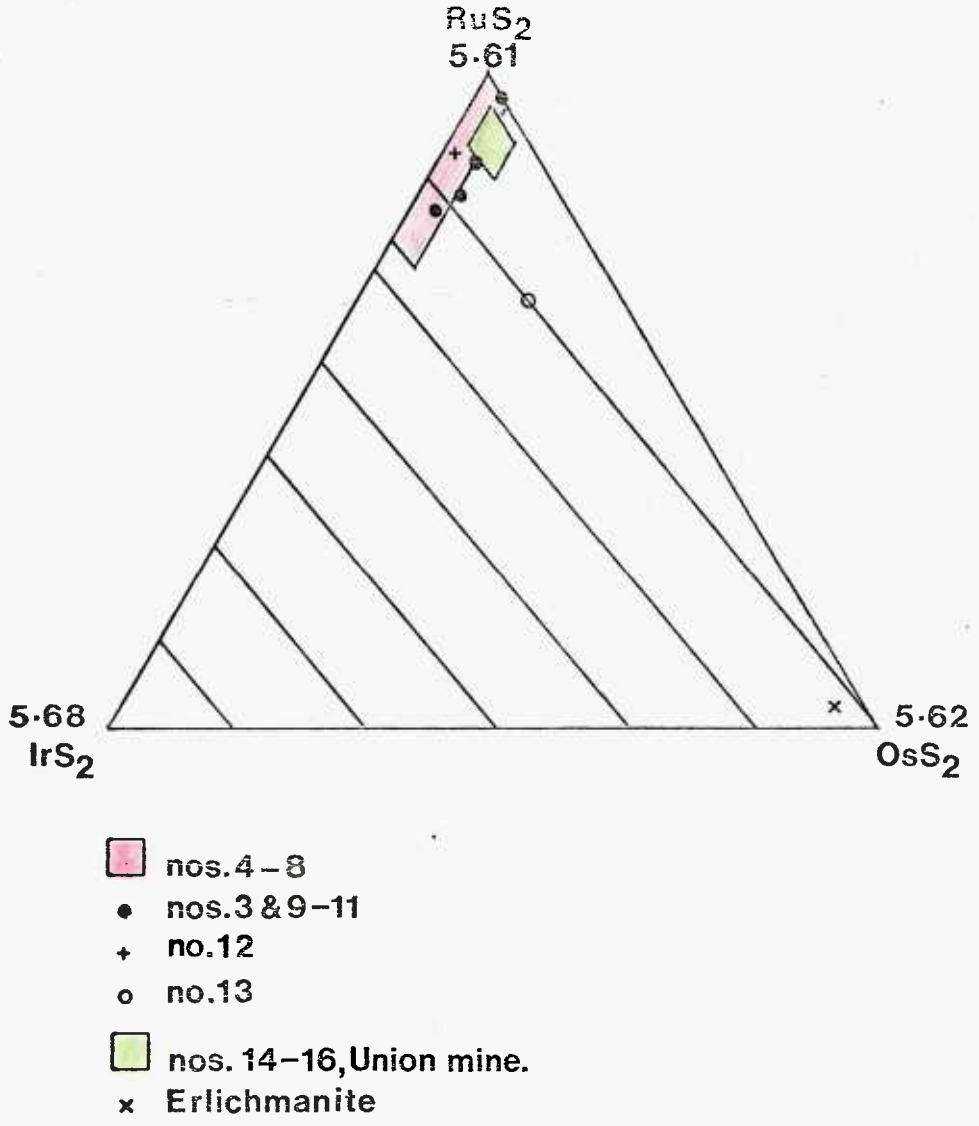

Fig. 6.19 Ternary composition diagram showing the range of composition exhibited by laurites in table 6.10, and the corresponding range of theoretical cell sizes.

1967) or erlichmanite is small, the iridium content of laurite grains in a particular deposit could be determined provided, as is generally the case, platinum, iron, and nickel contents were insignificant. This appears to be contrary to the opinion of Leonard et al (1969) who seem to have ignored the effect of iridium substitution and who confusingly use a measurement of the cell size of their Borneo laurite (a_o 5·614Å) as an indication of its composition being approximately ($Ru_{.5}$ $Os_{.5}$) S_2 despite an electron-probe microanalysis of the same grain giving 20·0% Ir with osmium only 'detected'.

X-ray powder diffraction data for laurite from Union mine is presented in table 6.11, and the pattern in figure 6.18. The d-spacings agree closely with those for Rustenburg laurite.

6.4 Other Sulphides Possibly Present

6.4.1 Other Sulphides and Sulphosalts have so far not been reported in the Merensky Reef or located by the author. If others are present then they are of very rare occurrence. Vysotskite (Pd, Ni, Pt)S and erlichmanite OsS_2, the only other sulphides described, may occur, particularly as they are closely related to braggite and laurite respectively. A number of platinum group element sulpharsenides have been found elsewhere, and some no doubt will be located in the Merensky Reef in the future. For the most part Pt, Ir, Os, Pd, and Ru can be accounted for, although there is still a problem in explaining most of the ruthenium content at Rustenburg mine, and part of it at Union mine. However the rhodium content also warrants attention, particularly as the average rhodium content of the ore at both mines is about 2·6 wt.% of the total content of platinum group elements plus gold, and no separate rhodium mineral has yet been found. Although rhodium is known to be present in trace amounts in sperrylite (0·7-1·2 wt.% Rh) and cooperite (0·0-0·02 wt.% Rh) at Western Platinum mine (Brynard et al. 1976), this cannot account for it all at Rustenburg and Union mines, where it has not been detected in any of the minerals analysed in this investigation. Vermaak and Hendriks (1976, p.1267) report that they too 'failed to identify any rhodium minerals in the Merensky ore', despite their earlier reference (p.1259) to an apparently very rare Pt-Rh-Cu-Ni-S phase with minor Ir and Co.

Table 6.12 Composition of known rhodium sulphides and sulparsenides expressed as atomic proportions assuming a whole number cation : anion ratio. All belong to the cubic system.

MINERAL NAME		COMPOSITION Ru	Rh	Pd	Os	Ir	Pt	Co	Ni	As	S
Hollingworthite	(1)	----	0.66	0.18	----	0.04	0.12	----	----	1.00	1.00
RhAsS	(2)	0.10	0.59	----	----	0.06	0.25	----	----	1.15	0.85
	(3)	0.27	0.52	----	----	0.01	0.20	0.08	0.04	1.05	0.95
	(4)	0.05	0.80	0.02	----	----	0.01	----	----	0.93	1.07
Irarsite	(7)	0.27	0.20	----	----	0.35	0.18	----	----	1.12	0.88
IrAsS	(4)	----	0.10	0.03	0.03	0.65	0.11	0.07	----	0.93	0.87
	(8)	----	0.04	0.04	----	0.74	0.04	----	0.13	1.08	0.92
Osarsite	(8)	0.44	.005	0.01	0.47	0.02	.005	----	0.04	1.07	0.93
OsAsS											
"Rh-Sperrylite"	(1)	----	0.33	0.05	----	0.27	0.35	----	----	1.19	0.81
Erlichmanite	(5)	0.01	0.08	0.01	0.86	0.04	----	----	----	----	2.00
OsS_2	(5)	0.44	0.10	----	0.48	----	----	----	----	----	2.00
	(6)	0.01	0.12	0.02	0.80	0.05	----	----	----	----	2.00

(1) Stumpfl and Clark (1965):- Driekop mine, Transvaal.
(2) Genkin (1968):- Nori'sk, U.S.S.R.
(3) Genkin et al (1966):- Onverwacht mine, Transvaal.
(4) Rucklidge (1969):- Werner Lake, Ontario.
(5) Snetsinger (1971):- California.
(6) Snetsinger (1971):- Ethiopia.
(7) Genkin et al (1963):- Onverwacht, Transvaal.
(8) Snetsinger (1971):- California.

The rhodium content could be largely accounted for as being in solid solution in one or more of the relatively abundant base-metal sulphides, or even the silicates. The first important clue to its occurrence comes from the results of the analysis of Rustenburg and Union mine concentrates by Johnson and Matthey Ltd, which showed that the rhodium content of the 'metallics' concentrates is negligible and that of the sulphide flotation concentrates is high (Zermatten, pers.comm. 1962). Zermatten concluded from this that rhodium is not a constituent of ferroplatinum, cooperite, braggite, gold, or laurite, and that in the flotation concentrates it is not in the metallic state but combined as a sulphide or similar compound. At this time none of the rhodium sulphides, sulpharsenides, or arsenides in table 6.12 had been discovered, although rhodium was known in small amounts in alloys of the platinum group elements, which would not be expected to occur in any sulphide flotation concentrates. A confirmatory emission spectrographic study of + 90% purity samples of pyrrhotite, pentlandite, and pyrite by Vermaak and Hendriks (1976) indicated that they contained the bulk of the 'soluble' rhodium (soluble in leach solutions). However, as pointed out in chapter 3.2.3, whether the rhodium occurs in solid solution, as submicroscopic inclusions of a rhodium mineral, as 'dispersed colloidal particles' (Vermaak and Hendriks), or in some other way, is at present purely speculative in the absence of any unambiguous evidence.

It was within this background and during the initial stages of familiarisation with the properties of known platinum group minerals from other localities, that the author's attention was directed by A. P. Millman to several unidentified phases in a nugget from Yubdo, Ethiopia. Subsequent analyses of these showed two of them to be new rhodium sulphides. Publication of the data on these new minerals, after several refinements of the electron-probe microanalyses, is at present in press. Because of this and because these minerals could be present in the Merensky Reef they are described below. Their occurrence is also important with regard to [redacted] the formation and distribution of platinum group elements and minerals during serpentinisation and birbiritisation [redacted].

6.4.2 Prassoite[1] and Zappinite[2] - New Rhodium Sulphides

Introduction. The geology and general distribution of platinum and gold in the ultrabasic complex of the Ubdo district, in the Wallaga Province of Ethiopia, have been described by Duparc et al (1927), Molly (1927, 1959), Augustithis (1965) and Ottemann and Augustithis (1967), who have shown this ultrabasic mass to be of a

(1) Mineral and name approved by the Commission on New Mineral and Mineral Names, I.M.A. April, 1971.
(2) Name approved and reserved for anisotropic rhodium sulphide by above Commission in April, 1971. New data being submitted for mineral approval.

Uralian type, consisting of a central zone of platiniferous dunite enclosed by a less platiniferous pyroxenite. The dunite is overlain for the most part by a hard platiniferous brownish rock, the 'birbirite' of Duparc et al., believed to be derived from the dunite by some form of hydration alteration with leaching of magnesium (Augustithis, 1965). A lateritic eluvium occurs as a layer of 2 - 10 metre thickness forming a capping over the dunite, birbirite and pyroxenite. Economic quantities of platinum have been recovered from this eluvium, especially from those parts overlying the dunite, in the form of small nuggety grains (Molly, 1959), but the grades of the primary source rocks and the birbirite are uneconomic. The minerals are named after A. Prasso, A.R.S.M., and A. Zappin who first discovered these deposits in 1924.

The two eluvial platinum specimens studied were about 1·5cm in diameter, and were irregular and cavernous consisting dominantly of native platinum, coated and penetrated by reddish limonitic material. Two previous chemical analyses of similar composite material from this area by Molly (1928) gave Pt 73·45, 79·48; Os 1·41, 2·70; Ir 0·65, 0·82; Rh 0·62, 0·75; Pd 0·22, 0·49; Au 3·48, 0·49 and Fe 18·88, 16·50 weight percent. The PGE content of the rocks and eluvium was first attributed to native platinum and sperrylite (Augustithis, 1965). Later Ottemann and Augustithis (1967) revealed that the platinoid assemblage

was more complex and described the occurrence of a new mineral 'roseite' (Os, Ir)S, which was disapproved by the I.M.A. Commission on New Minerals and Mineral Names in 1968. They also reported a mineral of approximate composition Os 60, Ir 40 weight percent which they called osmiridium, but being strongly anisotropic and hexagonal it should be called iridosmine since the former name is reserved for isotropic and cubic Os-Ir alloys. A later study by Snetsinger (1971) of a specimen of 'roseite in ferroplatinum' provided by Augustithis characterised a further new mineral named erlichmanite OsS_2, which may be the same as the partly discredited 'roseite' since no osmium monosulphide was found.

The nuggets examined in this study have been found to consist of a platinum matrix with an Fe content of approximately 6 weight percent, enclosing euhedral laths of iridosmine containing 7 - 9 weight percent Ir, and euhedral laurite crystals containing minor Ir, Pt, Cu and Fe (fig. 6.20). In addition two new rhodium sulphide minerals containing Ir, Pt, Cu, and Fe in important amounts occurred (figs. 6.21 and 6.22). Both of these minerals are different from the four unidentified minerals indicated by the qualitative electron-probe microanalyses of Ottemann and Augustithis (1967). These were (a) a grey anisotropic sulphide of Ni, Pd, Rh, and Fe; (b) a yellowish isotropic sulphide with a high Fe content, a higher Ni content than (a) with some Co and a little Pd; (c) a greyish blue sulphide of low reflectance containing Pd, Rh and Pt;

(d) a phase containing major Ru with some Rh and Pd, possibly a sulphide.

Prassoite occurs as anhedral, sparsely distributed grains up to 0.2 mm in size, exhibiting smooth embayed boundary relationships with the enclosing platinum matrix, and often associated with euhedral iridosmine laths in the manner illustrated in figure 6.22 and 6.23. It is isotropic and its colour in air is medium grey compared with the enclosing bright creamy white platinum. It is slightly darker than associated bluish grey laurite.

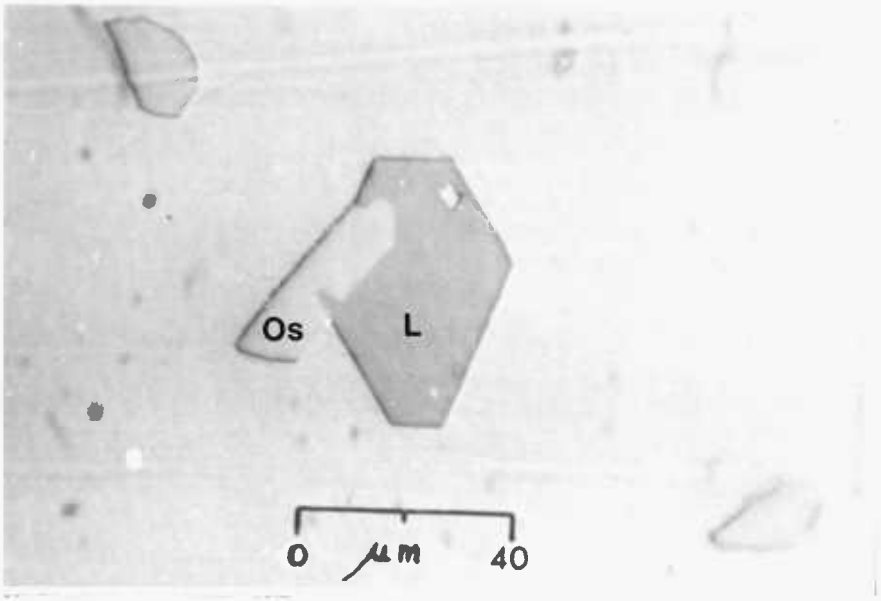

Fig. 6.20 Reflected light photomicrograph of intergrown euhedral crystals of laurite (L) and iridosmine (Os) in a matrix of native platinum. Yubdo District, Ethiopia.

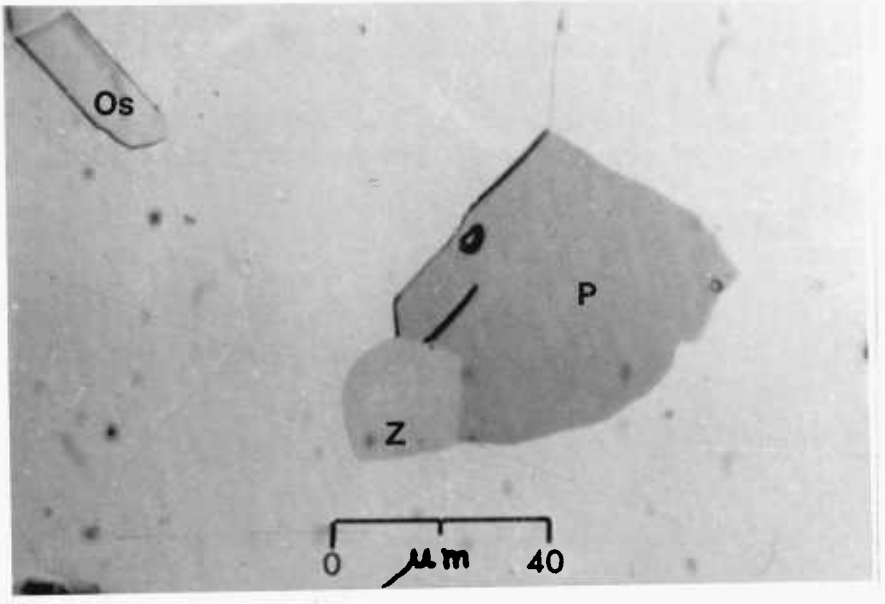

Fig 6.21 Anhedral grain of prassoite (P), with subhedral zappinite (Z) at boundary. Matrix is platinum with an inclusion of iridosmine (Os). Yubdo District, Ethiopia. Scale 1 cm = 14 µm.

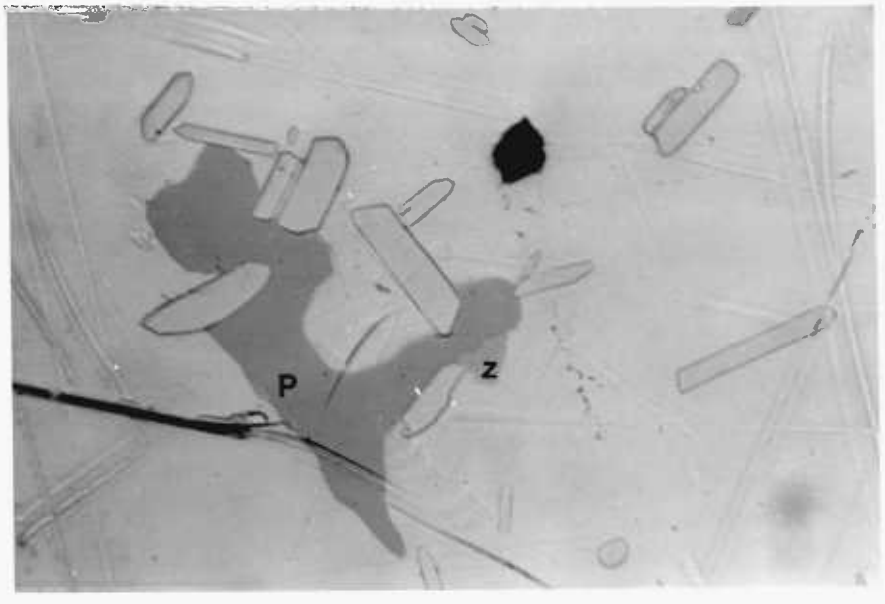

Fig. 6.22 Anhedral prassoite (P) with two small grains of zappinite (Z) at the boundary with the matrix platinum. The light grey laths are iridosmine. Yubdo District, Ethiopia. Scale 1 cm = 20 µm.

Table 6.13 Spectral reflectance values for prassoite and zappinite from Yubdo, Ethiopia, together with the standard silicon values measured by the N.P.L.

λ in nm.	Silicon std. N.2538.36	Prassoite, Rh_4S_5	Zappinite, Rh_3S_4	
		R_n	R_g	R_p
440	43.1%	41.0%	49.7%	48.4%
460	41.3	40.4	49.4	47.8
480	40.0	39.9	49.3	47.9
500	38.9	39.8	49.9	48.2
520	38.0	39.9	50.5	48.8
540	37.2	39.5	50.6	48.8
560	36.6	39.7	51.6	49.7
580	36.0	39.5	51.3	49.6
600	35.5	39.3	50.8	49.2
620	35.1	39.2	51.2	49.7
640	34.8	38.9	51.8	50.2
660	34.4	38.7	52.2	50.4

Reflectance measurements in air at twelve points in the visible spectrum were made using a Reichert reflex spectral microphotometer with a X 35 air objective, 5 mm mirror diaphragm and a 24 μm field diameter (table 6.13); comparison was made with a silicon standard (N2538.36) previously measured by the National Physical Laboratory, Teddington. The possible effect of flare was

considered negligible because of the relatively small difference in reflectance between the standard and prassoite. The interpolated reflectance R_n at 589 nm for prassoite is 39.4%.

The Van der Veen line test for polishing hardness showed prassoite to be harder than platinum and softer than iridosmine. Four Vickers microhardness measurements with a 25 g load gave a range of VHN_{25} 627 - 762 kg/mm^2. It was found necessary to use a low load because of the small grain size. The equipment used was a Leitz Durimet and the procedure followed was that described by Young and Millman (1964).

Electron-probe microanalyses by the author and Kelly of three separate grains of prassoite yielded the results in table 6.14, with an average formula of $(Rh_{0.59}\ Fe_{0.17}\ Cu_{0.15}\ Ir_{0.08})_{6.03}\ S_{7.00}$ approximating to the generalised formula of Rh_6S_7. The instrument used was a Cambridge Microscan Mark I which had a 20° take-off angle; all the analyses were conducted at 25kV with a beam current of about 120 mμA. The standards were an analysed Elba pyrite for Fe and S, a 70/30 Pt/Rh alloy for Pt and Rh, pure Ir and pure Cu. Full matrix-effect corrections were done using a 'Mark I' program by Mason, Frost and Reed (1969). A recent check analysis of prassoite by Steed (pers comm.,1975) employing a Cambridge Microscan Mark III at 25kV, pure metal standards, stoichiometric pyrite for S, and a carbon coating on the polished section, gave the result no. 4 in table 6.14. This result was obtained by applying a full matrix-effect correction to one set of measured values obtained from the average of three different grain analyses. The correction program used was again by Frost, Mason, and Reed

Table 6.14 Eleotron-probe microanalyses of prassoite from Yubdo, Ethiopia, by Kingston and Kelly in 1969 (1) - (3), and Steed in 1975 (4).

	(1)	(2)	(3)	(4)
Rh	46.9	47.5	47.9	42.72
Ir	13.7	14.6	(9.3)	13.71
Pt	----	----	----	0.06
Cu	7.6	7.3	7.5	7.22
Fe	7.6	7.6	7.5	6.79
S	29.9	29.3	28.6	29.03
	105.7	106.3	100.8	99.53

Empirical Formulae

(1) $(Rh_{0.58}Ir_{0.09}Cu_{0.15}Fe_{0.18})_{5.95}S_{7.00}$

(2) $(Rh_{0.58}Ir_{0.10}Cu_{0.14}Fe_{0.18})_{6.08}S_{7.00}$

(3) $(Rh_{0.61}Ir_{0.06}Cu_{0.16}Fe_{0.17})_{6.06}S_{7.00}$

(4) Average of three grain analyses

Average Summarised Formula

$(Rh, Fe, Cu, Ir)_{6.03}S_{7.00}$

$(Rh_{0.57}Ir_{0.10}Cu_{0.16}Fe_{0.17})_{3.99}S_5$

(—— ditto ——)$_{5.6}S_7$

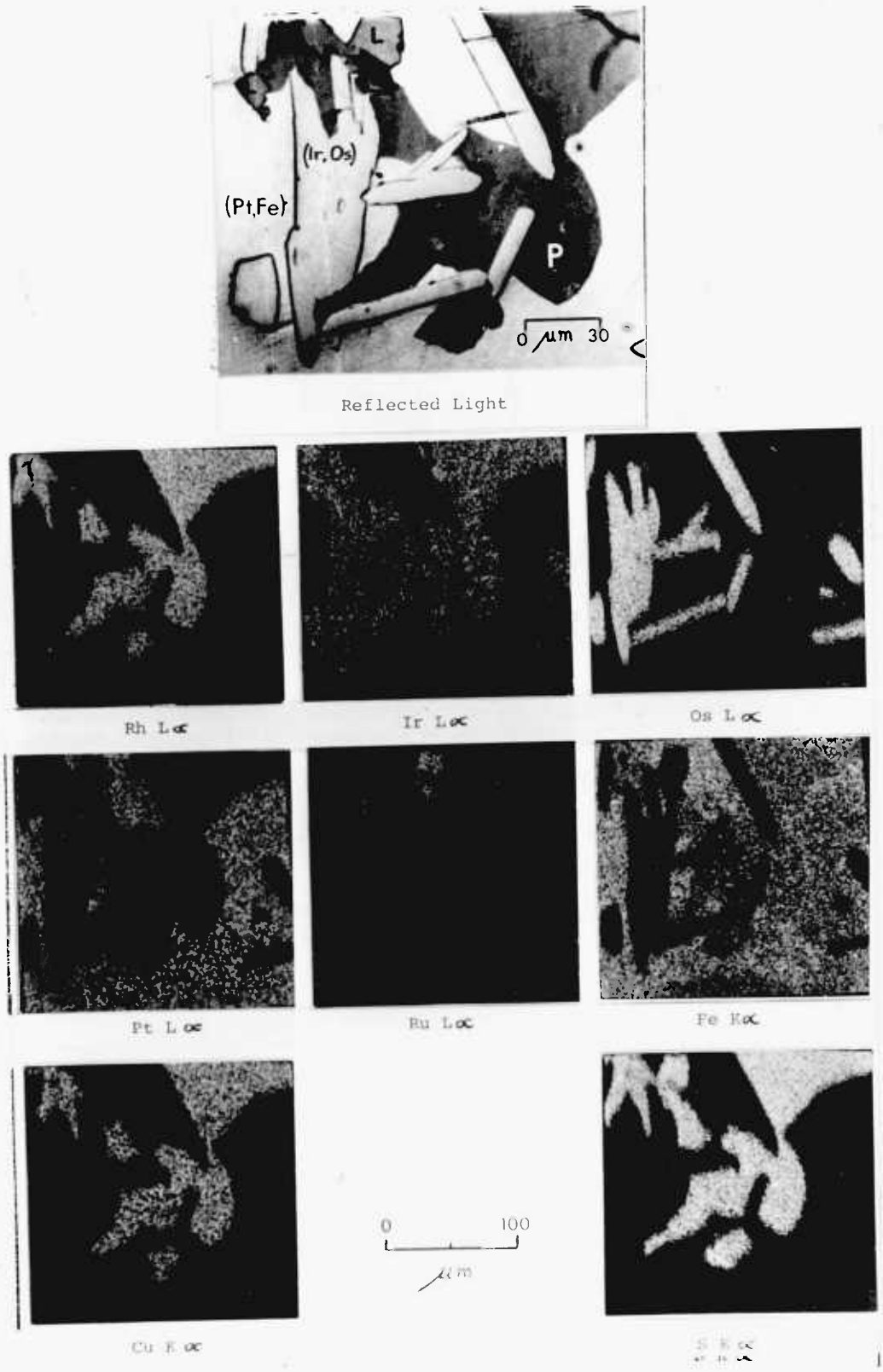

Fig. 6.23 Prassoite (P) and laurite (L) with euhedra of iridosmine (Os) in a matrix of platinum. Reflected light photomicrograph and X-ray scanning micrographs showing the distribution of Rh,Ir,Os,Pt,Ru,Fe,Cu,S.

Table 6.15 X-ray diffraction data for prassoite, Rh_4S_5, from the Yubdo district of Ethiopia. (Cu K radiation, Ni filter and 11.483 cm camera). Cell size a_o = 9.853Å ± 0.001 standard deviation.

h	k	l	d(calc.) Å	d(obs.) Å	I(obs.)
1	1	1	5.6884	5.72	90
2	2	0	3.4834	3.48	30
3	1	1	2.9707	2.97	100
2	2	2	2.8442	2.84	30
4	0	0	2.4631	2.46	70
3	3	1	2.2603	2.26	15
4	2	2	2.0111	2.01	15
5	1	1	1.8961	1.895	60
4	4	0	1.7417	1.741	70
5	3	1	1.6654	1.667	25
5	3	3	1.5025	1.504	20
6	2	2	1.4853	1.486	10
4	4	4	1.4221	1.422	20
5	5	1	1.3796	1.378	10
6	4	2	1.3166	1.317	5
5	5	3	1.2827	1.283	30
8	0	0	1.2316	1.233	15
5	5	5	1.1377	1.138	15
8	4	0	1.1015	1.101	25
7	5	3	1.0815	1.082	5
9	3	1	1.0328	1.033	15
8	4	4	1.0056	1.006	30
9	3	3	0.9902	0.9926	5
9	5	1	0.9525	0.9528	15
9	5	3	0.9188	0.9186	5
7	7	5	0.8884	0.8887	5
8	8	0	0.8708	0.8714	10
9	5	5	0.8608	0.8611	5
9	7	3	0.8357	0.8365	5
10	6	2	0.8327	0.8330	5
8	8	4	0.8210	0.8209	20
8	8	4	0.8210	0.8208	5
9	7	5	0.7914	0.7913	20
9	7	5	0.7914	0.7913	5
12	4	0	0.7789	0.7788	30
12	4	0	0.7789	0.7789	15

(MK 2). This result indicates the empirical formula to be $(Rh_{0.57}\ Fe_{0.17}\ Cu_{0.16}\ Ir_{0.10})_4\ S_5$. The difference between the two formulae is considered to be largely the result of improved matrix-effect corrections in the recent programme by Frost et al., and the inevitable refinements in analytical technique since the first set of consistent analyses were made in 1969. Because of this, the latter metal:sulphur ratio of 4:5 is accepted as being closest to the truth.

X-ray powder data for prassoite are given in table 6.15. All the reflections were indexed assuming a cubic symmetry and the cell size calculated as a_o 9.853 ± 0.001 standard deviation. An attempt was made to correlate this data with that by Juza et al, (1935) on the Rh-S artificial system. No X-ray powder data or cell-sizes were found to be comparable with those of prassoite. However, there was a correspondence of the strongest reflections with those of synthetic $CuRh_2S_4$ (A.S.T.M. index, file no. 17-644) which is cubic with a_o 9.72 Å.

Zappinite is rare in the sections studied and occurs as small subhedral grains, up to 0.03 mm in size, associated with prassoite (fig. 6.22). Its colour in air is grey with a brownish tint of a "stannite" type hue compared with the enclosing brighter native platinum; in comparison prassoite appears a darker grey with no colour tint.

Zappinite shows weak reflection pleochroism in air and oil, but distinct anisotropy under crossed nicols. Reflectance values are presented in table 6.13. The apparatus and determinative procedure was as described under prassoite. The interpolated

Table 6.16 Electron-probe microanalyses in weight percent of zappinite from Yubdo, Ethiopa, by Kingston and Kelly in 1969 (1), and Steed in 1975 (2) and (3).

	(1)	(2)	(3)
Rh	58.9	51.49	54.27
Ir	10.4	11.93	16.29
Pt	9.5	11.73	0.78
Cu	----	0.17	0.18
Fe	----	0.08	0.07
S	25.0	24.83	28.44
	103.8	100.23	100.03

Empirical Formulae

(1) $(Rh_{0.85}Ir_{0.07}Pt_{0.07})_6S_7$

(2) $(Rh_{0.80}Ir_{0.10}Pt_{0.10})_{4.04}S_5$

(3) $(Rh_{0.85}Ir_{0.14}Pt_{0.01})_{2.09}S_3$ or $(Rh_{0.85}Ir_{0.14}Pt_{0.01})_{4.89}S_7$

Average Summarised Formulae

$(Rh_{0.83}Ir_{0.12}Pt_{0.05})_3S_4$

$(Rh_{0.84}Ir_{0.10}Pt_{0.06})_{3.15}S_4$

or

(-------ditto------)$_{3.93}S_5$

reflectance at 589nm is R_g 51.5% and R_p 49.4%. Because of the small size of the grains no reliable indentations could be made. However, it is a little softer in polishing hardness than prassoite, and harder than native platinum. It thus has an estimated hardness of VHN_{25} 500 kg/mm^2.

Electron-probe microanalyses of three grains of zappinite are given in table 6.16. Analysis (1) was done in 1969. A further two analyses of zappinite by Steed (pers comm. 1975) are in general agreement with the 1969 analysis, but indicate metals: sulphur ratios of 2:3 and 4:5 as opposed to 6:7. An average of the two recent analyses gives an empirical formula of $(Rh_{0.82}\ Ir_{0.12}\ Pt_{0.05}\ (CuFe)_{0.01})_3S_4$. Because of the small grain size and rarity of zappinite, no X-ray powder data have yet been obtained. Until this becomes available for comparison with synthetic compounds a 3:4 ratio is considered the better solution.

In Conclusion, prassoite and zappinite are the first sulphides of rhodium to be chemically and optically defined. However, the composition of a rhodium sulphide as $\lesssim$20 µm inclusions in isoferroplatinum, which may be equivalent to either of these, has recently been reported from the Witwatersrand gold field by Feather (1976). Unfortunately no X-ray powder data or optical and physical characteristics are given for this phase, which has an average cation: anion ratio from five grain analyses of 0.53:0.47, and a composition in the range of Rh 33.7-71.7, Ru 27.0-3.8, Pt 13.3-2.5, Ir and Os < 0.1, Ni 0.2-4.7, Fe < 0.1-3.1, and S 27.5 - 18.5 weight percent.

Reference to table 6.12 shows that an isotropic rhodium diarsenide hollingworthite $(Rh,Pd,Pt,Ir)(As,S)_2$ containing As 32.6

and S 13.9 wt.% has been described from the Driekop mine in the Bushveld, where it is associated with cubic rhodian sperrylite $(Pt,Rh)As_2$. A pyrite-type structure has been postulated for hollingworthite, similar to that of sperrylite of cell-size a_o 5.967 (Berry and Thompson, 1962). Irarsite, an isotropic iridium diarsenide $(Ir,Ru,Rh,Pt)(As,S)_2$ containing Rh 7.2 wt.%. with a cell size of a_o 5.777 has been reported by Genkin et al.,(1966) from the Transvaal, and erlichmanite OsS_2, with Rh 3.8 wt.% and a_o approximately 5.62 Å, by Snetsinger (1971). Cubic prassoite with a cell-size of a_o 9.853 Å, is structurally unrelated to erlichmanite and the above rhodium-bearing arsenides and sulpharsenides. The three rhodium-bearing phases observed by Ottemann and Augustithis (1967) are different in composition from prassoite and zappinite, but the limited published optical and analytical data for these three phases do not allow close comparison.

[redacted] The existence of prassoite and zappinite in the Merensky Reef is considered very probable.

CHAPTER 7

PLATINUM GROUP ARSENIDES AND ANTIMONIDES

7.1 Sperrylite $PtAs_2$

7.1.1 Introduction. Sperrylite was first discovered and described from the Vermilion deposit, Sudbury, by Wells in 1889. It was first reported in the Bushveld by Spencer, and Wagner in 1926 (in Wagner, 1929) as well formed bright tin-white crystals of cubic habit and up to 1.85 cm across occuring in the pegmatitic deposits in the Potgietersrust district. Schneiderhohn (1929) also reported on sperrylite in this district in samples of the pegmatitic veins and lenses, and the lime-silicate rocks developed at the contact of the norite and the underlying dolomite. He did not, however, find any sperrylite in any samples of the Merensky Reef. Wagner (1929 p.17) was the first to report sperrylite in the Merensky Reef, although Bannister (1932) was the first to quantitatively confirm its presence by X-ray diffraction.

Chemical analyses of sperrylite by Wells (1889), Cooper (in Wagner, 1929), and others, all gave a composition close to the ideal $PtAs_2$ with up to 1.66 wt.% Rh, and 0.5-0.7 wt.% Cu,Fe or Sb. Subsequent electron-probe microanalyses have confirmed this composition and have shown that it is generally quite pure, with only minor substitutions by Rh,Ir,Os,Ni,Co,Fe and Sb. The first reported electron-probe microanalysis of sperrylite in the Merensky Reef was by Schwellnus et al (1976) who reported an analysis of Pt 56.59, Os 0.58, Ni 0.10, Pb 3.00, Bi 0.72, Sb trace, S 0.74, and As 37.77 weight percent. The presence of Pb and Bi is considered to require confirmation. Brynard et al (1976) have also reported the composi-

tion from three analyses of sperrylites from the Merensky Reef at Western Platinum mine as being Pt 59.3, 56.2, 57.1, As 39.6, 44.2, 42.8, Pd 0.0, 0.2, 0.1, Rh 0.7, 1.2, 1.2, and Cu 0.1, 0.1, 0.1, weight percent. The only other ananlysis for Bushveld sperrylite is by Tarkian and Stumpfl (1975) for Driekop mine. They give an analysis of Pt 55.1, Ir 1.8, Sb 2.7, S 0.4, and As 37.6 wight percent. Cabri and Laflamme (1976) and Feather (1976) have also provided a large number of analyses for sperrylites from Sudbury, and the Witwatersrand respectively. All these analyses show that sperrylite in general, and particularly sperrylite from the Merensky Reef, is relatively free of significant substitutions by other elements.

The first examination of the structure of sperrylite by X-ray diffraction was by Aminoff and Parsons in 1928 (Strunz, 1970) on material from Vermilion mine Sudbury. They determined the cubic cell edge as a_o 6.00 Å. Bannister (1932) refined the structure further and gave a value of a_o 5.94 Å for the Bushveld sperrylite, the structure being cubic type T_h^6 - Pa3, and Z = 4. Thompson (1962) refined the Sudbury sperrylite to a_o 5.967Å.

The properties of sperrylite in reflected light are well established as white in air with a bluish tint in oil (fig. 7.1), isotropic, having a reflectance at 589nm/$_{\lambda}$ at Rustenburg mine between 52.2 - 53.5%, and exhibiting little spectral dispersion as shown by the spectral reflectance values in table 7.1. All reported values of hardness fall within the range of first measurements made by Gray and Millman (1962) of VHN_{100} 960-1277 for large crystals from Potgietersrust mine.

Table 7.1 Reflectance values for sperrylite by (1) Gray and Millman (1962), (2) Vyalsov (in Uytenbogaardt & Burke, 1971), (3) Tarkian and Stumpfl (1975), and (4) Schwellnus et al. (1976).

λnm	Reflectance in % (1)	(2)	(3)	(4)
470	51.2(b)	55.0	54.1	53.0
546	56.4(g)	55.5	52.8	53.7
589	53.5(y)	55.5	52.1	53.1
650	55.7(r)	52.0	52.5	52.2

7.1.2 Rustenburg and Union mine Sperrylite

Identification of sperrylite in the concentrates was initially by qualitative electron-probe microanalysis and X-ray powder diffraction (table 7.2 and fig. 6.18), combined with a comparison of its properties with reference specimens of sperrylite from Potgietersrust mine and Sudbury. Subsequently its euhedral form, colour, reflectance, and isotropism enabled it to be confidently distinguished from the other isotropic phases, in particular laurite. Only platinum and arsenic were detected with certainty, although osmium and iridium were indicated in trace amounts (fig.7.2).

Occurrence. Sperrylite has not been located by the author in polished sections of the ore, and is only of minor importance in the 'metallic' table concentrates, in which it occurs as large euhedral grains in part modified by embayments. Despite earlier beliefs, and later statements (Liebenberg, 1970) of sperrylite's

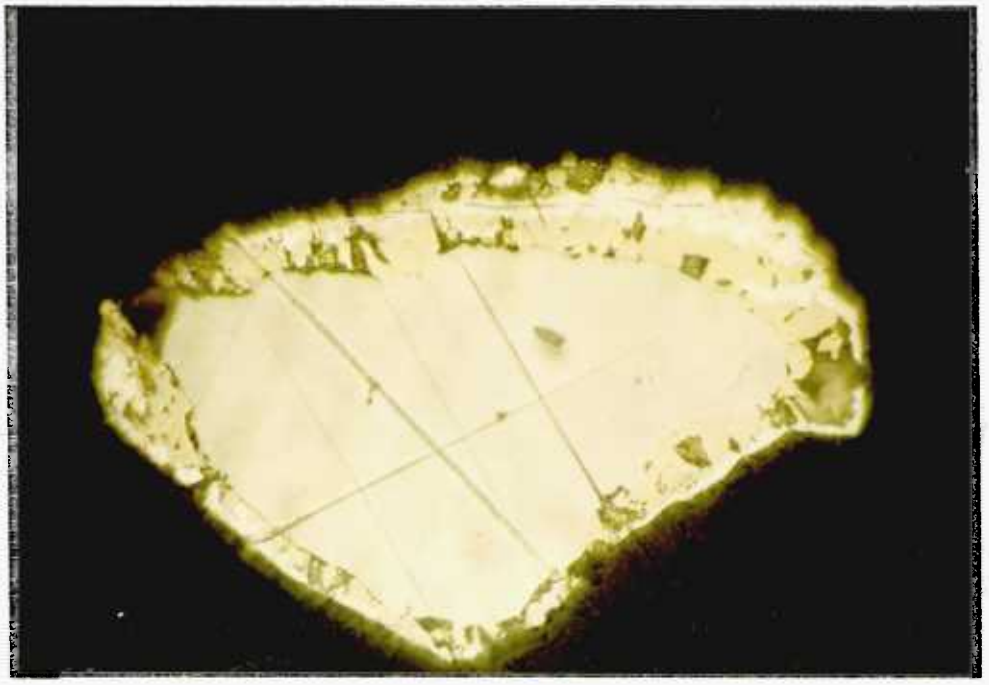

Fig 7.1 A concentrate grain of sperrylite from Union mine enclosed by pyrrhotite (brown) and rimed by platinum-iron alloy (white) which has formed from the release of platinum during the corrosion of sperrylite by pyrrhotite. Union mine.

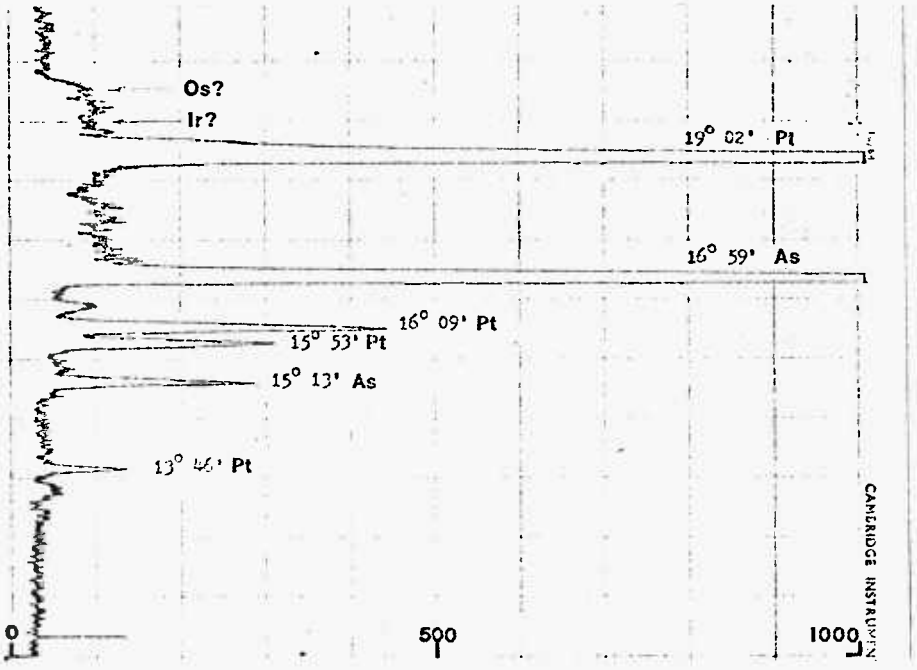

Fig. 7.2 Electron-probe microanalyser chart-recorder scan for Bragg-angle range 11 - 23° using a lithium fluoride crystal, and showing the positive detection of major Pt and As, and the uncertain indication of Os and Ir in sperrylite from Union mine.

Table 7.2 X-ray powder data for sperrylite $PtAs_2$ from Rustenburg mine and Potgietersrust (cu radiation, Ni filter and using 11·483 cm camera), compared to sperrylite from Vermilion mine, Sudbury, by Berry & Thompson (1962).

	Rustenburg		Potgietersrust		Vermilion
I	d (meas)	I	d (meas)	I	d(calc)
8	3·44	8	3·42	4	3·445
10	2·98	9	2·97	6	2·983
6	2·66	6	2·66	3	2·668
6	2·43	6	2·43	3	2·436
8	2·11	8	2·10	5	2·109
10	1·798	10	1·791	10	1·799
4	1·722	5	1·717	2	1·722
3	1·654	5	1·650	2	1·655
4	1·591	5	1·588	3	1·595
4	1·366	6	1·362	3	1·369
5	1·334	6	1·327	4	1·334
2	1·317	3	1·296	2	1·302
1	1·271	1·5	n.m.	1	1·273
4	1·217	6	1·211	4	1·218
6	1·147	8	1·143	7	1·148
2	1·108	4	1·103	2	1·108
1	1·089	3	1·085	2	1·089
4	1·054	6	1·050	4	1·055
4	1·008	6	1·005	4	1·009
4	0.993	6	0·990	4	0·995
	n.d.		n.d.	½	0·981
1	0·966	3	0·964	1	0·968
3*	0·943	6	0·940	2	0·944
3*	0·909	6	0·908	3	0·910
1*	0·907				
3*	0·899	6	0·897	3	0·900
1*	0·889	1	n.m.	1	0·890
	n.d.		n.d.	1	0·880
3*	0·835	6	0·835	3	0·836
3*	0·827	6	0·827	4	0·828
2*	0·819	2	n.m.	2	0.820
2*	0·811	2	n.m.	2	0·812
5*	0·797	8	0·797	6	0·798
8*	0·776	10	0·777	6	0·777

n.m. not measured

n.d. not detected

* $K\alpha_1$ ' radiation.

importance at Rustenburg mine, Vermaak and Hendriks (1976) have also confirmed its rarity in the ore, and report that sperrylite forms only 0.29 vol.% of the total amount of precious minerals. However, at Western Platinum mine (Brynard et al., 1976) sperrylite forms 50.3 vol.% of the total precious mineral content. This is one example of the important variations which occur in the platinum-mineral proportions along the strike of the Merensky Reef, and is a warning to those who generalise about the mineralogy of this deposit.

Although the grains so far seen in the concentrates are generally free of attached sulphides, a clue to its mode of intergrowth in the ore is seen in figure 7.1. In this example sperrylite is being replaced by pyrrhotite and the platinum released as a result has given rise to a zone of textural-type III platinum-iron alloy by segregation, as described in chapter 5.1.3. Vermaak and Hendriks say little about the mode of occurrence of sperrylite in the western Bushveld, but they do show a photomicrograph which illustrates its occurrence as a large euhedral rectangular crystal enclosed dominantly by pyrrhotite and partly by pentlandite. No reaction with pyrrhotite is evident although the crystal is slightly embayed and rounded where it is in contact with pentlandite. Their studies, however, indicate a stronger affinity of sperrylite for a pentlandite and chalcopyrite matrix. The relationship of sperrylite to other platinum group minerals is at the moment obscure. Even Vermaak and Hendriks only mention observing intergrowths of sperrylite with laurite, about which they comment that these were "too sparingly present to have warranted the researchers remarking

on the details of aggregation". Liebenberg (1970) reports sperrylite in the Merensky Reef of the Lydenburg District as enclosing chalcopyrite, and at Potgietersrust as being interstitial to the silicates or having cross-cutting relationships towards the sulphides and silicates. Despite the abundance of sperrylite at Western Platinum mine, Brynard et al (1976) unfortunately do not comment on its occurrence in the ore, and merely interpret euhedralism of the concentrate grains as an indication that it was "one of the first minerals to crystallize". It is considered that the limited evidence at Rustenburg and Union mines tends to more strongly suggest crystallisation at an early magmatic sulphide stage than at a late 'residual' hydrothermal one.

7.2 Palladium arsenide

A quantitative electron-probe microanalysis of a small rectangular bluish grey grain of medium reflectance, and associated with a palladium antimonide phase, showed only major palladium and arsenic present. Before any quantitative work could be done the grain fragmented under the electron beam. No further occurrences have yet been found. This Rustenburg occurrence is still the only one reported of a Pd-As phase in the Merensky Reef. The author first reported this as arsenopalladinite which was then considered to be of composition Pd_3As. However, since then several distinct Pd-As phases have been described from other deposits (Cabri et al. 1975; Clark et al. 1974; Cabri et al. in press Canad. Min.). Arsenopalladinite is a redefined term now used specifically for a triclinic phase of composition $Pd_8(As,Sb)_3$ where As:Sb is approximately 5:1.

7.3 Palladium antimonide

7.3.1 Introduction. A palladium antimonide was first reported by Adam in 1927 to occur in the pegmatitic ore of Farm Tweefontein in the Potgietersrust district of the Transvaal. A chemical analysis by Adam (in Wagner, 1929) gave a composition of Pd 70.4, Sb 26.0, Fe(as Fe_2O_3) 0.9, and insolubles 1.4 weight percent. A partial analysis by Millin at the same time gave Pd 70.35 and Sb 27.95 wt. percent. Both analyses corresponded to the formula Pd_3Sb. This mineral was named stibiopalladinite by Wagner. Its reflected-light properties were given by Wagner as white with a yellowish or bronzy-pink tint, isotropic or very faintly anisotropic, high reflectance, and Mohs hardness of 4-5. Schneiderhohn (in Wagner, 1929) describes it as isotropic and resembling sperrylite, with stibiopalladinite being of similar reflectance and displaying a yellowish-pink tint in comparison. Reflectance values determined by Frick (1929) were between 56-57% in green, orange, and red light. Stibiopalladinite was first reported in the Merensky Reef by the author in 1966. Prior to this Stumpfl (1961) had described nine new minerals from Driekop mine, amongst which were three palladium minerals of compositions Pd_2CuSb, Pd(Sb,Bi), and Pd_8CuSb_3. The only other report of stibiopalladinite in the Merensky Reef has been at Western Platinum mine by Brynard et al (1976). They report it as rare and accounting for 0.4 vol.% of the total precious minerals.

An examination of stibiopalladinite from the type area by Desborough et al.(1973) gave a mean composition from the electron-probe microanalysis of seven grains of Pd 67.8 ± 0.5, Cu 1.9 ± 0.1, and Sb 31.2 ± 0.5 weight percent, corresponding to the formula

$(Pd_{4.83}Cu_{0.23})Sb_{1.94}$. X-ray powder and precession photography indicated a hexagonal or perhaps orthorhombic structure, with the powder data indexed provisionally according to a cell of a_o12.80, b_o15.04 and c_o11.36 Å. Its reflected-light properties were described as yellowish white in air with lavender, pinkish, and greenish tints in some orientations, and a slightly darker and richer yellow in oil; reflection pleochroism in air weak from pale yellow to yellowish white; and anisotropy distinct in air and oil. The reflectance range in air at 589nm was given as Rg' 55.1 - 58.2, and Rp' 55.1 - 57.2, and the VHN_{50} of 589 - 644. Clark et al (1974) also examined six grains of type stibiopalladinite, and confirmed the Pd_5Sb_2 composition with electron-probe microanalyses which gave a compositional range of Pd 66.56 - 67.12, Cu 1.56 - 1.94, and Sb 30.58 - 31.48 weight percent. The grains they studied were considered not to be bireflectant, although a variation between grains was found (related to composition presumably) giving a range at 589 nm in air of 55.28 - 56.31 %. A weak to distinct anisotropy was observed.

Finally Cabri and Chen (1976) re-examined more type stibiopalladinite which was weakly anisotropic and showed no observable bireflectance. Analyses of six grains gave a composition range of Pd 67.0-68.0, Sb 30.3-30.7, Cu 1.6-1.7, As 0.2, and Sn 0.1-0.2 weight percent, which they concluded to be best represented by $Pd_{5-x}Sb_{2-x}$ (between Pd_5Sb_2 to Pd_8Sb_3) where x is approximately 0.05, and Cu substitutes for Pd, and As, Sn for Sb. They considered the structure to be hexagonal with a_o 7.598(2), and c_o 28.112(9) Å.

A number of other palladium antimonides have been

defined since 1966. These are:

Mertieite $Pd_{5+x}(Sb,As)_{2-x}$ where x is 0.1-0.2 (Desborough et al., 1973). Its characteristics are:- pseudohexagonal, a_o 15.04, c_o 22.41 Å, possibly monoclinic; mean composition of varieties I and II given respectively as Pd 72.9 and 72.3, Cu 1.2 and < 0.1, Sb 15.3 and 24.7, As 9.2 and 3.3 weight percent; colour brassy yellow and bireflectant, with range of reflectance at 589 nm of Rp' 52.7 - 58.8 and Rg' 55.3 - 61.4%; distinctly anisotropic under crossed nicols; and VHN_{50} of 561 - 593. Cabri et al (1975) re-examined variety II and considered it to be hexagonal stoichiometric $Pd_8(Sb,As)_3$ with a_o 7.546(2), c_o 43.18(1) Å.

Isomertieite $(Pd,Cu)_5(Sb,As)_2$ (Clark et al.,1974). Its characteristics are:- cubic with a_o 12.283 Å, and a composition range of Pd 71.96 - 72.90, Cu 0.93 - 1.13, As 10.74 - 10.99, Sb 15.41-15.74 weight percent; colour pale yellow with reflectance range according to composition of 55.05 - 57.49 % at 589 nm; VHN_{100} of 587-597; isotropic under crossed nicols in most cases.

Sudburyite PdSb (Cabri et al., 1974). Its characteristics are:- hexagonal with a_o 4.06(2), and c_o 5.59 (2) Å; compositional range of Pd 31.1 - 45.2, Ni 10.3 - 0.48, Sb 57.7 - 45.3, Bi 0.53 - 5.4, Te 0.07 - 3.9, As 0.71 - 2.04 weight percent; colour white with yellow tint, and bireflectant with a composition dependent range of reflectance values at 589 nm of Rp' 57.6 - 61.5, and Rg' 61.7 - 65.4; weakly to moderately anisotropic under crossed nicols; VHN_{25} of 281 and 311.

7.3.2 Palladium antimonide from Rustenburg mine is considered to be either mertieite II or stibipalladinite, although some recently

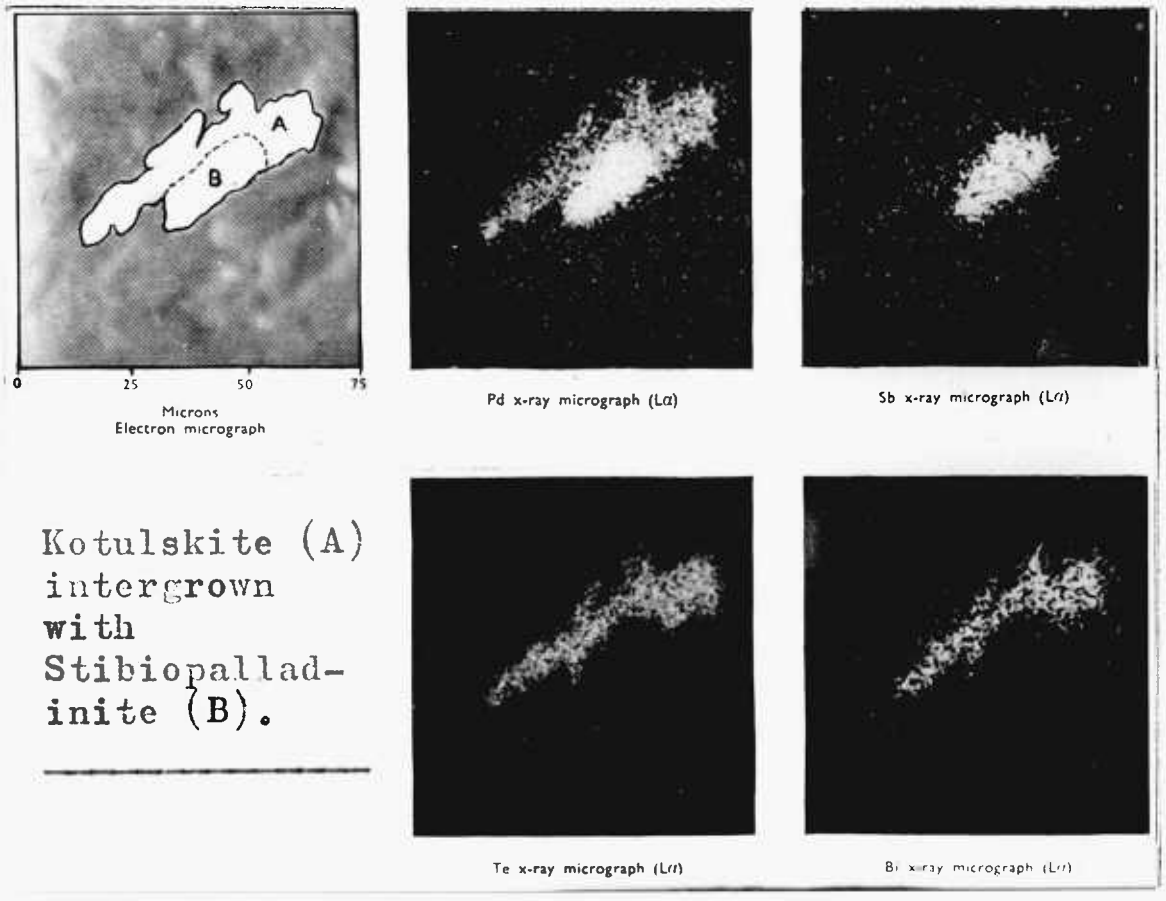

Fig. 7.3 X-ray scanning micrographs showing the distribution of palladium, antimony, tellurium, and bismuth from an electron probe microanalysis of a composite grain of kotulskite Pd(Te,Bi) and palladium antimonide Pd_4Sb. The grain is enclosed in a late stage silicate microveinlet. Rustenburg mine.

located isotropic yellowish grains in a high grade concentrate from Union mine require investigation and could be isomertierite.

Palladium antimonide at Rustenburg mine has been found intergrown with kotulskite in a small embayed grain enclosed in a late-stage silicate microveinlet (figure 7.3). The palladium antimonide was greyish white with a pinkish tint in comparison to kotulskite. It was distinctly anisotropic. Its reflectance was a little less and its hardness greater than kotulskite. A further occurrence at Rustenburg was as a composite grain composed of a euhedral rectangular crystal of palladium arsenide attached to the antimonide by a silicate vein.

The mean composition of the palladium antimonide grain illustrated in figure 7.3 from two analyses was Pd 76.5, Sb 22.0, Bi 1.5, and Fe 0.5 (table 7.3). This gives an atomic ratio of 4:1 compared with the 4:1.5 ratio of mertieite II by Cabri et al.(1975). However, with the present ambiguity in the interpretation of the X-ray powder data for mertieite, in particular mertieite II, together with the close structural and compositional similarity between it and stibiopalladinite, it is not possible to draw any further conclusions without considerably more data.

Table 7.3 Electron-probe microanalyses of palladium antimonide from Rustenburg mine.

kV	wt.% before correction				wt.% after correction			
	Pd	Sb	Bi	Fe	Pd	Sb	Bi	Fe
35	72.8	10.5	1.5	0,5	76.0	18.0	1.5	0.5
25	74.3	15.4	1.5	0.5	77.0	26.0	1.5	0.5
			Mean Wt. %		76.5	22.0	1.5	0.5
			Atomic Proportions		3.97	1.0	0.04	0.05

note: correction for absorption only.

CHAPTER 8

PLATINUM GROUP BISMUTHOTELLURIDES

8.1 Introduction

8.1.1 The Discovery of platinum group tellurides in the Merensky Reef was by the author (1966). However, the presence of a Pd-Bi-Te compound at Union Mine had previously been deduced in 1952 from the detection of bismuth and tellurium during the chemical analysis of a non-magnetic portion of a concentrate by Lever, Todd and Powell of Johnson and Matthey Ltd. (pers comm,). In 1962, during a preliminary investigation of the PGM in polished sections of the Rustenburg ore with the electron-probe microanalyser, the author found a number of white strongly anisotropic laths and blebs, occurring in chalcopyrite and at the margins of the iron-copper-nickel sulphide aggregates, to be bismuth tellurides of platinum and palladium. No X-ray powder data at that time was obtained for these minerals because of their small size and rarity. Meanwhile in 1961 Genkin and Korolev, in a paper describing a procedure for the identification of small mineral grains by X-ray diffraction analysis and microspectrographic methods, described similar minerals which occurred as minute grains in chalcopyrite, pyrrhotite, and occasionally violarite in the upper sectors of vertical veins of the Monchegorsk platinum deposits. In 1963 Genkin et al. defined these minerals more precisely, showing them to be hexagonal and naming one of them moncheite, $(Pt,Pd)(Te,Bi)_2$, and the other kotulskite with the uncertain formula of $Pd(Te,Bi)_{1-2}$. They also gave new data on cubic michenerite which, instead of being as originally thought

$PdBi_2$, was shown to contain tellurium as a major constituent and to have a composition $Pd_{0.72}Pt_{0.21}Te_{1.02}Bi_{0.98}$.

8.1.2 The Author's Results from a study of these minerals in the Merensky Reef at the Rustenburg and Union mines were published in 1966 together with descriptions of three other new bismuthotellurides. One of these is of composition $(Pd,Pt)(Te,Bi)_2$ and was named merenskyite after Dr. Hans Merensky. This mineral is isostructural with moncheite, although a complete isomorphous solid solution series does not appear to exist between them. The second new mineral is a mercurian palladium bismuthotelluride (Mineral A) which is distinctly different from any of the other tellurides, being grey and apparantly isotropic, with a composition determined from one electron-probe microanalysis of a 5 μm diameter grain to be close to (Pd,Hg)(Te,Bi). This mineral could be the same as temagamite Pd_3HgTe_3, which is considered to be orthorhombic (Cabri et al. 1973). The third mineral, Mineral C, is similar to kotulskite in appearance but has considerably more bismuth, with a composition of $(Pd_{0.98}Pt_{0.02})(Te_{0.56}Bi_{0.44})_{0.86}$. The possible existence of a fourth mineral optically the same as merenskyite but of composition $Pd_3(Te,Bi)_5$, was also indicated. The study also showed for the first time that kotulskite is Pd(Te,Bi).

No other platinoid tellurides have been definitely confirmed in this study, although some of the creamy white grains which are isotropic are probably michenerite, and not, as first thought, merely basal sections of hexagonal kotulskite. This is supported by the report of michenerite in the Merensky Reef from unspecified localities in the western Bushveld by Vermaak and Hendriks (1976).

They, however, provide no data to substantiate their identification. Since 1966, merenskyite has been verified in composition and structure in at least seven other deposits throughout the world (Rucklidge, 1969; Cabri, 1974; Cabri and Gilles Leflamme, 1976; McCallum et al., 1976; Page et al., 1976). Moncheite from Atok mine (Schwellnus et al., 1976), and moncheite and kotulskite from Western Platinum mine (Brynard et al., 1976) are the only platinoid tellurides to have been so far reported in other specific outcrops of the Merensky Reef.

8.1.3 The General Occurrence of these bismuthotellurides is late in the paragenesis, as is evident from their invariable close association or intergrowth with chalcopyrite. They occur commonly as equant anhedral grains 1-15 μm in size enclosed partially or completely by chalcopyrite and rarely by pentlandite. In this form they are often to be found in the vicinity of braggite crystals which are fractured and veined by chalcopyrite, as in figures 8.1 and 6.11. Very small fine white acicular crystals of 1-<1μm in width have also been seen in chalcopyrite, especially close to the margin with the silicates. These are presumed to be platinum and palladium bismuthotellurides. Clusters of small grains are to be found isolated in later silicate microveinlets cutting the primary silicates or following cleavage directions. These are again associated or/and intergrown with chalcopyrite blebs disseminated along the veinlets as in figure 8.2. Larger euhedral to subhedral lamellae of 0.3 - 0.6 mm are more rarely found as illustrated in figures 8.3 and 8.7. These occur at the silicate-sulphide boundaries, and in these cases are enclosed by pentlandite as well as

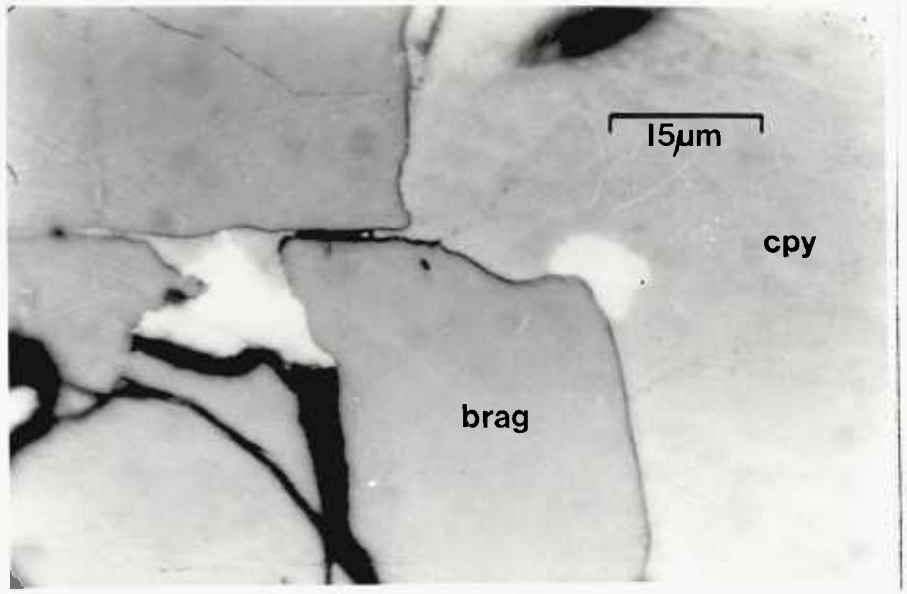

Fig. 8.1 Photomicrograph of polished section showing two grains of moncheite $Pt(Te,Bi)_2$ (white) associated with chalcopyrite (cpy) which encloses fractured braggite (Pt,Pd,Ni)S (brag). Rustenburg mine.

Fig. 8.2 Platinoid bismuthotellurides (white) associated with chalcopyrite in late stage silicate microveinlets replacing the primary silicates. Photomicrograph of polished section. Rustenburg mine.

chalcopyrite. Except for mineral A, all these tellurides of platinum and palladium are bright white to cream in colour, are anisotropic to varying degrees according to orientation, and crystallise in the hexagonal system.

8.1.4 Electron-probe Microanalysis. The instrument used for this study was a Cambridge Microscan Mark 1. Details of this and the correction procudures used are given in chapter 3. The standards used were an analysed 50/50 Pt:Pd alloy (kindly given by Johnson and Matthey & Co., Ltd), an analysed specimen of calaverite, $(Au,Ag)Te_2$, for tellurium, an analysed specimen of coloradoite, HgTe, for mercury determinations, and spectrographically pure bismuth. The specimens for analysis were coated with a 50-75 A thick film of aluminium.

8.2 Moncheite $(Pt,Pd)(Te,Bi)_2$

This was the second recorded occurrence of moncheite (Kingston, 1966) and it provided confirmation that moncheite from the Urals was valid as a new mineral.

8.2.1. The Occurrence of moncheite at Rustenburg and Union mines is usually in the form of blebs 1-10 μm across, and fine acicular laths up to 10 μm in length which are generally only visible at magnifications of greater than X400. Moncheite is nearly always enclosed at least in part by chalcopyrite, and occurs at or near to the clusters or small grains in microveinlets along partings in the altered silicates. It is particularly abundant in the immediate area of other platinum group minerals (fig. 6.11). The study of Vermaak and Hendriks (1976) supports this qualitative conclusion. They determined that 98.59 vol.% of all moncheite occurrences were at the sulphide-gangue contact (51·87 vol.%) and within veinlets in

the silicates and oxides (46·72 vol.%). At the sulphide-gangue contact 40·38 vol.% occurred within chalcopyrite.

Only one large lath of sufficient size to enable its extraction for X-ray powder analysis (200 x 60 μm size) has so far been located. This occurred at a sulphide:silicate contact as a subhedral lath, which in this exceptional case was enclosed by pyrrhotite and pentlandite (figs. 8.3 & 8.5). It is considered that this lath was originally formed by the replacement of pyrrhotite, but was later centrally 'corroded' by pentlandite which now separates two optically continuous pieces of the lath. The final texture probably has been modified by subsequent diffusion and recrystallisation processes which, as discussed earlier (chapter 5.1) may have given rise to the euhedral ferroplatinum crystals in the pyrrhotite.

8.2.2 The Optical and Physical Properties of the type moncheite from the Urals is described by Genkin et al as a white mineral showing noticeable pleochroism in air, strongly anisotropic, and having a reflectance in air with orange light of approximately 56 - 60%. Hardness is given as lower than chalcopyrite and higher than kotulskite and michenerite.

The Colour of moncheite in this study is a bright greyish-white in air, showing a weak pleochroism. Under oil immersion it is light grey and exhibits a distinct pleochroism. Compared with ferroplatinum (fig. 8.3) it appears more grey and less creamy, especially under oil. When enclosed by braggite it appears greyish white but is a bright white against chalcopyrite (figs. 8.2 & 8.4).

The Reflectance in sodium light, by visual comparison,

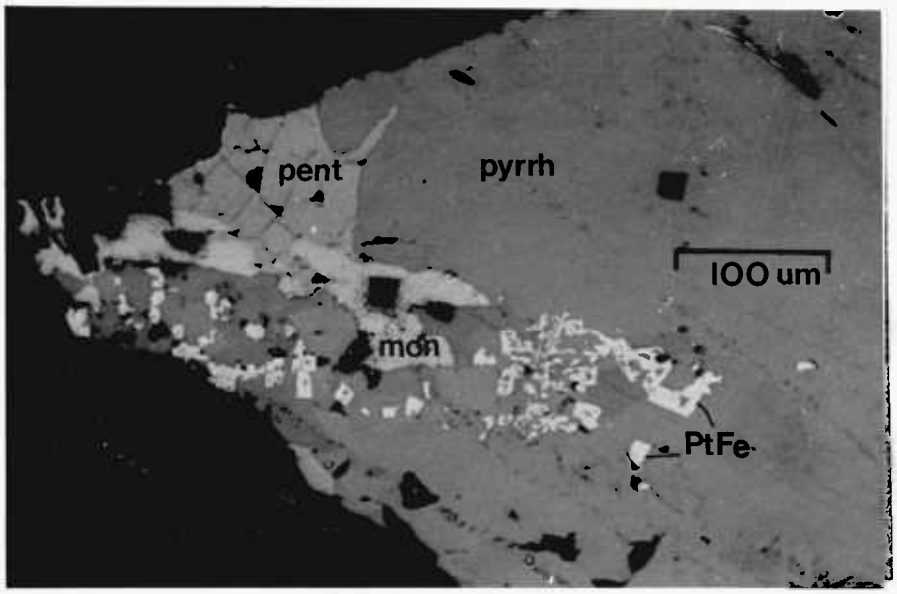

Fig. 8.3 A lath of moncheite (mon) and euhedral crystals of platinum-iron alloy (Pt,Fe) showing cubic outline, intergrown with pyrrhotite (pyrrh) and pentlandite (pent). Photomicrograph of polished section. Rustenburg mine. Scale 1 cm = 50 μm.

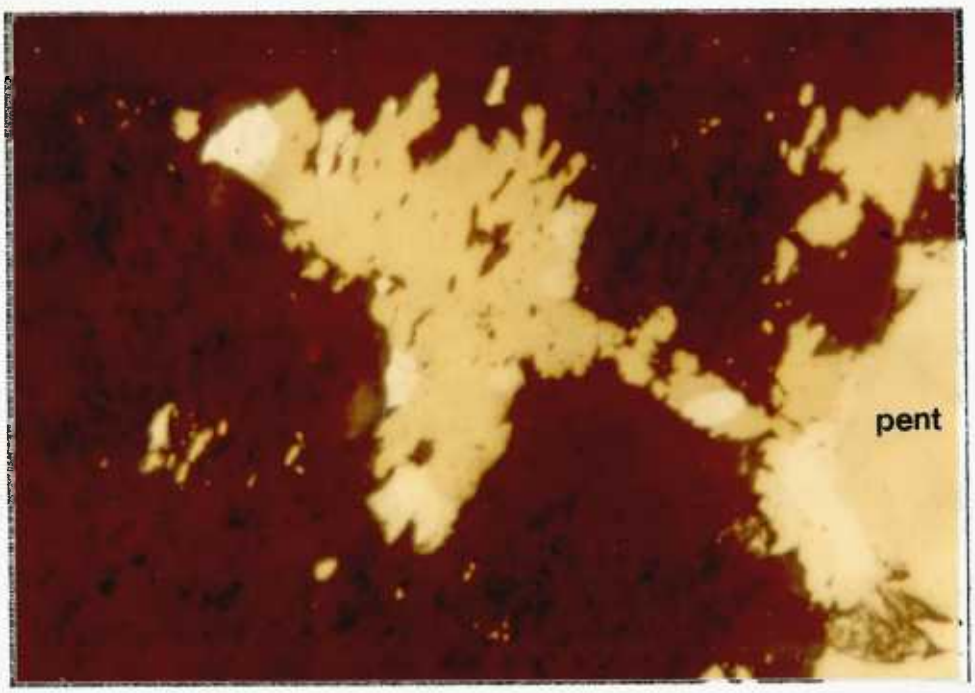

Fig. 8.4 Grains of moncheite and merenskyite (white) associated with chalcopyrite. Union mine. Scale 1 cm = 10 μm.

lies between pentlandite and ferroplatinum and is very much greater than braggite or cooperite. Reflectance values for two of the largest grains showing the strongest anisotropy were determined in air with the Reichert reflex spectral microphotometer, using a x60 objective and 2mm mirror diaphragm. An N.P.L. Measured pyrite (N.1915.1), loaned by S.H.U. Bowie of the Atomic Energy Division, was used as a standard. These values are given in table 8.1. for comparison with moncheite from Atok mine (Schwellnus et al, 1976). Although the values for one grain from Atok mine agree closely with the present study, the R_o of the other grain is considerably higher. This is difficult to explain as there is no appreciable difference in composition between the two Atok mine grains.

Table 8.1 Spectral reflectance values in % for moncheite from Rustenburg mine (R) compared with values by Schwellnus et al. (1976) for moncheite from Atok mine (A).

Loc. Grain	R_o 470nm	546nm	589nm	650nm	R_e, 470nm	546nm	589nm	650nm
R 2	53.0	53.2	52.9	52.7	56.8	58.8	58.1	59.6
R 3	53.9	53.7	53.3	52.7	56.5	56.6	56.1	54.9
A 10	58.4	56.7	57.3	58.0	59.4	58.9	59.7	60.5
A 11	50.3	52.4	51.6	51.7	54.9	54.4	57.5	57.7

The hexagonal structure determined by X-ray powder diffraction is supported by the constant low values at each wavelength. Since R_e is greater than R_o, moncheite is optically positive with an average reflectance and near maximum bireflectance at 589nm of 53.1% and 5% respectively. The dispersion profiles do not contradict the

observed colour, and the author cannot understand the subjective criticism of Ramdohr (1969), which appears to be based on his apparant general aversion to quantitative reflectance measurements, that "regarding the trend of dispersion, the data do not look very reliable".

Finally a comparison of the compositions of the two measured grains (analyses (2) & (3), table 8.2) shows differences of Pt 8.6, Pd 3.7, Bi 9.5, and Te 5.6 wt. percent. However, this appears to result in no significant difference in reflectance of R_o, although an increase in Pd content can be expected to increase the reflectance, since the palladium end-member, merenskyite, has an R_o at 589nm which is 12 units of reflectance % higher than moncheite.

The Anisotropy under crossed nicols is from distinct to strong in air, according to orientation, with light yellowish to dark brown polarisation colours. Cabri and Laflamme (1976) report them as shades of grey for Sudbury moncheite.

The Hardness, according to observations of its polishing relief, is approximately the same as pentlandite (VHN_{100} 222, VHN_{50} 264, Young & Millman, 1964) greater than chalcopyrite and less than pyrrhotite. No reliable indentation microhardness measurement could be obtained either because of the small size of even the largest grains (fig. 8.3). [redacted]. Values of VHN_x 57.5 for moncheite by Schwellnus et al (1976), and VHN_{10} 92 (range 73 - 111) by Cabri and Laflamme (1976), disagree with its observed polishing hardness, as well as with values for the other platinoid tellurides exhibiting a similar polishing relief.

8.2.3 The Composition. The results of quantitative micro-

Table 8.2 Electron-probe microanalyses in weight percent of moncheite from Rustenburg mine by Kingston (1966), compared to quantitative microspectrographic analyses of type moncheite from the Monchegorsk deposit by Genkin et al. (1963), and electron-probe microanalyses of moncheite from Atok mine by Schwellnus et al. (1976), and Western Platinum mine by Brynard et al.,(1976).

Loc.	RUSTENBURG MINE					MONCHEGORSK				ATOK MINE		W.PLATINUM	
No.	(1)	(2)	(3)	(4)	(5)	(6)	(7)	(8)	(9)	(10)	(11)	(12)	(13)
Pt	18.6	28.4	37.0	42.0	38.4	22.3	27.4	25.9	30.8	40.14	38.61	38.8	38.4
Pd	9.3	3.7	----	----	----	7.0	9.2	6.9	4.6	0.24	0.33	0.2	0.5
Bi	10.2	7.5	17.0	17.0	16.2	31.7	29.9	12.9	9.2	6.58	11.16	7.2	11.2
Te	40.3	40.7	35.1	35.3	45.8	39.0	33.5	54.3	55.4	48.07	44.17	54.9	49.4
Fe	}				----					-----	-----		
Cu	} 7.0	8.0	3.0	3.0	}	----	----	----	----	-----	-----		
Ni	}				(1.2)					0.09	0.08		
Os										0.69	0.68		
Pb										2.34	2.66		
As										0.16	0.31		
Sb										tr	tr		

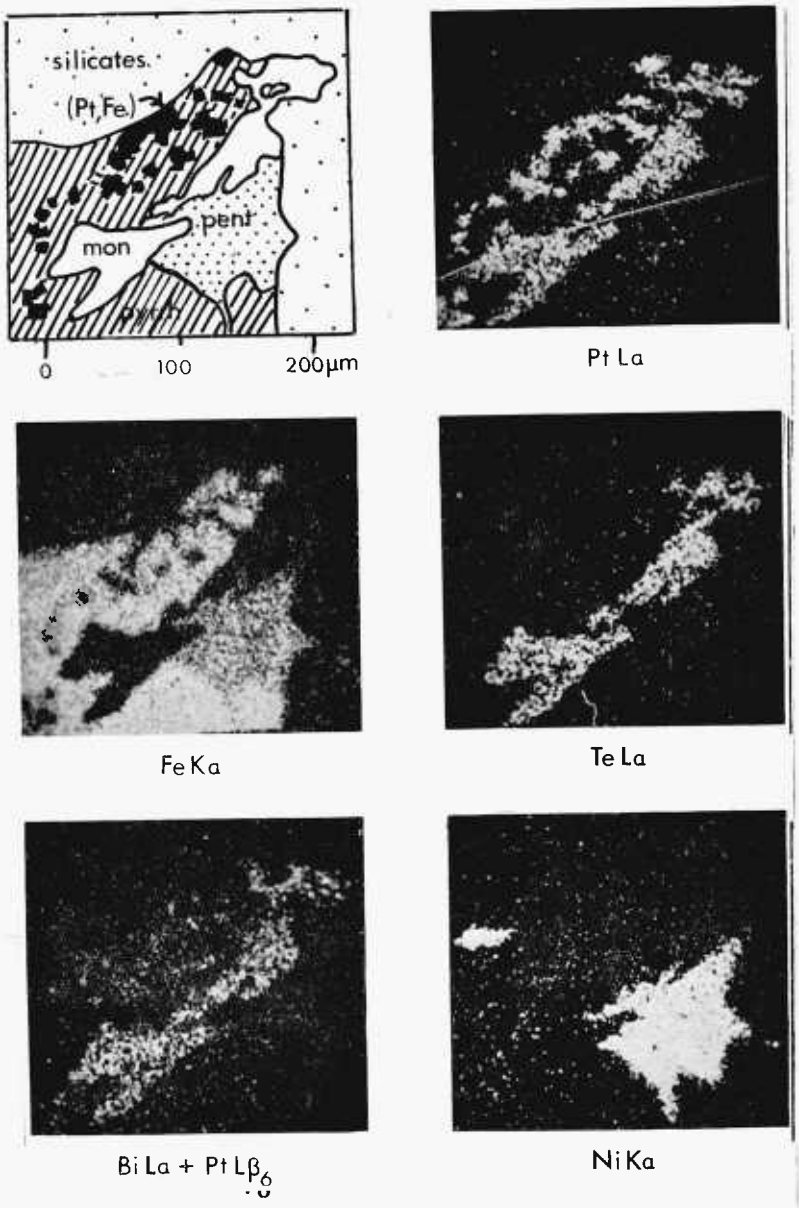

Fig. 8.5 X-ray scanning micrographs of area illustrated in figure 8.3 showing the distribution of platinum, iron, tellurium, bismuth, and nickel in an intergrowth of moncheite $Pt(Te,Bi)_2$ (mon) and ferroplatinum (Pt,Fe) in pyrrhotite (pyrrh) and pentlandite (pent). Rustenburg mine.

spectrographic analyses of four grains of moncheite from the Monchegorsk deposit by Genkin et al., and the results of electron-probe microanalyses of moncheite from Rustenburg and Atok mine are tabulated for comparison in table 8.2. The analyses 1,2,3 and 4 of the present study were obtained under conditions of constant specimen-current, and have only been corrected for absorption using a correction procedure by Tong (1961). They are, however, considered to be sufficiently accurate to help confirm the grains as being moncheite, for comparison with the type moncheite, and to further confirm that compositional trends involve the substitution of Pd for Pt, and Bi for Te.

One of the largest grains (no.3, fig. 8.3 & 8.5), confirmed later by X-ray powder analysis to be moncheite, was reanalysed at constant beam current. The analysis was corrected for absorption, atomic number, and fluorescence by the method outlined in chapter 3.4.3, and is presented in table 8.2 under analysis 5; giving a Pt:(Te,Bi) ratio of 1 : 2.22 . This ratio is when the 3.0 wt.% of combined Cu,Ni, and Fe is ignored from the first analysis as being due to irradiation of the surrounding base-metal sulphides. However, reference to figure 8.3 and 8.5 shows that at least the copper content cannot be ignored, since the enclosing sulphides are pyrrhotite and pentlandite. In addition, Schwellnus et al (1976) report 0.08 - 0.09 wt.% Ni in moncheite from Atok mine, as well as Pb 2.34 - 2.66, Os 0.68 - 0.69, trace Sb, As 0.16 - 0.31, and S 0.37 - 0.44 weight percent. Cabri and Laflamme (1976) also report 0.13 - 0.48 wt.% Ni in Sudbury moncheite. Therefore it is concluded that Rustenburg moncheite does contain small amounts of copper and

nickel, and that their detection under the electron-probe micro-analyser cannot be completely attributed to subsurface irradiation of enclosing base-metal sulphides, especially with grain 3 (fig. 8.3) which is fairly large, and which is enclosed in the area of analysis by pyrrhotite. In the other analyses (1,2, and 4, table 8.2) where the grains were very small and enclosed by chalcopyrite (fig. 8.1), the high percentages of (Cu,Ni,Fe) are still considered to be largely due to Cu & Fe radiation as a result of subsurface irradiation of chalcopyrite. When this is taken into consideration a 1:2 ratio is not incompatible with the results of this study since as is the case with analysis 5, the addition of as little as 1·2 wt.% combined Cu and Ni would give the ideal ratio.

The absence of nickel in moncheite at Monchegorsk together with the occurrence of less than 0·1 wt.% Ni for Atok mine and less than 2 wt.% for Rustenburg mine suggests that there is a very limited solid solution series with melonite. Palladium contents indicate a limited solid solution also towards merenskyite, the latter forming a complete series, according to Rucklidge (1969), in the direction of melonite $NiTe_2$, or more correctly palladian bismuthian melonite $(Ni,Pd)(Te,Bi)_2$. This is discussed further under merenskyite.

8.2.4 X-Ray Powder Data for the Rustenburg moncheite are given in table 8.3, together with the type moncheite and artificial $PtTe_2$. The unindexed d-values may be due to contamination by pyrrhotite and pentlandite during extraction from the polished section. Of the eleven indexed lines, nine correlate closely with those for the type moncheite. Only a very weak diffraction pattern was obtained as a

Table 8.3 X-ray powder data for moncheite $(Pt,Pd)(Te,Bi)_2$ from Rustenburg mine (Cu radiation, Ni filter and 11.483 cm diameter camera), and for moncheite from Monchegorsk (Genkin et al.,1963).

	Rustenburg			Monchegorsk	
Hex. Cells	a_o 4·062 ± 0·002 c_o 5·346 ± 0·003			a_o 4·049 ± 0·004 c_o 5·288 ± 0·005	
hkil	d calc	d obs	I obs	d obs	I obs
0001*	5·325	5·25	50	5·32	60
--	---	3·02	40	3·07	20
$10\bar{1}1$*	2·932	2·94	100	2·93	100
--	---	2·73	10	--	--
0002	---	---	--	2·66	10
$10\bar{1}2$*	2·124	2·12	60	2·11	80
--	---	2·08	20	--	--
$11\bar{2}0$*	2·028	2·03	60	2·02	70
$11\bar{2}1$*	1·896	1·885	20	1·888	40
--	---	1·798	40	1·712	20
0003	---	---	--	--	--
--	---	1·728	30	--	--
$20\bar{2}1$*	1·668	1·668	40	1·664	60
$10\bar{1}3$*	1·587	1·588	20	1·575	50
--	---	1·534	20	--	--
$20\bar{2}2$*	1·467	1·471	20	1·462	70
0004	---	---	--	1·324	40
$21\bar{3}0$*	1·328	1·328	20	--	--
$21\bar{3}1$*	1·289	1·289	40	1·282	70
$20\bar{2}3$	---	---	--	1·242	30
$10\bar{1}4$*	1·247	1·248	10	--	--
$21\bar{3}2$	---	---	--	1·182	50

Footnote

* These indices were checked, assuming a hexagonal symmetry, using a modified version of a computer programme by W.D.Hoff et al.(1965). In this programme the indices were accepted if $\overline{(\sin^2\theta_o - \sin^2\theta_c)}$ 0·003. The drift constant K (Hess, 1951) was assumed proportional to $\frac{1}{2}(\cos^2\theta/\sin\theta\cos^2\theta/\theta)$. Standard deviations of a and c were also determined. All reflections indexed were included in the determination of the cell parameters.

result of the minute quantity of powder available from the lath shown in figure 8.3. Therefore, differences from type moncheite may in part be due to measurement error, particularly in the back reflection region. However, Genkin et al must have encountered the same problem. The eleven indexed spacings were checked (Frost, pers. comm), assuming a hexagonal symmetry, using a modified version of a computor programme by W.D.Hoff et al (1965). All reflections indexed were included in the determination of the cell parameters which gave a_o 4.062(2), c_o 5.346(3) Å, compared to type moncheite of a_o 4.049(4), c_o 5.288(5) Å, and artificial $PtTe_2$ of a_o 4.026, c_o 5.221 Å (Gronvold et al., 1960). These values are further confirmed by Cabri and Laflamme (1976) with their cell dimensions for Sudbury moncheite of a_o 4.040(1), and c_o 5.297(6) Å.

A new mineral, 'chengbolite' $PtTe_2$, recently reported from China (Sun et al., 1973) is probably moncheite. This mineral was discredited by an I.M.A. vote in March 1975. The data for this mineral were reported as a_o 4.041, c_o 5.220 A; VHN_x 142 kg/mm^2; composition range Pt 35·86 - 39·4, Pd 2·2 - 3·96, Te 58·16 - 68.0 weight percent; strongest d-lines of 2.896(10), 2.086 (9), 1.560(8) 1.096 (7), and 1.001 (7) Å; and reflectance of 51·6 - 42·1 % at an unspecified wavelength.

8.3 Kotulskite Pd(Te,Bi)

8.3.1 The Occurrence of Kotulskite was first reported from the Monchegorsk deposit by Genkin et al (1961,1963) as being intergrown with moncheite and michenerite, and as separate grains enclosed in chalcopyrite. An approximate formula of $Pd(Te,Bi)_{1-2}$ was given. A similar phase from Rustenburg mine, considered to be kotulskite from

the evidence of the X-ray powder data (table 8.6), has a composition from two fully corrected electron-probe microanalyses of Pd(Te,Bi). Its occurrence at both Rustenburg and Union mines is the same as for moncheite. However, whereas moncheite has not been found intergrown with any other telluride, kotulskite is usually intimately intergrown with merenskyite as follows:-

(1) as a small-size lammellar intergrowth, as illustrated in figure 8.6, which can easily be overlooked because of kotulskite's general similarity to merenskyite. With the smallest grains this intergrowth can only be discerned in oil using the highest magnification. This intergrowth appears to be formed by a guided replacement of merenskyite by kotulskite. As pointed out in 1966, this can give rise to errors during analyses, and will be discussed later with regard to the composition of merenskyite.

(2) As an easily resolved replacement intergrowth, as illustrated in figure 8.7, in which a lath of merenskyite is clearly being replaced by kotulskite. This again will be discussed more fully under merenskyite.

(3) As an intergrowth showing a smooth and slightly embayed boundary, as in figure 8.8. Here the relationship is a little ambiguous.

Vermaak and Hendriks report that 83·79 vol.% of all kotulskite occurs enclosed in gangue, and 10·46 vol.% in chalcopyrite along sulphide-gangue contacts. They do not, however, report on the common merenskyite-kotulskite association.

8.3.2 The Optical and Physical Properties of the type kotulskite from Monchegorsk has been described as a cream-coloured and

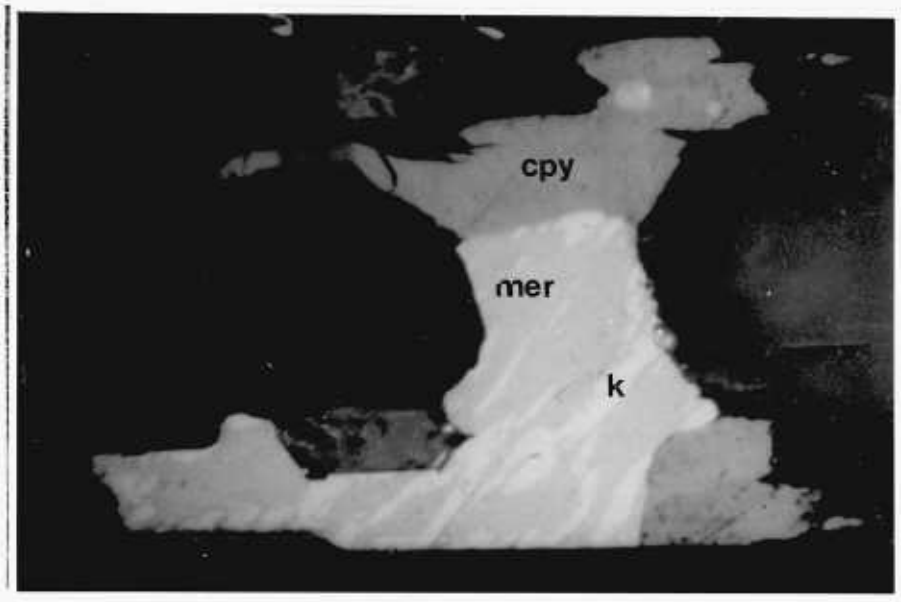

Fig. 8.6 A fine lammellar intergrowth of kotulskite (k) and merenskyite (mer) adjacent to chalcopyrite (cpy) and resolved under crossed nicols with the analyser slightly rotated. Rustenburg mine. Scale 1 cm = 10 um.

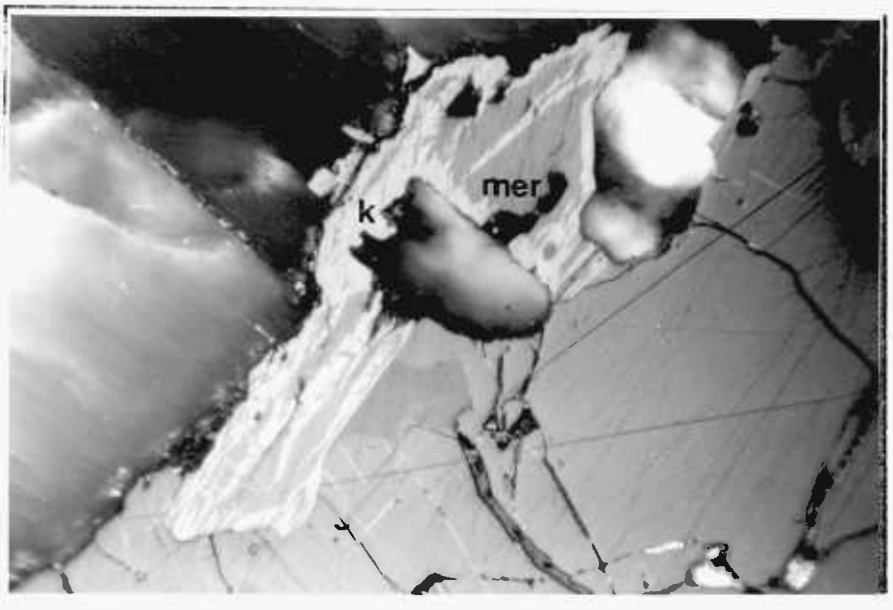

Fig. 8.7 A subhedral lath of merenskyite (mer) along a pentlandite-silicate contact showing partial replacement by kotulskite (k). Photomicrograph of polished section under crossed nicols to show texture. Rustenburg mine. Scale 1 cm = 33 µm.

strongly anisotropic mineral in air, with polarisation colours of brown to grey-blue, and as having a high reflectance (maximum 66%) in orange light (Genkin et al., 1963). Its hardness is given as lower than chalcopyrite and moncheite, and similar to michenerite.

The Colour of kotulskite from Rustenburg mine is a cream or pale yellow in air, and it exhibits a distinct pleochroism from a light cream to a slightly darker greyish cream. In oil it appears more yellow and the pleochroism is more distinct. Moncheite and merenskyite appear white in comparison with kotulskite. Chalcopyrite against kotulskite appears greenish yellow.

The Reflectance values (table 8.4) were obtained by the same method as for moncheite, except that a x32 objective was used. Although the values are a little ambiguous, it is considered to be most probably optically positive with an average R_o at 589nm of 62·5% compared to moncheite at 53·1% and merenskyite at 65%.

The Anisotropy is strong with polarisation effects from grey to dark bluish grey with the nicols completely crossed.

The Hardness from its polishing relief is greater than chalcopyrite and less than pentlandite and merenskyite. One grain was large enough to obtain two Vickers microhardness values, using a 15 g load, which gave an average of VHN_{15}=236. The indentation shape was symmetrical with no fractures and straight to very weakly concave sides. This may be compared with VHN_{15} 291 (range 277 - 322) obtained by Cabri and Laflamme (1976) from eight measurements on five grains of tellurium rich (26·6 - 28·1 wt.% Te) kotulskite from Sudbury.

8.3.3 The Composition. Two homogeneous and inclusion free

Table 8.4 Spectral reflectance values in percent for kotulskite from Rustenburg mine, corresponding to analyses (1) & (2) in table 10.5.

No.	R_o				$R_{e'}$			
	470nm	546nm	589nm	650nm	470nm	546nm	589nm	650nm
1	55.1	60.9	63.3	65.2	57.3	64.4	65.6	67.9
2	53.0	58.7	61.7	64.1	53.4	61.1	63.2	66.2

Table 8.5 Electron-probe microanalyses in wt.% of kotulskite and Mineral C from Rustenburg mine by Kingston (1966); a quantitative microspectrographic analysis of type kotulskite from Monchegorsk (Genkin et al., 1963); and an electron-probe microanalysis of a similar 'new mineral' from Bissersk by Stumpfl (1976).

	KOTULSKITE			MINERAL C	'NEW MINERAL'
	RUSTENBURG		MONCHEGORSK	RUSTENBURG	BISSERSK
	(1)	(2)	(3)	(4)	(5)
Pt	----	1.1	----	1.3	----
Pd	45.9	38.8	31.1	40.0	37.6
Bi	17.2	20.1	24.9	30.6	39.0
Te	38.0	36.1	44.0	23.3	19.0
Sb	----	----	----	----	3.8

grains of kotulskite from Rustenburg mine were analysed with the electron-probe microanalyser using constant beam-current conditions, and the initial percentages were corrected for absorption, atomic number, and fluorescence as outlined in chapter 3.4.3. The results are presented in table 8.5 together with the semiquantitative microspectrographic analysis of kotulskite by Genkin et al. X-ray scanning micrographs showing the distribution of palladium, tellurium, and bismuth in an intergrowth of kotulskite and merenskyite are presented in figure 8.8. These show clearly the difference in Pd and Te content between the two minerals, as well as the homogeneity of each. The formulae calculated from these analyses are $(Pd_{0.98}Pt_{0.02})(Te_{0.75}Bi_{0.25})_{1.02}$ and $Pd(Te_{0.78}Bi_{0.22})_{0.88}$. These give an average composition of $(Pd_{0.99}Pt_{0.01})(Te_{0.76}Bi_{0.24})_{0.95}$ which strongly supports an ideal stoichiometric ratio of 1 : 1 for this Rustenburg phase.

A similar phase "Sudbury kotulskite" has been recently described by Cabri and Laflamme (1976). In contrast to Rustenburg kotulskite this mineral is distinctly pinkish-cream with no observable bireflectance in air or oil, and its anisotropy under crossed nicols is weak to nil in air, and weak in oil. This is because of its marked difference in composition from the Rustenburg and type Monchegorsk kotulskite. The composition of "Sudbury kotulskite" is fairly constant giving a range from the analysis of four grains of Pd 37·7 - 38·3, Ni 0·00 - 0·05, Te 26·6 - 28·1. Bi 33·2 - 35·3, and Sb 0·06 - 0·32 weight percent. No X-ray data was obtained for this phase.

8.3.4 The X-Ray Powder Data (table 8.6) adds further confirma-

Table 8.6 X-ray powder data for kotulskite (Pd,Pt)(Te,Bi) from Rustenburg mine (copper radiation, Ni filter and 11.483 cm diameter camera), kotulskite $Pd(Te,Bi)_{1-2}$ from Monchegorsk (Genkin et al.,1963), and artificial PdTe (Thomassen, 1929).

	Rustenburg			Monchegorsk			Artificial PdTe	
Hex. Cells	a_o 4·145 ± 0·005 c_o 5·67 ± 0·01			a_o 4·19 ± 0·01 c_o 5·67 ± 0·01			a_o 4·127 ± 0·004 c_o 5·663 ± 0·005	
hkil	d calc	d obs	I obs	hkil	d obs	I obs	d obs	I obs
---‡	---	---	---	$10\bar{1}0$	3·65	30	3·58	10
$10\bar{1}1$*	3·032	3·03	100	$10\bar{1}1$	3·05	100	3·03	40
---	---	---	---	0002	2·85	10	--	--
$10\bar{1}2$*	2·224	2·22	90	$10\bar{1}2$	2·24	90	2·22	80
$11\bar{2}0$*	2·071	2·08	70	$11\bar{2}0$	2·09	90	2·07	60
$20\bar{2}1$*	1·711	1·72	20	$20\bar{2}1$	1·73	60	1·71	40
$10\bar{1}3$*	1·671	1·67	20	$10\bar{1}3$	1·68	60	1·67	50
$11\bar{2}2$	1·672							
$20\bar{2}2$*	1·515	1·52	30	$20\bar{2}2$	1·53	70	1·51	80
---	---	1·41	5	0004	1·42	20	1·42	25
$10\bar{1}4$*	1·318	1·32	10	$10\bar{1}4$	1·33	70	1·32	50
$21\bar{3}2$	1·319							
---	---	1·23	10	$20\bar{2}3$	1·31	30	1·30	25
$30\bar{3}1$	1·170	1·17	10	$21\bar{3}2$	1·24	80	1·22	100
$11\bar{2}4$*	1·169			$30\bar{3}0$	1·19	70	1·21	50
				$20\bar{2}4$	1·17	80	1·17	100

* See footnote to table 8.3. ‡ Strong blackening of the film in this region due to rubber.

tion of a 1:1 ratio, since it is in close agreement with artificial PdTe. This is further emphasised by the lack of agreement with the powder data for artificial $PdTe_2$. The close agreement of the indexed spacings and cell size, a_o 4.145(5) and c_o 5.67(1)Å, of the Rustenburg phase with Monchegorsk kotulskite, a_o 4.19(1) and c_o 5.67(1)Å, together with the compositional data, confirms that both can be considered as the same mineral, and that the correct formula for pure end-member kotulskite should be in future quoted as Pd(Te,Bi).

8.4 Mineral C $(Pd_{0.98}Pt_{0.02})(Te_{0.56}Bi_{0.44})_{0.86}$.

This telluride has similar optical properties to kotulskite. The composition (table 8.5, analysis 4) was determined on a grain of about 30 μm in diameter, which was simply interlocked with a 15 μm bleb of stibiopalladinite. This composite grain occurred in a late stage microveinlet cutting the early formed matrix silicates. Compared to kotulskite it had on average 12 wt.% more Bi, and tellurium was correspondingly 13·8 wt.% lower. Since this data was published in 1966, Stumpfl (1976) has provided an analysis of a 'new mineral' from Bissersk in the Urals (table 8.5, analysis 5) of composition expressed as $Pd_{2.00}Bi_{1.05}(Te_{0.84}Sb_{0.18})_{\Sigma=1.02}$. This would appear to be merely another example of Mineral C with some minor antimony substitution for either Te or Bi, and it is considered that the formulae might well be expressed as $Pd(Bi_{0.51}Te_{0.40}Sb_{0.09})_{1.04}$. The fact that this mineral is also white, strongly anisotropic, and with an estimated reflectance of greater than 60%, is further strongly suggestive that Mineral C from Rustenburg and 'the new mineral' from Bissersk are the same.

Mineral C is probably an intermediate member of a solid solution series trending towards an as yet unknown hexagonal PdBi by the progressive substitution of Bi for Te in kotulskite. Mineral C might therefore be called a bismuthian kotulskite.

8.5 Merenskyite (1)* $(Pd,Pt)(Te,Bi)_2$.

8.5.1 The Occurrence of merenskyite at Rustenburg mine is in the same manner as kotulskite, with which it has so far always been found to be intergrown. Its preference for chalcopyrite along sulphide-gangue contacts and within veinlets in the gangue is emphasised by the quantitative study of Vermaak and Hendriks, which produced occurrence figures for these two modes of 28·44 vol.% in chalcopyrite and 59·04 vol.% in the gangue. The modes of intergrowth with kotulskite are illustrated in figures 8.6, 8.7, and 8.8. These occurrences have been confirmed by electron-probe microanalysis, and are all examples from Rustenburg mine. Grains of identical properties to merenskyite have been found in the ore from Union mine but these have not as yet been confirmed as merenskyite by analysis. In nearly all cases it is clear that the intergrowths have been formed by the replacement of merenskyite by 'palladium-rich' kotulskite, and that a crystallographic control has operated. This provides further evidence for late stage palladium enrichment during sulphide fractionation, with resultant palladium metasomatism of earlier formed minerals. This also supports and complements the author's earlier observations on the replacement of cooperite by braggite.

(1)* Name approved before publication by the Commission on New Minerals and Mineral Names, International Mineralogical Association, June 1965.

Because of the similar appearance of kotulskite and merenskyite, and the fine nature of the replacement lamellae (often of the order of 1 μm in width), small-size grains exhibiting this intergrowth, as in the case of figure 8.6, are easily misinterpreted as either being of a homogeneous phase or a pleochroic homogeneous phase showing twin lamellae. In the present study several early analyses of these small telluride grains had to be rejected after a microscopic re-examination revealed a two phase intergrowth. The author's findings (1966) were confirmed by Cabri and Pickwick (1974). They also demonstrated the existence of even finer lamellar intergrowths in the Stillwater Complex, which appear to have resulted from the exsolution of kotulskite from merenskyite. The kotulskite lamellae in this case ranged in width from 0.2-0.5 μm. A 'bulk' analysis of this grain by them, using an electron-probe microanalyser, gave a 3:5 stoichiometry, although separate results for the matrix and lamellae indicated that they were compositionally distinct, with the matrix being merenskyite of a 1:2 stoichiometry and the lamellae "most probably" being kotulskite of 1:1 stoichiometry. The significance of this and other studies to the existence or not of the author's $Pd_3(Te,Bi)_5$ phase is discussed later.

However, at Rustenburg mine no indication of such a lamellar exsolution relationship between kotulskite and merenskyite has so far been found. All the intergrowths between these two are considered to be replacement, except in the case illustrated in figure 8.8, where the smooth embayed boundary relationship and absence of penetrating veinlets could be interpreted as the result of

exsolution or simultaneous deposition.

As far as could be resolved by optical microscopy, the analyses for kotulskite and merenskyite presented here represent homogeneous areas or grains. Later analyses of these two minerals in other deposits by other workers supports this opinion by their agreement with the author's results. It is obviously imperative that careful microscopic examination should preceed any electron-probe microanalyser studies of these tellurides. The composition, X-ray data, and reflectance values for type merenskyite were obtained from the study of the two identical and homogeneous merenskyite areas illustrated in figure 8.8.

8.5.2 The Optical and Physical Properties

The Colour of merenskyite is white in air compared to kotulskite, which appears a pale yellow colour (fig. 8.8). Moncheite and merenskyite are not easily distinguished from each other unless in close proximity, when merenskyite can be seen to have a higher reflectivity and appears slightly more creamy. Its reflection pleochroism in air is weak from white to greyish white; in oil it is more distinct, from white with a slight creamy tint to light greyish white.

The Reflectance values of merenskyite in figures 8.8 and 8.7 were obtained by the same method as for kotulskite, and are presented in table 8.7, in which it has been assumed that merenskyite is optically positive. Although of different reflectance, the dispersion profiles of the two grains are identical. The small difference in reflectance may be caused by the compositional difference (e.g. Pd 23·1 wt.% for No. 1, and Pd 33·2 wt.% for No. 2) or merely a difference in the quality of the polished surfaces. In the case of

kotulskite the relationship between composition and reflectance is opposite to that for merenskyite.

Table 8.7 Spectral reflectance values for merenskyite from Rustenburg mine corresponding to analyses (1) and (2) in table 8.8.

No.	R_o				R_e'			
	470nm	546nm	589nm	650nm	470nm	546nm	589nm	650nm
1	61.8	64.3	65.7	65.9	62.2	65.2	67.0	67.4
2	60.9	63.2	64.4	64.3	61.4	64.4	66.0	66.6

The Anisotropy in air is distinct to strong, according to orientation, with dark brown to light greenish grey polarization colours.

The Hardness from its polishing relief is less than pentlandite, greater than chalcopyrite, and just greater than kotulskite, i.e. just greater than VHH_{15} 236. No microhardness values were obtained for merenskyite because of either the small size of the grains (fig. 8.8), or the complexity of its intergrowth with kotulskite (fig. 8.7). No other natural hardness data has been reported, although measurements by Hoffman and Maclean (1976) on synthetic merenskyite of composition $PdTe_{1.5}Bi_{0.5}$ gave VHN_{25} of 237 - 247.

8.5.3 The Composition of type merenskyite from Rustenburg mine was determined from an electron-probe microanalysis of the

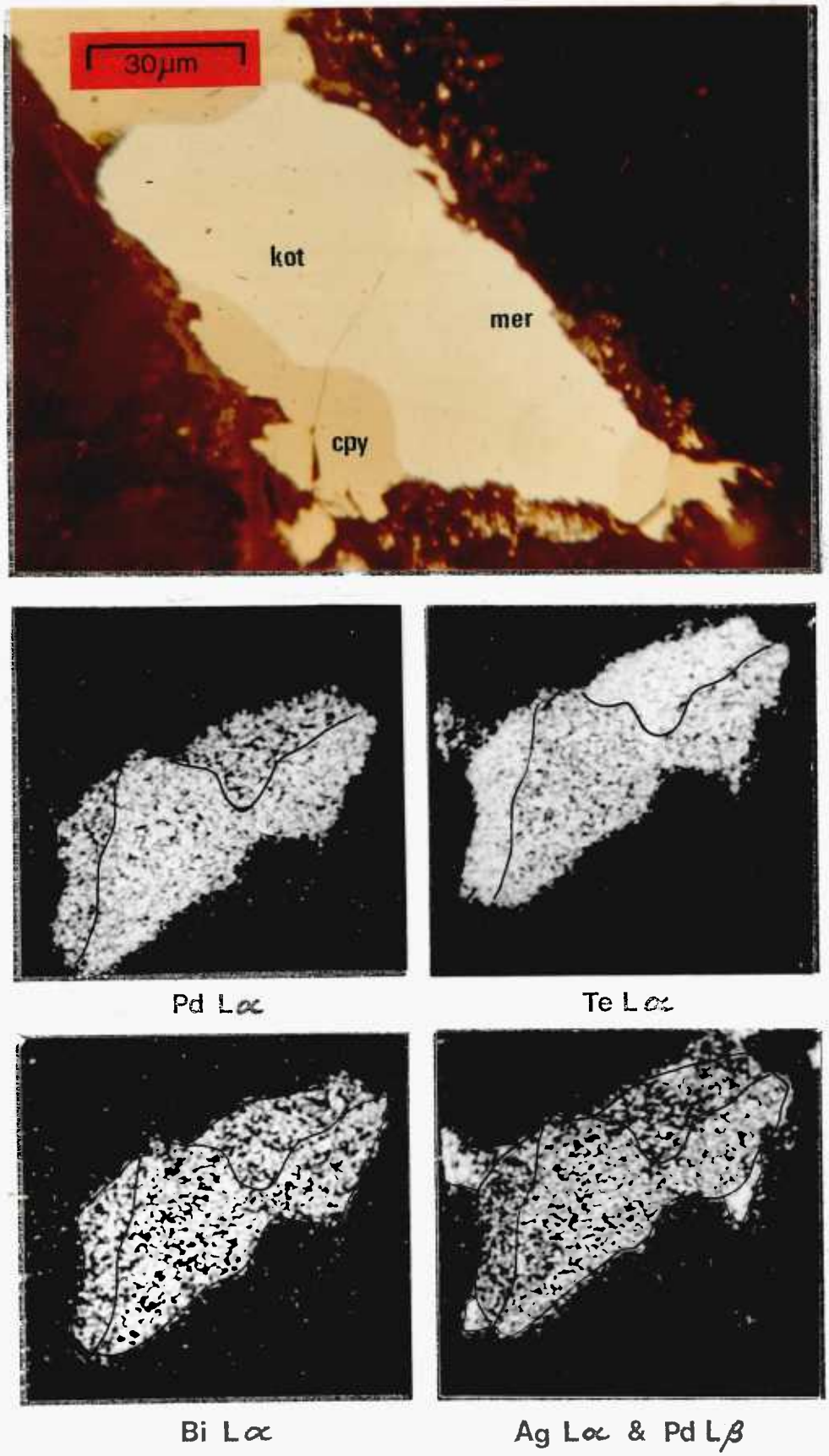

Fig. 8.8 Photomicrograph under plane polarised light, and X-ray scanning micrographs showing the distribution of Pd, Te, Bi and Ag in a composite grain of type merenskyite $Pd(Te,Bi)_2$ (mer) and kotulskite Pd(Te,Bi) (kot) intergrown with chalcopyrite (cpy) and a silver telluride (now largely volatilised) from Rustenburg mine.

Table 8.8 Electron-probe microanalyses of merenskyite from Rustenburg mine (Kingston, 1966) and the Sudbury District (Cabri and Laflamme, 1976), and merenskyite and palladian melonite from Werner Lake, Strathcona, and Falconbridge, Ontario (Rucklidge, 1969), and Temagami (Cabri et al. 1973).

	RUSTENBURG		SUDBURY DISTRICT				ONTARIO			TEM.
	(1)	(2)	(3)	(4)	(5)	(6)	(7)	(8)	(9)	(10)
Pd	23.1	33.2	26.3	18.3	27.2	12.7	18.3	7.4	2.1	29.2
Ni	----	----	0.5	6.1	0.16	0.19	5.9	11.3	17.1	----
Pt	1.8	----	----	----	----	18.8	0.37	3.7	1.5	----
Te	50.8	56.3	59.7	61.4	56.7	33.0	65.6	65.2	72.5	67.8
Bi	14.2	15.1	12.3	14.2	14.8	36.4	10.8	14.4	9.1	2.6
Sb	----	----	----	0.5	0.7	----	----	----	----	0.3

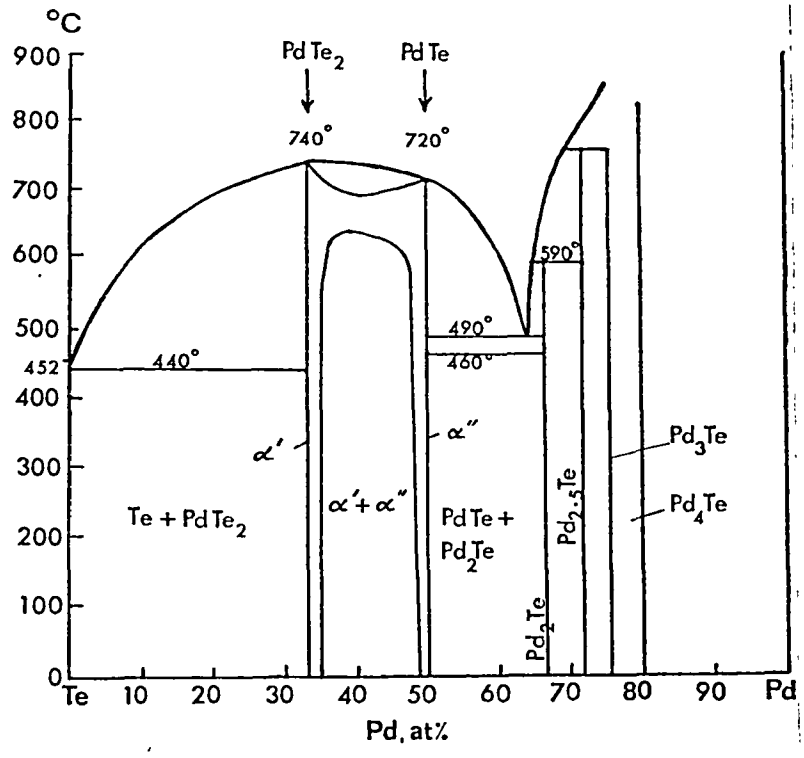

Fig. 8.9 Equilibrium diagram for Pd-Te alloys (after Medvedeva, Klochko, Kuznetsov, and Andreeva, 1961).

largest of the two homogeneous and inclusion free areas illustrated in figure 8.8, from which X-ray powder data were later obtained. Constant beam-current conditions were used, and the initial percentages were corrected for absorption, atomic number, and fluorescence as outlined in chapter 3.4.3. This analysis (table 10.8, anal.1) has a summation of 89·9 wt.% after correction, although before correction it was 93·4 wt.%. However, in this element combination the effect of the matrix corrections was found to be relatively small for all the elements and, although the corrections appear to have been of insufficient magnitude, it is considered that the atomic proportions are correct. Thus on the basis of this assumption, the analysis strongly suggests a (Pd,Pt):(Te,Bi) ratio of 1:2 with an empirical formula similar to $(Pd_{0.96}Pt_{0.04})(Te_{0.85}Bi_{0.15})_{2.06}$. Confirmation of a 1:2 stoichiometry for this type merenskyite was provided by the close agreement of the X-ray powder data for this phase (table 8.9) with that for artificial $PdTe_2$, as well as for moncheite. As with other tellurides in this study, only a minute quantity of powder could be obtained (see chpt. 3.4.2), and a 30-hour exposure was needed to obtain measurable lines.

A further electron-probe microanalysis (table 8.8, anal.2) of a phase optically identical to merenskyite, and intimately intergrown with kotulskite (fig. 8.7), suggested a 3:5 stoichiometry with an empirical formula of $Pd_3(Te_{0.86}Bi_{0.14})_{4.93}$. This was explained by the author in 1966 as being due <u>either</u> to an error produced by the inclusion of sub-outcropping (or outcropping) kotulskite in the irradiated zone of the analysis, as a result of the complexity of the replacement intergrowth, <u>or</u> that, on the basis

of an equilibrium diagram for Pd-Te alloys (fig. 8.9) produced by Medvedeva et al 1961, the $Pd_3(Te,Bi)_5$ phase consisted of merenskyite with PdTe or Pd(Te,Bi) in solid solution.

Medvedeva et al considered that in the $PdTe_2$ - PdTe region, in the range 640-690°C, the alloys formed a continuous series of solid solutions which break down below 640°C into a mixture of two solid solutions based on PdTe and $PdTe_2$. The existence of such a solid solution series at 660°C was also confirmed by Kjekshus and Pearson (1965) by the use of high-temperature X-ray powder diffraction. They also showed that at 500°C the two end-member phases PdTe and $PdTe_2$ had very limited ranges of solid solution, which may be designated as $Pd_{2-x}Te_2$, where x ranges from 0.04-0.23, and $Pd_{1-x}Te_2$, where x is from zero - 0.04. In the most recent study of this system, Hoffman and Maclean (1976) confirmed and refined these early findings, and concluded that a complete solid solution exists between $PdTe_2$ (synthetic merenskyite) and PdTe (synthetic kotulskite) from $575^{o\pm}$ 10° to $710^{o\pm}$ 10° C, and that with rising temperature synthetic merenskyite retreats towards $PdTe_2$, which melts congruently at $740^{o\pm}$ 3° C.

Since 1966 the problem of the existence of a variety of merenskyite with a 3:5 stoichiometry has been considered by other workers. From their work and the author's, five mineralogical alternatives have arisen which can give rise to a (Pd,Pt)(Te,Bi) ratio of 3:5. These are:

1. A fine and optically submicroscopic lamellar 'exsolution' intergrowth of kotulskite and merenskyite, as demonstrated by Cabri and Pickwick (1974).

2. A complex replacement intergrowth of merenskyite and kotulskite, such that electron-probe irradiation of underlying kotulskite beneath a homogeneous veneer of merenskyite is unavoidable.

3. A solid solution of merenskyite and PdTe, the existence of which has been demonstrated with regard to the synthetic Pd-Te system.

4. A distinct mineral species with closely similar optical properties to merenskyite.

5. A distinct mineral species with different properties from merenskyite. A possible example is the pinkish weakly anisotropic $(Pd_{0.74}Pt_{0.26})_3(Te_{5.01}$ with 0·1% Bi of Mihalik et al (1974). In this case the lack of bismuth and consequently higher tellurium content of 63·3 wt.% could be considered responsible for the difference in colour and anisotropy from the 3:5 stoichiometric 'merenskyite' at Rustenburg. However, lack of X-ray powder data in both cases prevents further comparison.

The existence of a Pd_3Te_5 phase with variable amounts of Pt and Bi substitution is therefore uncertain, and alternatives 1-4 could apply to the Rustenburg example. A scanning-electron microscopic examination of the analysed merenskyite area shown in figure 8.7 is required to determine whether fine submicroscopic inclusions of kotulskite are present. The high summation of the analysis of 104·6 % could be due to this, combined with 'beam wandering' during analysis. The presence of exsolution lamellae would overcome the difficulty of postulating the existence of a homogeneous mixed crystal at normal temperatures which exceeded the

limit imposed by Kjekshus and Pearson, and Hoffman and Maclean.

The existence of a solid solution can be used to explain the reason for the two different intergrowth types illustrated by figures 8.7 abd 8.8. The smooth embayed boundary relationship could be interpreted as the result of the complete unmixing of a kotulskite-merenskyite solid solution whereas unstable easily replaceable $Pd_3(Te,Bi)_5$ mixed crystals would be more susceptible to later palladium metasomatism and conversion to kotulskite. Moncheite is in contrast unreplaced by other PGM.

Only a limited solid solution appears to exist between moncheite and merenskyite, as shown by the platinum contents in table 8.8. However, Rucklidge (1969) provides evidence for extensive substitution of Pd by Ni in merenskyite, and suggests an almost complete solid solution series with melonite $NiTe_2$ on the basis of analyses of three intermediate members from Ontario (table 8.8, analyses 7,8, & 9). These gave Ni contents of 5·9, 11·3, and 17·1 wt. percent, with a corresponding depletion in Pd giving contents of 18·3, 7·4, and 2·1 wt. percent. He introduced the terminology for these intermediate members of nickeloan merenskyite (analysis 7), and palladian bismuthian melonite (analyses 8 & 9). Similarly platinian merenskyite could be used for analysis 1. Cabri and Laflamme (1976) helped confirm this solid solution series with a further nine analyses of palladian melonite from Sudbury. These exhibited a compositional range of Ni 9·4-17·1, Pd 12·7-2·1, Pt 0·0-3·7, Te 73·0-62·4, Bi 5·6-16·5, and Sb 0·55-1·04 weight percent. They also introduced a similar terminology based on merenskyite being $PdTe_2$. On this basis all merenskyite occurrences so far analysed

are bismuthian, and according to whether Pt or Ni is the second most important cation then it will be platinian bismuthian merenskyite or nickeloan bismuthian merenskyite. This is considered an unnecessary complication, since all merenskyites so far reported are 'bismuthian' and all except one have Bi contents lying within the small range of Bi 10·8 - 15·1 wt.%. This suggests that bismuth is an essential constituent of merenskyite. Similarly Bi contents appear to be essential to palladian melonites. Analysis 6 in table 8.8, of "platinian bismuthian merenskyite" by Cabri and Laflamme, despite the similarity of the X-ray powder data to that for synthetic $PdTe_2$ is possibly a distinct species lying between merenskyite and a hypothetical hexagonal $PtBi_2$.

Finally with regard to composition, Cabri and Laflamme demonstrated that a partial solid solution probably occurs between michenerite (cubic PdBiTe) and merenskyite, with which it is commonly associated in the Sudbury ores. This was confirmed by Hoffman and Maclean (1976).

8.5.4 X-Ray Powder Data presented in table 8.9 is still the only available data for natural merenskyite, although Cabri and Laflamme provide cell dimensions for a "platinian bismuthian merenskyite" (table 8.10, no.2). The crystal structure of the synthetic equivalent of merenskyite was shown by Thomassen (1929) to have a hexagonal sheet-like $Cd(OH)_2$ structure. This together with its excellent 0001 cleavage accounts for its characteristic laminar replacement by kotulskite.

Variations in the cell dimensions with composition are illustrated in table 8.10, in which an increase along the c-axis

Table 8.9 X-ray powder data for merenskyite from Rustenburg mine (Cu radiation, Ni filter and 11.483 cm diameter camera), and for artificial $PdTe_2$ (Thomassen, 1929).

	Merenskyite			Artificial $PdTe_2$		
Hex. Cells	a_o 3·978 ± 0·001 c_o 5·125 ± 0·002			a_o 4·028 ± 0·003 c_o 5·118 ± 0·004		
hkil	d calc.	d obs.	I obs.	hkil	d obs.	I obs.
---	---	3·07	30	---	---	---
$10\bar{1}1$*	2·921	2·92	100	$10\bar{1}1$	2·89	60
---	---	---	--	---	---	--
---	---	2·51	20	0002	2·56	20
$10\bar{1}2$*	2·088	2·10	60	$10\bar{1}2$	2·07	60
---	---	---	--	---	---	--
$11\bar{2}0$*	2·015	2·02	30	$11\bar{2}0$	2·02	40
---	---	---	--	---	---	--
---	---	---	--	---	---	--
0003*	1·726	1·73	20	0003	1·71	20
---	---	---	--	---	---	--
---	---	1·67	30	$20\bar{2}1$	1·65	30
---	---	1·61	20	$11\bar{2}2$	1·59	20
$10\bar{1}3$*	1·543	1·54	30	$10\bar{1}3$	1·54	70
---	---	1·46	10	$20\bar{2}2$	1·44	50
---	---	---	--	---	---	--
---	---	1·39	10	$11\bar{2}3$	1·30	20
0004*	1·288	1·29	10	0004	1·28	80

* see footnote to table 8.3.

Table 8.10 Cell dimensions of merenskyite from Rustenburg mine (1) (Kingston, 1966) compared to platinian merenskyite from Sudbury (2) (Cabri and Laflamme, 1976), synthetic merenskyite of varying bismuth content (3)-(7)(Hoffman and Maclean, 1976), melonite (8) (Strunz, 1970), and palladian melonite (9) (Cabri and Laflamme, 1976). Composition is expressed as atomic proportions.

Loc.	Pd	Pt	Ni	Te	Bi	Sb	a(A)	c(A)
1	0.96	0.04	----	1.75	0.31	----	3.978(1)*	5.125(2)
2	0.55	0.44	0.01	1.19	0.80	----	4.036	5.132
3	1.0	----	----	2.0	----	----	4.042(5)	5.124(8)
4	1.0	----	----	1.8	0.20	----	4.040(4)	5.169(4)
5	1.0	----	----	1.7	0.30	----	4.050(6)	5.186(6)
6	1.0	----	----	1.6	0.40	----	4.045(3)	5.205(3)
7	1.0	----	----	1.5	0.50	----	4.049(4)	5.231(4)
8	----	----	1.00	2.00	----	----	3.84	5.26
9	0.33	----	0.67	1.71	0.26	0.03	3.905(4)	5.248(4)

* number in parenthesis gives standard deviation expressed in units of the last decimal place.

with increasing Bi content is clearly demonstrated by Hoffman and Maclean. Substitution of Ni for Pd appears to decrease that a_o of merenskyite although this may be offset by the substitution of Pt.

8.6 Mineral A (Pd,Hg)(Te,Bi)

8.6.1 The Occurrence and Properties. This phase has so far only been located in the area shown in figure 8.2 as four blebs, ranging from 2 to 5 μm in diameter, intergrown at the margins of merenskyite grains associated with chalcopyrite. Its colour in air is light grey compared to merenskyite, but under oil immersion it becomes slightly darker with a brownish tint. Its reflectance values at the four standard wavelengths are R_{470nm} 48·8%, R_{546nm} 53·3% R_{589nm} 55·6%, R_{650nm} 53·9%. It appears to be isotropic, although any weak anisotropy under crossed nicols could not be distinguished with certainty on such small grains enclosed by strongly anisotropic merenskyite. Its hardness from its polishing relief was softer than merenskyite and chalcopyrite.

8.6.2 The Composition was determined by electron-probe microanalysis of the largest (5 μm) grain. Because of this small size, a certain proportion of the underlying and enclosing merenskyite may have been irradiated as well. Consequently the analysis could be considered to be only semiquantitative. The analysis after full matrix corrections gave Pd 27·8, Hg 12·0, Te 38·5, Bi 1·6 wt. percent. This suggests a (Pd,Hg):(Te,Bi) ratio of 1:1, and an empirical formula of $(Pd_{0.81}Hg_{0.19})(Te_{0.97}Bi_{0.03})$.

Since this was reported by the author in 1966, Cabri et al (1973) have described a new mineral from Ontario, temagamite Pd_3HgTe_3, of composition within the ranges of Pd 34·6 - 35·1,

Hg 21·5 - 22·6, Te 41·6 - 42·3, Bi 0·0 - 0·5, Sb 0·0 - 0·3 weight percent. This mineral is described as white with a grey tinge in air and oil, weakly anisotropic with a measured bireflectance on one grain of R_{470nm} 52.8 - 51.8, R_{546nm} 53.9 - 52.9, R_{589nm} 55.0 - 54.2, R_{650} 57.7 - 57.1, and a micro-indentation hardness value from one identation of VHN_{25} 92. Temagamite was usually closely associated with merenskyite, hessite, and stuetzite inclusions in chalcopyrite. An orthorhombic symmetry was proposed with cell dimensions of a 11.57, b 12.16, c 6.76, $\pm$ 0.001 A.

It is probable that temagamite is the same mineral as mineral A from Rustenburg.

8.7 Michenerite - cubic PdBiTe.

The presence of michenerite in the Merensky Reef has only recently been brought to the attention of the author by Vermaak and Hendriks (1976). However, although they record its distribution in the ore, they give no confirmatory analytical evidence of its existence there in the first place. Even qualitative observations have been omitted. Since michenerite is nearly identical in colour and reflectance and similar in composition to kotulskite, a quantitative electron-probe microanalysis, or X-ray diffraction with a qualitative analysis, would be needed to distinguish it. The fact that michenerite is isotropic is no certain guide, since basal sections of kotulskite are also isotropic. It may be that an assumption was made by Vermaak and Hendriks that all isotropic grains looking like kotulskite were michenerite.

At the time of the author's publication on the bismuthotellurides in the Merensky Reef, data for michenerite was

incorrect and conflicting, and it was not until 1973 that Cabri et al., and Childs and Hall, fully redefined it. Prior to this, therefore, any isotropic grains similar to kotulskite were merely considered to be basal sections. Later reports of the common occurrence of michenerite with merenskyite in other deposits made the author aware of its possible occurrence in the Merensky Reef, although this has not yet been investigated at Rustenburg or Union mines. However, until quantitative evidence is provided, its reported occurrence cannot be fully accepted, especially as it would constitute the first recorded occurrence for this deposit.

CHAPTER 9

GENERAL DISCUSSION

9.1 Geochemical Considerations

9.1.1 Introduction

Since the discovery of platiniferous deposits in the Bushveld numerous reviews of the PGE geochemistry have been published. Some of the more notable ones are by Vogt (1927), Rankama and Sahama (1950), Goldschmidt (1954), Wright and Fleischer (1965), Yushko-Zakharova and Ivanov (1967), Mertie (1969), and Crocket (1969). These publications, together with recent ore genesis type reviews (Naldrett and Cabri, 1976) and 'thoughts' (Stumpfl, 1974; Stumpfl and Tarkian, 1976; Cabri, 1974; Cousins and Vermaak, 1976), and various specific geochemical papers, add up to a considerable sum of knowledge and opinion on PGE geochemistry.

Over the last decade it has become increasingly evident that, although previously considered to form a geochemically coherent group, fractionation amongst the PGE does take place during endogenic and exogenic processes, and that the PGM are not the inert substances once generally envisaged but may undergoe dissolution and differential leaching, redeposition, and recrystallisation, even in the exogenic environment. Thus the PGM will not only be restricted to primary orthomagmatic deposition from a basic magma but may also be formed by pneumatolytic, hydrothermal, metamorphic, and supergene processes. This behaviour has been particularly stressed by Stumpfl (1974), and Stumpfl and Tarkian (1976).

A further advance is in our understanding of the parti-

tioning of the PGE between the various rock forming silicates and oxides as well as the closely associated ore sulphides. Studies of the PGE content of chromite, and the primary sulphides pyrrhotite, pentlandite, and chalcopyrite has attracted particular attention (Gijbels et al, 1973; Keays and Crocket, 1970; Chyi and Crocket, 1976; Crocket et al, 1976; and others). These studies involving neutron activation analysis show that at least some incorporation and partitioning of the PGE in these lattices occurs, and that discrete PGM cannot always be used to account for all the PGE content of a rock or mineral concentrate.

The origins of these important geochemical concepts about the PGE are not as recent as many publications give the impression. Fifty years ago fractionation of the PGE was reported by Wagner (1929, p.110) with regard to the supergene oxidation of the Merensky Reef when he recorded that "palladium was clearly more susceptible to leaching by oxygenated surface waters" than platinum since the Pt:Pd ratio in the oxidised ore was 7 - 10% higher than in the unoxidised ore. It is also clear from the observations and conclusions on the various genetic types of platinum deposits studied by Wagner in the Bushveld Complex that he, and also Schneiderhohn, realised the importance of pneumatolytic and hydrothermal processes in PGM deposition.

With regard to trace element work, Schneiderhohn's excellent spectrographic study (1929) is generally overlooked because he did not see or perhaps recognise any of the discrete PGM associated with the base-metal sulphides he was analysing. However, when considering his painstaking method of extraction under the

microscope it is likely that his samples were just as uncontaminated with platinum minerals than present day samples concentrated by initial crushing of the rock followed by heavy liquid or/and dry electromagnetic-density separation, with final 'purification' by acid leaching and microscopic monitoring. Even had he found discrete PGM in his ore samples his conclusion from his data still must have been that the PGE occur at least in part in the lattices of the base-metal sulphides. It is important to remember that, although he concluded that before oxidation of the ore the PGE occurred completely in solid solution in the base-metal sulphides, it was known and reported by others (Cooper, 1928; Adam, 1929; Wagner, 1929;) that discrete PGM occur in the Merensky Reef as well as other genetic ore types in the Bushveld. It is strange, therefore, that in many of the later reviews and papers so much was made of disproving Schneiderhohn's conclusion. That a large quantity of the PGE content in these Bushveld deposits is accounted for by the existence of distinct PGM has never been in doubt by those exploiting the deposits since mining of them began. They would have been amused to have been told that their grey very heavy concentrates which they were so carefully packaging for the refinery were not platinum minerals. The only controversy to be inspired by Schneiderhohn's work should have been on the extent and the physico-chemical nature of the incorporation of PGE in various mineral lattices. The latter aspect still being a relatively unknown quantity, although the application of the crystal field theory may elucidate the substitution problems involved.

Even in connection with the paragenesis of the Merensky

Reef ore minerals it is the author's opinion that Schneiderhohn's conception was basically sound, and his sequence of events of (1) liquid magmatic deposition, (2) pneumatolytic deposition, (3) hydrothermal deposition, and finally (4) exogenic oxidation can be used as a framework within which details such as chromite and sulphide formation in relation to T^{o},P,fO_2,fS_2, and FeO content of the magma, and sulphide-oxide/silicate immiscibility, postcumulus growth and trace element redistribution etc. are fitted.

Thus at least from the time of the discovery and exploration of the Merensky Reef and other PGE deposits in the Bushveld it was recognised particularly that: (1) fractionation of the PGE could occur during geological processes, (2) PGE mineralisation could be produced from orthomagmatic, pneumatolytic, hydrothermal, and supergene processes, (3) PGE could occur in the lattice of base-metal sulphides but predominantly occured as discrete platinum minerals in ores of the Merensky Reef type. It is interesting that it took nearly 40 years before the conclusions of these pioneers were reincarnated, and before reliable geochemical data became available to confirm and greatly elaborate upon their findings. The following considerations aim to incorporate aspects of ore mineral paragenesis and ore genesis of the Merensky Reef at Rustenburg and Union mines within a broad geochemical context of PGE partitioning at the various stages of the geochemical cycle.

9.1.2 Primordial Fractionation

The platinum metals (table 9.1) are transition elements of the second and third transition series, a transition element being defined as one which has a partly filled d or f shell. This

Table 9.1 Some Physical characteristics of the platinum metals.

Properties		Ru	Rh	Pd	Os	Ir	Pt
Atomic no.		44	45	46	76	77	78
Atomic wt.[1]		101.07	102.905	106.4	190.2	192.2	195.09
Density.[5]		12.45	12.41	12.02	22.61	22.65	21.45
Crystal typ.		H.C.P	F.C.C	F.C.C	H.C.P	F.C.C	F.C.C
Space grp.		C6/mmc	Fm3m	Fm3m	C6/mmc	Fm3m	Fm3m
Atomic rad.[1] in angstroms		1.33	1.34	1.37	1.35	1.35	1.38
Ionic radius							
VAL.	C.N						
1 +	---	n.d.f.	unstable[4]	unstable[4]	unstable[4]	unstable[4]	unstable[4]
2 +	4	stable[4]	unstable[4]	0.80[2,6]	n.d.f.	unstable[4]	0.80[2,6]
3 +	6	stable[4]	0.68-0.75[2] [6]	n.d.f.	stable[4]	stable[4]	unstable[4]
4 +	6	0.63(3) 0.62(6) 0.67(2)	0.68(2) 0.65(6)	0.65(2) 0.64(6)	0.65[3] [6]	0.65(6) 0.64(3) 0.68(2)	0.65 (2) 0.64(6)
6 +	(6)	stable[4]	unstable[4]	unstable[4]	0.69(2)	stable[4]	unstable[4]
7 +	?	stable[4]	n.d.f.	n.d.f.	unstable[4]	n.d.f.	n.d.f.
8 +	?	stable[4]	n.d.f.	n.d.f.	stable[4]	n.d.f.	n.d.f.
Electron[4] Structure.							
	K	2	2	2	2	2	2
	L	8	8	8	8	8	8
	M	18	18	18	18	18	18
	N	8-7	8-8	8-10	32	32	32
	O	1	1	-	8-6	8-9	8-9
	P	-	-	-	2	0	1

Table 9.1 contd.

Ionization Potential in e.v.(7)	Ru	Rh	Pd	Os	Ir	Pt
1 +	7.364	7.461	8.334	8.732	9.1	8.962
2 +	16.758	18.072	19.423	(17)	(18)**	18.558
3 +	28.459	31.049	32.921	(28)**	(28)**	(29)
4 +	(47)	(46)	(49)	(42)**	(39)*	(41)
5 +	(63)	(67)	(66)	(54)*	(57)*	(55)
6 +	(85)**	(105)**	(90)**	(70)**	(77)**	(70)**
7 +	(115)**	--	--	--	--	--
Electrode Potential(4)	**Ru**	**Rh**	**Pd**	**Os**	**Ir**	**Pt**
$M \rightarrow M^2$	-0.45	-0.6	-0.64	-0.7	-1.0	-0.73
$M^2 \rightarrow M^3$	-0.3	-0.9	n.d.f.	-0.3	-1.0	n.d.f.
$M^3 \rightarrow M^4$	-1.3	-1.4	-1.29	n.d.f.	(-1.2)	-0.72
$M^4 \rightarrow M^6$	-1.7	-1.4	n.d.f.	-0.85	-1.4	n,d,f.
$M^6 \rightarrow M^7$	-1.6	n.d.f.	n.d.f.	n.d.f.	n.d.f.	n.d.f.
$M^7 \rightarrow M^8$	-1.0	n.d.f.	n.d.f.	-1.0	n.d.f.	n.d.f.
Electro- negativity (7)	(a) 2.05 (b) 1.42	2.1 1.45	2.0 1.35	(2.1) 1.52	2.1 1.55	2.1 1.44

References and notes

(1) Strunz (1970). (2) Ahrens, (1952) in Strunz (1970).(3) Pauling (1927), in Strunz(1970). (4) Latimer & Hildebrand, 1951. (5) Mertie (1969). (6) Razin & Khomenko (1969). (7) Ahrens (1964)

(a) Pauling et al (1951) in Ahrens (b) Little and Jones (1960), in Ahrens.

VAL - Valency. CN - Coordination number.

n.d.f. - no data found.

H.C.P. is 'hexagonal close packed'; F.C.P. is 'face centred cubic'.

* - corrected from Razin & Khomenko by author.

** - extrapolated by author.

Ionization potentials in parentheses are uncertain according to Ahrens (1964).

includes also those elements which have partially filled d or f shells in any one of their commonly occurring oxidation states. As a result of the Lanthanide contraction the PGE atomic radii, and the ionic radii are closely similar. This similarity also extends to other characteristics like ionization potential, electrode potential, electronegativity, anion affinity, and heats of formation of the oxides. They, therefore, form a geochemically coherent group in that they are invariably found together. However, as illustrated in table 9.1, the atomic properties are sufficiently different to give rise to detectable fractionation during natural and artifical chemical and physical processes.

The first natural evidence of their ability to fractionate comes from meteorite data. This data shows that the PGE are strongly siderophile, with average contents for the individual metals ranging from 0.1-2.0 ppm in chondrites and 1-10 ppm in irons (Crocket 1969). Their siderphilic character is further emphasised by their distribution within ordinary chondrites where their concentrations in the metallic phase are roughly 1000 times that in the silicates (Crocket, 1972). Goldschmidt's (1954) and Wright and Fleischer's (1965) data for chondrites indicates that in the coexisting troilite and metallic phases Pd especially and also Ru and Os are equally distributed between them, whereas Pt,Ir,and Rh are preferentially enriched in the metallic nickel-iron phase. The chalcophile character of Pd was also reported by Crocket (1972) who demonstrated a strong positive correlation with As and Sb. Goldberg et al (1951) noted that in individual iron meteorites the platinum and palladium content appeared to increase with increasing nickel, whereas

ruthenium decreases. Crocket (1972) also confirms a strong positive correlation of Pd with Ni as well as with Cu and Au, although a poor correlation with the other noble metals. He, however, considered that Pt decreases with increasing nickel, and that it correlates strongly with Ru but only weakly with the others.

These fractionation trends indicated in meteorites are broadly reflected in some aspects of the ore-mineral paragenesis of the Merensky Reef. Thus the late stage Pd-Ni metasomatism of cooperite to form braggite, and the replacement of 'platinum' merenskyite by 'palladium' kotulskite as reported in this thesis are evidence for the fractionation of palladium, particularly from platinum, and its close association with nickel. The strong positive correlation of Ir,Os,Ru, and Pt shown by Crocket (1972) and their probable positive correlation with Rh expresses itself in the composition of laurite, and its notable defficiency in palladium.

9.1.3 Magmatic Fractionation

Since basic and ultrabasic rocks, in particular chromitites, dunites, peridotites, pyroxenites, and serpentinites, are the source of economic amounts of PGE, it is clear that the first fractionation trend is for the PGE as a whole to be concentrated in the early stages of magmatic differentiation. Also being very weakly lithophilic the PGE will rarely enter the silicate lattices, especially if there are sulphide phases present. Because of this lack of affinity for the silicate lattices the PGE may be carried through the differentiation process and become concentrated and transported in hydrothermal derivatives. Hydrothermal transportation of PGE was first recognised in the Waterberg District (Wagner, 1929), and since

then there has been an increasing awareness and acceptance of the importance of this mechanism for PGE mineralisation. The awareness has been particularly promoted by Stumpfl (1961,1974,1976) who has championed the 'hydrothermal platinum' cause for many years. Recent studies by Mihalik et al (1974) on the Messina copper deposit in S.Africa, and McCallum et al (1976) on the New Rambler Mine, Wyoming, have particularly reinforced his contentions. These hydrothermal deposits are characterised by the PGE being largely in the form of tellurides and bismuthotellurides; minerals which are also the last to have formed in the Merensky Reef from a residual volatile-rich phase after the formation of the main bulk of the sulphides (Kingston, 1966). Mobilisation of PGE during serpentinisation is also proving to be an important PGM-formation and redistribution process (Rucklidge,1971; Razin, 1971).

The importance of post-intrusive crystallisation differentiation as opposed to pre-intrusive magma fractionation in the concentration of PGE can be demonstrated by comparing the concentration factors for platinum and palladium necessary firstly to produce their average abundance values in the Bushveld mafic zone rocks, and secondly to produce the ore grade values in the Merensky Reef. From the abundance data for the Mafic Zone rocks by Hagen (1954) a useful average abundance figure for Pt of 0.04 ppm and for Pd of 0.037 ppm can be taken as representing the probable content of the Mafic Zone magma. This gives a WA(Pd) ratio (Cousins and Vermaak, 1976, p.292) of 0.48 which compares with a WA(pd) ratio of 0.50 for the chilled marginal gabbro of the Skaergaard intrusion (Wright and Fleischer, 1965). Hagen's figures are given below. Values for

silicic rocks are not included since these are not considered to be differentiates of the mafic zone magma.

	Pt	Pd	
Bushveld Gabbros	0.021	0.031	ppm
Bushveld Norites	0.038	0.051	
Bushveld Peridotite	0.017	0.012	
Bushveld pyroxenite	0.048	0.059	
Bushveld anorthosite	0.075	0.032	
Average value	0.040	0.037	ppm

Values of crustal abundance for Pt and Pd are taken as 0.005 and 0.015 ppm respectively, for Ir,Os,Rh, and Ru a maximum of 0.001 ppm, and for Au 0.004 ppm (Wright and Fleischer, 1965). The average grade of the Merensky Reef is taken as 10 ppm, corresponding to individual metal values as in table 9.2.

Table 9.2 Platinum metal grade values for the Merensky Reef at Rustenburg(1) and Union(2) mines, together with the corresponding concentration factors(A) relative to crustal abundance figures and (B) relative to concentration in the original magma.

PGE	Grade in ppm		Concentration Factors			
	(1)	(2)	(1) A	(1) B	(2) A	(2) B
Pt	5.8	6.6	1160	145	1320	165
Pd	2.7	2.8	180	73	187	76
Ir	0.07	0.01	70	388	10	55
Os	0.06	0.005	60	375	5	31
Ru	0.6	0.3	600	545	300	272
Rh	0.3	0.3	300	n,d	300	n.d
Au	0.4	0.2	100	n.d	50	n.d

n.d. - No data.

It is evident from these figures that the processes of magma formation are less important than magma crystallisation in the formation of a deposit like the Merensky Reef, since the magma concentration factors for Pt and Pd are 8 and 2.5 respectively compared with a crystallisation concentration factor of Pt 145 and 165, and Pd 73 and 76 for Rustenburg and Union mines respectively. However, of special interest is the preferential concentration of platinum in the Merensky Reef relative to palladium. In terms of WA ratios this enrichment in platinum can be alternatively expressed as WA(Pd)0.32 and 0.30 for Rustenburg and Union mines respectively, compared to WA(Pd) 0.48 for the original magma. This platinum enrichment in the iron-rich Merensky Reef pyroxenite clearly reflects its strong siderophilic character, whereas the weaker affinity of palladium for this environment reflects its equally strong siderophile and chalcophile character. It also follows from the above reasoning that if one considers the Merensky Unit as a single differentiation unit, then the hanging wall anorthositic rocks must be impoverished in platinum relative to palladium. Thus the differentiation trend for the unit is one of palladium enrichment or fractionation upwards. This relative enrichment or persistence of palladium towards the acid pole of a differentiating basaltic magma is known from other studies, notably Crocket and Skippen (1966). They suggested that during freezing of basaltic magma the palladium was probably rejected from common silicates, and thereby enriched in residual liquids due to the highly covalent character and the square planar orientation of its bonds.

Cousins and Vermaak (1976) have demonstrated that by

arranging the various platiniferous deposits of the Bushveld into a 'stratigraphic order' their WA(Pd) ratios show an upward decrease. Thus in successively later formed and increasingly iron rich platiniferous deposits the Pt : Pd ratio increases. From this they concluded that although fractionation towards an acid pole favours palladium enrichment, which they called the Sudbury trend, any tendency towards iron enrichment highlights the siderophile nature of platinum and favours platinum enrichment relative to palladium. Thus in the case of the Merensky Unit of differentiation they considered that the basal Merensky Reef pyroxenite and sulphides provided the necessary iron-rich environment for platinum to respond to its siderophile nature and become relatively enriched against palladium, whereas palladium responded to differentiation of the unit towards an acid pole by being relatively enriched upwards in the hanging wall anorthositic rocks. Fractional crystallisation of the interstitial sulphides in the Merensky Reef would similarly lead to progressive enrichment of palladium in the increasingly more copper-rich and acid residual liquid fractions. This "Sudbury trend" of palladium enrichment is mineralogically evident in the Merensky Reef as a progressive paragenetic increase in the importance of palladium in the composition of the platinum group minerals, as well as in the base-metal sulphides as a trace constituent. Thus within a slightly oversimplified framework of base-metal sulphide paragenesis of pyrite, pyrrhotite, pentlandite, and finally chalcopyrite, the earliest platinum group minerals at Rustenburg mine are palladium deficient graphic Pt-Fe alloy and cooperite, followed by 'palladium rich' braggite resulting largely from Pd and Ni metasomatism, and finally

palladium rich bismuthotellurides associated with chalcopyrite and which exhibit further evidence of palladium enrichment in the replacement of merenskyite by kotulskite.

This fractionation of palladium from platinum in the ore is further supported by Vermaak and Hendriks (1976) who have shown that pyrrhotite contains the bulk of the submicroscopic "invisible" platinum and no palladium, whereas pentlandite contains the bulk of the "invisible" palladium and very little platinum. After using the analysed Bi and Te content of chalcopyrite to account for nearly all the detectable PGE content, they concluded that chalcopyrite contained little or no "invisible" platinum, palladium or ruthenium. Crocket et al (1976) adds further support to the correlation of Pd with pentlandite and nickel at Western Platinum mine by showing that pentlandite rich sulphide aggregates were characterised by above average Pd contents. These results correlate broadly with the observed main location of the various platinum group minerals described in this thesis. Thus cooperite and graphic Pt-Fe alloy are the main PGM to be found in pyrrhotite, and braggite is the main one to be found partly or completely enclosed by pentlandite, and clearly pre-dating chalcopyrite which veins it. The lack of "invisible" PGE in chalcopyrite correlates with the paragentic observation that the bulk of the PGM in the Merensky Reef crystallised before chalcopyrite and therefore left little over, especially after PGE combination with Bi,Te, and Sb, to be incorporated in the lattice of chalcopyrite.

Fractionation of Ru,Rh,Os, and Ir in the course of the formation of the Merensky Reef is more difficult to define, because

of a general lack of analytical data for these elements arising from their very low concentration in the ore, the ore minerals, and the enclosing silicates and oxides. For the original magma Gijbels et al (1974) quote estimates of Ir 0.18 ppb, Os 0.16 ppb, and Ru 1.1 ppb. Table 9.2 indicates their low content in the ore, and their concentration factors. Gijbels et al analysed separates of orthopyroxene, plagioclase, and chromite from the eastern Bushveld and concluded that Ru,Os, and Ir were progressively depleted in the magma as differentiation proceeded, and that the ratio of any one of these elements between the separates was 1 : 16 : 700. They also reported a tendency for the orthopyroxenes to be enriched in Ru relative to Os and Ir. Greenland (1971) showed that Ir decreased systematically upwards through the Great Lake dolerite sheet, in Tasmania, from the mafic dolerite (0.25 ppb) to the granophyre (0.006 ppb), its differentiation trend closely paralleling that of chromium. He considered that the substitution of Ir^{4+} for Cr^{3+} in chromite accounts for this correlation, although Gijbels et al (1976) found a tendency for Ir to be impoverished relative to Os and Ru in their chromite concentrates, and Crocket et al (1976) considered Ir to show a stronger relative enrichment in the sulphides of the Merensky Reef at Western Platinum mine than Pd; their order of enrichment being Ir > Pd > Au > Pt.

In the Merensky Reef at Rustenburg and Union mines the higher concentration factors (A & B in table 9.2) of Ru compared to Ir and Os suggests some fractionation. Some separation of Ru from Os and Ir can also be inferred from the common occurrence of Os and Ir with platinum in Ru defficient platinum-iron alloy and sperrylite.

The fact that there is insufficient laurite to account for much of the Ru at Rustenburg mine suggests a possible tendency for Ru to occur in the lattices of the base metal sulphides. This, together with the findings of Crocket et al that Ir is also relatively enriched and homogeneously distributed in the base-metal sulphides and, the common substitution of Ir and Os for Ru in laurite, points to the overall geochemical coherency of these three in the Merensky Reef. Finally the absence of any rhodium minerals to account for the relatively high Rh content at both mines could be explained by accepting the conclusions of Grimaldi and Schnepfe (1969) that, as in the case of chromite in the Stillwater Complex, the rhodium occurs almost entirely within the chromite lattice. However, data on the content of "invisible" Pt,Pd, and Rh in the base metal sulphides of the Merensky Reef by Vermaak & Hendriks (1976) can be used to contradict this. They found equal amounts of Rh in pyrite, pyrrhotite, and pentlandite, with none in chalcopyrite.

The presence of the platinoid bismuthotellurides is of interest as regards the geochemical behaviour of tellurium during the fractional crystallization of the sulphides. Their occurrence is in agreement with investigations by Sindeeva (1959) and others who have demonstrated that tellurium, although a close analogue of sulphur and selenium, tends to form independent minerals even when present in very low concentrations rather than to form solid solutions in the base metal sulphides. This is explained as a result of the quite different atomic size and electronegativity of tellurium compared to sulphur. Selenium readily substitutes for sulphur, as shown by Zaryan (1962) and others, and where the concentration of

selenium is low, independent selenium minerals will be unlikely to form. In the Merensky Reef no selenides have yet been found, although traces of selenium are probably present in the sulphides. Platinoid selenides were first reported from the Urals in the copper-nickel sulphide ores of the Norilsk region by Zainullin and Pashinkin (1960), but compared with the platinoid tellurides they were rare even though there was more selenium than tellurium present in the ore. The results of microscopic and chemical investigations of the distribution of tellurium in ores related to basic and ultrabasic intrusives by Zainullin (1960), Pshenichnii (1961), Zaryan (1962), and others, show that tellurium is concentrated in the later stages of crystallization and in particular in the chalcopyrite-rich ores. The tellurium in the Merensky Reef follow this trend. Bismuth appears to behave in a similar way and in these ores substitutes for tellurium as demonstrated in the various analyses of moncheite in table I. This substitution would be expected from the close similarity in atomic radius of bismuth (1·55Å) and tellurium (1·43Å).

A further point of interest is with regard to the low nickel content of the bismuthotellurides in the Merensky Reef, particularly merenskyite (table 8.8), when compared to other reported occurrences. This can be explained by the fact that the environment of chalcopyrite-bismuthotelluride deposition would have been depleted in nickel by the prior formation of pentlandite together with the nickel replacement of Pt in the cooperite lattice.

Finally, the fractionation trends for the PGE which can be discerned from undertaking whole rock, mineral concentrate,

or individual mineral analyses are merely superficial expressions of the complex physico-chemical and crystallochemical intricacies of crystallisation, involving ultimately the question of the suitability or unsuitability of these particular elements to be accepted into the various possible crystal structures during or after they are formed. The factors controlling the incorporation of atoms and ions into crystal structures are many, and have been and are still a subject for lengthy discussion. Some particularly authoritative discourses on this subject are by Goldschmidt (1937)*, Ahrens (1953, 1964), Ringwood (1955), Tauson (1965), and Zehmann (1969). In the case of the PGE such a discussion is backed by a deficiency in reliable data on their chemical and crystallochemical properties. Some of these properties are given in table 9.1 and can be used to predict and support observed trends or possible, probable, or proved lattice substitutions. Although the substitution of PGE in base-metal sulphide lattices is theoretically acceptable, and in practice has been demonstrated as conclusively as is possible within the limitations of present day analytical procedures, substitution in silicate and oxide lattices, in particular chromite, is still not proved. The siderophilic nature of the PGE, together with the recognition of minute inclusions of base-metal sulphides entraped by chromite and silicate growth, and PGM and base metal sulphides along cleavages and alteration veinlets, are arguments used by mineralogists against the validity of the geochemical results obtained from the analysis of mineral concentrates. Cousins and Vermaak (1976) and Vermaak and Hendriks (1976) have summarised some of the facts with regard to chromite substitution in particular, and the author

* Goldschmidt, V.M. (1937). J.Chem. Soc. p.655.

is inclined to agree with their unconvinced attitude to suggestions of diadochic substitution of PGE in such lattices. The experiences of the Merensky Reef do little to convince the author of any significant contribution of PGE from such a source.

9.2 Ore Mineral Paragenesis

It has been generally shown (Haughton et al, 1974; Page, 1971; MacLean, 1969) that in iron-rich systems the separation of an immiscible sulphide liquid from a basaltic magma is favoured by an increase in oxygen fugacity and a decrease in sulphur fugacity, Fe^{2+}, and possibly temperature. Assuming the system is closed to sulphur, the principal control appears to be compositional changes measurable in terms of relative ferrous iron depletion or enrichment. Thus Haughton et al consider that although the crystallization of any silicates or oxides will increase the relative concentration of sulphur in the melt, the separation of pyroxenes and plagioclase which are less iron-rich than the parent magma, will cause the magma to become enriched in FeO and thus cause the magma to move off the sulphide saturation surface. However, as discussed also by Page for the chromitites of the Stillwater Complex (1971), the removal of large amounts of Fe^{2+} from the magma in the region of chromite precipitation results in a decrease in the sulphide capacity of the magma and the segregation of immiscible iron-sulphide-oxide liquid droplets which are carried down and accumulated with the chromite. Continued sulphide precipitation depends then on the differentiation trends of the silicate and oxide phases. Haughton et al consider that in a closed system there is not likely to be sufficiently large changes in the fO_2:fS_2 ratio to strongly influence the sulphur solubility.

In the case of the Merensky Reef at Rustenburg and Union mines there is a clear correlation with the occurrence of a chromitite band and the concentration immediately above of sulphides (chapter 3.1.3). At Rustenburg mine this sulphide concentration also corresponds with the bulk of the PGE content of the ore. At Union mine, however, the bulk of the PGE content is immediately below the top chromitite band although again there is a correspondence with base-metal sulphide concentration. However PGE, although in uneconomic quantities, are also concentrated with sulphides immediately above.

Although the concentration of sulphides and PGE is understandable in relation to precipitation and accumulation of the bottom chromitite band at Rustenburg mine, it is less so in the case of the top chromitite band, particularly at Union mine. However the evidence presented in this thesis that the potholes were formed after the accumulation of the bottom chromitite band and PGE-rich and sulphide-rich Reef pegmatitic pyroxenite may account for this, since it is considered that pothole formation involved the combination of disturbances of the footwall cumulate crystal mush and fairly turbulent magmatic currents. The potholes are, therefore, evidence of 'disturbances' prior to the formation of the top chromitite band and the further removal of PGE from the magma by the precipitation of the PGE-scavenging base-metal sulphides. The increase in oxygen fugacity and the related decrease in ferrous content of the magma necessary for sulphide segregation during this period of instability may be directly related to an influx of new magma as well as changes in the magma produced by phenomena like

"roof foundering" as suggested by Naughton et al (1974). The top chromitite band can be used as evidence of this change and can therefore be considered to represent a pause or retrograde step in the differentiation of the Merensky Unit. The mechanism proposed by Vermaak (1976) for the formation of the'boulder-like' pegmatitic patches in the Reef pyroxenite is an attractive one, although the formation of a plagioclase raft has very little to support it. Also the formation of a pegmatitic facies is clearly not a prerequisite for PGE or sulphide concentration, as is evident from its absence or lack of correlation with the 'ore grade section' in some other outcrops of the Merensky Reef.

The extensive removal of PGE from the magma by the sulphide liquid is evident in the fact that the bulk of these metals plus gold are concentrated in the interstitial crystalline sulphide aggregates, and that the PGM are clearly an intimate part of the total sulphide paragenetic picture. This thesis clearly shows that the PGM have not resulted from their introduction by hydrothermal fluids as suggested by Lauder (1970), and as implied by Stumpfl (1974). However Stumpfl has altered his opinion recently (Stumpfl and Tarkian, 1976) under the recent weight of published evidence and has conceded that in situ magmatic crystallisation of an interstitial sulphide liquid, as proposed by Schneiderhohn (1929) and first supported by the author in 1966, is responsible for the bulk of the PGE and PGM occurrences in the ore section.

Some of the interpretations and findings in this thesis are supported by recent experimental work. The relevance of Hoffman and MacLean's work and others on the Pd-Bi-Te system to the meren-

skyite-kotulskite intergrowth relationship has already been dealt with in chapter 8. They were concerned with the artifical equivalents and their solid solution relationships. However, in the ore the main relationship between the two phases is one of replacement, although some intergrowths can be explained by complete segregation from a solid solution. In addition Skinner et al (1976) have presented some tentative results for the Pt-Pd-Fe-As-S system, and the relevance of their conclusions will be dealt with briefly.

The system Pt-Pd-S

Skinner et al summarised the binary phase relations at 1000°C as follows: The join Pt-S contains a single binary compound, PtS(cooperite) whereas the join Pd-S is occupied by an extensive liquid field but does not contain any binary solids. However a ternary phase equivalent to braggite and showing an extensive compositional range from $(Pd_{0.40}\ Pt_{0.60})S$ to $(Pd_{0.84}\ Pt_{0.16})S$ does occur. They also observed that the substitution of Pd for Pt in cooperite amounts to approximately 30 atomic percent, and that the metal:sulphur ratio in cooperite and braggite does not depart significantly from 1:1.

These findings agree with the available compositional data for these two minerals, and with the author's affirmation of braggite and cooperite as distinct and recognisable species. Their observed substitution of Pd in the PtS phase supports the replacement origin for much of the braggite at the two mines. However it is also clear that some of the braggite could have formed in its own right at a similar time to cooperite. The author's recommendation for a reinvestigation of vysotskite is also supported by its

absence in the artificial system.

The system Pt-Pd-As

Skinner et al reported the existence of two stable phases, a Pt-Pd alloy and Pt As_2 (sperrylite). They noted that Pt As_2 and Pt-Pd alloy cannot coexist at 1000°C or higher temperatures, and concluded that the association of sperrylite with the alloy must therefore arise by reaction at submagmatic temperatures. This is supported in this thesis by the association of graphic Pt-Fe alloy in pyrrhotite enclosing and replacing sperrylite. They also support the author's conclusions on the purity of sperrylite in their statement that "the main phase $PtAs_2$ has a very restricted compositional range, less than 1 at.% Pt being replaced by Pd.

The system Pt-As-S

Skinner et al concluded that the two binary phases PtS and $PtAs_2$ are stable and coexist with each other, and that neither phase shows any tendency toward solid solution. This supports the observed absence of any intergrowth relationships in the ore between these two, and also the lack of As in cooperite and S in sperrylite.

The system Pt-FeS

Skinner et al concluded that pyrrhotite contained small but detectable (under the electron-probe microanalyser) amounts of Pt, presumably in solid solution. Cooperite was also present as a binary phase and accepts less than 0·5 at.% Fe into its lattice. Four Pt-Fe alloy phases were observed i.e. a face-centered cubic platinum-iron solid solution; a primitive cubic phase (isoferroplatinum); a tetragonal phase (tetraferroplatinum); and a gamma-iron solid solution. They noted that in the assemblage pyrrhotite

cooperite + alloy the alloy is isoferroplatinum. The stable co-existence of these phases supports the author's interpretation of a high temperature segregation origin for the Pt-Fe alloy textural types I - IV involving pyrrhotite and cooperite.

In their final discussion Skinner et al support a fractional crystallisation origin for the PGM, and also the enrichment of Pd and other rare elements relative to Pt in the liquid remaining after pyrrhotite crystallisation. The data in this thesis provides considerable evidence to support fractional crystallisation as being the main process for PGM formation. Detailed explanations of the various textural types found in the ore and concentrates have been offered for the first time. Finally a paragenesis diagram on the basis of fractional crystallisation is presented for the ore minerals in figure 9.1. This diagram is at present offered as a basis for discussion, and represents a first attempt by anyone at providing such a diagram for the Merensky Reef ore minerals. There is still an immense amount of research to be done and we should not be lulled into inactivity by the recent spate of publications on the subject. The study and interpretation of the PGM textures provides a particularly rewarding field for future study.

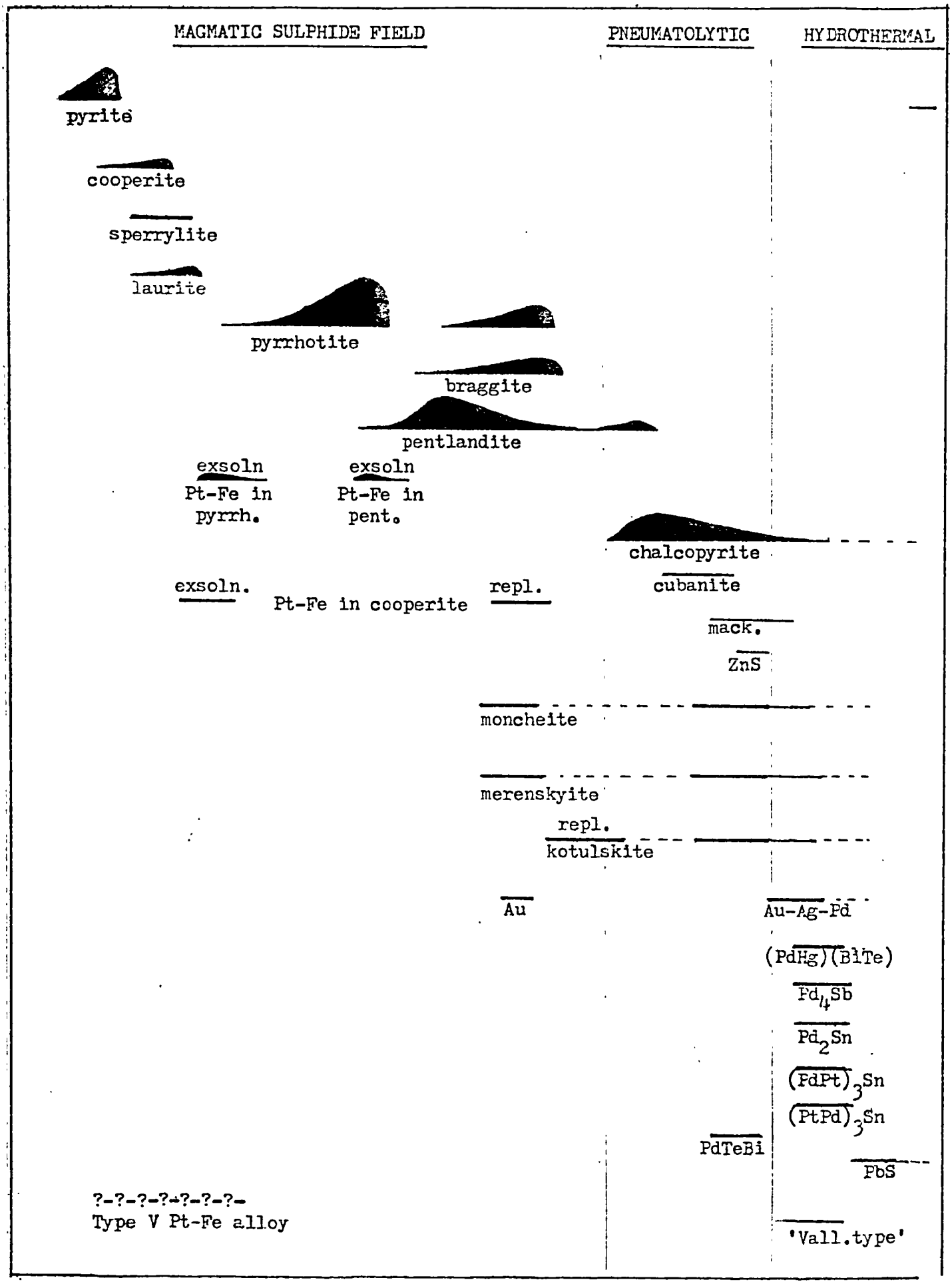

Fig. 9.1 Ore Mineral Paragenesis Diagram for the Merensky Reef at Rustenburg and Union Mines.

CHAPTER 10

SUMMARY OF CONCLUSIONS

1. As a climax to a natural progression of crustal instability evident at various stages in the deposition of the Transvaal System, the final collapse of the area of the Bushveld Basin coincided with a sill phase of basic magma injection into the Pretoria Series, an epicrustal phase of volcanism and metasomatism, a phase of intrusion and differentiation of the Mafic Zone magma as marginal arcuate sheets, and finally a central intrusion of the Bushveld Granite.

2. Visible mineral layering, unconformities, disconformities, the characteristic cyclic differentiation units of the Critical Zone, and cryptic compositional trends are all compatible with progressive differentiation of the Mafic Zone magma by fractional crystallisation and gravity settling, together with periodic influxes of new magma.

3. The Merensky Reef is a platiniferous and sulphide-rich pyroxenite forming a basal cumulate fraction of a cyclic differentiation unit (The Merensky Unit) of chromitite - pyroxenite - norite - anorthostic norite - anorthosite, which was terminated by the onset of a final cyclic unit (The Bastard Unit), at the base of which was formed the Bastard Reef pyroxenite.

4. Personal field observations on the structural and lithological characteristics of the Merensky Reef and associated hanging wall and footwall rocks at Rustenburg mine demonstrate and emphasise that the variable nature of the Merensky Reef is due to its differing environments of accumulation at 'normal reef elevation', in

'potholes' or over 'koppies'.

5. New and more detailed field evidence on the structure of potholes and koppies supports the opinion that magmatic currents were responsible for the scouring and enlargement of existing downwarps in the footwall to produce the Bastard Potholes, and for scouring new and shallower hollows, producing the Normal Potholes.

6. The latest genetic model by Vermaak (1976) to account for the cyclicity in the Critical Zone and the pegmatitic Reef provides an attractive explanation of many of the facts, but is in part contradicted by the author's suggested mode of formation for the potholes.

7. Available PGE distribution data for the Merensky Reef show that peak PGE plus gold values correspond to the bottom chromitite band at Rustenburg mine, and the top chromitite band at Union mine, although the bulk of the PGE content of the 'ore section' occurs immediately above these chromitite bands. At Rustenburg mine this corresponds to the pegmatitic Reef, and at Union mine to the finer grained Merensky pyroxenite.

8. The formation of a pegmatitic pyroxenite is not a prerequisite for PGE concentration, although the formation of a chromitite band appears to be so.

9. In the pyroxenite above the chromitite bands the PGE content is mainly accounted for as discrete PGE sulphides, arsenides, antimondes, bismuthotellurides, and graphic Pt-Fe alloy intergrown with the base metal sulphides. In the chromitite bands it is considered most likely that alloys, particularly Pt-Fe alloy, are the dominant

PGE minerals, although the great majority of the PGE content is considered to be 'submicroscopic'.

10. Recent studies on the occurrence of PGE in mineral separates have added further weight to the probability that solid solution in the base-metal sulphides, and even in the silicates and chromite, accounts for a significant proportion of the PGE content of the ore. Rhodium is a particularly important example where no discrete PGE mineral has been found in the ore to account for it. However, the problem of whether substitution of PGE in silicate and oxide lattices can or does occur is highly controversial and difficult to resolve.

11. The most common PGM in the ore are braggite, cooperite, and graphic Pt-Fe alloy at Rustenburg mine, and laurite and graphic Pt-Fe alloy at Union mine. The bismuthotellurides of Pt and Pd found by the author, although rare relative to the total PGM content, are as easily found in polished sections of the ore because of their invariable concentration with chalcopyrite.

12. The nature of the macro- and microtextures formed by the intergrowth of the base metal sulphides with each other, with the PGM, and with the enclosing silicates and oxides, are consistent with an origin from the fractional crystallisation of an entraped liquid platiniferous sulphide phase within the interstices of a cumulus aggregate of silicate and oxide crystals. This mechanism, together with the inclusion of sulphide liquid during adcumulus growth of silicates and oxides, the reaction of intercumulus liquid with cumulus minerals, and deposition of material from residual hydro-

thermal fluids as a final product of intercumulus liquid crystallisation, accounts for all the observed textural and mineralogical features, and dispenses with theories involving an external hydrothermal source of PGE mineralisation.

13. Pyrite enclosed by pyrrhotite is poor in nickel and is considered to have been the first base-metal sulphide to crystallise. The textural evidence shows that the common replacement relationship between granular 'mosaic' pyrrhotite and pyrite is the result of desulphurisation of pyrite in the solid state after the main bulk of the pyrrhotite and pentlandite had formed, and before chalcopyrite. The replacement may correspond in time to the recrystallisation of myrmekitic Pt-Fe alloy in pyrrhotite, and to the replacement of cooperite by braggite.

14. The bulk of the pentlandite is considered to have crystallised directly from the sulphide liquid after pyrrhotite. Later pentlandite occurs as exsolution flames in pyrrhotite.

15. Chalcopyrite is the latest formed major sulphide phase.

16. A brown 'valleriite-looking' phase of the same composition as Rustenburg mackinawite may have been mistaken for valleriite by previous workers. No valleriite was found in this study. Rustenburg mackinawite appears to be structurally different from Outokumpu mackinawite.

17. The textures formed by the intergrowth of Pt-Fe alloy are classified into five textural types. Types I,II, and III are considered to represent variations on the segregation of Pt-Fe alloy from a

Pt-Fe-sulphide mixed-crystal.

Type I has involved exsolution by co-nucleation and the mutual growth of Pt-Fe alloy and pyrrhotite to produce a normal eutectoid texture.

Type II results from exsolution from a mixed crystal containing either a high concentration of Pt or which has been undercooled.

Type III may have either formed from the slow cooling of a mixed crystal or the recrystallisation of a myrmekitic texture.

Type IV is considered to largely result from the desulphurisation of cooperite in response to a lowering of the sulphur fugacity, and probably corresponds in time to the similar breakdown of pyrite to pyrrhotite.

Type V is considered to have formed by simple euhedral crystal growth, largely from the silicate walls or in the interstices of the chromite aggregates.

18. The properties of Type V Pt-Fe alloys in the concentrates indicate that both isoferroplatinum and tetraferroplatinum are present.

19. No reliance can be put on the use of indentation microhardness as a tool for determining the iron content of natural Pt-Fe alloys. The same probably applies to measurements of reflectance.

20. A new Pt-Au-Fe alloy has been detected.

21. The first report of 'palladic gold' in the Merensky Reef by the author is supported.

22. The detection of minute granules of a possible silver-palladium

alloy in palladian electrum is a further illustration of the need for careful ore microscopic observation prior to any meaningful analytical work.

23. Gold, electrum, and palladian electrum are generally formed at the time of chalcopyrite crystallisation, but some may result from the replacement of cooperite by braggite.

24. On the basis of a historical review of the facts regarding the discovery of cooperite, it was clearly Bannister and Hey who first isolated and defined it, and thus technically discovered it.

25. Published results confirm an ideal metal:sulphur ratio of 1:1 for braggite and cooperite. This is supported by the present study although cooperite from Rustenburg may be an exception.

26. The composition of seven braggite grains from Rustenburg mine fall within the range of $(Pt_{0\cdot39-0\cdot54}\ Pd_{0\cdot24-0\cdot40}\ Ni_{0\cdot19-0\cdot28})\ S$, and trend towards PdS rather than vysotskite in the ternary composition diagram. Vysotskite needs to be reinvestigated.

27. The compositional variation and antipathy between palladium and nickel in braggite from Rustenburg reflects its origin largely from the late stage palladium metasomatism of cooperite.

28. The common occurrence of braggite intergrown with cooperite together with their similarity in reflected-light has led to confusion in the literature over their properties. This study provides new data on their properties, and shows that they are sufficiently different to confidently distinguish between cooperite and brag-

gite where they are found intergrown, although confirmation by X-ray powder diffraction analysis or electron-probe microanalysis is usually necessary for the certain identification of solitary grains of either.

29. X-ray powder patterns of cooperite and braggite are especially diagnostic.

30. The use of electron-probe microanalysis for their identification without microscopic examination can give rise to errors where braggite is intergrown with cooperite, or confusion where the palladium and nickel content of braggite is low or that of cooperite high.

31. A thorough examination of the crystal structure of cooperite is required along the lines of Childs and Hall (1973).

32. The study of cooperite and braggite provides further evidence for the geochemical fractionation of palladium from platinum during the formation of the Merensky Reef.

33. Laurite is pre-pentlandite in its time of formation and grew as euhedral crystals from the silicate walls into the sulphide melt.

34. A high proportion of Ru in the ore at both mines appears to occur in the lattices of the base-metal sulphides.

35. The Ir-Os-Pt-Ru zoned laurite crystal from Union mine is apparantly unique. Substitution of iridium and osmium in laurite and Pt-Fe alloy probably accounts for the bulk of their content in the ore.

36. Osmium substitution is probably the most effective in raising the reflectance of laurite although measurements of reflectance are unsuitable for compositional determinations where specimens from a variety of localities are involved.

37. Osmium substitution is mainly responsible for a decrease in hardness in laurite.

38. Reliable indentation microhardness values for laurite are difficult to obtain, although the indentation features are particularly diagnostic as a determinative parameter.

39. The range within which the cell size of most laurites can be expected to fall are from a_o 5·61 - 5·63 Å.

40. The electron-probe microanalyses for several grains of the new cubic rhodium sulphide (a_o 9.853(1)) are best represented by the empirical formula $(Rh_{0.57}Fe_{0.17}Cu_{0.16}Ir_{0.10})_4 S_5$.

41. The composition of the optically anisotropic mineral 'zappinite' is best represented by the formula $(Rh_{0.82}Ir_{0.12}Pt_{0.05}(CuFe)_{0.01})_3 S_4$.

42. The large difference between the amount of sperrylite at Rustenburg and Union mines (0.3 vol.%) to that at Western Platinum mine (50.3 vol.%) further emphasises the large variation in the platinum group mineral proportions along the strike of the Merensky Reef, and the need for more localised and comparative studies.

43. Some sperrylite (if not all) crystallised prior to pyrrhotite, and its rarity in the Rustenburg and Union mine ores compared to Western Platinum mine may be due to its replacement by Type I - III Pt-Fe alloy intergrowths.

44. A detailed study is required on the Pd-Sb phases in the Merensky Reef. The Pd_4S phase located in this study conforms more closely to mertieite II than stibiopalladinite.

45. The original composition and structure of merenskyite determined by the author has been verified many times since then by other workers. However lengthy terminology like "platinian bismuthian nickolean merenskyite" should be discouraged.

46. Mineral A is probably the same as the more recently described temagamite.

47. Mineral C is similar to kotulskite but with considerably more bismuth, and is probably the same as the recently described new mineral from Bissersk.

48. The question of the existence of a $Pd_3(Te,Bi)_5$ phase is still problematical.

49. The early findings of the author's that kotulskite was Pd(Te,Bi) has been verified by other workers.

50. The bulk of the platinoid bismuthotellurides crystallised with chalcopyrite. Some very large crystals appear to have grown from the silicate margins prior to chalcopyrite and even pentlandite formation.

51. The relationship between merenskyite and kotulskite in this ore is largely one of replacement, although examples showing mutual boundary relationships are probably formed by complete segregation of a kotulskite-merenskyite solid solution. The replacement process could coincide with the similar palladium metasomatism of cooperite.

52. Electron-probe microanalysis of the bismuthotellurides without ore microscopic and X-ray diffraction controls can lead to the erroneous proposal of 'new unnamed minerals'.

53. Reflectance measurements, combined with qualitative observations of their reflected-light properties and intergrowth relationships, can enable fairly confident identifications to be made on a routine basis.

54. This thesis has provided additional mineralogical evidence which increases our conception of the presently emerging picture of PGE mobility and fractionation during geological processes. In particular it has emphasised that the PGM are an intimate part of the total sulphide paragenetic picture, are not foreign minerals or metals introduced into a 'favourable horizon' from some hypothetical external source, and were formed at all stages of the magmatic base-metal sulphide crystallisation time scale. The textural data and interpretations which have been presented are supported by the recent tentative conclusions on the artificial Pt-Pd-Fe-As-S system by Skinner et al (1976).

ACKNOWLEDGEMENTS

I would like to express my sincere thanks to my colleague and supervisor, Professor A.P.Millman, for his guidance and encouragement during the course of the research at Imperial College, London, and for his patience over the author's delay in presenting the results in the form of a thesis. I would also like to thank him and Professor J.Platt, together with the other staff of the Department of Mineral Exploitation, University College,Cardiff, for enabling me to have the necessary study leave to complete this thesis, and to undertake further research in Europe. In this respect I am very grateful to University College for granting me a study leave, and to the Leverhulme Trust for generously providing a Leverhulme Faculty Fellowship in European Studies for me to continue my work in Europe with various specialists in this field.

I am grateful also to Johannesburg Consolidated Investment Co. Ltd. for their help and permission to study the field relationships and collect specimens of the Merensky Reef at Rustenburg and Union mines from July to September of 1962. I would especially like to record my debt to the late Dr. Joe Zermatten for his kindness and assistance and his generous provision of a collection of polished sections of concentrates from the two mines. In respect to this visit I thank the Vernon Hobson Bequest Fund of the Institution of Mining and Metallurgy and the Hilary Bauerman Fund from Imperial College for financial assistance.

I am grateful to many, in both the Geology Department of Imperial College and the Mineral Exploitation Department at University College, for their assistance over the years and in the final preparation of this thesis. I would especially like to acknowledge the assistance of Mr.T.K.Kelly for his help in the electron-probe microanalysis of these minerals and, Mr. R.Curtis and Dr. M.T.Frost for their guidance in obtaining and processing the X-ray data.

I am especially indebted to Mrs. Pat Fackrell for undertaking the laborious task of typing the manuscript and conscientiously ensuring that it was free of typographical error. Finally my grateful thanks also go to my wife and children for their moral support and patience during the writing of this thesis.

REFERENCES

ADAM, H.R.(1927) A note on a new palladium mineral from the Potgietersrust platinum fields. Chem.Met.Min.Soc. S.Africa. 27, 249-250.

ADAM, H.R.(1928) Determination of platinum metals in ores and concentrates. Chem.Met.Min.Soc.S.Africa 28.

ADAM, H.R.(1929) 'Contribution on paper by Cooper (1928)'. Chem. Met.Min.Soc. S.Africa 29.

ADAM, H.R.(1931) Notes on platinum group minerals from Rustenburg and Potgietersrust Districts, Transvaal. Geol.Soc. S.Africa Trans. 33, 103-109.

AHRENS, L.G.(1953) The use of ionization potentials - Part 2. Anion affinity and geochemistry. Geochim.Cosmochim. Acta. 3, 1-29.

AHRENS, L.H.(1964) The significance of the chemical bond for controlling the geochemical distribution of the elements - Part 1. Physics and Chemistry of the Earth. 5, 1-56. Pergamon Press, Editors Ahrens, Press, Runcorn.

AMINOFF, G. and PARSONS, A.L.(1928) Structure of sperrylite. Univ. Toronoto Stud.Geol.Ser. 26.

ARIAS, M.(1968) Unpublished report on alluvial platinum concentrates from Colombia, Alaska and Urals.

AUGUSTITHIS, S.S. (1965) Mineralogical and geochemical studies of the platiniferous dunite-birbirite-pyroxenite complex of Yubdo/ Birbir, W.Ethiopia. Chemie der Erde. 24, 159-196.

BANNISTER, F.A.(1932) The examination and identification of platinoid minerals in concentrates from the Transvaal. Mineral.Mag. 23, 195.

BANNISTER, F.A. and HEY, M.H.(1932) Determination of minerals in platinum concentrates from the Transvaal by X-ray methods. Mineral.Mag. 23, 188.

BANNISTER, F.A.(1937) The discovery of braggite. Zeitschr. Kristallogr. 96, 201.

BARTHOLOME, P.(1957) Theoretical considerations on the separation of the sulphides and their crystallization. Econ.Geol. 52, 895-903.

BEATH, C.B.,COUSINS, C.A. and WESTWOOD, R.J.(1961) The exploitation of the platiniferous ores of the Bushveld Igneous Complex with particular reference to Rustenburg Platinum mine. Trans. 7th Commonwealth Min.Metall.Congress.

BERRY, L.G.,and THOMPSON, R.M.(1962) X-ray powder data for ore minerals: the Peacock Atlas. New York.Geol.Soc. Amer.Memoir 85.

BIRKS, L.S.,BROOKS, E.J., ADLER,I., and MILTON,C.(1959) Electron probe analysis of minute inclusions of a copper-iron mineral. Am.Mineral. 44, 974-978.

BOROVSKII, I.B.,DEEV, A.N.,and MARCHUKOVA, I.D.(1959) Application of the method of local X-ray spectrographic analysis to the study of minerals of the platinum group. Geologiya Rudnykh Mestorozhdenii, no.6.

BRYNARD, H.J.,DE VILLIERS, J.P.R., and VILJOEN, E.A.(1976) A mineralogical investigation of the Merensky Reef at the Western Platinum mine, near Marikana, South Africa. Econ. Geol. 71, 1299-1307.

CABRI, L.J.(1972) The mineralogy of the platinum-group elements. Miner.Sci.Eng. 4,no.3, 3-29.

CABRI, L.J.(1974) Some observations on the geochemistry of the platinum-group elements. Trans.Geol.Soc.S.Africa. 77, 65-67.

CABRI, L.J.(1976) Glossary of platinum-group minerals. Econ.Geol. 71,no.7,1476-1480.

CABRI, L.J.,and CHEN,TZONG T.(1976) Stibiopalladinite from the type locality. Am.Mineral. 61, 1249-1254.

CABRI, L.J.,CLARK, A.M., CHEN, TZONG T.(1977) Arsenopalladinite from Itabira, Brazil, and from the Stillwater Complex, Montana. Can.Mineral. 15, 70-73.

CABRI, L.J.,and FEATHER, C.E.(1975) Platinum-iron alloys: a nomenclature based on a study of natural and synthetic alloys. Can.Mineral. 13, 117-126.

CABRI, L.J., GILLES LAFLAMME, J.H.,and STEWART, J.M.(1973) Temagamite, a new palladium-mercury telluride from the Temagami copper deposit, Ontario, Canada. Can.Mineral. 12, 193-198

CABRI, L.J.,and GILLES LAFLAMME, J.H.(1974) Rhodium, platinum and gold alloys from the Stillwater Complex. Can.Mineral. 12, part 6.

CABRI, L.J.,and GILLES LAFLAMME, J.H.(1974) Sudburyite, a new palladium-antimony mineral from Sudbury, Ontario. Can.Mineral 12, part 4, 275-279.

CABRI, L.J., and GILLES LAFLAMME, J.H.(1976) The mineralogy of the platinum-group elements from some copper-nickel deposits of the Sudbury area, Ontario. Econ.Geol. 71, 1159-1195.

CABRI, L.J.,GILLES LAFLAMME, J.H., STEWART. J.M., ROWLAND, J.F., and TZONG T.CHEN(1975) New data on some palladium arsenides and antimonides. Can.Mineral. 13, 321-335.

CABRI, L.J., and HALL, S.R.(1972) Mooihoekite and haycockite, two new copper-iron sulfides, and their relationship to chalcopyrite and talnakhite. Am.Mineral. 57, 689-708.

CABRI, L.J., and HARRIS, D.C.(1972) The new mineral insizwaite ($PtBi_2$) and new data on niggliite (PtSn). Mineral.Mag. 38, 794-800.

CABRI, L.J., and HARRIS, D.C.(1975) Zoning in Os-Ir alloys and the relation of the geological and tectonic environment of the source rocks to the bulk Pt:Pt-Ir-Os ratio for placers. Can. Mineral. 13, 266-274.

CABRI, L.J.,HARRIS, D.C., and GAIT, R.I.(1973) Michenerite(PdBiTe) and froodite ($PdBi_2$) confirmed from the Sudbury area. Can. Mineral. 11, 903-912.

CABRI, L.J.,and PICKWICK, K.M. (1974) A complex bismuthian palladium telluride intergrowth from the Stillwater Complex, Montana. Econ.Geol. 69, 263-266.

CABRI, L.J., and TRAILL, R.J. (1966) New palladium minerals from Noril'sk, Western Siberia. Can. Mineral. 8, 541-550.

CAMERON, E.N. (1963) Optical symmetry from reflectivity measurements. Am.Mineral. 48, 1070-1079.

CAMERON, E.N. (1969) Postcumulus changes in the Eastern Bushveld Complex. Am.Mineral. 54, 754-779.

CAMERON, E.N.,and DESBOROUGH, G.A. (1969) Occurrence and characteristics of chromite deposits - Eastern Bushveld Complex. Econ. Geol. Monograph 4, 23-40.

CASTAING, R. (1951) Application des sondes electroniques a une methode d'analyse ponctuelle chimique et cristallographique. Theis, Faculty of Science, University of Paris.

CHILDS, J.D., and HALL, S.R.(1973) The crystal structure of braggite (PtPdNi)S. Acta Cryst. B29, 1446-1451.

CHILDS, J.D., and HALL, S.R. (1973) The crystal structure of michenerite, PdBiTe. Can.Mineral. 12, 61-65.

CHYI, L.L.,and CROCKET, J.H.(1976) Partition of platinum,palladium, iridium, and gold among coexisting minerals from the Deep Ore Zone, Strathcona mine, Sudbury, Ontario. Econ.Geol.71,1196-1205.

CLARK, A.M., CRIDDLE, A.J., and FEJER,E.E.(1974) Palladium arsenide-antimonide from Itabira, Minas Gerais, Brazil. Mineral. Mag. 39, 528-543.

CLIFFORD, T.N. (1970) The Structural framework of Africa. African Magmatism and Tectonics. Editors: Clifford,T.N.,& Gass, I.G., Edinburgh, Oliver and Boyd. p1-26.

COERTZE, F.J. (1963) Structures in the Merensky Reef at the Rustenburg Platinum mine. Ann.Geol.Surv. 2, Pretoria, p.69.

COERTZE, F.J. (1970) The geology of the western part of the Bushveld Igneous Complex. Geol.Soc.South Africa. Special Publication no.1, 5-22.

COOPER, R.A. (1928) A new platinum mineral in the Rustenburg norites. Journ,Chem.Met.Min.Soc.S.Africa. 28, 281. Also Mineral. Mag. 21, (1931) p.618, and Mineral.Abstr. 4-10.

COUSINS, C.A. (1959) The structure of the mafic portion of the Bushveld Igneous Complex. Trans. Geol.Soc.S.Africa.62, 179-201.

COUSINS, C.A., and FERINGA, G. (1964) The chromite deposits of the western belt of the Bushveld Complex. The geology of some ore deposits in southern Africa.Geol.Soc.S.Africa. 2, 183-202.

COUSINS, C.A.(1964) The platinum deposits of the Merensky Reef. The geology of some ore deposits in southern Africa.Geol.Soc. S.Africa. 2, 225-237.

COUSINS, C.A.(1969) The Merensky Reef of the Bushveld Igneous Complex. Econ.Geol.MON. 4, 239-251.

COUSINS, C.A.(1973) Platinoids in the Witwatersrand system. J.S.African Inst.Min.Met. 73, 184-199.

COUSINS, C.A.(1973) Notes on the geochemistry of the platinum group elements. Trans.Geol.Soc.S.Africa., 76, 77-81.

COUSINS, C.A., and KINLOCH, E.D.(1976) Some observations on textures and inclusions in alluvial platinoids. Econ. Geol. 71, 1377-1398.

COUSINS, C.A., and VERMÁAK, C.F. (1976) The contribution of southern African ore deposits to the geochemistry of the platinum group metals. Econ.Geol. 71, 287-305.

CROCKETT, R.N. (1969) The geological significance of the margin of the Bushveld basin in Botswana. Unpub.Ph.D.thesis, Univ. London.

CROCKET, J.H.(1969) Platinum metals. Handbook of Geochemistry: New York, Springer-Verlag.Ed.Wedepohl,K.H.vol. 2, chap.78.

CROCKET, J.H. (1972) Some aspects of the geochemistry of Ru,Os,Ir and Pt in iron meteorites. Geochim.et Cosmochim. Acta.36,517-535.

CROCKET, J.H.(1972) Some aspects of the geochemistry of Ru,Os,Ir and Pt in iron meteorites. Geochim.et Cosmochim. Acta. 36, 517-536.

CROCKET, J.H.,KEAYS, R.R.,and HSIEH,S.(1968) Determination of some precious metals by neutron activation analysis. J.Radioanal. Chem. 1, 487-507.

CROCKET, J.H.,MACDOUGALL,J.D.,and HARRISS,R.C.(1973) Gold, palladium and iridium in marine sediments. Geochim.et Cosmochim. Acta. 37, 2547-2556.

CROCKET, J.H., and SKIPPEN, G. (1966) Radioactivation determination of palladium in basaltic and ultrabasic rocks. Geochim. et Cosmochim. Acta. 30, 129-141.

CROCKET, J.H., TERUTA, YUKO, AND GARTH, J.(1976) The relative importance of sulfides, spinels, and platinoid minerals as carriers of Pt,Pd,Ir, and Au in the Merensky Reef at Western Platinum Limited, near Marikana,S.Africa. Econ.Geol.71,1308-1323.

DALY, R.A.(1928) The Bushveld igneous complex of the Transvaal. Geol.Soc.Am.Bull. 39, 703-768.

DALY, R.A., and MOLENGRAAFF, G.A.F. (1924) Structural relations of the Bushveld igneous complex, Transvaal. J.Geol. 32, 1-35.

DAVIES, R.D., ALLSOPP, H.L., ERLANK, A.J., and MANTON, W.I.(1970) Sr-isotopic studies on various layered mafic intrusions in southern Africa. Geol.Soc.S.Africa. Special Pub.1, 576-593.

DESBOROUGH, G.A.,FINNEY, J.J. and LEONARD, B.F.(1973) Mertieite, a new palladium mineral from Goodnews Bay, Alaska. Am.Mineral 58, 1-10.

DIETZ, R.S. (1964) Sudbury structure as an astrobleme. J.Geol. 72, 412-414.

DUPARC, L., MOLLY, E., and BORLOZ,A.(1927) Sur la birbirite, une roche nouvelle. Compt.Rend.Soc.Phys,de Geneve. 44, no. 3.

EDWARDS, A.B. (1960) Textures of the ore minerals. Australian Inst.Min.Met.

EHMANN, W.D., BAEDECKER, P.A.,and McKOWN, D.M.(1970) Gold and iridium in meteorites and some selected rocks. Geochim. et Cosmochim. Acta. 34, 493-507.

ELCOCK, E.W. (1956) Monograph on order-disorder phenomena; in Methuen's Monographs on Physical Subjects.

EVANS, R.C. (1966) An introduction to crystal chemistry. Cambridge Univ.Press.Second edition.

EVANS, H.T., BERNER, R.A., and MILTON, C. (1962) Valleriite and mackinawite. Annu.Meet.Geol.Soc.Am.Houston Texas. Abstract.

EVANS, H.T., MILTON, C., CHAO, E.C.T., ADLER, T., MEAD, C., INGRAM B., and BERNER, R.A.(1964) Valleriite and the new iron sulphide mackinawite. U.S.Geol.Surv.Prof.Pag. 475-D, 64-69.

FEATHER, C.E. (1976) Mineralogy of platinum-group minerals in the Witwatersrand, South Africa. Econ.Geol.71,1399-1428.

FERGUSON, J., and BOTHA, E. (1963) Some aspects of igneous layering in the basic zones of the Bushveld Complex.Trans.Geol.Soc. S.Africa. 66, 259-278.

FERINGA, G. (1959) The geological succession of a portion of the north-western Bushveld (Union Section) and its interpretation. Trans.Geol.Soc. S.Africa. 62, 219-232.

FOCKEMA, R.A.P., and MENDELSOHN, E. (1954) Notes on an unusual occurrence of chromite in the eastern Bushveld. Trans.Geol. Soc. S.Africa. 57, 77-82.

FOURIE, G.P. (1959) The chromite deposits in the Rustenburg area. S.African Geol.Surv. Bull. 27.

FOURIE, P.J.(1969) Die geochemie van granitiese gesteentes van die Bosveldstollingskomplex. D.SC.Thesis.Univ.Pretoria. (quoted in Hunter, D.R. (1973) Mineral.Sic.Eng. 5, p.73).

FRICK, H. (1930) Reflexionsmessungen an Erz- und Metallanschliffen mit Hife eines Reflexions-Photometerokulars. Neus Jahrb. fur Mineral. 61A, 31-86.

GASKELL, T.F. (1937) Z.Kristallogr. 96, 203-213

GASPARRINI, E., and HIEMSTRA, S.A.(1975) Paolovite (Pd_2Sn) from the Atok mine in the Merensky Reef. Trans. Geol.Soc. S.Africa. 78, 167-169.

GENKIN, A.D. (1968) Minerals of the platinum metals and their associations in the copper-nickel ores of the Noril'sk deposits. Akad.Nauk SSSR,Inst.Geol.Rudn.Mestorozhd., Petrogr. Mineral Geokhim., 106pp (in Russian).

GENKIN, A.D., and KOROLEV, N.V. (1961) Procedure for the identification of small mineral grains in ores. Geo. Rudn. Mestorozhd. no. 5.

GENKIN, A.D., and ZVYAGINTSEV, O.E. (1962) Vysotskite, a new sulfide of palladium and nickel. Zapiski Vses. Mineral. Obshch. 91, 718-725 (in Russian)

GENKIN, A.D., ZHURAVLEV, N.N., and SMIRNOVA, E.M. (1963) Moncheite and kotulskite - new minerals - and the composition of michenerite. Ibid 92, no. 1, 33-50 (in Russian)

GENKIN, A.D., EVSTIGNEEVA, T.L., TRONEVA, N.V., and VYAL'SOV, L.N. (1969) Polarite, Pd (Pb,Bi), a new mineral from copper nickel sulfide ores. Ibid. 98, 708-715.

GENKIN, A.D., MURAV'EVA, I.V., and TRONEVA, N.V. (1966) Zvyagintsevite, a natural intermetallic compound of palladium, platinum, lead and tin. Geol.Rudn. Mestorozhd. 8, 94-100 (in Russian).

GENKIN, A.D., YEVSTIGNEYEVA, T.L., VYAL'SOV, L.N., LAPUTINA,I.P., and TONEVA, N.V. (1974) Paolovite, a new mineral from copper nickel sulphide ores. Ibid. 16, 98-103.

GENKIN, A.D., ZHURAVLEV, H.N. TRONEVA, N.V., and MURAV'EVA, I.V. (1966) Irarsite, a new sulphoarsenide of iridium, rhodium, ruthenium and platinum. Zapiski Vses. Mineral. Obshch. 95, 700-712 (in Russian).

GIJBELS, R.H., MILLARD, H.T.Jr., DESBOROUGH, G.A., and BARTEL, A.J.(1974) Oxmium, ruthenium, iridium and uranium in silicates and chromite from the eastern Bushveld Complex South Africa. Geochim. et Cosmochim. Acta. 38, 319-337.

GOLDBERG, E., UCHIYAMA, A., and BROWN, H. (1951) The distribution of nickel, cobalt, gallium, palladium and gold in iron meteorites. 2, 1-25.

GOLDSCHMIDT, V.M. (1954) Geochemistry: Oxford Univ. Press. 730p.

GRAY, I.M., and MILLMAN. A.P. (1962) Reflection characteristics of ore minerals. Econ. Geol. 57, 325-349.

GREENLAND, L.P. (1971) Variation of iridium in a differentiated tholeiitic dolerite. Geochim. et Cosmochim. Acta. 35, 319-322.

GRIMALDI, F.S., and SCHNEPFE, M.M. (1969) Mode of occurrence of platinum, palladium, and rhodium in chromite. U.S.Geol. Surv. Res.Paper. 650-C,C149-C151.

HAGEN, J.C. (1954) Some aspects of the geochemistry of platinum, palladium and gold in igneous rocks with special reference to the Bushveld Complex, Transvaal. Unpub. Ph.D. thesis, M.I.T. 298p.

HALL, A.L. (1932) The Bushveld igneous complex of the central Transvaal. Geol.Surv. S.Africa. Memoir 28. 510p.

HAMILTON, W. (1970) Bushveld Complex - product of impacts? Geol. Soc. S.Africa Trans. Spec.Pub.1.367-374.

HARRIS, D.C. (1974) Ruthenarsenite and iridarsenite, two new minerals from the territory of Papua and New Guinea, and associated irarsite, laurite and cubic iron-bearing platinum. Can.Mineral. 12, part 4.

HARRIS, I.R. NORMAN, M., and BRYANT, A.W. (1968) a study of some palladium-indium, platinum-indium, and platinum-tin alloys. J.Less-common Metals, 16, 427-440.

HARRIS, D.C., and VAUGHAN, D.J.(1972) Two fibrous iron sulfides and valleriite from Cyprus with new data on valleriite. Am. Mineral. 57, 1029-1036.

HAUGHTON, D.R., ROEDER, P.L., and SKINNER, B.J. (1974) Solubility of sulfur in mafic magmas. Econ. Geol.69, 451-467.

HAWLEY, J.E., LEWIS, C.L., and WARK, W.J. (1951) Spectrographic study of platinum and palladium in common sulphides and arsenides of the Sudbury District, Ontario. Econ. Geol, 46, 149-162.

HESS, J.B. (1951) Acta Cryst. 4, p.209.

HIEMSTRA, S.A. (1956) An easy method to obtain X-ray diffraction patterns of small amounts of material. Am,Mineral.41, p.519.

HOFFMAN, E., AND MACLEAN, W.H. (1976) Phase relations of michenerite and merenskyite in the Pd-Bi-Te system. Econ.Geol. 71, 1461-1468.

HUNTER, D.R. (1976) Some enigmas of the Bushveld Complex. Econ. Geol. 71, 229-248.

JUZA, R., HUELSMANN, O., and MEISEL, K. (1935) Uber die Sulphide des Rhodiums. Zeit. anorg. Chem. 225, 369-385.

KEAYS, R.R., and CROCKET, J.H. (1970) A study of precious metals in the Sudbury Nickel Irruptive. Econ. Geol. 65, 438-450.

KEAYS, R.R., and DAVISON, R.M. (1976) Palladium, iridium, and gold in the ores and host rocks of nickel sulfide deposits in Western Australia. Econ. Geol. 71, 1214-1228.

KELLY, T.K. (1966) Mass absorption coefficients and their relevance in electron-probe microanalysis. Inst. Min.Met.Earth Sci. Sect. 75, p.59.

KENT, L.E. (1957) Discussion of a paper by Brock, B.B.Tans. Geol. Soc. S.Africa. 60.

KINGSTON, G.A. (1966) The occurrence of platinoid bismuthotellurides in the Merensky Reef at Rustenburg platinum mine in the western Bushveld. 35, 815-834.

KINGSTON, G.A. (1966) Discussion. Trans.Inst.Min.Met.(Sect.B) 75, B98-B99.

KINGSTON, G.A.(1967) The occurrence of two new rhodium sulphide minerals in elluvial 'platinum nuggets' from Yubdo district of Ethiopia. Min.Soc.G.B.Meet.Oxford.

KINGSTON, G.A. (1971) Unpub.presentation on 'the importance of electron-probe microanalysis in the study of platinum minerals and platiniferous ores'. Univ.Wales Intercollegiate Colloquium, Swansea.

KUOVO, O.,VUORELAINEN, Y., and LONG, J.V.P. (1963) A tetragonal iron sulphide. Am. Mineral. 48, 511-524.

LATIMER, W.M., and HILDEBRAND, J.H.(1956) Reference Book of Inorganic Chemistry. The Macmillan Co.

LAUDER, W.R.(1964) 'Mat' formation and crystal settling in magma. Nature. 202, no. 4937.

LAUDER, W.R.(1970) Origin of the Merensky Reef. Nature. 227, 365-366.

LEBEDEEVA, S.I. (1963) The determination of the microhardness of minerals. Izdatelstvo Nauka. S.S.S.R,Moskva. 122p.

LEGG, C.A.(1967) Some chromite-ilmenite associations in the Merensky Reef, Transvaal. Am.Mineral. 54, 1347-1354.

LEGG, C.A. (1967) Some aspects of the mineralogy of chromite with special reference to chromite of the Bushveld Igneous Complex. Unpub.M Sc Thesis.Univ.London.

LEONARD, B.F.,DESBOROUGH, G.A., and PAGE,N.J. (1969) Ore microscopy and chemical composition of some laurites. Am.Mineral.54, 1330-1346.

LEVER, TODD, AND POWELL (1952) Mineral constituents of South African concentrates. Johnson-Matthey Research Lab.Rep. (unpub.)

LIEBENBERG, L.(1970) The sulphides in the layered sequence of the Bushveld Igneous Complex. Geol.Soc.S.Africa Spec.Pub.1,108-207.

MALAN,D.J. (1960) Economic mineral distribution in the Merensky Reef - Union Section. Unpub.J.C.I.report.

MASON, B.(1966) Principles of Geochemistry. Third Edition. John Wiley and Sons, Inc.

MASON, P.K., FROST, M.T. AND REED, S.J.B. (1969) B.M. - I.C - N.P.L. Computer programme for calculating corrections in quantitative X-ray microanalysis. Natl.Phys.Lab.,I.M.S. Report 1 (MK 1) Modified recently to MK 2.

McCALLUM, M.E., LOUCKS, R.R., CARLSON, R.R., COOLEY, E.F., and DOERGE, T.A. (1976) Platinum metals associated with hydrothermal copper ores of the New Rambler Mine, Medicine Bow Mountains, Wyoming. Econ. Geol. 71, 1429-1450.

MCDONALD, J.A. (1965) Liquid immiscibility as one factor in chromitite seam formation in the Bushveld Igneous Complex. Econ. Geol. 60, 1674-1685.

MEDVEDEVA, Z.S., KLOCHKO, M.A., KUZNETSOV, V.G., and ANDREEVA,S.N. (1961) Equilibrium diagram of the palladium-tellurium system. Russian J.Inorg.Chem. 6, no. 7.

MERTIE, Jr.J.B. (1969) Economic geology of the platinum metals. Geol.Surv.U.S.Prof.Paper 630. 120p.

MIHALIK, P., HIEMSTRA, S.A., and DE VILLIERS, J.P.R.(1975) Rustenburgite and atokite, two new platinum-group minerals from the Merensky Reef, Bushveld Igneous Complex. Can.Mineral.13, 146-150.

MIHALIK, P.,JACOBSEN, J.B.E., and HIEMSTRA, S.A.(1974) Platinum group minerals from a hydrothermal environment. Econ. Geol. 69, 257-262.

MOLLY, E. (1928) Platinum-bearing deposits of Birbir. Schweizer Mineral.u Petrogr.Mitt. 8(1),240-257.

MOLLY, E. (1959) Platinum deposits of Ethiopia. Econ.Geol. 54, 467-477.

MUNSON, R.A. (1968) The synthesis of iridium disulphide and nickel diarsenide having the pyrite structure. Inorg. Chem.7,389-390.

NALDRETT, A.J., and CABRI, L.J.(1976) Ultramafic and related Mafic rocks: Their classification and genesis with special reference to the concentration of nickel sulphides and platinum-group elements. Econ. Geol. 71, 1131-1158.

NEWMAN, S.C. (1973) Platinum.Trans.Inst.Min.Met.82, Sect.A.A52-A68.

OFTEDAL, J. (1928) Z.fur Phys.Chem. 135, 129.

OTTEMANN, J., and AUGUSTITHIS, S.S. (1967) Geochemistry and origin of 'platinum nuggets' in lateritic covers from ultrabasic rocks and birbirites of W.Ethiopia. Mineralium Deposita 1, 269-277.

PAGE, N.L. (1971) Comments on the role of oxygen fugacity in the formation of immiscible sulfide liquids in the H.Chromitite Zone of the Stillwater Complex, Montana. Econ.Geol. 66, 607-610.

PAGE, N.J., and JACKSON, D.(1967) Preliminary report on sulfide and platinum-group minerals in the chromitites of the Stillwater Complex, Montana. U.S.Geol.Surv.Paper 575-D.D123-D126.

PENFIELD, S.L. (1889) The crystalline form of sperrylite. Am.J. Sci. 37, 71-73.

PHILIBERT, J. (1962) A method for calculating the absorption correction in electron-probe microanalysis. 3rd Int. Symposium X-Ray Optics, X-Ray Microanalysis (New York, Academic Press, 1963), p.379.

PXHENICHNII, G.N. (1961) Mode of occurrence and distribution pattern of tellurium in sulphide ores. Geochemistry, no. 8, 751-762.

RAMDOHR, P. (1969) The ore minerals and their intergrowths. London, Pergamon.

RANKAMA, K., and SAHAMA, T. (1950) Geochemistry (Chicago).

RAZIN, L.V. (1971) Problems of the origin of platinum metallization of forsterite dunites. Int.Geol.Rev. 13, 776-788.

RAZIN, L.V., and KHOMENKO, G.A.(1969) Accumulation of osmium and other platinum-group metals in chrome spinel in platinum-bearing units. Geochem.Int.6, 546-557.

RAZIN, L.V., KHVOSTOVA, V.P., and NOVIKOV, V.A. (1965) Platinum metals in the essential and accessory minerals of ultramafic rocks. Geochem. Int.2, 118-131.

RINGWOOD, A.E.(1955) The principles governing trace element distribution during magmatic crystallisation. Part 1: The influence of electronegativity. p.189-202. Part 2: The role of complex formation p.242-254. Geochim.et Cosmochim. Acta.7.

ROWE, J.J. (1969) Fractionation of gold in a differentiated tholeiitic dolerite. Chem.Geol. 4, 421-427.

RUCKLIDGE, J. (1969) Electron microprobe investigations of platinum metal minerals from Ontario. Can.Mineral.9, part 5.

RUCKLIDGE, J. (1971) Mobilisation of nickel and platinun metals during serpentinization of ultramafic rocks. Platinum Conf. Univ.Melbourne. (in Stumpfl,E.(1974) Min.Sci.Eng.p137).

SAMPSON, E. (1932) Magmatic chromite deposits in southern Africa. Econ.Geol. 27, 113-144.

SANTOKH SINGH, D. (1965) Measurement of reflectivity with the Reichert Microphotometer. Trans.Inst.Min.Met. 74, 901-916.

SCHMIDT, E.R.(1952) The structure and composition of the Merensky Reef and associated rocks on the Rustenburg Platinum Mine. Trans.Geol.Soc.S.Africa. 55, 233-279.

SCHNEIDERHOHN, H.(1929) The mineragraphy and spectrography of the sulphidic platinum ores of the Bushveld Complex. In P.A.Wagner: The Platinum Deposits and mines of S.Africa. 206-246.

SCHNEIDERHOHN, H.(1929) Central bl.fur Mineral.A,193-202.

SCHNEIDERHOHN, H.,and RAMDOHR, P.(1931) Lehrbuch der Erzmikroskopie. 2nd.Ed.Berlin.(in German).

SCHWELLNUS, J.S.I.,HIEMSTRA, S.A., and GASPARRINI, E.(1976) The Merensky Reef at the Atok Platinum mine and its environs. Econ. Geol. 71, 249-260.

SKINNER, B.J.,et al.(1976) Phase relations in the ternary portions of the system Pt-Pd-Fe-As-S. Econ.Geol. 71, 1469-1475.

SMIT, P.J.,HALES, A.L., AND GOUGH, D.I.(1962) The gravity survey of the Republic of South Africa. S.Africa Geol.Surv. Handbook 3. 354p.

SNETSINGER, K.G. (1971) A platinum-metal nugget from Trinity County, California. Am.Mineral. 56, 1101-1105.

SNETSINGER, K.G. (1971) Erlichmanite (OsS_2), a new mineral. Am. Mineral. 56, 1501-1506.

SNETSINGER, K.G. (1972) Osarsite, a new osmium-ruthenium sulf-arsenide from California. Am.Mineralogist. 57, 1029-1036.

SNETSINGER, K.G. (1973) Chromian aluminian magnetite and two rhodium alloys in a platinum nugget from Goodnews Bay, Alaska. Am.Mineral. 58, 189-194.

SPENCER, L.J. (1926) Sperrylite from Potgietersrust.Mineral.Mag. p.94-97.

SPENCER, L.J.(1932) Notes on platinum group minerals from Potgietersrust and Rustenburg districts, Transvaal. Discussion of paper by Adam,H.R. Proc.Geol.Soc.S.Africa. p.152-153.

SPRY, A. (1974) Metamorphic Textures.Pergamon Press.

STRUNZ, H.(1970) Mineralogische Tabellen.Leipzig.

STUMPFL, E.F.(1961) Some aspects of the genesis of platinum deposits. Econ.Geol. 57, 619-623.

STUMPFL, E.F.(1961) Some new platinoid-rich minerals, identified with the electron microanalyser. Min.Mag. 32, 833-847.

STUMPFL, E.F.(1967) On the occurrence of native platinum with copper sulphides at Congo Dam, Sierra Leone. Inst.Geol.Sci. Overseas Div.,Min.Resources Sect.reprint from Overseas Geol. Mineral Resources 1966, 10, 1-10.

STUMPFL, E.F.(1972) Compositional variations in the hollingworthite-irarsite group. Neues Jahrb.Mineral. 9, 406-415.

STUMPFL, E.F. (1974) The genesis of platinum deposits:Further thoughts. Minerals Sci.Eng. 6, 120-141.

STUMPFL, E.F.,and CLARK,A.M.(1965) Electron-probe microanalysis of gold-platinoid concentrates from southeast Borneo. Trans.Inst. Min.Met. 74, 933-946.

STUMPFL, E.F., AND CLARK, A.H. (1965) Hollingworthite, a new rhodium mineral, identified by electron probe microanalysis. Am. Mineral. 50, 1068-1074.

STUMPFL, E.F.,and TARKIAN, M.(1973) Natural osmium-iridium alloys and iron-bearing platinum:new electron-probe and optical data. Neues Jahrb.Mineral. 7/8,313-322.

STUMPFL, E.F.,and TARKIAN, M.(1976) Platinum genesis: new mineralogical evidence. Econ.Geol. 71, 1451-1460.

SUN, W.-C.et.al. Acta Geol.Sinica.no.1, 89-93 (in Chinese).

SUTARNO, O.K.,and REID, K.I.(1967) Chalcogenides of the transition elements.V.Crystal structures of the disulphides and ditellurides of ruthenium and osmium.Can.J.Chem.45, 1391-1400.

TARKIAN, M.,and STUMPFL, E.F.(1974) (Pt,Pd)(Bi,Sb), a new mineral. Neues Jahrb.Mineral. 11, 514-517.

TARKIAN, M.,and STUMPFL, E.F.(1975) Platinum mineralogy of the Dreikop mine, S.Africa. Mineralium Deposita. 10, 71-85.

TAUSON, L.V.(1965) Factors in the distribution of the trace elements during the crystallisation of magmas. Physics and Chemistry of the Earth.vol. 6, 215-249.

TAYLOR, S.R.(1965) The application of trace element data to problems in petrology. Ibid.p.133-213.

THEISEN, R.(1961) Analyse d'une methode de calculs de correction de microanalyseur electronique.Euratom Pub. EUR 11.

THOMASSEN, L.(1929) Uber die kristallstrukturen einiger binarer verbindungun der platinmetalle. Zeitschr. Physik. Chemie. B2, 349-379.

TOMA, S. (1975) Mineralogical studies on some synthetic alloys and minerals of the platinoid group. Unpub. PhD thesis (Leeds).

ULMER, G.C. (1969) Experimental investigations of chromite spinels. Econ.Geol.Monograph 4, 114-131.

UYTENBOGAARDT, W.(1968) Tables for microscopic identification of ore minerals.(Facsimile of 1951 edition). Hafner Pub.Co.London.

UYTENBOGAARDT, W., and BURKE, E.A.J.(1971) Tables for microscopic identification of ore minerals. Second Revised Ed. Elsevier Pub.Co.London.

VAN ZYL, J.P.(1970) The petrology of the Merensky Reef and the associated rocks on Swarklip 988, Rustenburg district. Geol. Soc.S.Africa. Spec.pub.1, 80-107.

VAUGHAN, D.J.(1969) Nickelian mackinawite from Vlackfontein, Transvaal. Am.Mineral. 54, 1190-1192.

VERMAAK, C.F.(1970) The geology of the lower portion of the Bushveld Complex and its relationship to the floor rocks in the area west of the Pilanesberg, Western Transvaal. Trans.Geol. Soc.S.Africa.Spec.Pub. 1, 242-265.

VERMAAK, C.F.(1976) The Merensky Reef - Thought on its environment and genesis. Econ.Geol. 71, 1270-1298.

VERMAAK, C.F.,and HENDRIKS, L.P.(1976) A review of the mineralogy of the Merensky Reef, with special reference to new data on the precious metal mineralogy.Econ.Geol. 71, 1244-1269.

VISSER, DJ.L.(1957) The structural evolution of the Union. Geol. Soc.S.Africa. Proc. 60, 103-159.

WAGNER, P.A.(1924) Magmatic nickel deposits of the Bushveld Complex in the Rustenburg district, Transvaal. Geol.Surv.S.Africa Memoir no. 21. 181p.

WAGNER, P.A.(1929) The Platinum Deposits and Mines of South Africa. Edinburgh, Oliver and Boyd.

WARTENWEILER (1928) In discussion of paper by Cooper. J.Chem.Met. Min.Soc.S.Africa. 28, p281.

WELLS, H.L.(1889) Sperrylite, a new mineral. Am.J.Sci. 37, 67-70

WILLEMSE, J.(1959) The "floor" of the Bushveld igneous complex and its relationships, with special reference to the eastern Transvaal (Presidential Address),Geol.Soc.S.Africa Proc. 62.

WILLEMSE, J.(1964) A brief outline of the geology of the Bushveld Igneous Complex. In 'The Geology of Some Ore Deposits of Southern Africa'.Geol.Soc.S.Africa. 2, 91-128.

WILLEMSE, J.(1969) The geology of the Bushveld Igneous Complex, the largest repository of magmatic ore deposits in the World.Econ. Geol.Monograph 4.pp.1-22.

WILLIAMS, K.L.(1962) The preparation of small powder samples from thin and polished sections. Am.Mineral. 47.

WISE, E.M.(1953) in 'The Platinum Metals' by C.C.Allen. Can.Dep. Mines and Tech.Surv.Min.Resources Div.,Min.Rep.3, 1960, 68p.

WOHLER, F.(1866) Ueber ein neues Mineral von Borneo: Laurit. Gesch. Wiss.Gottingen Nachr. pp.155-160.

WRIGHT, T.L., and FLEISCHER, M. (1965) Geochemistry of the Platinum Metals. Bull.U.S.Geol.Surv.no.1214-A, 23p.

YOUNG, B.B.,and MILLMAN, A.P.(1964) Microhardness and deformation characteristics of ore minerals. Trans.Inst.Min.Met.73, 437-466.

YUSHKO-ZAKHAROVA, O.Ye.,BYKOV,VYKOV,V.P.,KULAGOV,E.A.,AVDONIN,A.S. CHERNYAYEV,L.A.,and YURKINA,K.V.(1970) Isomorphism in the platinum metals. Geochem.Int. 7, 788-796.

YUSHKO-ZAKHAROVA, O.Ye.,IVANOV,V.V.,RAZINA,I.S.,and CHARNYAYEV, L.A.(1967) Geochemistry of Platinum Metals. Geochem.Int. 4, 1106-1118.

ZAR'YAN,R.N.(1962) Selenium and tellurium in ores of the Kafan deposit. Geochemistry no.3.267-274.

ZEMANN, J.(1969) Handbook of Geochemistry.Ed.Wedepohl, K.H. vol. I,chap.2, 12-36.

ZHURAVLEV, N.N.,GENKIN, A.D., and STEPANOVA, A.A.(1968) O rentgenometricheskikh osobennostiyakh Noril'skoge kuperita.Zap. Vses.Mineral.Obshch. 97, 85-88.

ZIEBOLD, T.O.,and OGILVIE, R.E.(1964) an empirical method for electron microanalysis. Anal.Chem. 36, 322-327.

Reprinted from the *Mineralogical Magazine*, London, June 1966,
Vol. 35, pp. 815–834

The occurrence of platinoid bismuthotellurides in the Merensky Reef at Rustenburg platinum mine in the western Bushveld

By G. A. KINGSTON

Department of Mining Geology, Imperial College of Science and Technology, London S.W.7

(With Plate XII)

[Read 29 April 1965]

Summary. Four different palladium and platinum bismuthotellurides, one containing major mercury, have been identified in the ore from Rustenburg mine on the Merensky Reef. The composition of each phase was determined by electron-probe microanalysis, and X-ray powder data are presented for three of these phases. Quantitative spectral reflectivity values at 470, 546, 589, and 650 mμ were obtained on areas of 1–10μ. Similar phases have been located in the ore from Union mine.

Two of these phases are shown to be moncheïte and kotulskite. From two electron-probe microanalyses, kotulskite is shown to be Pd(Te,Bi). The other two phases are new minerals: analysis of one of them gives the composition $(Pd,Pt)(Te,Bi)_2$, containing 23·1 % Pd, 1·8 % Pt, 50·8 % Te, 14·2 % Bi, with strongest X-ray powder lines at 2·92 (10), 2·10 (6), 2·02 (3), and 1·54 Å (3), and cell parameters a 3·978 ± 0·001, c 5·125 ± 0·002; it is probably isostructural with moncheïte, and an isomorphous series may exist between them; the name *merenskyite* is proposed for this mineral, after Dr. Hans Merensky who was mainly responsible for discovering the platinoid bearing 'reef'; it is commonly intergrown with kotulskite. For the second new phase (*Mineral A*), no X-ray data could be obtained, but a single electron-probe microanalysis gave a composition of Pd 27·8 %, Hg 12 %, Te 38·5 % and Bi 1·6 % suggesting the empirical formula (Pd,Hg)(Te,Bi).

THE Merensky Reef, named after the geologist Dr. Hans Merensky who was responsible for the prospecting programme that led to its discovery in 1924, is a layer of feldspathic pyroxenite containing economic amounts of copper, nickel, and platinoid elements. It occurs in the lower part of the intrusive norite or mafic zone of the Bushveld Igneous Complex, which is a vast composite body of extrusive, hypabyssal, and plutonic rocks in the central Transvaal of South Africa. The Merensky Reef or Merensky Horizon forms a generally continuous layer that has been located and followed around most of the norite outcrop. It is at present being exploited in the western sector of this mafic zone at Rustenburg mine, about 50 miles west of Pretoria, and also at Union mine, 55 miles north of Rustenburg and about 6 miles west of Northam.

The Merensky Reef at Rustenburg is a composite layer at the base of which is a thin chromite band, resting on an undulating but sharp contact with the footwall spotted anorthositic norite. The chromite band, about one inch in thickness, grades rapidly up into a coarse feldspathic pyroxenite commonly known to those exploiting this horizon as the 'Reef', averaging about one foot in thickness. The Reef or pegmatoid (as suggested by Willemse (1964)) contains disseminated interstitial segregations of copper–iron–nickel sulphides with which the platinum group minerals are commonly associated. At or near the top of the Reef is found a thin irregular and discontinuous chromite band of about $\frac{1}{4}$ in. thickness. The Reef or pegmatoid is overlain by a less coarse feldspathic pyroxenite known to the miners as the 'Merensky'. The contact between the two is sometimes sharp and sometimes gradational. The 'Merensky' pyroxenite is also gradational into the overlying hanging-wall spotted anorthosite, although generally the top of it is about two feet above the Reef.

In the northern outcrop of the Merensky Reef at Union mine these units are still present although considerably thicker. The bottom one-inch thick chromite band, resting on the undulating surface of the footwall spotted anorthosite, is overlain by a very coarse feldspathic pyroxenite of 10 to 18 feet in thickness that can be equated to the 'Reef' pegmatoid at Rustenburg. A continuous one-inch thick chromite band occurs at the top of this coarse pyroxenite, and is overlain by up to 20 feet of a finer grained pyroxenite similar to the 'Merensky' pyroxenite at Rustenburg. This grades upwards, after about 75 feet, into a spotted anorthosite. It is of interest to note that whereas at Rustenburg mine the entire width of the pegmatoid, including the top and bottom chromite bands, is mined, at Union mine a combination of the great width of the pegmatoid and the generally much lower platinoid content of the bottom chromite seam renders the extraction of the whole 'Reef' uneconomic (Beath, Cousins, and Westwood, 1961). Fairly typical geological sections through the Merensky Reef at Rustenburg and Union mines are illustrated in fig. 1.

Up to the commencement of the author's investigations in 1962, the platinoid mineralogy of the Merensky Reef was generally thought to be fairly simple, consisting of five or six major platinoid minerals together with a large proportion of platinum metal content accounted for by Schneiderhohn (1929) as occurring in solid solution in the base metal sulphides pyrite, pyrrhotine, pentlandite, and chalcopyrite. However workers on other platiniferous deposits, in particular Stumpfl (1961),

Borovskii *et al.* (1959), and Genkin *et al.* (1961, 1963), have described a great variety of new platinoid minerals and it was thus reasonable to suspect that many of these new phases, together with other unreported ones, were present in the Merensky Reef. During the present study all the previously recorded platinoid minerals from this deposit have been

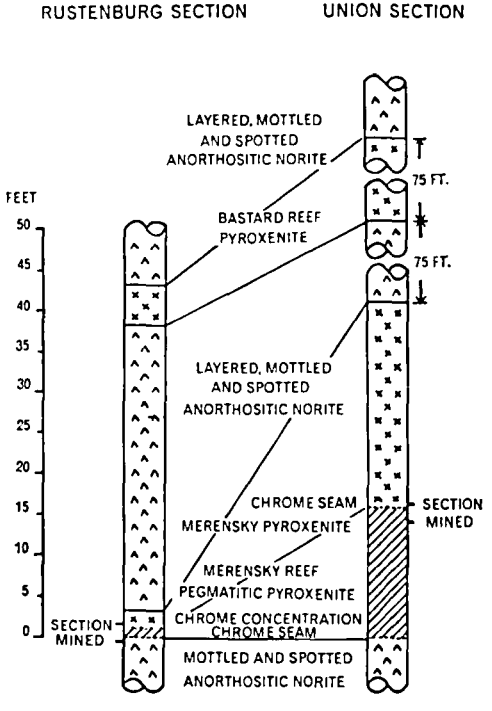

FIG. 1. Geological sections through the Merensky Reef zone at Rustenburg and Union mines (after Beath, Cousins, and Westwood, 1961).

recognized, and their identification confirmed with the electron-probe microanalyser and X-ray powder analysis. A number of new phases were identified, the most interesting of which are the platinoid bismuthotellurides. The frequencies of occurrence of the platinoid minerals in polished sections of the ore from Rustenburg mine and Union mine are:

	Rustenburg	*Union*
ferroplatinum (Pt,Fe)	minor	common
palladic gold (Au,Pd)	rare	rare

	Rustenburg	*Union*
palladic electrum (Au,Ag,Pd)	minor	minor
cooperite PtS	common	minor
braggite (Pt,Pd,Ni)S	common	minor
laurite RuS_2	rare	common
sperrylite $PtAs_2$	minor	minor
arsenopalladinite Pd_3As	v. rare	not located
stibiopalladinite Pd_xSb	v. rare	not located
moncheïte $(Pt,Pd)(Te,Bi)_2$	rare	rare
kotulskite Pd(Te,Bi)	rare	rare
merenskyite $(Pd,Pt)(Te,Bi)_2$	rare	rare
mineral A $(Pd,Hg)_x(Te,Bi)_y$	v. rare	not located

More phases are undoubtedly present. Iridium, osmium, and rhodium are known to be present in appreciable quantities but have not yet been detected as separate mineral phases in the ore although minor quantities do occur in most of the above minerals.

Determinative techniques

Electron-probe microanalysis. The electron-probe microanalyser used in this study is a Cambridge Microscan Mark 1. This is a scanning analyser with a vertically incident electron beam and X-ray detection at an angle of 20° to the surface of the specimen. It does not have paraxial optics, but positioning is facilitated by the use of a back-scattered electron image also obtained at an angle of 20° to the surface.

The counts for the characteristic radiation are detected with a semi-focusing spectrometer that incorporates a flow-proportional counter with a 'dead time' of 5 μsec. A pulse-height analyser is used for discrimination against unwanted noise while scanning photographs are being taken, but it is rarely used while counting in order to avoid errors due to pulse-height depression.

The count rates were corrected for statistical errors due to the 'dead time' of the electronics, and also for counts due to the background radiation. The apparent mass percentages given by these corrected count rates were further corrected to allow for the following phenomena: absorption of the characteristic X-rays by the matrix (using the method proposed by Philibert (1962)); fluorescence produced by the characteristic radiation (using Castaing's formula (1951)); the effect of the difference in atomic number of the constituent atoms of the mineral (using Ziebold's correction method (1964)); and a correction for overvoltage was made by a modification to Philibert's formula made by Duncumb (1964). Background fluorescence effects were ignored. The values of the absorption coefficients used in the above corrections were those given by Kelly (1966).

The standards used in the present investigation were an analysed 50/50 Pt:Pd alloy (kindly given by Johnson and Matthey & Co., Ltd.), an analysed specimen of calaverite, $(Au,Ag)Te_2$, for tellurium, an analysed specimen of coloradoite, HgTe,

for mercury determinations, and spectrographically pure bismuth. All specimens for analysis were polished using diamond abrasives on cloth laps as described by Barringer (1953). They were subsequently cut down to size and coated with a 50–75 Å thick film of aluminium to render the surface electrically conducting to the electron beam.

X-ray diffraction. In this particular investigation a procedure was required which would enable a very small (0·3–0·01 mm) and previously analysed grain to be extracted, with minimum contamination from the enclosing silicates and sulphides, and to be suitably mounted for X-ray powder analysis. A steel needle, a tungsten carbide pick, and a microdrill were found too unmanageable and not practical for extracting such small grains. However, by using a diamond marker in the way described by Williams (1962) it was found that with practice very small areas can be removed with some precision. A method devised by A. P. Millman (*pers. comm.*), which entails using the Leitz Durimet microscope fitted with a standard Leitz wedge-type scratch diamond, was found to have a much greater precision of positioning.

The diamond, after being lowered on to the required spot, is moved, using the micrometer stage, in the opposite direction to the normal one used for scratch purposes. A mound of mineral powder is formed at the end of the scratch, the length of which can be very precisely controlled. The mineral powder is mounted as follows: a clean glass slide is taken and a spot of 'Cow' gum or other rubber solution is allowed to adhere to it; the slide is then inverted and held over the polished section whilst still observing the powdered area under the ore microscope with a low-power objective (some refocussing is required because of the intervening glass slide); the rubber-cement spot, which can now be seen through the back of the glass, is lowered on to the powdered area to engulf the fragments of broken mineral. After a short while the solvent begins to evaporate and the cement can be rolled into a ball containing the mineral powder. The slide and adhering rubber ball are then raised from the surface of the polished section. Further grinding of the powder can be accomplished between two slides, as described by Hiemstra (1956), followed by the mounting of the ball on the end of a glass fibre. The ball should generally not be greater than 0·5 mm in diameter. The larger the ball the more scattering of X-rays occurs with consequent fogging of the film. An X-ray photograph of a globule of pure cement should be taken first since some varieties yield lines in the front reflection region.

Before destroying the rare mineral grains of these bismuthotellurides some preliminary experiments, similar to those by Hiemstra (1956), and Genkin and Korolev (1961), were carried out on cleavage fragments of galena to determine approximately the minimum quantity of material required to produce a distinct powder pattern. It was found that a cleavage fragment of dimensions $0{\cdot}06 \times 0{\cdot}05 \times 0{\cdot}025$ mm and of approximate weight 0·6 μg produced a weak but measurable pattern.

Spectral reflectivity measurements. Quantitative spectral reflectivity values at wavelengths of 470, 546, 589, and 650 mμ were obtained with the Reichert reflex spectral microphotometer, which incorporates a

photomultiplier tube and wedge dielectric filter. A description of this together with the results of standardization experiments are given by Santokh Singh (1965). This instrument enables rapid and accurate spectral reflectivity measurements to be made on areas down to 1 μ diameter and is invaluable for routine determinative work on opaque minerals. In the present context the size of the area used for any particular mineral grain corresponded to the maximum flawless and flat area available and ranged from 1 to 10μ diameter. The rarity of grains of a suitable size and having a flat area limited the number of reflectivity values that could be made.

The author is indebted to S. H. U. Bowie of the Atomic Energy Division for the loan of an N.P.L. Measured pyrite (N.1915.1), which was used in the present study as a standard.

Indentation microhardness values were obtained where possible with a Durimet hardness tester fitted with a Vickers diamond, as described by Young and Millman (1964). Because of the general by small grain size of these platinoid bismuthotelluride phases in polished sections of the ore, only a 15 g load could be used to produce a reliable indentation value. The relative hardness, deduced from the polishing relief, was assessed for each phase.

Bismuthotellurides of platinum and palladium

Although this is the first time that platinoid minerals of tellurium and bismuth have been found and described in the Merensky Reef, the presence of a Pd–Bi–Te compound was demonstrated in 1952 by chemical analyses of a non-magnetic portion of a concentrate from the northern extension of this horizon at Union Mine by F. M. Lever, R. Todd, and A. R. Powell of Johnson and Matthey Ltd. (*pers. comm.*). In 1962, in a preliminary investigation of the platinoid minerals with the electron-probe microanalyser, the author found a number of white strongly anisotropic laths, occurring in chalcopyrite and at the margins of the iron–copper–nickel sulphide segregations, to be bismuthotellurides of platinum and palladium. No X-ray powder data at that time could be obtained for any of these phases because of their small size. Meanwhile in 1961 Genkin and Korolev, in a paper describing a procedure for the identification of small mineral grains by X-ray powder analysis and microspectrographic methods, described the occurrence of similar phases from the Monchegorsk deposit. In 1963 Genkin *et al.* defined these minerals more precisely, naming two of them *moncheïte*, $(Pt,Pd)(Te,Bi)_2$, and *kotulskite*, $Pd(Te,Bi)_{1-2}$, as well as giving more data on *michenerite*,

$PdBi_2$, which was shown to contain tellurium as a major constituent. Recently Stumpfl (*pers. comm.* 1965) has also detected by electron-probe microanalysis the presence of a platinum bismuthotelluride from the Dreikop platinum pipe in the eastern Bushveld.

The results of the present study confirm the presence of moncheïte and kotulskite in the Merensky Reef at Rustenburg mine. Two other bismuthotellurides are shown to be new platinoid phases: one of composition $(Pd,Pt)(Te,Bi)_2$, named *merenskyite* after Dr. Hans Merensky, is possibly isostructural with moncheïte and an isomorphous series may exist between the palladium and platinum end members; the second new phase (*Mineral A*), for which no X-ray data are yet available, is a grey isotropic mineral having a composition close to (Pd,Hg)(Te,Bi). A preliminary investigation of the ore from Union mine has also revealed the presence of moncheïte and a palladium bismuthotelluride phase optically similar to merenskyite. A more detailed electron-probe study has still to be completed. It is hoped that more occurrences of these phases will be found at Union mine so that a comprehensive study can be made of them.

These bismuthotellurides occur late in the paragenesis as equant grains 1–3μ in size enclosed partially or completely by chalcopyrite and occasionally pentlandite (pl. XII, fig. A). Larger euhedral to subhedral lamellae of 0·3 to 0·6 mm are more rarely found. Often clusters of small grains are to be found isolated in microveinlets in the silicates together with disseminated blebs of chalcopyrite. Except for the mercury phase (*Mineral A*) all these platinoid minerals are white to cream in colour, are anisotropic, and crystallize in the hexagonal system.

Moncheïte

Moncheïte (Genkin *et al.* 1961, 1963) was reported to occur as minute grains in chalcopyrite, pyrrhotine, and occasionally violarite in the upper sectors of vertical veins of the Monchegorsk platinum deposits, commonly intergrown with michenerite and kotulskite. Moncheïte from the Merensky Reef at Rustenburg mine is similarly associated with kotulskite and other platinum tellurides enclosed by or adjoining chalcopyrite. Generally it is in the form of blebs or fine laths of the order of 1 to 10μ in size (pl. XII, fig. A). Only one large lath of sufficient size to enable its extraction for X-ray powder analysis ($200 \times 60\mu$) has so far been located. This occurred at a sulphide: silicate contact as a subhedral lath penetrating pyrrhotine along a pentlandite: pyrrhotine boundary (fig. 2); pl. XII, fig. D).

Optical and physical properties. Moncheïte from Rustenburg is a bright

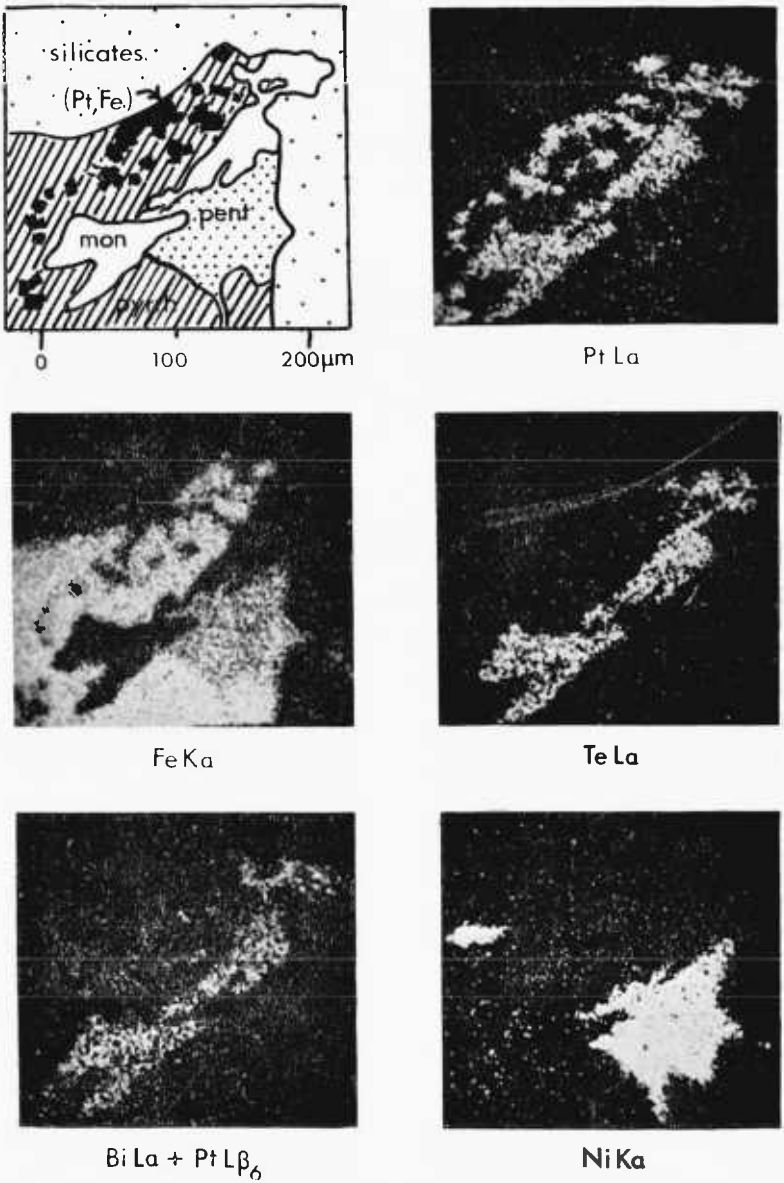

FIG. 2. X-ray scanning micrographs showing the distribution of platinum, iron, tellurium, bismuth, and nickel in an intergrowth of moncheïte $Pt(Te,Bi)_2$ (mon) and ferroplatinum (Pt,Fe) in pyrrhotine (pyrrh) and pentlandite (pent) in a polished section of the 'Reef' pyroxenite.

greyish-white mineral showing weak pleochroism in air. Under oil immersion it is a light grey and exhibits a distinct pleochroism. Compared with ferroplatinum it appears more grey and less creamy especially under oil. When enclosed by braggite it appears greyish white but is a bright white against chalcopyrite. Its anistropy is from distinct to strong in air, according to orientation with light yellowish brown to dark brown polarization colours. Although a reliable indentation microhardness measurement was not obtained, it was seen to be approximately of the same hardness as pentlandite when applying the pseudo-Becke line test. Its reflectivity in sodium light, by visual comparison, was between pentlandite and ferroplatinum and very much greater than braggite or cooperite. Accurate measurements are given in table II. The measurements were made in air using a ×60 objective and 2 mm mirror diaphragm. Two of the largest grains were measured.

Composition. The results of quantitative microspectrographic analyses of four grains of moncheïte from the Monchegorsk deposit by Genkin *et al.*, and the results of electron-probe microanalyses of moncheïte from Rustenburg are tabulated for comparison in table I. The analyses 1, 2, 3, and 4 were under conditions of constant specimen-current, and after correction for absorption, using a correction procedure by Tong (*pers. comm.*), they were still far from satisfactory but sufficiently accurate to illustrate substitutional trends in the moncheïte members.

One of the grains (table I, anal. 3; pl. XII, fig. D; fig. 2), confirmed by X-ray powder analysis to be moncheïte, was reanalysed at constant beam-current. The analysis was corrected for absorption, atomic number and fluorescence by the method previously outlined. This is presented in table I under analysis 5. The empirical formula from this approximates to that of the type moncheïte, $(Pt,Pd)(Te,Bi)_2$.

The X-ray data for the Rustenburg moncheïte are given in table II together with the type moncheïte and the probable palladium end-member merenskyite. The unindexed spacings may be due in part to contamination by pyrrhotine and pentlandite during extraction from the polished section. Of the eleven indexed lines, nine agree closely with those for the type moncheïte. The discrepancies in intensity towards the back reflection region are probably the result of the minute quantity of powder available and also possible disorder in the lattice.

Kotulskite

Kotulskite was first reported from the Monchegorsk deposit by Genkin *et al.* (1961, 1963) and an approximate formula given, $Pd(Te,Bi)_{1-2}$.

TABLE I. Results of electron-probe microanalyses and reflectivity values of some platinoid bismuthotellurides from Rustenburg Mine, and quantitative microspectrographic analyses of moncheïte and kotulskite from the Monchegorsk deposit by Genkin *etal.*, 1963.

	Moncheïte									*Kotulskite*						
	Rustenburg					*Monchegorsk*				*Rustenburg*		*Monchegorsk*	*Merenskyite Rustenburg*		*Mineral A Rustenburg*	*Mineral C Rustenburg*
Element	1	2	3	4	5	6	7	8	9	10	11	12	13	14	15	16
% *before correction*																
Pt	17·2	26·2	34·9	39·4	41·0					—	1·0		1·5	—	—	1·2
Pd	6·7	2·5	—	—	—					56·8	47·0		27·5	40·7	31·5	30·0
Bi	9·9	7·2	16·7	17·0	16·0					18·3	21·0		14·2	15·7	1·5	29·6
Te	38·6	39·8	30·8	35·6	45·0					32·1	31·0		50·2	54·0	35·3	17·2
Hg	—	—	—	—	—					—	—		—	—	11·9	—
(Fe,Cu,Ni)	5·0	6·0	3·0	3·0	—					—	—		—	—	—	trace
% *after correction*																
Pt	18·6	28·4	37·0	42·0	38·4	22·3	27·4	25·9	30·8	—	1·1	—	1·8	—	—	1·3
Pd	9·3	3·7	—	—	—	7·0	9·2	6·9	4·6	45·9	38·8	31·1	23·1	33·2	27·8	40·0
Bi	10·2	7·5	17·0	17·0	16·2	31·7	29·9	12·9	9·2	17·2	20·1	24·9	14·2	15·1	1·6	30·6
Te	40·3	40·7	35·1	35·3	45·8	39·0	33·5	54·3	55·4	38·0	36·1	44·0	50·8	56·3	38·5	23·3
Hg	—	—	—	—	—	—	—	—	—	—	—	—	—	—	12·0	—
(Fe,Cu,Ni)	7·0	8·0	3·0	3·0	—	—	—	—	—	—	—		—	—	—	trace
Reflectivity %																
λ mμ																
470	—	53·0	—	—	53·9	—	—	—	—	55·1	53·0	—	61·8	60·9	48·8	—
		56·8			56·5					57·3	53·4		62·2	61·4		
546	—	53·2	—	—	53·7	—	—	—	—	60·9	58·7	—	64·3	63·2	53·3	—
		58·8			56·6					64·4	61·1		65·2	64·4		
589	—	52·9	—	—	53·3		←	56 60	→	63·3	61·7	66 %	65·7	64·4	55·6	—
		58·1			56·1					65·6	63·2	max.	67·0	66·0		
650	—	52·7	—	—	52·7	—	—	—	—	65·2	64·1	—	65·9	64·3	53·9	—
		59·6			54·9					67·9	66·2		67·4	66·6		

TABLE II. X-ray powder data for moncheïte $(Pt,Pd)(Te,Bi)_2$ and merenskyite $(Pd,Pt)(Te,Bi)_2$ from Rustenburg mine (Cu radiation, Ni filter and 11·483 cm and 6 cm diameter cameras respectively), and for moncheïte from Monchegorsk (Genkin *et al.*, 1963) and artificial $PdTe_2$ (Thomassen, 1929)

	Moncheïte					*Merenskyite*				*Artificial $PdTe_2$*		
	Rustenburg			*Monchegorsk*								
Hexagonal cells	*a* 4·062 ±0·002	*c* 5·346 ±0·003		*a* 4·049 ±0·004	*c* 5·288 ±0·005	*a* 3·978 ±0·001		*c* 5·125 ±0·002		*a* 4·028 ±0·003	*c* 5·118 ±0·004	
hkil	*d calc.*	*d obs.*	*I obs.*	*d obs.*	*I obs.*	*hkil*	*d calc.*	*d obs.*	*I obs.*	*hkil*	*d obs.*	*I obs.*
0001*	5·325	5·25	50	5·32	60	—	—	—	—	—	—	—
—	—	3·02	40	3·07	20	—	—	3·07	30	—	—	—
$10\bar{1}1$*	2·932	2·94	100	2·93	100	$10\bar{1}1$*	2·921	2·92	100	$10\bar{1}1$	2·89	60
—	—	2·73	10	—	—	—	—	—	—	—	—	—
0002	—	—	—	2·66	10	—	—	2·51	20	0002	2·56	20
$10\bar{1}2$*	2·124	2·12	60	2·11	80	$10\bar{1}2$*	2·088	2·10	60	$10\bar{1}2$	2·07	60
—	—	2·08	20	—	—	—	—	—	—	—	—	—
$11\bar{2}0$*	2·028	2·03	60	2·02	70	$11\bar{2}0$*	2·015	2·02	30	$11\bar{2}0$	2·02	40
$11\bar{2}1$*	1·896	1·885	20	1·888	40	—	—	—	—	—	—	—
—	—	1·798	40	1·712	20	—	—	—	—	—	—	—
0003	—	—	—	—	—	0003*	1·726	1·73	20	0003	1·71	20
—	—	1·728	30	—	—	—	—	—	—	—	—	—
$20\bar{2}1$*	1·668	1·668	40	1·664	60	—	—	1·67	30	$20\bar{2}1$	1·65	30
$10\bar{1}3$*	1·587	1·588	20	1·575	50	—	—	1·61	20	$11\bar{2}2$	1·59	20
—	—	1·534	20	—	—	$10\bar{1}3$*	1·543	1·54	30	$10\bar{1}3$	1·54	70
$20\bar{2}2$*	1·467	1·471	20	1·462	70	—	—	1·46	10	$20\bar{2}2$	1·44	50
0004	—	—	—	1·324	40	—	—	—	—	—	—	—
$21\bar{3}0$*	1·328	1·328	20	—	—	—	—	1·39	10	$11\bar{2}3$	1·30	20
$21\bar{3}1$*	1·289	1·289	40	1·282	70	0004*	1·288	1·29	10	0004	1·28	80
$20\bar{2}3$	—	—	—	1·242	30							
$10\bar{1}4$*	1·247	1·248	10	—	—							
$21\bar{3}2$	—	—	—	1·182	50							

* These indices were checked, assuming a hexagonal symmetry, using a modified version of a computer programme by W. D. Hoff *et al.* (1965). In this programme the indices were accepted if $|(\sin^2\theta_o - \sin^2\theta_c)| \leqslant 0{\cdot}003$. The drift constant K (Hess, 1951) was assumed proportional to $\frac{1}{2}(\cos^2\theta/\sin\theta + \cos^2\theta/\theta)$. Standard deviations of a and c were also determined. All reflections indexed were included in the determination of the cell parameters.

A similar phase from Rustenburg mine, considered to be kotulskite from the evidence of the X-ray powder data (table III), is shown to be Pd(Te,Bi) from two accurate quantitative electron-probe microanalyses. Kotulskite occurs in the Monchegorsk platinum deposit intergrown with moncheite and michenerite, and as separate grains enclosed

TABLE III. X-ray powder data for kotulskite (Pd,Pt)(Te,Bi) from Rustenburg mine (copper radiation, Ni filter and 11·483 cm diameter camera), kotulskite $Pd(Te,Bi)_{1-2}$ from Monchegorsk (Genkin *et al.*, 1963), and artificial PdTe (Thomassen, 1929)

	Kotulskite						*Artificial PdTe*	
	Rustenburg			*Monchegorsk*				
	a	*c*		*a*	*c*		*a*	*c*
Hexagonal cell	4·145 ±0·005	5·67 ±0·01		4·19 ±0·01	5·67 ±0·01		4·127 ±0·004	5·663 ±0·005
hkil	*d calc.*	*d obs.*	*I obs.*	*hkil*	*d obs.*	*I obs.*	*d obs.*	*I obs.*
†	—	—	—	$10\bar{1}0$	3·65	30	3·58	10
$10\bar{1}1$*	3·032	3·03	100	$10\bar{1}1$	3·05	100	3·03	40
—	—	—	—	0002	2·85	10	—	—
$10\bar{1}2$*	2·224	2·22	90	$10\bar{1}2$	2·24	90	2·22	80
$11\bar{2}0$*	2·071	2·08	70	$11\bar{2}0$	2·09	90	2·07	60
$20\bar{2}1$*	1·711	1·72	20	$20\bar{2}1$	1·73	60	1·71	40
$10\bar{1}3$*	1·671	1·67	20	$10\bar{1}3$	1·68	60	1·67	50
$11\bar{2}2$	1·672							
$20\bar{2}2$*	1·515	1·52	30	$20\bar{2}2$	1·53	70	1·51	80
—	—	1·41	5	0004	1·42	20	1·42	25
$10\bar{1}4$*	1·318	1·32	10	$10\bar{1}4$	1·33	70	1·32	50
$21\bar{3}2$	1·319							
—	—	1·23	10	$20\bar{2}3$	1·31	30	1·30	25
$30\bar{3}1$	1·170	1·17	10	$21\bar{3}2$	1·24	80	1·22	100
$11\bar{2}4$*	1·169							
				$30\bar{3}0$	1·19	70	1·21	50
				$20\bar{2}4$	1·17	80	1·17	100

* See footnote to table II. † Strong blackening of the film in this region due to rubber.

in chalcopyrite. At Rustenburg mine it also occurs enclosed by or adjoining chalcopyrite, especially at the periphery of the chalcopyrite where it abuts against the silicates. It is along the sulphide–silicate boundaries that the larger grains of this phase and the other tellurides occur. Kotulskite is also invariably intergrown with the new palladium bismuthotelluride, *merenskyite*, which occasionally replaces it but often shows mutual boundary relationships (fig. 3; pl. XII, fig. c).

Optical and physical properties. Kotulskite from Rustenburg is a cream or pale yellow mineral in air and exhibits a distinct pleochroism from a light cream to a slightly darker greyish cream. In oil it appears more yellow and the pleochroism is more distinct. Moncheite and merenskyite compared with pale yellow kotulskite appear white and are easily distinguished. Chalcopyrite against kotulskite appears greenish yellow. It exhibits a strong anisotropy with polarization effects from grey to dark bluish grey with the nicols completely crossed. Its polishing relief, com-

pared with associated minerals, indicated it to be harder than chalcopyrite and softer than pentlandite and merenskyite. One grain of this phase was large enough to obtain two Vickers indentation microhardness values using a 15 g load. The average of the two indentations gave a value of $VMH_{15} = 236$. The indentation shape for kotulskite was symmetrical with no fractures and straight to very weakly concave sides. Accurate quantitative measurements of reflectivity are given in table I. The measurements were made in air using a $\times 32$ objective and 2 mm mirror diaphragm.

Composition. Two grains of kotulskite from Rustenburg mine were quantitatively analysed with the electron-probe microanalyser using constant beam-current conditions, and the initial percentages were corrected for absorption, atomic number, and fluorescence as outlined previously. The results are presented in table I together with the semi-quantitative microspectrographic analysis of kotulskite from Monchegorsk by Genkin *et al.* X-ray scanning micrographs showing the distribution of palladium, tellurium, and bismuth in an intergrowth of kotulskite and merenskyite are presented in fig. 3.

A phase, Mineral C, with similar optical and physical properties to kotulskite, and which with stibiopalladinite formed a small composite grain of about 30 μ diameter in a late stage microveinlet cutting the early formed matrix silicates, showed, on analysis under conditions of constant specimen-current (table I), a large bismuth content compared to the previous analyses of kotulskite; tellurium was correspondingly lower.

The X-ray data for the Rustenburg kotulskite are tabulated in table III together with the type kotulskite and artificial PdTe for comparison. Although the powder was exposed for 26 hr at 40 kV and 22 mA only ten lines could be measured to a reasonable degree of accuracy. The fall-off in line intensity towards the back reflection region is again probably caused by the extremely small quantity of powdered mineral available. The close agreement with artificial PdTe strongly supports the empirical formula Pd(Te,Bi) for kotulskite derived by electron-probe microanalysis. This is further emphasized by the lack of agreement with the powder data for artificial $PdTe_2$.

Merenskyite[1]

Merenskyite occurs in the same manner as kotulskite with which it is very commonly intergrown (fig. 3; pl. XII, fig. c). In reflected light it is

[1] Name approved before publication by the Commission on New Minerals and Mineral Names, International Mineralogical Association, June 1965.

easily distinguished from kotulskite, which is pale yellow in colour, whereas merenskyite is white in comparison. Moncheïte and merenskyite are not easily distinguished from each other, unless in close proximity, when merenskyite can be seen to have a higher reflectivity and appears slightly more creamy.

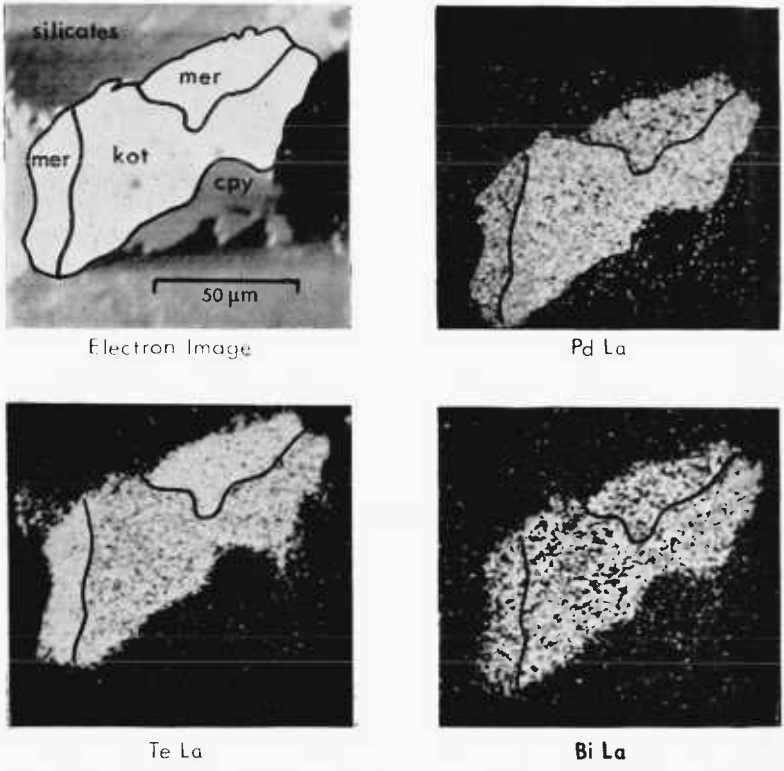

FIG. 3. X-ray scanning micrographs showing the distribution of palladium, tellurium and bismuth in a composite grain of merenskyite $Pd(Te,Bi)_2$ (mer) and kotulskite Pd(Te,Bi) (kot) intergrown with chalcopyrite (cpy). Because of poor contrast the respective phases have been outlined.

Optical and physical properties. In air merenskyite is white with a weak pleochroism from white to greyish white. In oil the reflection pleochroism is more distinct, from white with a slight creamy tint to light greyish white. It is distinctly to strongly anisotropic, according to orientation, with dark brown to light greenish grey polarization colours. No Vickers

indentation microhardness values were obtained for this phase because of the small size of the grains. The polishing relief indicated its polishing hardness to be less than pentlandite, greater than chalcopyrite, and just greater than kotulskite. Precise reflectivity values are given in table I; measurements were made in air using a $\times 32$ objective and 2 mm mirror diaphragm.

Composition. An electron-probe microanalysis of a large grain (fig. 3) of this phase, from which X-ray powder data were later obtained, was made using constant beam-current conditions and correcting the initial percentages for absorption, atomic number, and fluorescence. This analysis (table I, anal. 13) gives a (Pd,Pt): (Te,Bi) ratio of 1·0: 2·06 indicating the empirical formula $(Pd,Pt)(Te,Bi)_2$. The X-ray data for this phase are presented in table II together with artificial $PdTe_2$ and moncheïte for comparison. As with previous phases only a minute quantity of powder could be obtained and a 30-hr exposure at 40 kV and 22 mA with Cu-$K\alpha$ radiation was needed to obtain a reasonable photograph. The similarity of the patterns for merenskyite and moncheïte suggests that they are probably isostructural, merenskyite being the palladium end-member of a possible solid solution series, and the close agreement of both patterns with that for artificial $PdTe_2$ helps to confirm the above formula. The X-ray data compared with those for artificial PdTe do not show such a close similarity.

A further electron-probe microanalysis (table I, analysis 14) of a phase optically identified as merenskyite and intimately intergrown with kotulskite (pl. XII, fig. c) suggested the empirical formula $Pd_3(Te,Bi)_5$. This may be an error, probably present in many probe analyses of chemically similar phases complexly intergrown, caused by the inclusion of sub-outcropping kotulskite in the irradiated zone of the analysis. However, in an equilibrium diagram for Pd–Te alloys (fig. 4) (Z. S. Medvedeva *et al.* (1961)) it is significant that in the $PdTe_2$–PdTe region, in the range 640–690° C, the alloys form a continuous series of solid solutions, which break down below 640° C into a mixture of two solid solutions based on PdTe and $PdTe_2$. This could account for the $Pd_3(Te,Bi)_5$ phase as consisting of merenskyite with PdTe or Pd(Te,Bi) in solid solution. This relationship also helps to account for the invariable occurrence of kotulskite, equivalent to PdTe, as an intimate intergrowth with merenskyite.

In conclusion it appears that merenskyite is the palladium end-member of a possible solid-solution series with the platinum end-member moncheïte. It may also form a complete solid-solution series with

kotulskite at high temperatures and only a partial one at normal temperatures, an indication being the possible existence of $Pd_3(Te,Bi)_5$.

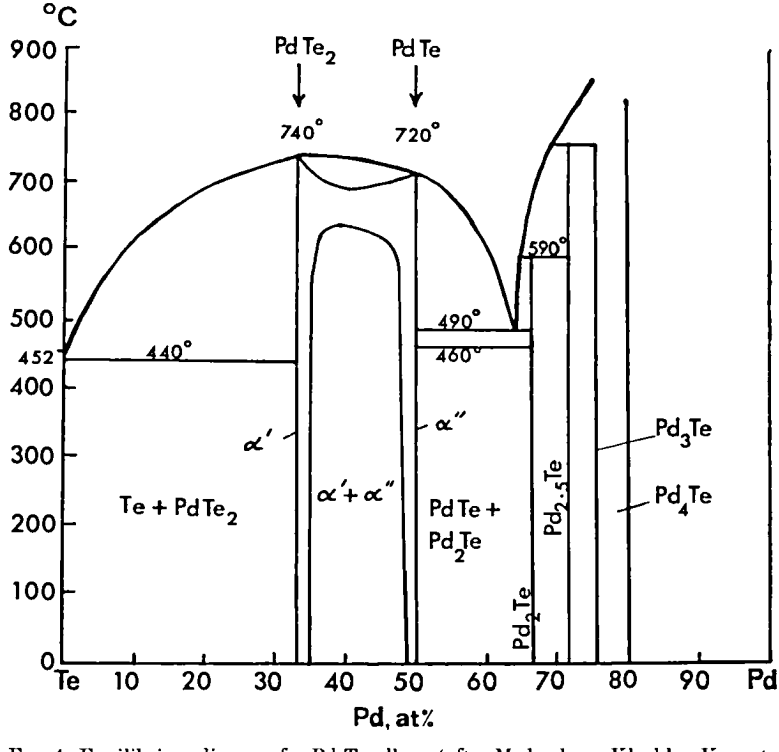

FIG. 4. Equilibrium diagram for Pd-Te alloys (after Medvedeva, Klochko, Kuznetsov, and Andreeva, 1961).

Mineral A, $(Pd,Hg)_x(Te,Bi)_y$

This phase has so far only been located as four blebs, ranging from 2 to 5 μ in diameter, intergrown with merenskyite. Its colour in air is light grey but under oil immersion it is slightly darker with a brownish tint. It appears to be isotropic. Values of reflectivity for this phase are presented in table II. From an examination of polishing relief it is softer than merenskyite and chalcopyrite.

The composition of this phase as determined with the electron-probe microanalyser is at present only semiquantitative because of the small grain size and the consequent errors involved in such an analysis (table I, anal. 15). This suggests a (Pd,Hg):(Te,Bi) ratio of 1:1. The only other

palladium–mercury minerals reported in the literature are potarite, PdHg, and allopalladium, whose exact composition is uncertain but which appears to contain palladium and mercury.

Paragenetic considerations

Although the mode of emplacement and the details of the subsequent differentiation of the mafic zone of the Bushveld Igneous Complex are still somewhat controversial, there are few who would not concede that it was produced from a melt of basaltic composition, which did undergo at least part of its differentiation *in situ*. Thus the paragenesis of the minerals composing the Merensky Reef can be considered in the light of fractional crystallization and sulphide immiscibility in an oxide-silicate melt. One can envisage, as a result of these two processes combined with gravity settling and related phenomena, the formation at one stage of a compact coarsely crystalline aggregate of mainly pyroxenes with subordinate feldspars, with a sulphide melt rich in volatiles filling the interstices. Reaction takes place between this sulphide melt and the early silicates producing reaction minerals such as hornblende and biotite. Graphite may also be formed at this time. Meanwhile from the interstitial sulphide melt the base metal sulphides and platinoid minerals begin to crystallize out in a certain order. In the Rustenburg mine this order is relatively simple and early pyrite is followed by pyrrhotine, exsolution pentlandite and primary pentlandite, and finally chalcopyrite with exsolved cubanite and mackinawite. One of the earliest formed platinum minerals is ferro-platinum, which is commonly associated with pyrrhotine either as a fine graphic intergrowth, suggesting a eutectic relationship, or as euhedral partially corroded grains. The platinoid sulphides and arsenides are slightly later and generally occur as euhedral aggregates or isolated grains enclosed in pentlandite but often fractured and veined by chalcopyrite. The bismuthotellurides, stibiopalladinite, and arsenopalladinite are the latest formed platinoid minerals and are commonly associated with chalcopyrite as included blebs and laths or as discrete grains along sulphide–silicate boundaries. They are also found as clusters or small grains in microveinlets along partings in the altered early silicates. These microveinlets may have been formed by reaction of residual fugitive constituents with the early silicates. Thus the platinoid bismuthotellurides appear to be of late crystallization and may be associated with the residual 'pegmatitic' phase after the formation of the main bulk of the sulphides as postulated by Schneiderhohn (1929).

The tendency at present is to allocate platinum minerals to a later

stage of crystallization (Stumpfl, 1962) than was envisaged in past conceptions of the geochemical behaviour of the platinum metals by Schneiderhohn (1929) and Rankama and Sahama (1950). This trend of opinion began as a result of the location of numerous new platinoid phases in deposits and ores that from field evidence were of a relatively late stage of crystallization compared to the early magmatic sulphides of the Merensky Reef. Notable among these discoveries are those from the Dreikop dunite pipe in the eastern Bushveld by Stumpfl (1961), from the Urals, Norilsk, and Monchegorsk by Borovskii (1959), Genkin (1959, 1961, 1963), and Betechtin (1961), and from Sudbury by Hawley and Berry (1958). However, as regards the Merensky Reef it is apparent that not all the platinum minerals are of a late stage of crystallization as has been suggested by Willemse (1964). In fact, the chief platinoid minerals at Rustenburg mine, cooperite and braggite, appear to have crystallized early from the interstitial magmatic sulphides.

The presence of these platinoid bismuthotellurides is of interest as regards the geochemical behaviour of tellurium during the fractional crystallization of the sulphides. Their occurrence is in agreement with investigations by Sindeeva (1959) and others who have demonstrated that tellurium, although a close analogue of sulphur and selenium, tends to form independent minerals even when present in very low concentrations rather than to form solid solutions in the base metal sulphides. This is explained as a result of the quite different atomic size and electronegativity of tellurium compared to sulphur. Selenium readily substitutes for sulphur, as shown by Zaryan (1962) and others, and where the concentration of selenium is low, independent selenium minerals will be unlikely to form. In the Merensky Reef no selenides have yet been found, although traces of selenium are probably present in the sulphides. Platinoid selenides were reported from the Urals in the copper–nickel sulphide ores of the Norilsk region by Zainullin and Pashinkin (1960), but compared with the platinoid tellurides they were rare even though there was more selenium than tellurium present in the ore. The results of microscopic and chemical investigations of the distribution of tellurium in ores related to basic and ultrabasic intrusives by Zainullin (1960), Pshenichnii (1961), Zaryan (1962), and others, show that tellurium is concentrated in the later stages of crystallization and in particular in the chalcopyrite-rich ores. The tellurium in the Merensky Reef appears to follow this trend. Bismuth appears to behave in a similar way and in these ores substitutes for tellurium as demonstrated in the various analyses of moncheïte in table I. This substitution would be expected

from the close similarity in atomic radius of bismuth (1·55 Å) and tellurium (1·43 Å).

Acknowledgements. This paper constitutes part of a research programme into the mineralogy of the Merensky Reef of the Western Bushveld. I am very grateful for financial assistance from the Vernon Hobson Bequest Fund of the Institution of Mining and Metallurgy and the Hilary Bauerman grant from Imperial College. I am also indebted to Johannesburg Consolidated Investment Co. Ltd. for their help and permission to study the field relations and collect specimens of this platiniferous horizon at Rustenburg and Union mines from July to September of 1962. I would especially like to thank Dr. J. Zermatten of J.C.I. for his kindness and assistance and his generous provision of a comprehensive collection of polished sections of concentrates and ore from the two mines.

I would like to express my sincere thanks to Dr. A. P. Millman for his helpful suggestions and criticisms during the course of this investigation and in the preparation of this paper.

I am grateful to Mr. T. K. Kelly for his help in the electron probe microanalysis of these minerals and for correcting the initial results for absorption, atomic number, and fluorescence. In connexion with the electron probe microanalysis, Messrs. Johnson and Matthey Ltd. very generously provided standard platinoid alloys. Thanks are also owed to Mr. R. Curtis and Mr. M. T. Frost for their help in obtaining and processing the X-ray data.

References

Barringer (A. R.), 1953. Trans. Inst. Min. Metall., vol. 63 (Bull. Inst. Min. Metall., no. 563, Oct. 1953), p. 21.

Beath (C. B.), Cousins (C. A.), and Westwood (R. J.), 1961. The exploitation of the platiniferous ores of the Bushveld Igneous Complex with particular reference to Rustenburg Platinum Mine. Commonwealth Conference of Min. Metall.

Betechtin (A. G.) [Бетехтин (А. Г.)], 1961. Mikroskopische Untersuchungen an Platinerzen aus dem Ural. Neues Jahrb. Min.,Abh. vol. 97, p. 1.

[Borovskii (I. B.), Deev (A. N.), and Marchukova (I. D.)] Боровский (И. Б.), Деев (А. Н.), и Марчукова (И. Д.), 1959. Геол. рудн. месторожд. (Geol. ore-deposits), no. 6.

Castaing (R.), 1951. Application des sondes électroniques à une méthode d'analyse ponctuelle chimique et cristallographique. Thesis, Faculty of Science, University of Paris.

Duncumb (P.), 1964. Paper presented at the International Symposium on Electron Probe Microanalysis in Washington, D.C. (to be published).

[Genkin (A. D.)] Генкин (А. Д.), 1959. Геол. рудн. месторожд. (Geol. ore-deposits), no. 6, p. 74.

[—— and Korolev (N. V.)] —— и Королев (Н. В.), 1961. *Ibid.*, no. 5.

[——, Zhuravlev (N. M.), and Smirnova (E. M.)] ——, Журавлев (Н. М.) и Смирнова (Е. М.), 1963. Moncheite and kotulskite—new minerals and the composition of michenerite. Зап. Всесоюз. мин. общ. (Mem. All-Union Min. Soc.), vol. 92, p. 33 [M.A. **16**–283].

Gronvold (F.), Haraldson (H.), and Kjekshus (A.), 1960. Acta Chem. Scand., vol. 14. no. 9.

Hawley (J. E.) and Berry (L. G.), 1958. Canad. Min. vol. 6, p. 200.

Hess (J. B.), 1951. Acta Cryst., vol. 4, p. 209.

Hiemstra (S. A.), 1956. Amer. Min., vol. 41, p. 519.

Hoff (W. D.), Wallace (W.), and Kitchingman (W. J.), 1965. Journ. Sci. Instr., vol. 42, p. 171.

KELLY (T. K.), 1966. Inst. Min. Metall., Earth Sciences Section, vol. 75, p. 59.
[MEDVEDEVA (Z. S.), KLOCHKO (M. A.), KUZNETSOV (V. G.), and ANDREEVA (S. N.)] Медведева (З. С.), Клочко (М. А.), Кузнецов (В. Г.) и Андреева (С. Н.), 1961. Журн. неорг. хим. (Journ. Inorg. Chem.), vol. 6, no. 7.
PHILIBERT (J.), 1962. A method for calculating the absorption correction in electron prove microanalysis. 3rd Internat. Sympos. X-Ray Optics, X-Ray Microanalysis (New York, Academic Press, 1963), p. 379.
PSHENICHNII (G. N.) [Пшеничный (Г. Н.)], 1961. Geochemistry (translation of Геохимия), no. 8, p. 751.
RANKAMA (K.), and SAHAMA (T.), 1950. Geochemistry (Chicago).
SANTOKH SINGH (D.), 1965. Trans. Inst. Min. Metall., vol. 74, p. 901.
SCHNEIDERHOHN (H.), 1929. In P. A. Wagner—The platinum deposits and mines of South Africa. (Edinburgh: Oliver and Boyd).
SINDEEVA (N. D.) [Синдеева (Н. Д.)], 1959. quoted by Zaryan in Geochemistry, no. 3, 1962.
STUMPFL (E. F.), 1961. Min. Mag., vol. 32, p. 833.
—— 1962. Econ. Geol., vol. 57, p. 619.
THOMASSEN (L.), 1929. Zeitschr. physikal. Chem., Abt. B, vol. 2, p. 349.
WILLEMSE (J.), 1964. Geol. Soc. South Africa, vol. 2 (The geology of some ore deposits of southern Africa.)
WILLIAMS (K. L.), 1962. Amer. Min. vol. 47, p. 974.
YOUNG (B. B.) and MILLMAN (A. P.), 1964. Trans. Inst. Min. Metall., vol. 73, p. 437.
ZAINULLIN (G. G.) [Зайнуллин (Г. Г.)], 1960. Geochemistry (translation of Геохимия), no. 3, p. 273.
ZARYAN (R. N.) [Зарьян (Р. Н.)], 1962. Ibid., no. 3, p. 267.
ZIEBOLD (T. O.) and OGILVIE (R. E.), 1964. Anal. Chem., vol. 36, p. 322.

[*Manuscript received 2 September 1965.*]

EXPLANATION OF PLATE XII

FIG. A. Two grains of moncheïte $Pt(Te,Bi)_2$ (white) associated with chalcopyrite (cpy) which encloses fractured braggite (Pt,Pd,Ni)S (brag).

FIG. B. Platinoid bismuthotelluride grains (white) associated with chalcopyrite (light grey) in microveinlets in the silicates (dark grey).

FIG. C. A subhedral lath of merenskyite (mer) along a pentlandite: silicate contact showing partial replacement by kotulskite (k) Pd(Te,Bi). Crossed nicols.

FIG. D. A lath of moncheïte $Pt(Te,Bi)_2$ (mon) and euhedral crystals of ferroplatinum (Pt,Fe) showing cubic outline, intergrown with pyrrhotine (pyrrh) and pentlandite (pent).

[*Note*: μm, on the scales on Plate XII, is a micro-metre, equal to a micron (μ), and not to be confused with a millimicron, mμ.—*Ed.*]

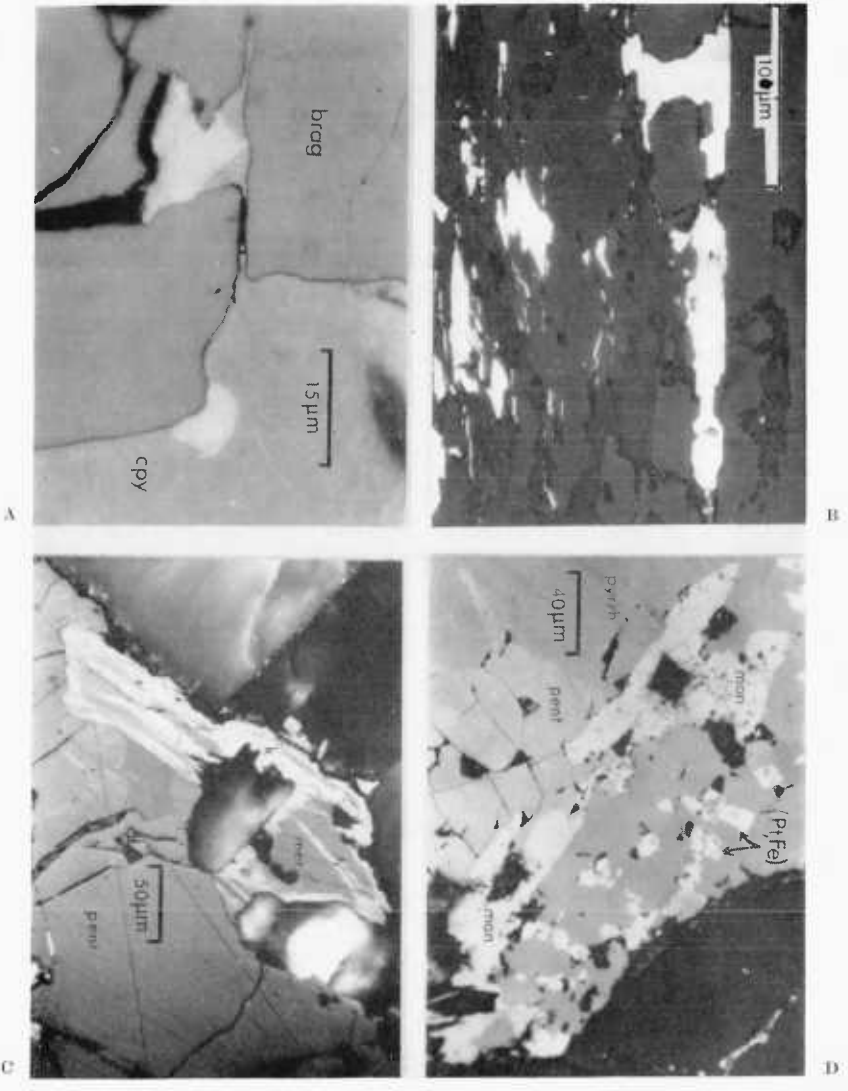

G. A. KINGSTON: PLATINOID BISMUTHOTELLURIDES

MAP 1

RUSTENBURG MINE
C2 W—9

REEF FACIES

K	KOPPIE
	NORMAL
PH	POTHOLE

SCALE 1:200

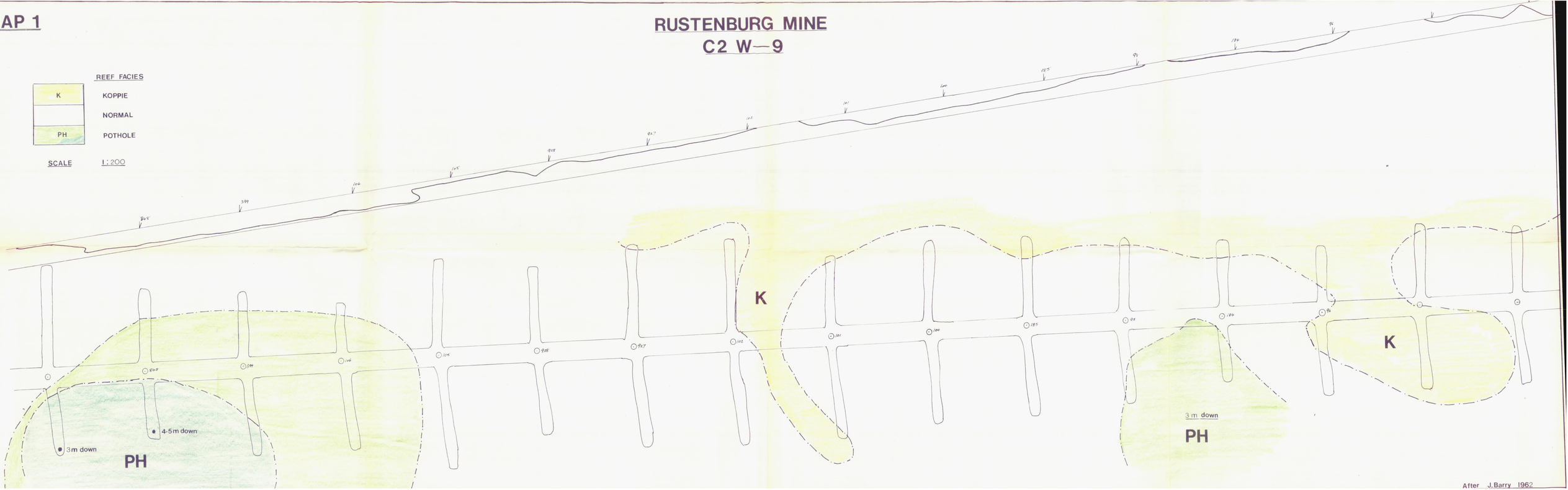

After J.Barry 1962

RUSTENBURG MINE

N

SCALE 1:200

T 16

STOPE FACE

REEF/KOPPIE CONTACT

NORMAL REEF FACIES

KOPPIE REEF FACIES

PEGMATITIC ANORTHOSITIC NORITE

SULPHIDE PEGMATITE

T 14

T 13

9 HAULAGE

Dyke

W1E — 9W

SECTION

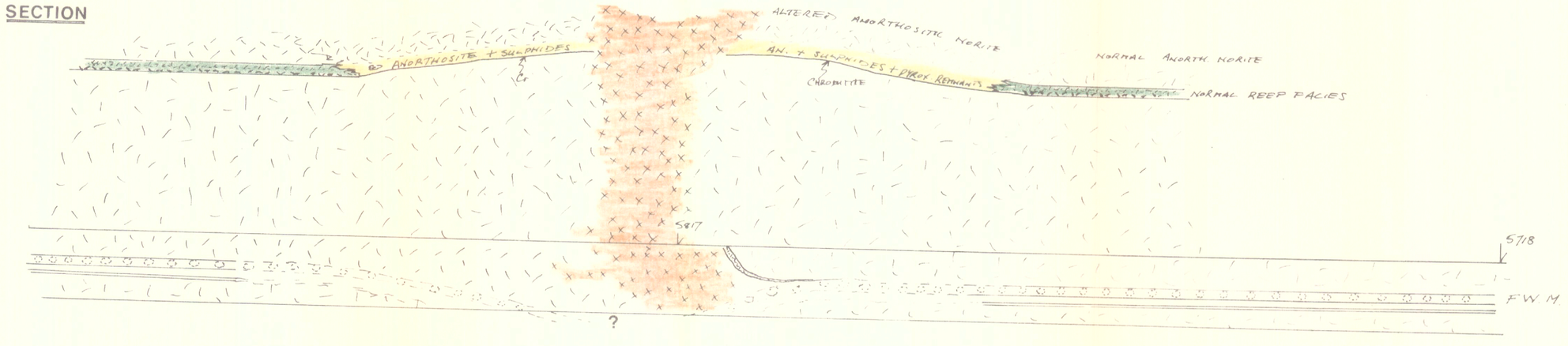

KINGSTON 1977